Development of Field Portable Solid Phase Microextraction Samplers for Performing On-site Environmental Analysis

by

Jonathan Grandy

A thesis
presented to the University of Waterloo
in fulfillment of the
thesis requirement for the degree of
Doctor of Philosophy
in
Chemistry

Waterloo, Ontario, Canada, 2018

Examining committee membership

The following served on the Examining Committee for this thesis. The decision of the Examining Committee is by majority vote.

External Examiner	NAME: Xing-Fang Li Title: Professor
Supervisor(s)	NAME: Janusz Pawliszyn Title: University Professor
Internal Member	NAME: Mario Gauthier Title: Professor
Internal-External Member	NAME: Carol Ptacek Title: Professor
Other Member(s)	NAME: Scott Hopkins Title: Associate Professor

Authors Declaration

This thesis consists of material all of which I authored or co-authored: see Statement of Contributions included in the thesis. This is a true copy of the thesis, including any required final revisions, as accepted by my examiners.

I understand that my thesis may be made electronically available to the public.

Statement of contributions

Many of the materials in Chapter 1 were already published in 2 separate publications including a book chapter entitled "Chapter 7. Novel and Emerging Air-Sampling Devices" of a book entitled "Comprehensive Analytical Chemistry Volume 70 Monitoring of Air Pollutants" (Elsevier, **2015**, pp 209-235) which was co-authored by Saba Asl Hariri and supervised by Janusz Pawlisyzn and a review article entitled, "Advances in Solid Phase Microextraction and Perspective on Future Directions: Environmental Analysis" (*Anal. Chem*, **2018,** 90 (1), pp 302-360 which was co-authored by Nathaly Reyes-Garcés, Emanuela Gionfriddo, German Augusto Gómez-Ríos, Md. Nazmul Alam, Ezel Boyacı, Barbara Bojko, Varoon Singh, and Janusz Pawliszyn. In all cases, of the excerpts that were used in this thesis, I certify that I am the sole author of the selected materials with all other authors mentioned being responsible for the writing of their own respective sections in the aforementioned publications. Final amalgamation and submission of these publications were performed by Patricia Forbes (book editor) and Nathaly Reyes-Garcés (leading author) respectively.

Most of Chapter 2 was already published in one manuscript entitled, "Development of a standard gas generating vial comprised of a silicone oil–polystyrene/divinylbenzene composite sorbent," (*J. Chrom, A,* **2015**, 1410, pp 1-8) **w**hich was co-authored by German Augusto Gómez-Ríos and supervised Janusz Pawliszyn. In all cases, experimental planning and design, experimental work conducted in the laboratory, data analysis, interpretation, and writing were performed by the author of the thesis.

Most of Chapter 3 was already published in one manuscript entitled, "Solid Phase Microextraction On-Fiber Derivatization Using a Stable, Portable, and Reusable Pentafluorophenyl Hydrazine Standard Gas Generating Vial," (*Anal. Chem*, **2016**, 88, pp 6859-6866) which was co-authored by Justen Poole, German Augusto Gómez-Ríos, Emanuela

Gionfriddo and supervised Janusz Pawliszyn. In most cases, experimental planning and design, experimental work conducted in the laboratory, data analysis, interpretation, and writing were jointly performed by the author of the thesis and Justen J. Poole. The experiment described in Section 3.2.7 of this thesis was performed jointly by Justen J. Poole and Emanuela Gionfriddo with the author of this thesis assisting with experimental design, set-up of materials, data interpretation and writing. The experiment described in Section 3.3.6 of this thesis, including experimental planning and design, experimental work conducted in the laboratory, data analysis, interpretation, and writing were performed solely by the author of the thesis and remains unpublished outside of this thesis.

Most of Chapter 4 was already published in one manuscript entitled, "Development of a Carbon Mesh Supported Thin Film Microextraction Membrane As a Means to Lower the Detection Limits of Benchtop and Portable GC/MS Instrumentation," (*Anal. Chem,* **2016**, 88, pp 1760-1767) which was co-authored by Ezel Boyacı and supervised Janusz Pawliszyn. In all cases, experimental planning and design, experimental work conducted in the laboratory, data analysis, interpretation, and writing were performed by the author of the thesis. The experiments described in Sections 4.2.6 and 4.3.3 of this thesis including experimental planning and design, experimental work conducted in the laboratory, data analysis, interpretation, and writing were performed solely by the author of the thesis and remain unpublished outside of this thesis.

Most of Chapter 5 was already published in two manuscripts entitled, "Inter-laboratory validation of a thin film microextraction technique for determination of pesticides in surface water samples," (*Anal Chimica Acta,* **2017**, 964, pp 74-84) which was co-authored by Hamed Piri-Moghadam, Emanuela Gionfriddo, Angel Rodriguez-Lafuente, Heather L. Lord, and supervised by Terry Obal and Janusz Pawliszyn, and, "Development and Validation of Eco-Friendly

Strategies based on Thin Film Microextraction for Water Analysis," (Green Chemistry, in-review) which was co-authored by Hamed Piri-Moghadam, Emanuela Gionfriddo, Md. Nazmul Alam, and supervised by Janusz Pawliszyn. In most cases, of the excerpts taken from these respective manuscripts, experimental planning, and design, experimental work conducted in the laboratory or on-site, data analysis, interpretation, and writing were jointly performed by the author of the thesis, Hamed Piri-Moghadam, and Emanuela Gionfriddo. The experiment described in Section 5.2.4 of this thesis was designed, conducted, and data analyzed by Angel Rodriguez-Lafuente and Heather L. Lord while, Hamed Piri-Moghadam, and Emanuela Gionfriddo, and the author of this thesis, only assisted in experimental planning, data interpretation and writing for the respective portion of the study.

Chapter 6 consists of unpublished works from a project entitled "Development of a Hydrophilic-Lipophilic Balanced Thin Film Solid Phase Microextraction Device for the Balanced Determination of Volatile Organic Compounds" which was co-authored by Varoon Singh and supervised by Janusz Pawliszyn. In most cases, experimental planning and design, experimental work conducted in the laboratory, data analysis, interpretation, and writing were performed by the author of the thesis. The experiments described in Sections 6.2.3, 6.2.9, 6.3.1, 6.3.6 of this thesis, including experimental planning and design, experimental work conducted in the laboratory, data analysis, interpretation, and writing were performed jointly by the author of the thesis and Varoon Singh.

Chapter 7 consists of unpublished works from a project entitled "Design, Construction and Validation of Robust, Self-Sealing and Analyte Stabilizing Deep Ocean Samples for Manual and Robotic Operation" and was authored solely by the author of this thesis. In most cases, experimental planning and design, experimental work conducted in the laboratory, data analysis,

interpretation, and writing were performed by the author of the thesis. Sampler design and construction were performed jointly by the author of this thesis, Harmen Van-der-Heide and Johnathan Rose. Deep ocean ROV samplings were coordinated by Verena Tunnicliffe and Johnathan Rose while they were performed by Woods Hole Oceanographic Institution, the ROPOS team of the Canadian Scientific Submersible Facility Ltd and the Schmidt Ocean Institute.

Abstract

Since being introduced in 1989 solid phase microextraction (SPME) techniques have continually evolved from within the analytical chemistry community due in large part to their clean, portable and easy to handle design. It is no surprise then that these devices lend themselves well to on-site sampling approaches making their use in conjunction with field portable instrumentation a growing trend. However, as with any emerging analytical methodology, it is important that these entirely on-site approaches are developed such that they deliver comparably reliable and sensitive results to accepted techniques. As such, presented herein, various novel morphologies and analytical methodologies based on the principles of solid phase microextraction were developed and validated as a means to improve the reliability and sensitivity of on-site environmental analysis.

As an opening project, a portable in-vial standard analyte generator capable of delivering a highly reproducible gaseous headspace is proposed. The vial is comprised of a silicone diffusion pump fluid spiked with appropriate calibration or derivatization compounds, such as modified McReynolds probes (benzene, 2-pentanone, pyridine, 1-nitropropane, 1-pentanol, and n-octane) or pentafluorophenyl hydrazine (PFPH), respectively. The spiked silicone oil is then mixed with polystyrene/divinylbenzene (PS/DVB) particles and enclosed in a 20 mL headspace vial. Using the McReynolds calibration mixture, headspace concentrations were found to be substantially decreased in comparison to prior hydrocarbon pump oil based vials hence, the amount of standard loaded onto SPME fibers was at most, half that of the previous vial design. Appropriately, depletion for all compounds after 208 successive extractions was shown to be less than 3.5%. Smaller proportions of standards being used at each extraction resulted in a vial that depleted slower while remaining statistically repeatable over a wider number of runs. Indeed, it was found that this depletion could be predicted using a theoretical, mass-balance model. At a 95 % level of

confidence, the ANOVA test demonstrated that prepared vials were statistically identical, with no significant intra- or inter-batch variations. Storage stability in varying conditions such as light exposure and temperature was also validated over 10 weeks for vials prepared with the reactive and unstable, pentafluorophenyl hydrazine in addition to the McReynolds probes. To demonstrate amenability for on-site environmental applications, a battery operated vial oven was constructed and employed in tandem with portable GC/MS instrumentation for the on-site PFPH derivatization and quantitation of formaldehyde from car exhaust. By using a combination of SPME fibers and needle trap devices (NTD's) the concentration of this formaldehyde in aerosol particles could be determined and differentiated from the free gaseous concentration. Following these validatory experiments, varying standard headspace generating mixtures were continuously used to evaluate the portable GC/MS instrument while providing a means for on-site quality control.

As the main accomplishment of this thesis a durable, high surface area, and easy to handle thin film microextraction (TFME) device is proposed. The membrane is comprised of poly-divinylbenzene resin particles suspended in a high-density polydimethylsiloxane glue spread onto a carbon mesh support. This novel design was shown to exhibit a substantially lesser amount of siloxane bleed during thermal desorption while providing a statistically similar extraction efficiency towards a broad spectrum of compounds when compared to an unsupported DVB/PDMS membrane of similar size that had been prepared with former methods. At a 95 % level of confidence, the ANOVA test demonstrated that these membranes were also statistically similar, with no significant intra- or inter-batch variations. In an initial validation, membranes cut to 4 cm long, 4.85 mm wide and coated 30-40 μm thick (per side), were shown to extract 21.2, 19.8, 18.5, 18,4, 26.8, and 23.7 times the amount of 2,4-dichlorophenol 2,4,6-trichlorophenol,

phorate-D10, fonofos, chlorpyrifos, and parathion respectively, from a 10 ppb aqueous solution than a comparable 65 μm DVB/PDMS SPME fiber.

Following these initial developments, these carbon mesh supported DVB/PDMS membranes were established as highly sensitive, accurate and green alternative to classical liquid-liquid extraction (LLE) for the determination of 23 multi-class pesticides from surface water samples. This signal improvement was made evident by method limits of detections (MLOD's) in the low ng L^{-1} range for most of the pesticides studied while only requiring 30 mL of sample. Furthermore, these MLOD's were shown to be at least 10 times lower than those achieved using an EPA certified, LLE method performed at an accredited analytical laboratory participating in the study. Moreover, the method accuracy was validated through double-blind split analyses of 18 surface water samples. Good agreement between the two methods was achieved with accuracy values between 70-130% for the majority of analytes tested. This methodology was further explored on-site with the design and deployment of a portable TFME sampling case to be used in conjunction with the portable GC/MS instrumentation. Although the chosen pesticides were found to be more-or-less absent from the 4 riparian sampling locations, a wide variety of untargeted compounds could still be detected and identified using the portable TFME-GC-TMS method. As such, the on-site method repeatability was still deemed acceptable with %RSD's for the untargeted compounds around 20% (n=5). Moreover, by use of a BTEX standard headspace generating vial, the portable GC/MS was shown to remain stable over the entire 1-month sampling period.

Furthering the development of carbon mesh supported TFME, a highly sensitive HLB-PDMS thin film microextraction device for the balanced determination of VOC compounds of varying polarity was prepared. In addition to exhibiting a 50+ fold increase in sensitivity when compared to a 65 μm DVB/PDMS SPME fiber, these membranes extracted approximately double

the amount of McReynolds probes versus a more comparable DVB/PDMS TF-SPME device of identical size. Inter-membrane extraction efficiencies for these compounds were determined to be reproducible at 95% confidence for all 4 of the coating chemistries tested including the DVB/PDMS membranes, and those prepared with 3 different HLB compositions. Further method reliability was established by confirming that, once extracted, the McReynolds standards were stable on the HLB/PDMS membranes stored in the thermal desorption tubes on the autosampler rack for at least 120 hours for 5 of the 6 standards and only 24 hours for pyridine at 95% confidence. Finally, a real-world proof of concept application determining chlorination by-products from a private hot tub was performed, successfully identifying, 2-chloroethylamine 3-chloro-1-propanamine, and dichloroacetonitrile with %RSD's less than 10%.

Finally, as a side project, the goal of pushing on-site sampler design to its fullest was explored by means of the construction of a self-sealing coated bolt sampler for the analysis of deep ocean environments via divers and ROV submersibles. These samplers employ HLB particles which have been coated onto recessed stainless steel bolts by use of polyacrylonitrile (PAN) glue. 6 coated bolts are then inserted into a self-sealing, polytetrafluoroethylene (PFTE) bodied sampler designed to preserve extracted compounds for extended periods. To verify this stability, 3 samplers were deployed on-site at a waste-water treatment facility outflow pipe via kayak. Post-sampling, the samplers were stored using 3 storage conditions including A: immediate desorption, B: 3 days at 23 ^{o}C), C: 12 days at 23 ^{o}C and D: 12 days in a -80 ^{o}C freezer. All bolts tested were statistically indistinguishable when analyzed using principal component analysis (PCA). Furthermore, 10 randomly selected, volatile, features were also demonstrated to give a statistically identical response at a 95% level of confidence using the ANOVA test. Finally, in a cutting-edge application, these samplers were tailored for use on an ROV submersible and employed for the on-

site sampling of hydrothermal vents at 2 locations along the Pacific Rim with 2 corresponding control extractions also performed from ambient waters away from these vents such that significant features could be differentiated. Separation and analysis of all samples were performed using an HPLC equipped orbit-trap mass spectrometer and 100's of statistically unique features could be determined from the vents by use of multivariate statistical analysis.

Acknowledgments

I would like to express my thanks to my supervisor, Professor Janusz Pawliszyn, for giving me the opportunity and support to work within his research group with a particular thanks for sharing his valuable ideas, encouragement, and enthusiasm making this thesis possible.

I would also like to thank my advisory committee members including, Prof. Mario Gauthier, Prof. Edgar Lee, and Prof Wojciech Gabryelski for providing their time and advice throughout my studies and thesis preparation.

I also would like to extend my gratitude to those who agreed to provide their time and comments required for the examination of my thesis and related defense including my external examiner, Xing-Fang Li, and my internal/external examiner, Carol Ptacek.

I also extend my sincerest gratitude to our many collaborators including those scientists from Torion Technologies of Perkin Elmer for their instrument and training support; those who assisted us from Supelco of Millipore-Sigma with their continued financial support and supply of raw materials used in the construction of our samplers; to Verena Tunnicliffe and Johnathan Rose of University of Victoria who worked with the Woods Hole Oceanographic Institution, the ROPOS team of the Canadian Scientific Submersible Facility Ltd and the Schmidt Ocean Institute on our behalf to facilitate the deployment of our deep sea samplers.

Finally, I would like to give a special thanks to all those who assisted me professional and with their friendship from within Professor Pawlisyzn's Research Group. Particularly, I would like to thank Dr. German Augusto Gómez-Ríos, Justen J Poole, Dr. Emanuela Gionfriddo, Dr. Hamed Piri-Moghadam, Dr. Ezel Boyacı, Dr. Nathaly Reyes-Garcés, Varoon Singh, and Dr. Angel Rodriguez-Lafuente, for their assistance and mentorship throughout our many co-authored publications. I would also like to thank those members from our university support staff including Harmen Van-der-Heide of the Science Machine Shop, Krunomir Dvorski of the Science

Electronics Shop, and Catherine Van Esch, and Kim Rawson, of our graduate administrative support, for their help and advice throughout my studies.

Dedication

I dedicate this thesis to my family and friends, particularly to my parents, who, through their loving support have made it possible for me to be where I am today, Thank you.

Table of Contents

List of Tables

List of Figures

List of abbreviations

ACN	acetonitrile
BTEX	benzene, toluene, ethylbenzene, (o)xylene
CAR	Carboxen
CIS	cooled injection system
CW	Carbowax
DI	direct immersion
DMF	dimethylformamide
DVB	divinylbenzene
ECD	electron capture detector
EI	electron impact ionization
ESI	electrospray ionization
FID	flame ionization detector
GC	gas chromatography
GC/MS	gas chromatography/mass spectrometry
GC/TMS	gas chromatography/toroidal ion trap mass spectrometry
HDPE	high-density polyethylene
HLB	hydrophilic-lipophilic balance
HPLC	high-performance liquid chromatography
HPLC/MS	high-performance liquid chromatography/mass spectrometry
HS	headspace
ID	inner diameter
IMS	ion mobility spectrometry
IS	internal standard
LC	liquid chromatography
LDR	linear dynamic range
LLE	liquid-liquid extraction
LOD	limit of detection

LOQ	limit of quantification
MCL	maximum contaminant levels
McReynolds	a mixture containing benzene, 2-pentanone, 1-nitropropane, pyridine, 1-pentanol, octane
MDL	method detection limit
MLOQ	method limit of quantification
MOEE	Ontario Ministry of Environment and Energy
MS	mass spectrometry
MS/MS	tandem mass spectrometry
ND	not detected
NIST	National Institute of Standards and Technology
OPLS-DA	Orthogonal Projections to Latent Structures Discriminant Analysis
PA	polyacrylate
PAHs	polycyclic aromatic hydrocarbons
PAN	polyacrylonitrile
PCA	principle component analysis
PCBs	polychlorinated biphenyls
PCDDs	polychlorinated dibenzodioxins
PDMS	polydimethylsiloxane
PEG	poly(ethylene glycol)
PFP	pentafluorophenyl
PFPH	pentafluorophenyl-hydrazine
P&T	purge-and-trap
PS	polystyrene
PTFE	polytetrafluoroethylene
rpm	revolutions per minute
RSD	relative standard deviation
RT	retention time
SBSE	stir bar sorptive extraction

SD	standard deviation
SEM	scanning electron microscopy
SPE	solid phase extraction
SPME	solid phase microextraction
S.S.	stainless steel
SVOCs	semi-volatile organic compounds
TDU	thermal desorption unit
TFME	thin film microextraction (interchangeable with TF-SPME)
TF-SPME	thin film-solid phase microextraction (interchangeable with TFME)
THMs	trihalomethanes
TMS	toroidal ion trap mass spectrometry
U.S. EPA	United States Environmental Protection Agency
VOCs	volatile organic compounds
VVOCs	very volatile organic compounds

Chapter 1 Introduction

Preamble

This chapter has been partially published as two separate works including a book chapter and review article respectively:

1: Jonathan Grandy, Saba Asl-Hariri, Janusz Pawliszyn; Chapter 7: Novel and Emerging Air Sampling Devices, *Elsevier*; Comprehensive Analytical Chemistry; (V. 70 Monitoring of air pollutants); **2015** pp 209-235. Materials for Sections 1.2.1, 1.2.2, 1.3, 1.3.1, and 1.3.2 are reprinted from this book chapter publication with the permission from Elsevier Publishing. These excerpts have remained unchanged in this thesis as per the terms of the reprint permissions. Copyright for this work remains the property of Elsevier publications and any further request for re-use of this information should be requested directly from them (ISBN: 978-0-444-63553-2)

2: Nathaly Reyes-Garcés, Emanuela Gionfriddo, German Augusto Gómez-Ríos, Md. Nazmul Alam, Ezel Boyacı, Barbara Bojko, Varoon Singh, Jonathan Grandy and Janusz Pawliszyn; Advances in Solid Phase Microextraction and Perspective on Future Directions; *Anal. Chem*, **2018,** 90 (1), pp 302-360. Materials for Sections 1.1, 1.2, 1.4, 1.4.1, and part of 1.5 are reprinted from this review article publication with the permission of the American Chemical Society (ACS). Copyright for this work remains the property of ACS publications and any further request for re-use of this information should be requested directly from them (DOI: 10.1021/acs.analchem.7b04502)

1.1 Challenges in the sampling and analysis of on-site environments

Among the different steps involved in the analytical process, the sample collection and

preparation steps can certainly be said to be the most critical to the attainment of reliable results for environmental applications.[1] Such a consideration stems from the relatively high likelihood that errors performed during said samplings can easily go unnoticed due to the highly variable nature of real-world environments, as well as the comparatively low levels of replication and quality control measures that can be reasonably employed in comparison to those found in a traditional laboratory setting.[2–4] Furthermore, as sampling precedes all other steps of the analytical process, any error made during this step will be propagated throughout the rest of the analysis, potentially resulting in false or weakened conclusions.[5] As such, it is imperative that samplers designed for environmental applications remain sensitive enough to extract given compounds of interest while still being robust and easy enough to handle such that they are approachable by those working in the industry.

1.2 Solid Phase Microextraction (SPME) techniques for on-site sample preparation

Since the initial introduction of the SPME approach in 1989,[6] SPME techniques have been very well explored within the environmental analytical chemistry field, with a query of the Web of Sciences database yielding over 1000 related publications since 1992 (as of September 2017). In fact, as an environmentally friendly sampling technology, it is unsurprising that much of the initial SPME research targeted environmental applications. In their two initial publications Pawliszyn, Belardi, and Arthur employed polyamide-coated fused silica fibers for the extraction and thermal desorption of chlorinated organic contaminants from water. These contaminants, consisting of various polychlorinated biphenyls (PCBs); chlorinated aliphatic hydrocarbons; and a benzene, toluene, ethylbenzene, and xylene (BTEX) mixture, represented the first compounds to ever be extracted by use of SPME as a sampling methodology in publication.[6,7] These early GC-SPME fibers, although not as repeatable or sensitive as their contemporary counterparts, posed an

inherent advantage over traditional solvent-based sample preparation methods, as they vastly increased analytical throughput while avoiding the use of the very same organic solvents they were intended to measure.

More contemporary works have continued to explore these advantages, as exemplified by an inter-laboratory study conducted by Rodriguez-Lafuente et al.[8] This study involved the direct comparison of analytical figures of merit obtained via SPME-GC in lieu of liquid-liquid extraction (LLE) (US-EPA 8270) for the determination of 25 different pesticides from surface water and groundwater samples.[8] The findings of this study revealed that in addition to providing a much faster, fully automated analytical throughput, the DVB/PDMS SPME-GC methodology also provided noticeably lower limits of detection, allowing for the positive detection of 342 of the 350 compounds tested versus the 287 detections attained via LLE. This sensitivity difference was most pronounced at the 0.8 $\mu g\ L^{-1}$ spike point, which is below that of the reporting detection limit of the LLE method performed by the partnered accredited laboratory. Furthermore, only one SPME-GC run, using 15.5 mL of sample, was required to determine all 25 pesticides from a given sample, while the US-EPA 8270 method required 3 runs per sample (encompassing acidic, neutral, and basic conditions) consuming a total of 800 mL of sample, and 150 mL of dichloromethane. Unsurprisingly, the SPME method was considered far more environmentally friendly, with an Eco-scale greenness factor of 82 (out of 100) versus a value of 51 for LLE.[9] The two techniques were verified to have a comparable level of accuracy, with 65% of the SPME results and 71% of the LLE results (n=280) falling within the 70%-130% range of the true concentrations of compounds when double-blind split analyses were performed.

1.2.1 Fundamentals of solid phase microextraction

Much like what is observed with any other phase partitioning interface, microextraction methods are governed by a standard thermodynamic equilibrium between the analyte

concentration in the sorbent phase, C_f, and that in the sample, C_s, as dictated by a distribution constant K_{fs} giving rise to Eq. 1.1 [5]:

$$K_{fs} = \frac{C_f}{C_s} \qquad \text{Eq. 1.1}$$

Furthermore, by performing simple algebraic rearrangement and knowing that the sum of the analyte extracted and that which remains in the sample at equilibrium has to equal the amount initially in the system, we can generate Eq. 1.2 where n is the amount of analyte extracted, C_0 is the initial concentration of the sample, K_{fs} is the fiber-sample distribution coefficient, V_s is the volume of the sample and V_f is the fiber volume:[5,10,11]

$$n = C_0 * \frac{K_{fs}V_s}{K_{fs}V_f + V_s} \qquad \text{Eq. 1.2}$$

Favorably, when sampling of ambient air is performed on-site, it can generally be assumed that the sample volume is infinite ($V_s >>> V_f$) such that the sample volume can be factored out and eliminated from Eq. 1.2 giving rise to the much simpler Eq. 1.3: [5,10,11]

$$n = C_s K_{fs} V_f \quad \rightarrow \quad C_s = \frac{n}{K_{fs}V_f} \qquad \text{Eq. 1.3}$$

This simplified expression gives rise to one of the major advantages of using SPME for the atmospheric analysis of VOCs. In this way, the concentration of a given analyte may be calculated using a known K_{fs} at a given temperature as long as equilibrium has been achieved. Hence equilibrium calibration acts as a calibration curve-free method for the determination of VOCs in gaseous samples. It is worth noting, however, that one would still need a spiked analyte amount versus response curve for the analytical instrument employed (for GC analysis this can be generated by performing liquid injection of a known amount of standard). Typically, SPME extractions are described by being in either the equilibrium or pre-equilibrium regime. Furthermore, when less than 50% of the equilibrium amount has been extracted, the extraction can still be considered as a zero sink where the kinetics of analyte uptake remain linear.[5,10,11] When

in this linear regime, the rate of analyte uptake ($\frac{dn}{dt}$) and therefore the sensitivity is dictated purely by kinetics which are in turn controlled by the surface area A, of the coating, the thickness of the stagnant, boundary layer (δ) of matrix surrounding the coating, the static diffusion constant D_s of the analyte in this air and finally the analyte concentration in the sample. These values give rise to Eq. 1.4: [5,10,11]

$$\frac{dn}{dt} = C_s(\frac{D_s A}{\delta}) \qquad \text{Eq. 1.4}$$

A wide variety of factors can greatly affect the values of both the boundary layer thickness and the distribution coefficient regardless of the SPME mode being performed. With air sampling, the two most important factors would have to be the air temperature, which alters both values, and the linear velocity of the sample (air flow rate) which shrinks the boundary layer thus resulting in faster extraction kinetics. When the temperature is increased, the analyte-dependant diffusion coefficient also increases thus enhancing the extraction kinetics; however, the opposite may be said about the distribution constant meaning less analyte will be sorbed at equilibrium.[5,10,11] Furthermore, a similar phenomenon is seen with regard to the molecular weight of the analyte. Generally speaking as molecular weight increases, the partial pressure of the analyte in air drops. That combined with an increasing similarity in structure to that of the polymeric coating results in an increase in the fiber constant, K_{fs}. However, larger molecules also have a much lower static diffusion coefficient meaning that the kinetics will also decrease. These relationships can give rise to a number of difficulties when trying to optimize a microextraction method as compromises must be made between sampling kinetics and equilibrium sensitivity. Depending on the experimental goal and target analyte(s), the analyst will need to properly select an appropriate sorbent coating and, if possible, control the sample temperature and flow rate. Although these relationships may

not necessarily limit SPME application, they do most certainly require a reasonable understanding of the fundamentals that govern them in order to use microextraction to its fullest.

1.2.2 Selection and characteristics of commercial, GC amenable SPME sorbent coatings

As previously alluded to there are currently a wide variety of SPME sorbents available for gaseous sampling (Table 1.1). Generally speaking, polymeric sorbents have seen increased use in the extraction of organic analytes from otherwise complex sample matrices. Much like liquid-liquid extraction, a polymeric material can be chosen to more closely match the structure and polarity of the analyte of interest so as to increase the affinity of said analyte for the coating. A quick search of the Web of Science Publications statistics indicates that the 100 µm thick polydimethylsiloxane (PDMS) extraction phase has been, by far, the most widely used SPME extraction phase worldwide. The nonpolar structure of PDMS makes it highly appropriate for the extraction of similarly nonpolar organic analytes.[12] Furthermore, as the molecular weight of a given compound and its boiling point increases, the kinetics of extraction decrease concurrently.[5,11,13] Hence the use of a thinner, 7 µm, PDMS coating is regarded preferential for SVOCs as it is more likely for equilibrium to be achieved with shorter sampling times, allowing for the ability to perform a simpler equilibrium-based calibration technique.[5,11,14] However, pure PDMS coatings are not without their downsides. For starters, their nonpolar nature makes them inappropriate for the sampling of more polar analytes such as short chain alcohols and carbonyl compounds.[15] For these analytes, the choice of a more polar, PEG coating would be ideal.[5,15]

Much like PDMS, PEG coatings are prepared by cross-linking of a relatively low molecular weight prepolymer that gives a liquid-like sorbent where absorption is the predominant extraction mechanism. As such, these sorbents exhibit linear analyte uptake with increasing analyte concentration. However, exposing these sorbents to exceedingly high levels of high-affinity VOCs

(mid to high ppm level) can eventually cause the sorbents to swell and break off of the solid support. Despite their ease of use, these absorptive liquid coatings just do not offer the sensitivity and sorbent strength demonstrated by solid sorbent particles.[16–20]

The use of solid sorbent particles suspended in PDMS has been shown to vastly increase the sensitivity of SPME techniques, while their bipolar nature reduces analyte selectivity resulting in much more multipurpose coatings.[16–20] This strength stems from the general porosity of the sorbent. The poly(divinylbenzene) (DVB) particles used in commercial SPME fibre production, for instance, are normally considered to be mesoporous (20-500 Å pore diameter) with a porosity of 1.54 mL g^{-1}.[5] As such, these mid-strength particles have found a particular niche for the analysis of atmospheric SVOC compounds such as polychlorinated dibenzodioxins (PCDD's) and polycyclic aromatic hydrocarbons (PAH's), which can be commonly found in fly ash from industrial smokestacks, for example.[16] It is worth noting that DVB/PDMS fibers will still extract any analyte that has been classically analyzed using PDMS alone.[18] Furthermore, because of their bipolar nature, these fibers can also be applied for the sampling of carbonyls and other polar compounds. Although DVB/PDMS will also extract highly volatile compounds, those fibers prepared with the microporous (2-20 Å pore diameter), Carboxen (Car), activated carbon particles have been proven to be much more sensitive for this application.[5,17,18]

Indeed, the Car/PDMS fiber is currently the strongest SPME sorbent commercially available for environmental air analysis. As such, these fibers are the best choice when a given analyst only wishes to target the most volatile pollutants such as BTEX from car exhaust or trihalomethanes (THM's) emitted from chlorinated water.[17,18] However, the strength of the Carboxen sorbent has also been shown to have a considerable downside as well. When less volatile components are extracted it can prove very difficult, if not impossible, to thermally desorb them

from the carbon particle. Hence, to account for this limitation the multifunctional DVB/Car/PDMS fiber was developed.

Commonly referred to as the 'sandwich' fiber, DVB/Car/PDMS devices are prepared such that the stronger Carboxen sorbent is at the center of the fiber, protected within the DVB/PDMS layer.[5] This arrangement allows the higher-affinity SVOC compounds to be trapped by the weaker DVB sorbent well before it ever reaches the activated carbon at the center of the fiber. Furthermore, any volatile component which would typically be weakly extracted by DVB can permeate through the overcoating and instead be adsorbed by Carboxen. Hence, the sandwich fiber is particularly useful when broad-spectrum untargeted analysis is performed.[19,20] Such a coating would be very useful in applications where an analyst wishes to screen a range of compounds in a given sample in a single analytical run.

In terms of physical characteristics, all the currently available SPME architectures, the fiber-based geometry is by far the most popular configuration worldwide. Before use, these fibers are typically placed within a plunger-operated fiber holder as shown in Figure 1.1. This assembly is used to move the delicate fiber coating (A) in and out of the protective stainless steel needle (B). As such, it is always important to keep the sorbent coating withdrawn into the needle unless sampling or desorption in a GC injector is being performed. Furthermore, the fiber should always be kept deep inside the protective needle anytime the assembly is pushed through a barrier such as the septum of a GC inlet, only exposing the fiber for thermal desorption after the septum has been pierced. Although this clarification may seem obvious, it represents one of the most common errors performed by first time SPME users.

Commercial SPME fibers for GC applications are generally 2 cm long and possess a coating thickness of anywhere between 7 and 100 µm (more commonly between 60 and 100 µm).

Using a 65 µm thick DVB/PDMS fiber on a 0.120 mm diameter fused silica core as an example, we obtain a sorbent volume of 0.880 mm^3 and a cylindrical surface area of 15.6 mm^2. These factors become exceedingly important in determining the sensitivity of a given SPME technique depending on whether the extraction is in the equilibrium regime or kinetic regime, respectively.

Table 1.1 Analyte dependant selection of SPME polymeric sorbents for GC amenable sampling.

Sorbent material (coating thickness)	Analyte Properties	Example Analyte(s)	Extraction Mode	Comments	Refs
PDMS (100 µm)	Non-polar, highly volatile	BTEX (mid, high concentration)	Absorption	Most commonly used, poor sensitivity	[5,12]
PDMS (7 µm)	Non-polar, semi-volatile	PCB's, PAH's (high conc.)	Absorption	Faster equilibrium, lowest sensitivity	[5,14]
PEG (60 µm)	Polar, broad volatility	Alcohols, carbonyls	Absorption	More common for aqueous sampling	[5,15]
DVB/PDMS (65 µm)	Bipolar semi-volatile	PCB's, PCDD's	Adsorption	Best for SVOC's	[5,16]
Car/PDMS (75 µm)	Bipolar Highly volatile	THM's, BTEX (trace concentrations)	Adsorption	Strongest sorbent, tough to desorb SVOC's	[5,17,18]
DVB/Car/PDMS (50 µm/30 µm)	Bipolar, broad volatility	Untargeted, broad range screening	Adsorption	Multipurpose	[5,19,20]

Abbreviations: 1: PDMS- polydimethylsiloxane, 2: PEG- poly(ethylene glycol), 3: DVB- divinylbenzene, 4: Car- Carboxen, 5 BTEX- benzene, toluene, ethylbenzene, xylene 6: PCB's- polychlorinated biphenyls, 7: PAH's polycyclic aromatic hydrocarbons, 8; PCDD's- polychlorinated dibenzodioxins, 9; THM's- trihalomethanes

1.3 On-site calibration using SPME

Although calibration is not required for performing untargeted, qualitative, screening analyses of atmospheric air, choosing the proper calibration method becomes imperative if one wishes to perform quantitation. Furthermore, for on-site sampling, it becomes increasingly difficult, or impossible, to control the environmental conditions such as air, temperature, and velocity. In these cases, it is always necessary to measure these values such that they can be replicated back in the lab if classical calibration approaches are to be used. Furthermore, many important constants such as the fiber/sample distribution coefficient and the analyte static air diffusion coefficient are dependent on these values.[5,10,11] Moreover, extraction time and fiber desorption time must be optimized prior to going on-site so as to ensure the best analytical signal possible.[5,21] SPME techniques can be calibrated using many classical approaches including external calibration, internal calibration, and internal standardization.[22] However, with the exception of external calibration, none of these methods can be used for on-site air monitoring. Interestingly enough, recent advancements in standard gas/headspace generation have made it increasingly easy to perform targeted quantitation of atmospheric pollutants using external calibrants.[3,23] As previously discussed, equilibrium-based calibration can be very easily performed for any target analyte that achieves equilibrium in a reasonable time.[22] However, this may prove impractical for large PAHs and other heavy analytes that may require in excess of an hour to reach equilibrium. For these compounds, it would indeed be preferential to use one of the available diffusion or kinetic-based calibration methods.[22]

1.3.1 Interface Model Based on Diffusive Laws

The interface model is an example of a diffusion-based calibration technique (Figure 1.1). This method relies on careful regulation of the boundary layer thickness so as to control the

extraction kinetics. As such, it is important that the extraction mode remains in the zero sink, linear regime of the equilibrium profile and that both the air temperature and velocity are constant and known.[5,10,22] Furthermore, the diffusion coefficient of the target analyte at the given temperature must be known or derived empirically. If these three values are known, the interface model can be employed using Eq. 1.5, where C_s is the sample concentration, n is the absolute amount of analyte extracted, B_3 is the geometric factor of a cylinder which has a value of 3, D_s is the sample diffusion coefficient, A is the surface area of the coating, t is the sampling time and d is the boundary layer thickness which is itself described by Eq. 1.6. Equation 1.6 further shows that the boundary layer thickness is determined by dividing the fiber diameter, d, by the Reynolds number, Re, and the Schmidt number, Sc. These constants are further described by Eq.'s 1.7 and 1.8 respectively with u_s representing the linear velocity of the sampled air and v signifying kinematic viscosity of the matrix: [5,22]

$$C_s = \frac{n\delta}{B_3 D_s A t} \qquad \text{Eq. 1.5}$$

$$\delta = 9.52 \frac{d}{Re^{0.62} Sc^{0.38}} \qquad \text{Eq. 1.6}$$

$$Re = 2\frac{u_s d}{v} \qquad \text{Eq. 1.7}$$

$$Sc = \frac{v}{D_s} \qquad \text{Eq. 1.8}$$

Fortunately, what the interface modal lacks in mathematical simplicity is mitigated by a simplified analytical process that even allows the user to perform quantitation of an untargeted compound after it has been identified. This is because, much like equilibrium calibration, diffusive techniques remain calibration curve-free such that if a nanogram versus response relationship is known for the compound, and the prerequisite factors have been measured, quantitation may still be performed.

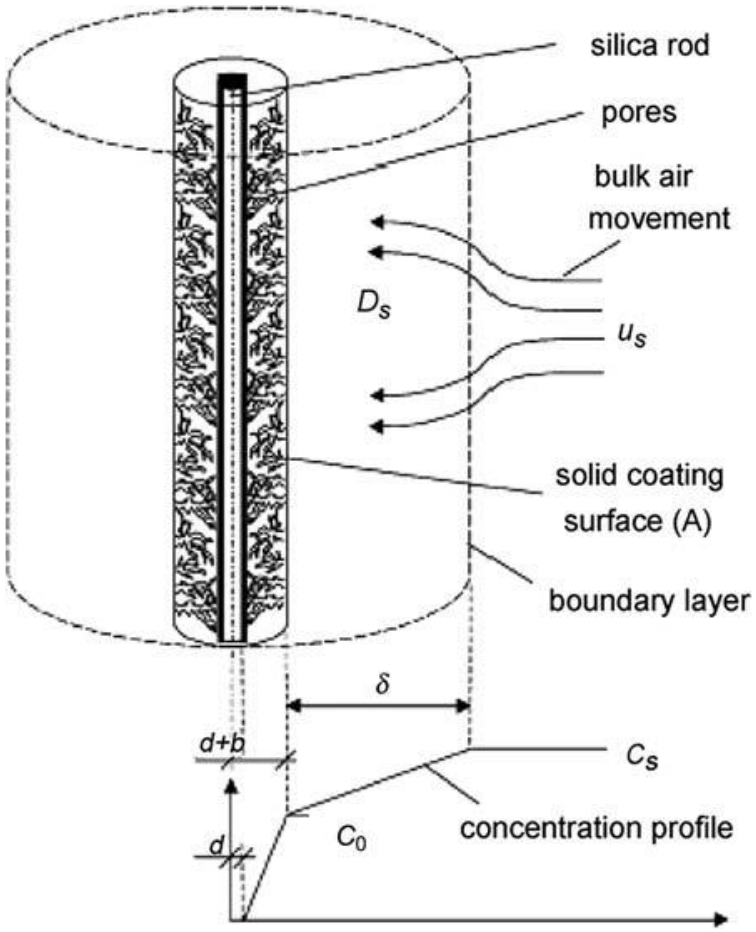

Figure 1.1 Schematic representation of the interface model of solid phase microextraction with a porous fiber coating highlighting the presence and importance of the gas flow rate-dependent boundary layer thickness d. As reproduced with permission from Ref. [23] Figure 5, p. 190.

1.3.2 Kinetic calibration techniques

Kinetic calibration can be performed in one of two ways. The first of these involves pre-loading a known amount of a deuterated analog of the target compound onto the fiber prior to performing an analytical extraction. Then, when the fiber is exposed to the sample matrix, this deuterated analogue will desorb from the fiber in an inverse pattern to that of the corresponding uptake of the target analyte as described by Eq. 1.9 where q_0 is the initial amount of standard loaded, q is the amount of standard remaining after the extraction, n_e is the amount of analyte that would be extracted at equilibrium and n is the actual amount of analyte extracted .[5,22] This equation

can be further rearranged to generate Eq. 1.10 thus calculating the concentration of the target analyte: [5,22]

$$\frac{n}{n_e} + \frac{q}{q_0} = 1 \qquad \text{Eq. 1.9}$$

$$C_0 = \frac{q_0 n}{K_{fs} V_f (q_0 - q)} \qquad \text{Eq. 1.10}$$

Despite the ease of use of Eq. 1.10, the method is rather impractical overall when actually employed. Firstly, it requires a standard be preloaded onto the fiber before the extraction; hence, it is inappropriate for untargeted analysis. Secondly, deuterated standards are exceedingly expensive and their availability is limited to a select list of compounds.

To avoid this limitation, standard-free kinetic calibration may be used instead.[5,22,24] In this method two separate extractions with times t_1 and t_2, in the linear regime are used to estimate the amount of analyte that would be extracted at equilibrium, n_e, by comparing the actual extracted amounts, n_1 and n_2, giving rise to Eq. 1.11: [5,22,24]

$$\frac{t_2}{t_1} \ln\left(1 - \frac{n_1}{n_e}\right) = \ln\left(1 - \frac{n_2}{n_e}\right) \qquad \text{Eq. 1.11}$$

Solving for n_e in this expression is exceedingly complex; however, Ouyang et al. who originally conceptualized Eq. 1.11 have suggested a simpler way to solve it. By arranging it into Eq. 1.12 with the addition of the surrogate constant Y, it is possible to then use an Excel table to determine n_e. With all other variables known from the experiment, one can prepare a table of estimated values for n_e substituting them into the Eq. 1.12 to solve for Y. At whatever point Y is found to be zero will indicate the true value for n_e.[24] Alternatively it could be possible to just use Excel's goal seek function to determine n_e when Y is equal to 0. Furthermore, once n_e has been calculated it just needs to be substituted back into Eq. 1.3 to calculate the sample concentration.[5,22,24]

$$Y = \frac{t_2}{t_1}\ln\left(1 - \frac{n_1}{n_e}\right) - \ln\left(1 - \frac{n_2}{n_e}\right) \qquad \text{Eq. 1.12}$$

Indeed, the use of standard-free kinetic calibration remains relatively underutilized in the literature. Not only is no deuterated standard required, there is an additional benefit that the only required constant is the fiber sample partitioning coefficient which can always be calculated experimentally if it is not already available in the literature. However, as previously mentioned this technique is limited by the requirement of ensuring the rate of analyte uptake remains in the linear, zero-sink regime of the extraction profile and requires twice the number of experiments to establish n_1 and n_2 at t_1 and t_2 respectively. It is important to also note that these calibration techniques not only apply to the standard fiber-based morphology of SPME but can indeed be utilized with various other configurations.

1.4 SPME samplers for varying environmental matrices

Beyond the standard fiber morphology, SPME technologies have continued to develop and change to address specific challenges imposed by the varying samples and locations targeted in the environment. When one considers environmental pollution and their related sampling matrices, the vastness of potential applications can initially appear daunting. Coming from all three of the earthly phases of matter, most pollution studies can be categorized as either air, water, or soil based, with further subcategorizations possible beyond that initial classification. Although by no means the panacea of sample prep, various SPME-based solutions to address each of these categories have been explored in recent years. Technologies such as needle trap devices (NTDs) for air sampling, cold fiber SPME for determination of soil contaminants, and GC-TFME for the ultra-trace detection of pollutants in surface waters[25] and metropolitan air[26] are just a select few of such specialized morphologies.[27–29] Like any technique, however, these samplers still require

routine quality control and an initial validation. As such, the repeatable delivery of standards tailored for SPME-based extractions that can be performed on-site is also necessary.

1.4.1 Needle trap devices for air analysis

Gaseous air samples lend themselves well to being sampled directly with standard SPME fibers, as the diffusion coefficients of most volatile organic compounds (VOC's) are high enough to allow for appreciable levels of extraction within short periods of time.[5,30,31] However, issues can arise once the analyst wishes to target organic compounds that are only semi-volatile (SVOC) in nature, as SVOCs have a tendency to bind to airborne particulate matter or aerosol-type particles, making them unavailable to SPME fibers which, as previously described, are only sensitive to the free analyte fraction.[5,32,33] Furthermore, the characterization of the environmental fate of a given compound, i.e., the percentage of a given compound that is particulate-bound, can yield additional information regarding the system under study.[12,34] With this application in mind, further developments in needle trap devices have been an ongoing endeavor to further assist in the characterization of environmental air.

As alluded to, one of the primary advantages of these sorbent packed needles lies in their ability to act as a filter and trap both the free form and particulate bound portion of small organic molecules in a given gaseous sample allowing for the determination of total analyte concentration. As with most filtration sampling methodologies needle trap based extractions are an exhaustive sampling technique and function by use of various sorbents which have been packed into the bore of a blunt tip needle.[32,35–37] In-line with what is expected with any exhaustive extraction technology, calibration with NTD methodologies is rather simple with the amount extracted being directly related to the sample concentration multiplied by the volume extracted (Eq. 1.13).

$$C_o = \frac{n}{V_s} \qquad \text{Eq. 1.13}$$

In terms of sampler design, there have been multiple formats of NTD needles proposed over the years.[27,32] The simplest format involved packing the tip of an open bore 22 gauge luer lock needle with appropriate sorbent particles (Carboxen, Tenax, DVB, etc…) which could then be attached to a gas-tight syringe or pump to draw gaseous sample through the needle tip.[27,32] However, this design was limiting during GC desorption as a supplementary desorption gas had to be manually applied via a gas-tight syringe at the needle hub during for appropriate desorption of the analytes. To overcome this limitation, modern needle trap devices are designed to seat directly into a specialized narrow-neck liner in the GC injector and instead force carrier gas through a small side hole which has been drilled above the NTD sorbent bed as to redirect instrument carrier gas to assist with analyte desorption.[27,32,38] Such needles include the 22 gauge extended tip NTD for benchtop GC instrumentation, shown in Figure 1.2, and a schematic of the 19-gauge blunt tip NTD (Figure 1.3) used in conjunction with the Tridion-9 portable GC-MS.

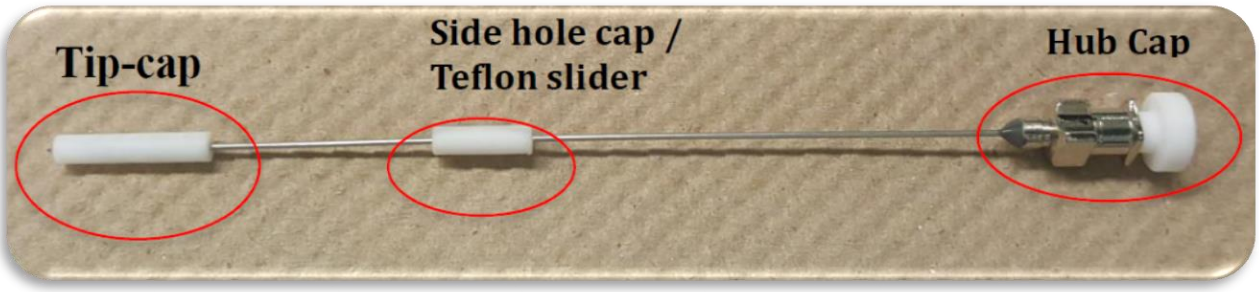

Figure 1.2: 22 gauge extended tip needle trap with appropriate PTFE caps.

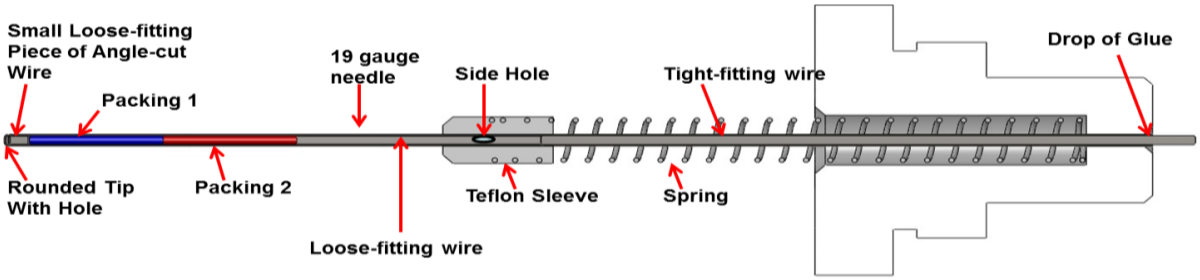

Figure 1.3: Schematic of 19 gauge blunt tip NTD used with Tridion-9 portable GC/MS instrumentation. (Courtesy: Torion Technologies of Perkin Elmer Inc. American Fork UT)

When combined with conventional open bed SPME devices which are themselves only sensitive to the free analyte fraction, it becomes possible to determine the particulate bound fraction of a given analyte by subtracting the free concentration determined by an SPME fiber from the total concentration determined via NTD. In an interesting exploration of this principle, Cheng et al. combined the use of 100 µm PDMS SPME fibers with a DVB packed NTD to determine the effectiveness of repellents emitted via mosquito coils,[12] and in the following work, from electronic vaporization mosquito mats.[34] Particularly in the mosquito mat study, a clear trend could be seen, with the 100 to 120 mesh DVB NTD extracting a much greater amount of the semi-volatile repellants than that extracted by the PDMS SPME design.[34] However, despite this novel advancement, this aforementioned study failed to fully explore the advantages of the approach by calibrating and comparing the free and particulate bound concentrations of the extracted analytes under study. Conversely, Reyes-Garces et al. better explored this advantage by comparing the free vs. total levels of alpha-pinene emissions from a pine branch on-site, which were found to be 3.3 and 7.8 ng mL $^{-1}$, respectively, using an SPME and NTD-enabled portable GC-IMS instrument.[39] This vast concentration difference is to be expected, as the mid-volatility alpha-pinene, with a boiling point of 155 ^{o}C, would much prefer to remain in the particulate-bound fraction at 23 ^{o}C.

In addition to these novel free versus total studies, NTD technologies have also been used on their own for the simple quantification of total pollutants in environmental air. In terms of more recent examples, NTDs employing a novel silica aerogel have also been used for the quantification of formaldehyde from indoor and outdoor air,[40] and chlorobenzenes from a standard air sample.[41] A bondesil C18 packed NTD was applied to develop a quantitative and fully automated headspace method for the determination of nine multi-residue musks from real wastewater treatment facility samples.[42] A high-resolution qualitative comparison of different marine diesel fuel emissions was

accomplished by use of a tri-bed PDMS, Carbopack B, and Carboxen 1000 NTD, introduced into a unique GC/REMPI/SPI-TOFMS, which is a form of NTD-GC enabled photoionization time-of-flight mass spectrometry.[43] A Silica composite carbon nanotube sorbent was applied to both SPME fibers and NTDs and compared in terms of MLODs vs DVB/PDMS analogues for the in-laboratory determination of perchloroethylene in air.[44] Finally, an entirely new approach using smaller NTDs to pre-concentrate large volume air samples, such as those from 3.5" sorbent tubes, was validated while incorporating the use of a hand-portable thermal desorption module.[45] This module essentially transfers analytes from 3.5" sorbent tubes onto a 19-gauge NTD, which can then be directly introduced to a standard GC injector. This methodology may have great implications in terms of future on-site analytical approaches; to date, it has already been coupled to portable GC-MS instrumentation and to the much more sensitive GC-TFME samplers.[1]

1.4.2 The thin film microextraction morphology of SPME

Due to their inherent larger sizes, the use of high volume, high surface area TF-SPME samplers has been shown to drastically decrease the limits of quantitation approachable for environmental applications.[1,25] In essence, these TFME devices are thin sheets of extraction phase ranging in the 10's to 100's of micrometers in thickness allowing for a vastly larger surface area to perform extraction. In particular, when extractions are performed in the pre-equilibrium regime of the extraction time profile, such as the norm for on-site samplings, the increase in surface area of the sorbent directly correlates to an increase in the amount of analyte extracted per unit time (Eq. 1.4).[5,10,11] Furthermore, if equilibrium is sought after, the added increase in total sorbent volume will also directly correlate to the amount extracted (Eq. 1.2, Eq. 1.3). Finally, so long as the extraction phase thickness denoted as (b-a) in Eq. 1.14, is kept constant between polymeric

similar SPME devices, the equilibrium time, t_{eq}, will remain unaffected. All these factors combined result in TF-SPME or TFME for short, being a much more sensitive SPME morphology.

$$t_{eq} = 3\delta K_{fs}(b-a)/D_s \qquad \text{Eq. 1.14}$$

Being an extension of solid phase microextraction, TFME shares many congruencies with traditional SPME fibers. A PDMS polymeric coating remains a popular choice for the development of thin film membranes.[29,46] Also, much like SPME fibers, many combined coatings such as CAR/PDMS, and DVB/PDMS can be applied to construct thin film membranes.[26,29,47] It is important to note that when these combined phases are prepared, the PDMS serves as a glue to hold the solid Carboxen or DVB particles in place. Furthermore, the fundamental sorptive mechanisms which govern fiber based SPME extractions still apply to the thin film membranes morphology. Consequently, the mathematical relationships used to calibrate traditional SPME hold true for TFME with a few exceptions. Such exceptions would include calibration techniques that employ fiber geometry.[29,48] However, like any technique, the introduction of TFME has not been without its challenges; particularly their large size has made them difficult to directly introduce into a GC thermal desorption.

1.4.2.1 Coupling of TFME with GC thermal desorption systems

One of the initial challenges of GC based TFME was finding a safe and reproducible method to desorb thin film membranes onto the instruments injector. One of the most rudimentary desorption methods employed involved having an analyst roll up the membrane and then place it in a standard split/splitless liquid injection liner that could then be manually inserted into an initially cooled GC injector port.[5,46] As a recent example this technique was used by Engler *et al.* in order to determine xenoestrogen porewater concentrations from soil samples.[48] After extraction, the pure PDMS membranes were rolled up and placed inside of a single tapper, liquid injection

liner. This liner was then manually placed into a GC injector that had been partially cooled to 220 ^{o}C and then immediately heated to 270 ^{o}C for xenoestrogen desorption.[48] Although the researchers were able to demonstrate reasonable analytical figures of merit for the selected SVOC analyte's with linear calibrations in and around one order of magnitude, this relatively cheap desorption method suffers from some major limitations. Firstly, it would be impossible to analyze any VVOC's or VOC's as such compounds would not reconstitute at the head of the GC column and would exhibit very broad desorption peaks and hence chromatographic peaks when using such a desorption method. Secondly, the researchers were unable to reuse their membranes likely because of high-temperature oxidation of the PDMS extraction phase. Finally, opening a GC injector at such a high temperature is ill-advised from any column manufacturer as this is well known to cause oxidation of the column's stationary phase, in addition to that of the membrane coating.

A more practical method to desorb such a membrane would be to use a secondary desorption unit mounted onto the GC-MS system. As such in their respective publications Jiang *et. al.* and Riazi Kermani *et al.* employed a GERSTEL thermal desorption unit – cooling injection system (TDU-CIS4) topped Agilent 6890-5973n GC/MS equipped with an MPS-2 autosampler to facilitate membrane desorption. Shown in Figure 1.4 below, this commercially available unit functions by employing both internally heated and cooled zones to safely and sharply move all analyte's from the TFME membrane to the GC column. This system works by first sealing the TFME membranes into the TDU module at near room temperature followed by helium purging as to avoid oxidation of the extraction phase or GC-column. With the CIS cryogenically cooled by liquid nitrogen (ca. -50 °C to -150 °C) the TDU is then heated to an appropriate TFME desorption temperature (200 ^{o}C to 300 ^{o}C) moving analytes from the TFME membrane to the cooled CIS where they are condensed and pre-concentrated prior to injection onto the GC/MS. Finally, to

facilitate sharp GC peaks, the CIS is then flash heated to temperatures approaching 275 °C moving analytes to the GC column.[26,47]

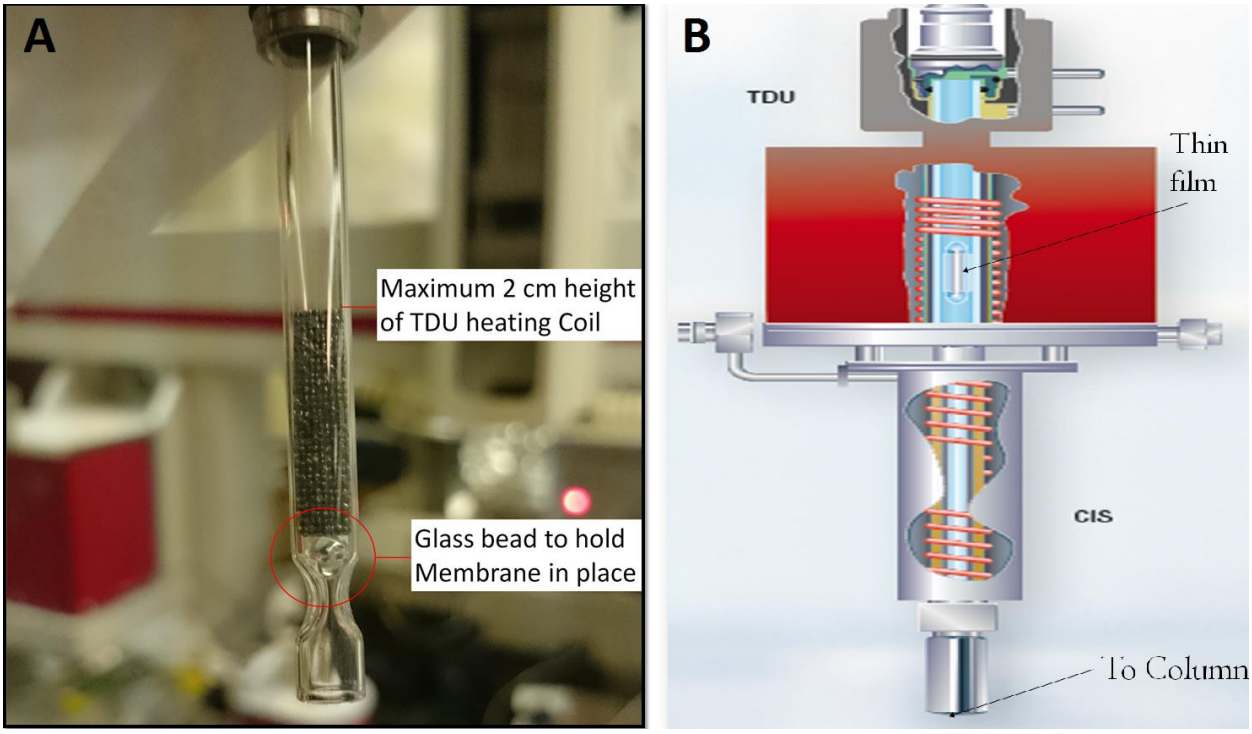

Figure 1.4: Coupling of TFME devices to benchtop GC/MS instrumentation using a GERSTEL TDU-CIS4 desorption systems showing, A) insertion of a DVB/PDMS carbon mesh supported membrane in a TDU tube, and, B) schematic of the TDU-CIS4 injection system. (acquired from Gerstel website)

1.4.2.2 Prior methodologies for the preparation of thin film membranes

In terms of TFME fabrication, the first and simplest membranes were prepared by simply cutting appropriately sized devices out of 127 µm or 254 µm thick sheets of pure PDMS.[46,49,50] Although simple, these devices were shown to perform much better than comparative pure PDMS fibers[49] and PDMS sorptive stir bars.[50] However, the lack of sorbent particles made such morphologies impractical for pushing down detection limits much more than particle loaded SPME membranes. As such in-house polymerization methods were required to make polymer loaded TFME membranes.[26,47]

Initially, Jiang *et al.* explored the fabrication of support-less, PDMS membranes by using Slygard 184 (Dow Corning Co.) PDMS pre-polymer mixture.[26] The components of this kit were mixed at a 10/100 w/w catalyst/PDMS base ratio and then spread onto a non-stick sheet Teflon using an Elometer 4340 bar coater to prepare TFME membranes approximately 60 µm – 100 µm.[51] The spread pre-polymer mixture was then heated under vacuum at 80 ^{o}C for 5 hours and then at 120 ^{o}C for 3 hours as to crosslink the PDMS.[7] To further improve these membrane Jiang then began evaluating the addition of 3-5 µm DVB particles by mixing 10:100, 20:100, and 30:100 w:w DVB:PDMS fractions for comparison. From this study, an optimum mixture was then determined to be 20:100 w:w DVB:PDMS (16.67% DVB), which gave the highest signal without compromising the physical characteristics of the membrane.[26,51] Membranes prepared using pure PDMS and the optimized DVB/PDMS mixture were then qualitative compared to a commercial DVB/PDMS SPME fiber for the extraction of alkyl-benzene compounds in air with, unsurprisingly, the DVB/PDMS TFME membrane giving the highest signal for the chosen analytes. Finally, as a proof of concept, these DVB/PDMS TFME membranes were then successfully applied for the quantitation of benzene and naphthalene emitted from car exhaust within Waterloo city streets.[26]

Moving in a slightly different direction Riazi-Kermani *et al.* explored the use of fiberglass fabric as a solid support for the TFME device.[47] To accomplish this, undisclosed proportions of DVB/PDMS and CAR/PDMS were prepared in a dichloromethane slurry. After mixing, the catalyst was added to initiate the cross-linking reaction of the PDMS and approximately 1.5 mL of this slurry was then deposited onto a pre-silanized sheet of fiberglass fabric which had been affixed to a spin coating wafer. The set-up was then spun at 1000-1250 rpm for 30-40 s evenly distributing the mixture throughout the fiberglass fabric which was then placed into a vacuum oven

at 80 ^{o}C for 2 hours to complete the polymerization. Final membranes were then cut in a house-like shape with dimension 2 cm x 2 cm with a 1 cm peak. Due in part to their size, these membranes were demonstrated to exhibit superb sensitivity with equilibrium extraction amounts 50-150 x greater than their respective fiber counterparts. However, it was unfortunate that there was no discussion in terms of possible siloxane background and the related signal-noise ratio regarding these membranes.

1.5 SPME use on portable GC-MS instrumentation

SPME-based techniques ultimately lend themselves well to the performance of entirely on-site environmental analyses. However, in order to accomplish such a feat, appropriate field portable instrumentation must also be available, as well as be as hand-portable as SPME samplers. For adequate performance during in situ analysis, a field instrument must be compact and lightweight, with low power consumption so as to allow for battery operation.[52–54] The instrument and accompanying SPME device should also be durable enough to withstand both transportation and the operating environment.[53] An additional caveat is that many on-site end-users are likely to be non-technical in nature; hence, the entirety of the analytical process should be easy to perform. Such simplicity is essential in security applications, where the user is unlikely to have any formal training in analytical chemistry.[52,54]

Early portable instruments such as the vehicle portable, SRI developed GC-FID and GC-PID instruments have been in use for over 15 years.[30] Although older compared to more recently developed portable GC-MS instruments, these SRI systems highlight some of the earliest developments towards completely on-site SPME approaches and were able to achieve detection limits for BTEX in air ranging from 1-3 ppb with %RSDs below 5%, using standard 65 µm DVB/PDMS coatings.[30] Despite a high degree of quantitative reliability, the SRI GC instruments

are not without limitations. Without a mass spectrometer, it can be difficult to confidently determine the identity of unknown compounds from a given sample by use of GC retention indices (RTI) alone. Besides, the SRI GCs are also quite large, susceptible to moisture, and can only be considered portable if on a handcart or when operated out of the back of a vehicle.[30]

However, recent technological advancements have allowed for the development of low power, miniaturized mass analyzers, which have been successfully coupled with high speed, low thermal mass gas chromatography (GC) systems.[52–55] By miniaturizing the mass analyzer, the size and power consumption of the MS vacuum system can also be minimized. Maintaining an acceptable degree of quantitative ability, these systems are now capable of separating and identifying a large degree of unknown chemical compounds while operating solely on battery power.[56] When ruggedized and combined with field portable SPME devices, such portable gas chromatography-mass spectroscopy (GC-MS) systems are able to meet all of the aforementioned qualifications, enabling their suitability for true in situ chemical analysis.

A fairly comprehensive review entailing various current miniature mass analyzers covering a broad range of sample introduction interfaces was just recently published in 2016.[57] However, on-site instrumentation is a continuingly advancing field, especially in terms of recent environmental approaches. In terms of solid sample analysis, one such application utilized a 100 μm PDMS fiber for the on-site determination of PCBs from soil.[58] However, without cold-fiber techniques, an inorganic modifier consisting of $KMnO_4$ and H_2SO_4 needed to be added to release analytes from the soil matrix. Furthermore, in order to facilitate quantitative results, Zhang et al. utilized EPA method 8082, which compares the mass spectral peak areas of the unknown PCBs found in soil to that of certified Arochlor standards. Although the portable SPME-GC/MS methodology was found to not impart the same repeatability as that achieved by the comparable

benchtop methodology, it still served as a good semi-quantitative means to quickly identify PCB-contaminated soil.[58] In line with the forensic capabilities that many portable GC/MS instruments were initially designed for, Visotin et al. were able to employ such instrumentation with a 65 µm DVB/PDMS SPME fiber to accurately identify 38 of the 49 ignitable liquid residues in simulated arson samples in firefighting studies.[59] Although only qualitative in nature, such studies represent how approachable such methods may be to non-technical end-users.

1.6 Thesis objective

The general objective of the thesis is to further develop, validate and apply various novel SPME-based samplers for the conduction of entirely on-site environmental analysis. In particular, devices were designed to improve the sensitivity and reliability of portable GC-MS instrumentation for on-site environmental applications

The first goal was to develop an improved manner for the repeatable delivery of quality control standards as to ensure the reliable operation of a portable GC-MS instrument. To accomplish this requirement, a novel standard gas generating vial which comprised of a multi-component sorbent was developed and validated to be portable while giving repeatable extractions of volatile McReynolds standards, even after hundreds of uses. These vials were then further validated for the delivery of a pentaflurorphenyl hydrazine (PFPH) derivatization agent for the on-fiber derivatization of aldehydes. This PFPH vial was then applied on-site with SPME, NTD and the portable GC/MS instrument for the on-site derivatization and determination of free and total formaldehyde concentration from car exhaust.

The primary goal of the thesis was the development, validation, and application of an improved TFME membrane for the determination of anthropogenic pollutants in surface waters. As such, a novel carbon mesh supported TF-SPME device comprising of a PDMS glue and various

sorbent particles are presented herein. These membranes were demonstrated to vastly decrease the background siloxane bleed exhibited in the previous TFME designs while giving comparable extraction efficiencies. Furthermore, coupling these membranes with portable GC/MS instrumentation was shown to give method limits of quantitation (MLOQ's) for multi-residue pesticides, similar to that observed with conventional sample preparation used in conjunction with traditional benchtop GC/MS instrumentation.

As a final side project, the concept of designing novel SPME devices for the sampling of extreme environments was taken to its fullest by the development of a self-sealing, coated bolt, SPME device. These self-sealing samplers were shown to stabilize and maintain extracted analytes on their coated surface in ambient conditions allowing for unprotected transportation to and from distant, and harsh environments. Furthermore, to attest to their robustness, these samplers were successfully applied for the direct sampling of deep oceanic hydrothermal vents via a submersible remotely operable vehicle (ROV). Although these HPLC based samplers are not the primary focus of this thesis, the work remains a prime example of just how useful proper sampler design can be in addressing unique requirements imposed by varying natural sampling environments.

Chapter 2 Development and validation of a field portable standard gas generation system for the on-site delivery of standard analyte compounds

Preamble

The materials in this chapter have been published as research article: Jonathan Grandy, German Augusto Gómez-Ríos, Janusz Pawliszyn; Development of a standard gas generating vial comprised of a silicone oil–polystyrene/divinylbenzene composite sorbent; *J. Chrom, A,* **2015**, 1410, pp 1-8 Materials for all sections of this current Chapter are reprinted from this research article with the permission from the Journal of Chromatography A of Elsevier Publishing. (DOI: https://doi.org/10.1016/j.chroma.2015.07.063)

2.1 Introduction

Since its introduction in 1989, solid phase microextraction (SPME) has been well accepted by the analytical chemistry community due to its miniaturized format, ability for high throughput analysis, minimal need for organic solvent,[5,6,11] and combination of sampling and sample preparation into one easy to perform step, which has revealed SPME to be an ideal technique for on-site chemical analysis.[60–63] One issue presented, however, is that environmental factors such as temperature, and air/water velocity can be very difficult to control. Since SPME is an equilibrium based extraction technique driven by diffusion, uncontrollable temperatures, and fluid velocities can have a major impact on the amount of analyte extracted, as the distribution constant, K_{fs}, and the diffusion rate across the fiber boundary layer are, respectively, dependent on these factors.[62–65] These effects render many classical SPME calibration techniques, such as equilibrium extraction and in-lab external calibration, impractical for on-site analysis.[5,10] To address these issues, diffusion-based calibration methods such as the interface model have been proposed, allowing

SPME calibration to be performed while accounting for measured fluid velocity and temperature.[5,22,66] Nonetheless, these techniques are susceptible to fluctuations in these factors and do not account for matrix effects in complex samples. In such scenarios, it may be preferential to perform a kinetic type calibration, where an internal standard is loaded onto the fiber prior to performing an extraction from the sample matrix.[11,23,64–69] Desorption of this standard will then occur as sampling takes place. The use of internal standards also brings the advantage of correcting for potential signal drifts incurred by field portable GC–MS instruments.[70]

In order to effectively perform such calibrations on-site, one must be able to deliver standard to the fiber in a highly reproducible manner with a portable standard source. It is also essential that the amount of standard loaded is representative of the analyte concentration found in the sampling environment.[71] Previous efforts by Koziel *et al.* were able to demonstrate that a standard gas of VOC's could be generated in-lab by placing neat standards into a series of PTFE permeation tubes that were then placed into an enclosed gaseous flow through system.[72] Although this system was found to be appropriate for SPME and needle trap sampling it is inappropriate for onsite use due to size. Wang *et al.* demonstrated that even when extremely short extraction times were used, a very large amount of standard are extracted onto the fiber if headspace extraction of pure standard spiked into a vial was performed.[71] Such quick extraction times are also difficult to perform repeatedly when manual injection is used on-site. Spiking standards into a polydimethylsiloxane (PDMS) membrane or Tenax particles was also shown to generate too great of a headspace concentration to be useful. It was subsequently found that an appropriate standard gas generating vial could be produced by spiking a few milligrams of the standard into a hydrocarbon-based, ultra-low volatility mechanical pump-oil.[67,71] Furthermore Xie *et al.* were also able to demonstrate that an easy-to-use multiple standard gas generating system could be prepared

by spiking nano-liters of pure standard onto a solid PDMS powder.[70] These PDMS based vials were shown to exhibit acceptable intra-vial repeatability, as demonstrated by percent relative standard deviations (%RSD's) of about 4.5% after 114 headspace extractions were performed for 30 seconds using a 100 µm PDMS fiber. However, PDMS vials were still found to generate too high of a headspace concentration for trace applications, as several hundreds of nanograms of standards were still extracted. Additionally, where such small quantities, in the nanoliters, of the more volatile standards were spiked, it would be very difficult to produce multiple vials in a reproducible manner. Concurrently, another design was proposed by Gómez-Ríos *et al.*, who addressed these major shortcomings by spiking a couple of microliters of pure standard into a hydrocarbon pump-oil solution, which was then mixed with PS/DVB particles to produce a highly reusable and durable standard gas generating vial.[23] In this study, it was demonstrated that these vials were highly repeatable, showing that intra-vial RSD's were less than 4% for all McReynolds probes[73] after 160 extractions were performed for 1 min, using the strongly sorbing, 50/30 µm DVB/CAR/PDMS SPME fiber. Furthermore, it was demonstrated that different vials prepared from the same batch of pump oil were statistically identical at a 95% level of confidence.[23]

In this chapter, a significant enhancement of the previous standard gas generation system was achieved by using a silicone based, ultra-low volatility diffusion pump fluid. Similar to the previous design, the oil was first spiked with pure standards and then mixed with PS/DVB resin particles.[23] The use of silicone oil in combination with the PS/DVB particles proved to better retain the standards. Consequently, a lower headspace concentration of the standard was obtained, and a smaller fraction of the analytes was removed per extraction. Hence, a lesser extraction of standard resulted in a vial that depleted slower, giving a standard gas generating vial that remained

repeatable over a greater number of extractions. Additionally, better precision of the amount loaded was obtained when longer loading times were used.

2.2 Materials, instrumentation, and experimental methods

2.2.1 Materials and reagents

Benzene, 2-pentanone, pyridine, 1-nitropropane, 1-pentanol, and n-octane standards, as well as the styrene/divinylbenzene(PS/DVB) particles (Amberlite®XAD-4)[74] were purchased from Sigma–Aldrich (Mississauga, ON, Canada). Varian general-purpose mechanical pump oil was supplied by Varian Vacuum Technologies (Lexington, MA). KJLC 704 silicone pump fluid (tetramethyl tetraphenyl trisiloxane) was ordered from Kurt J. Lesker Company (Toronto, ON, Canada). 20 mL screw top vials and caps with 20 mm PTFE/silicone septa were purchased from Canada Life Sciences (Peterborough, ON, Canada). 40 mL screwtop vials and caps with 22 mm PTFE/silicone septa and 15 mL screw top vials with PTFE Mininert® valves were purchased from Sigma–Aldrich. HPLC grade methanol was obtained from Caledon Laboratories Ltd. (Georgetown, ON, Canada). Nanopure water was obtained using a Barnstead/Thermodyne NANO-pure ultrapure water system (Dubuque, IA, USA). Ultra-high purity helium was supplied by Praxair (Kitchener, ON, Canada). The Drierite desiccant was purchased from W. A. Hammond DRIERITE Co. (Xenia, OH, USA). Hamilton brand, 10 µL microsyringes were purchased from Sigma–Aldrich. Flex-Foil® gas sampling bags were supplied by SKC (Eighty Four, PA, United States). The vial heater block was constructed by the University of Waterloo electronics shop (Waterloo, ON, Canada). 65 µm divinylbenzene/polydimethylsiloxane (DVB/PDMS) and 50/30 µm divinylbenzene/carboxen/polydimethylsiloxane (DVB/CAR/PDMS,) SPME fiber assemblies were provided by Sigma–Aldrich.

2.2.2 Instrumental analysis method (GC/FID and GC/MS)

An Agilent 6890 GC-5973 quadrupole mass spectrometer (Agilent Technologies, Mississauga, ON, Canada) was used in this study. Chromatographic separations were performed using an SLBTM-5MB (30 m × 0.25 mm × 0.25 μm) fused silica column from Sigma–Aldrich with a helium flow rate of 1 mL min^{-1}. The column temperature was initially held at 40 °C for 1 min, gradually increased to 50 °C at a rate of 5 °C min^{-1}, then to 70 °C at a rate of 6 °C min^{-1}, and then held for 0.47 min. An injector temperature of 260 °C was used to desorb the DVB/PDMS fibers. Calibration was performed using liquid injection at the same split ratio to generate a nanograms injected versus instrument response relationship curve. During analysis, the transfer line, quadrupole and ion source were set at 280 °C, 150 °C and 230 °C, respectively. Ionization was achieved using electron impact ionization mode. Full scan mode (40–250 m/z) was used for all compounds, and quantitation was achieved using extracted ion chromatograms.

Chromatographic separations on the Acme 6100 GC-FID (Young-Lin, South Korea) were performed using an RTX-WAX (30 m × 0.25 mm × 0.5 μm) fused silica column from Restek with a helium flow rate of 1.3 mL min^{-1}. The column temperature was initially held at 45 °C for 1.5 min and then raised to 145 °C at a rate of 12 °C min^{-1}, then raised to 180 °C at a rate of 35 °C min^{-1} and held there for 30 s. Desorption of the DVB/PDMS and DVB/CAR/PDMS fibers were carried out for 1 min at a temperature of 260 °C with a split setting of 3:1. Calibration was performed using liquid injection at the same split ratio. The flame ionization detector (FID) was held at a constant temperature of 300 °C with a fuel mixture consisting of 30 mL min^{-1} of hydrogen, 300 mL min^{-1} of air and 30 mL min^{-1} of helium.

2.2.3 Development and preparation of the headspace standards

2.2.3.1 Cleaning of the PS/DVB particles

As discussed by Gomez-Rios et al., care must be taken to properly clean the PS/DVB particles in order to remove naphthalene, styrene, hydrocarbon, and phthalate impurities that were reported present in such materials by Daignault *et al.*[74,75] To accomplish this, approximately 200 mL of PS/DVB particles were placed into a 1 L beaker and manually agitated with 600 mL of Nano-pure water for 2 minutes, then immediately decanted. This procedure was repeated 3 additional times. Next, the particles were mixed with 600 mL of Nano-pure water and heated gently to 50 °C for 30 minutes, then decanted a total of 4 times. Following this, the same procedure was repeated, except 400 mL of HPLC-grade methanol were used instead.

After cleaning, the PS/DVB particles were then placed on an aluminum foil covered Petri dishes and placed in a vacuum oven at 60 ºC for 24 hours, under nitrogen. This is an essential step taken to remove any remaining methanol and impurities from the particles. It is important to note that excessive heating should be avoided as to prevent the decomposition of the resin.[74] The particles were then removed from the oven and placed in a desiccator under constant nitrogen flow for at least 48 hours.

2.2.3.2 Spiking of the pump oil solution

In order to remove any potential impurities, approximately 150 mL of the hydrocarbon-based, and silicone oil pump oil solutions were placed into 2 separate 400 mL beakers with stir bars. The oil was then heated to 120 ºC and agitated at a rate of 120 rpm under constant nitrogen flow for 24 hours.[67,75] After cooling, approximately 32 g of hydrocarbon oil and 40 g of silicone pump oil were placed into 40 mL headspace vials with 0.25-inch stir bars and capped with PTFE/silicone septa. The pure standards were then spiked into the oils through the septa using a

10 μL microsyringe. For the oil comparison study, 2 μL of each standard was spiked into each of the stock oil solutions. For the inter-vial reproducibility and storage stability studies, 2 μL of benzene, 3 μL of 2-pentanone, 4 μL of 1-nitropropane, 3 μL of pyridine, 6 μL of 1-pentanol, and 6 μL of octane were spiked into the silicone oil. For the vial depletion study, 2.2 μL of benzene, 3 μL of 2-pentanone, 6 μL of 1-nitropropane, 2.5 μL of pyridine, 7.5 μL of 1-pentanol, and 5 μL of octane were spiked into the stock silicone oil. Once the standards were added, the vials were vortexed for 2 minutes, followed by replacement of the punctured septa to avoid loss of volatile analytes. These vials were then sealed with Parafilm® and mixed at 1500 rpm for 48-hours.

2.2.3.3 Preparation of the standard gas generating vials

1.500 ± 0.005 g of the previously cleaned PS/DVB particles were accurately weighed into either 20 mL or 15 mL headspace vials to be used with the PTFE septa and Mininert caps, respectively. Then, 3.000 ± 0.010 g of the hydrocarbon oil, or 3.690 ± 0.010 g of the silicone oil were accurately weighed into the vials. Given their different densities, these oil masses were chosen to ensure the same volume of oil was added to each vial, and, consequently, the same headspace volume was obtained. Additionally, adding the same volume of each oil also ensured that the same amount of the standards were present in each vial for comparison. Once the oil had been added, the vials were immediately capped and then sealed with Parafilm®. The vials were then allowed to equilibrate for at least 72 hours before being used. The vials were then labeled with a 3 character code with each character representing the pump oil used, the batch number, and vial number from a given batch, respectively (*e.g.* vial S-1-3 would be the third vial prepared from the first batch of silicone oil based vials from a given set).

Table 2.1. Preparation parameters of PS/DVB standard gas generating vials.

Parameters	**Varian oil**	**Silicone oil**
Density (g/mL)	0.87	1.07
Mass of oil to fill each 40 mL vial (g)	32.483	39.980
Volume of standard spiked into each 40 mL vial (µL)	2.0	2.0
Mass of spiked oil placed into each gas generating vial (g)	3.000	3.690
Volume of oil placed into each std gas generating vial (mL)	3.45	3.45
Volume of McReynolds placed into each vial (µL)	0.185	0.185

2.2.4 Comparison of the different pump oil matrices

To determine the superior pump oil matrix, 4 standard gas generating vials were prepared using the Varian® general purpose mechanical pump oil (hydrocarbon oil), the silicone diffusion pump oil, a hydrocarbon oil–PS/DVB mixture, and a silicone oil–PS/DVB composite mixture. In order to maintain a consistent headspace volume with the oil–PS/DVB composite vials, standard pump oil vials were prepared by placing 6 mL of the spiked oil solutions into an empty 20 mL headspace vial. The vials were then heated to 50 °C in a Gerstel agitator unit. Extractions were performed for 30 s using a 65 µm DVB/PDMS Stableflex fiber. Automated SPME injections were performed using a CTC Combi-PAL system (Zwingen, Switzerland) installed on the Agilent 6890 GC and 5973 qMS. Replicate extractions were randomized to minimize the effects of any potential signal drift of the mass analyzer.

2.2.5 Evaluation of intra-batch and inter-batch vial reproducibility

To verify the intra- and inter-batch reproducibility of the gas generating system, 2 vials from 3 different batches were randomly selected and placed into an agitated water bath at 35 °C.

Extractions were performed for 1 min using a 65 µm DVB/PDMS stableflex fiber. Manual SPME injections were carried out on a Young-Lin Acme 6100 GC-FID. GC runtimes were 11 min, with complete separation of the analytes occurring in less than 9 min. Extractions were randomized to account for potential signal drift effects.

2.2.6 Determination of long-term vial storage stability

Long-term storage stability of the standard gas generating vials was evaluated by storing vials from batch one (vials S-1-X) under 3 different sets of conditions. For the duration of the experiment, vials S-1-3 and S-1-4 were stored at ambient temperature on a bench top with exposure to light, vials S-1-5 and S-1-7 were stored at ambient temperature in a dark cupboard, while vials S-1-6 and S-1-8 were stored in a dark refrigerator kept below 5 °C. These vials were prepared using resealable Mininert® valves as to minimize potential sample losses from punctured septa after use and prolonged storage.[67,75] Analysis of the vials was performed immediately after the initial 72 h equilibration, and then after 1, 3, 6, and 10 weeks of storage. The vials were held in an agitated water bath adjusted to 36 °C.Water temperature was monitored throughout the experiment and allowed to fluctuate within ±0.2 °C. Extractions were performed for 1 min using a 65 µm DVB/PDMS stableflex fiber. Manual SPME injections were performed on a Young-Lin Acme 6100 GC-FID. Quality control analyses were also performed to detect any inter-week drift that may have occurred during the experiment. Additionally, replicate extractions were randomized to minimize the effects of any potential signal drift.

2.2.7 Assessment and modeling of the vial depletion rate

To model the vial depletion rate, 208 successive 1 min extractions were made from a single, resealable Mininert® capped standard gas generating vial using a 50/30 µm DVB/CAR/PDMS stableflex fiber. The vial temperature was precisely maintained at 35 °C using a vial block heater

developed in-house by the University of Waterloo electronics shop. Manual SPME injections were performed on a Young-Lin Acme 6100 GC-FID. GC runtimes were 11 min, with complete separation of the analytes occurring in less than 9 min. With the exception of the first 15 extractions, only 1 out of every 3 extractions was injected onto the instrument for analysis. Additionally, 28 quality control analyses were also performed throughout the experiment to identify and correct for signal drift while performing the multi-day experiment. To obtain a reliable determination of the initial amount extracted from the gas generating vial, the first 15 extractions from the vial were analyzed. Additionally, these first 15 analyses made it possible to estimate the percent RSD associated with the method while using the heater block assembly. Attaining low RSD values was essential to confidently detect a depletion of 3.5% or less.

2.3 Results and discussion

2.3.1 Comparison of the different pump oil matrices

Selection of the optimum pump oil matrix is crucial to maximize the longevity and reproducibility of the standard gas generating vial. This reproducibility is especially important in quality control applications, such as instrumental signal drift checks during multi-day analyses. For this purpose, 4 standard gas generating vials, prepared using hydrocarbon-based mechanical pump oil, silicone diffusion pump oil, a hydrocarbon oil–PS/DVB mixture, and a silicone–PS/DVB mixture, were compared.

As can be seen from Figure 2.1 results demonstrated that vials prepared using a silicone oil–PS/DVB composite as a matrix generated substantially lower headspace concentrations, indicating a higher affinity for the calibration compounds, and therefore, lower Henry constants. When compared to the hydrocarbon oil–PS/DVB vial, the relative amounts extracted from the silicone oil–PS/DVB vials were found to continually decrease in accordance to compound

volatility by factors of 2–4 times for benzene and octane, respectively. Where experimental RSD values did not exceed 3% when compared to the aforementioned variations, the difference in amount extracted was accepted to be statistically valid without further hypothesis testing. As the same amount of standard and headspace was present in each of the oil–PS/DVB vials, it could be determined that the use of silicone oil greatly assisted in the retention of the McReynolds compounds for standard gas generation.

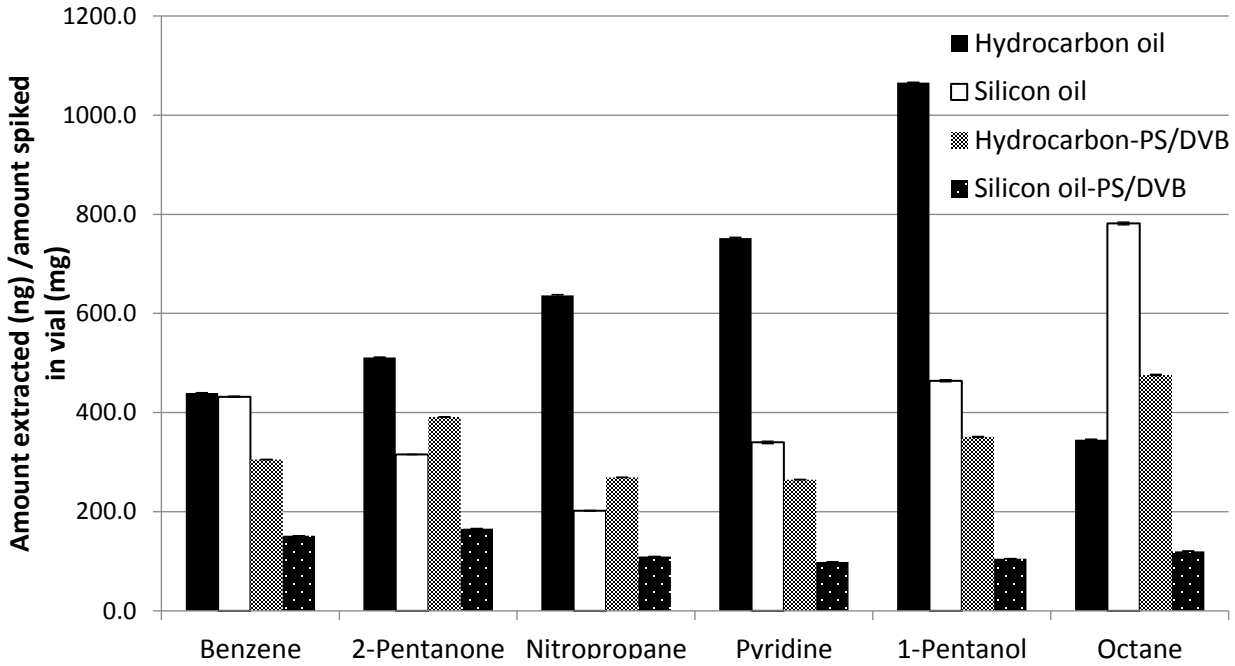

Figure 2.1 Nanograms of McReynolds extracted per milligram of analyte spiked into the standard gas generating vials prepared using different retention media after 1 min extractions were performed at 35 ◦C with a DVB/PDMS fiber.

To further support the involvement of oil in standard retention, vials prepared using only hydrocarbon or silicone oil as the retention media were also compared. It is important to note that 6 mL of oil was used to keep a consistent headspace volume of the oil–PS/DVB analogs. However, because the same spiked oil solutions were used to prepare the oil-only vials and those prepared with PS/DVB, and more oil had to be used in the oil-only vials to keep a consistent volume, there was a larger concentration of analyte available in the oil-only vials. As such the results shown in

Figure 2.1 were normalized by dividing the amount of standard extracted during analysis by the total amount of analyte present in the vial. As the composite sorbent matrix will obey Henry's Law this method of normalization is valid such that we can assure with certainty that differences among the systems tested are due to the analyte's affinity for the sorbent volume of the said system, rather than differences in the amount of standard present or the headspace volume.

Generally, with the exception of benzene and octane, the amounts of standard extracted from silicone–oil based vials were substantially lower. Such a trend seems to relate with the polarity of the analytes spiked onto the oil and the affinity of the oil for the analytes as indicated by log P values of 2.22 and 5.01 for benzene and octane, respectively. These non-polar analytes would, therefore, exhibit a greater affinity to the hydrocarbon oil, resulting in a lower headspace concentration. Despite this result, the silicone oil–PS/DVB vials provided much lower concentrations of benzene and octane when compared to any of the other vial configurations, suggesting that there exists a synergistic effect between the silicone oil and the PS/DVB resin with regards to analyte retention.

Since a lesser fraction of the standard is extracted each time, it could be hypothesized that the silicone oil–PS/DVB based standard gas generating vials would produce a more repeatable headspace concentration after many successive extractions had been performed. This repeatability could also be achieved by using shorter extraction times. However, by decreasing extraction time, precision would also decrease, as any variability experienced during the experimental method would become increasingly significant. Additionally, being able to generate a less concentrated headspace would also be advantageous in applications that require a much smaller amount of standard. Such applications could include quality control and tuning of contemporary mass spectrometry instruments where picograms of analyte would be sufficient.

2.3.2 Evaluation of intra-batch and inter-batch vial reproducibility

In a previous study, Gómez-Ríos and collaborators demonstrated that different vials prepared using the same spiked hydrocarbon pump-oil solution were statistically identical.[23] Consequently, intra-batch reproducibility was also addressed for the current study, with the additional challenge of also verifying inter-batch reproducibility. This additional task proved to be less challenging, as preparing spikes in silicone oil was an easier undertaking, given the higher affinity toward the compounds. By evaluating 2 vials randomly selected from each of the 3 different batches, these claims were demonstrated herein.

As presented in Figure 2.2, good agreement between vials chosen from the same batch and different batches was obtained. Furthermore, as can be observed in Table 2.2, ANOVA confirmed that the 6 vials analyzed were statistically identical with regards to all of the McReynolds probes ($F_{vial} < F_{crit}$ at 95% confidence). These results were attained with inter-vial percent RSD < 4% for every standard analyzed.

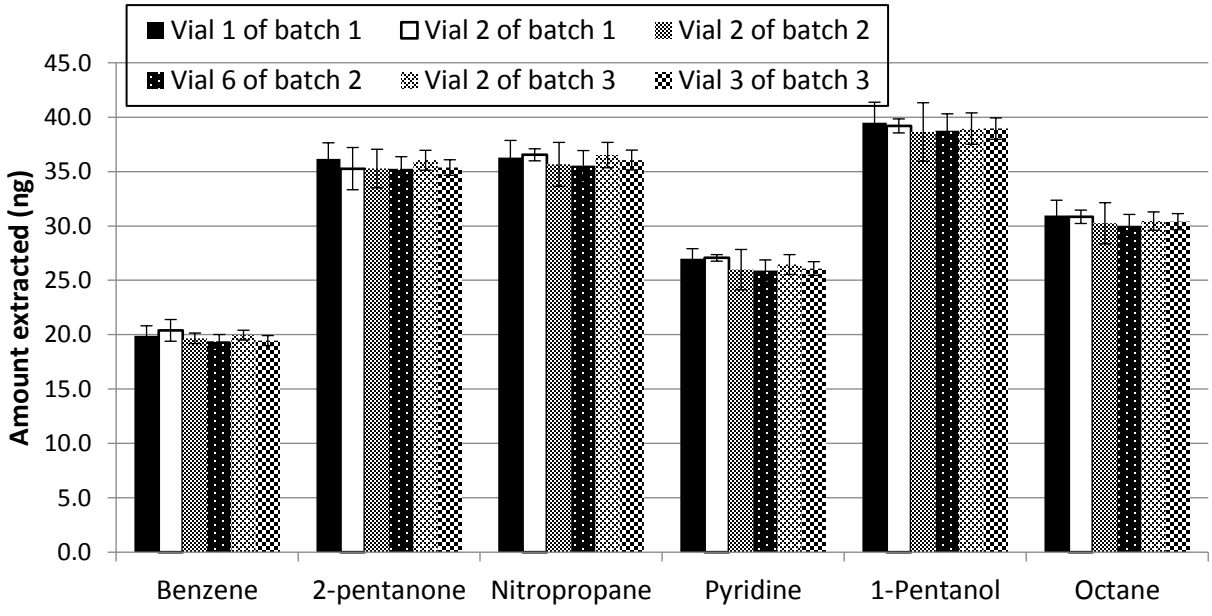

Figure 2.2 Inter-vial reproducibility of McReynolds standard gas generating vials when 1 min extractions were performed at 35 ◦C with a DVB/PDMS fiber from silicone oil–PS/DVB based standard gas generating vials.

Table 2.2 ANOVA testing of inter-batch reproducibility of the silicone oil-PS/DVB vials.

Compounds	Benzene	2-Pentanone	1-Nitropropane	Pyridine	1-Pentanol	Octane
F_{vial}	0.85	0.28	0.30	0.72	0.11	0.29
F_{crit}			3.11			
% RSD	3.4	3.5	3.3	3.8	3.7	3.4
2-factor ANOVA test of the first factor, inter-vial						
F_{vial}			1.37			
F_{crit}			2.34			

It is important to highlight that the method used to introduce the standard into the silicone oil is critical in order to attain inter-batch reproducibility. Through preliminary experimentation (data not shown), it was found that if standards were introduced to the oil by use of a disposable pipette, only intra-batch reproducibility could be achieved, as the repeatable release of standard could not be performed into the total volume of oil. Instead, the introduction of the standard into the oil by use of a micro-syringe through a PFTE septum was found to be preferential, thus preventing analyte evaporation while achieving a more precise delivery of the standard. Additionally, the Hamilton syringes used are stated to give an accuracy of ±1% of the nominal volume used (i.e. Hamilton, Syringe Care and Use Guide). Achieving reproducibility of the batches of vials is very important in multi-lab or commercial applications where different analysts may want to compare results attained using the same method or evaluate instrumental response throughout multiple analyses.

2.3.3 Determination of long-term vial storage stability

Another important feature for a successful in-vial standard gas generating system is the ability to confidently store vials for a prolonged period of time. In order to do so, determination of which conditions may result in premature degradation of the vial is a critical step in the development of a reliable system. In view of this, vial stability, under a variety of storage conditions, was examined for a period of 10 weeks. As smaller, 15 mL Mininert® capped vials

were used, a smaller headspace was available, resulting in lesser amounts of analyte being extracted than from mixtures prepared with standard 20 mL headspace vials.

It was demonstrated that benzene, the most volatile probe analyzed, 2-pentanone, 1-nitropropane, and 1-pentanol were shown to exhibit no-detectable loss regardless of the chosen storage method over the 10-week period. This observation was confirmed in Table 2.3 by use of ANOVA at 95% confidence. A visual representation of the stability associated with these results is fully graphed in Appendix A.

Table 2.3 ANOVA testing at 95% confidence demonstrating 10-week vial stability of silicone oil-PS/DVB vials.

Compounds	Benzene	2-Pentanone	1-Nitropropane	Pyridine	1-Pentanol	Octane*
F_{V1-3} RT,L	1.40	1.53	2.53	5.38	2.20	0.02
F_{V1-4} RT,L	1.82	1.48	3.08	4.82	2.71	0.66
F_{v1-5} RT,D	1.46	3.27	2.74	3.41	2.97	0.80
F_{V1-7} RT,D	0.28	0.30	0.52	0.34	0.78	13.89
F_{V1-6} F,D	0.57	0.22	0.53	0.20	0.09	1.53
F_{V1-8} F,D	0.91	1.29	0.87	2.07	1.46	0.35
F_{crit}			3.48			5.14

RT = room temperature, L = light exposure, D = storage in dark, F = storage in fridge

* Weeks 0, 1 and 10 were used for ANOVA calculations of octane

Unlike the other standards, vials stored with exposure to light were shown to incur losses for pyridine. This divergence was observable as a continually decreasing extraction efficiency from vials S-1-3 and S-1-4 which is shown in Appendix B Although this decline was observed to be slight, it was still significant at a 95% level of confidence. Pyridine has long been known as a particularly sticky, surface active compound; however, a brief review of the literature did not yield any details regarding pyridine instability when exposed to light. From this result, it can be concluded that future standard gas generating vials would benefit by being placed in amber colored vials. Additionally, further benefit may be attained by storing vials inside a dark cupboard when not in use.

Conversely, the variations observed for the octane results did not follow any definable trend. Values for weeks 3 and 6, which can be viewed in Appendix B were seen to be significantly higher than those observed initially and at weeks 1 and 10. It is possible that this variation may have been due to an undetected instrumental or temperature fluctuation when performing the experiments. For this reason, ANOVA testing for octane was only performed for weeks 0, 1, and 10, as can be seen in Table 2.3 With the exception of vial 1-7, the reduced ANOVA demonstrated that the amounts of octane extracted initially and at the latest time period of the study were statistically similar.

It was observed that vials stored in refrigeration exhibited a slightly smaller headspace concentration for octane (≤10%) than those stored at room temperature. Given that these vials were immediately moved into the refrigerator for the initial 72 h equilibration, after mixing the particles with the spiked silicone-oil solution, it could be hypothesized that due to the quick storage at low temperatures a small portion of the octane standard might have condensed into the smaller pores of the PS–DVB particles.[5] However, further experimentation would be needed to support this assumption. Thus, aiming to prevent inter-vial differences due to initial storage conditions, it would be preferential to allow the silicone oil mixture to equilibrate with the PS–DVB particles for at least 72 h at room temperature before placing them in the refrigerator.

2.3.4 Assessment and modeling of the vial depletion rate

As previously mentioned, intra-vial reproducibility and longevity are paramount in producing a practical standard gas generating vial. Ideally, less than 5% depletion should be observed in order to consider the vial reusable. Once this criterion has been exceeded, a switch would have to be made to an identical vial, or corrections would have to be made for vial depletion using a theoretical model in order to continue generating a statistically similar signal.

As can be seen in Figures 2.3 and 2.4, vial depletion was shown to be well below 5%, even after 208 extractions had been performed. More specifically, as shown in Table 2.4, experimental depletion was found to be 2.4%, 3.3%, 2.1%, 2.7%, 3.0%, and 1.5% for benzene, 2-pentanone, 1-nitropropane, pyridine, 1-pentanol, and octane, respectively. Collectively, the mass fractions removed for benzene, 2-pentanone, and 1-nitropropane were calculated to be 2.4%, 2.7%, and 2.2%, and 1.9%, 1.5% and 1.0% for pyridine, 1-pentanol, and octane, respectively. These first 3 values were in very good agreement with the experimental depletion determined by linear regression of the data. However, the experimental depletion was found to differ from the mass fraction by 34.5%, 66.4%, and 41.7% for the other 3 compounds, respectively. This much deviation was not unexpected due to the relatively small depletion observed in comparison to the method percent RSD values, which were found to be 2.1% or less. What was surprising was how closely results for the first 3 analytes were found to concur in the meantime. The disparity observed with the 3 least volatile standards may indicate that these compounds were not given adequate time to re-equilibrate with the vial headspace between successive extractions. This would likely not occur in real-world vial applications, as 2 out of every 3 extractions were dumped onto a dummy column; as such, the vial was only allowed to re-equilibrate for 5 min between each extraction, as opposed to a full GC run-time. Additionally, this process would have a cumulative effect and likely only occur significantly if multiple, proximate extractions are performed.

Table 2.4 Vial depletion from a silicone oil-PS/DVB vial based on experimental regression trend and total mass fraction extracted.

Compound	Benzene	2-Pentanone	1-Nitropropane	Pyridine	1-Pentanol	Octane
Experimental depletion trend						
Starting mass (ng)	20.5	29.7	58.1	20.6	41.5	15.1
Final mass (ng)	20.0	28.7	56.9	20.0	40.2	14.8
Amount remaining (%)	97.6	96.7	97.9	97.3	97.0	98.5
Amount removed (%)	2.4	3.3	2.1	2.7	3.0	1.5
RSD of first 15 runs (%)	1.2	1.7	1.6	1.6	1.5	2.1
Theoretical (mass fraction)						
Initial mass per vial (ng)	178185	223713	553321	225930	564826	324804
Total mass extracted (ng)	4257	6148	12106	4272	8595	3142
Mass remaining in vial (ng)	173927	217564	541215	221658	556231	321662
Amount remaining (%)	97.6	97.3	97.8	98.1	98.5	99.0
Amount removed (%)	2.4	2.7	2.2	1.9	1.5	1.0
Difference between models (%)	1.1	-19.0	4.4	-34.5	-66.4	-41.7

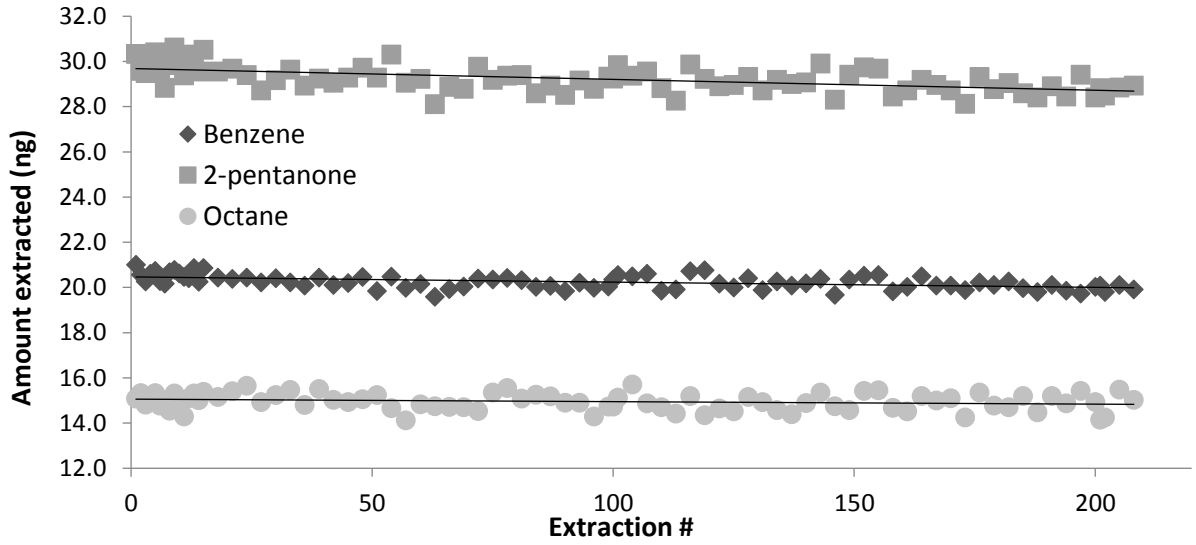

Figure 2.3 Vial depletion trend for benzene, 2-pentanone, and octane after 208 extractions performed at 35 ◦C for 1 min using a DVB/CAR/PDMS fiber from a silicone oil–PS/DVB based standard gas generating vial.

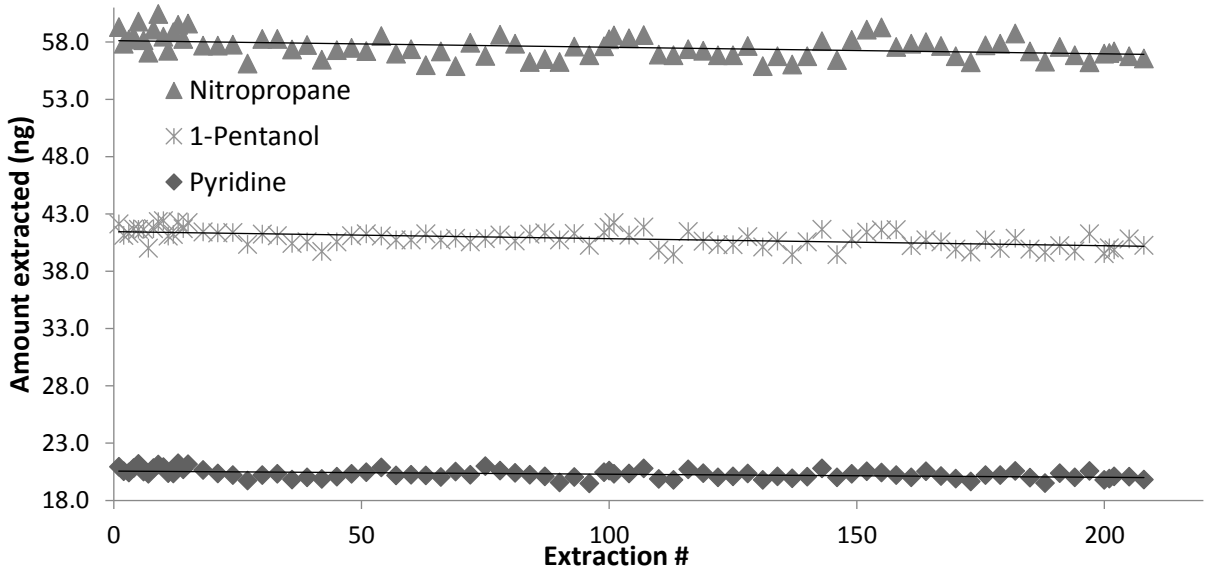

Figure 2.4 Vial depletion trend for 1-nitropropane, pyridine, and 1-pentanol after 208 extractions performed at 35 ◦C for 1 min using a DVB/CAR/PDMS fiber from a silicone oil–PS/DVB based standard gas generating vial.

Additional experimentation confirmed that 5 min was found to provide adequate recovery time after a few successive extractions. This additional study showed that there was no significant difference between recovery times of 5–10 min for octane, the most strongly retained standard. However, as aforementioned, it is possible that a cumulative effect may have been present if the vial was continuously not allowed to return to equilibrium before another extraction was performed. This effect would grow in significance when a large multitude of unrelenting extractions were performed, as was done in the depletion study. With this in mind, it would be more prudent to allow at least 10 min for a vial to re-equilibrate between each successive extraction, which is in agreement with standard GC runtimes.

Although very little depletion was observed, correction was still undertaken by using the experimentally determined depletion rate as well as a newly proposed equation that models the depletion based on the mass fraction extracted at each extraction. Ideally, the best correction model is one that would generate continuously repeatable results, which would be represented as a

hypothetical zero slope line as shown in Figure 2.5 As expected, the corrections made using the regression equation generated from the experimental rate of depletion gave near zero slope results. However, this correction method would prove to be impractical for common use. This impracticality stems from the fact that the amount extracted, and therefore depletion rate would change anytime a different fiber coating, extraction time, or extraction temperature were used. Instead, it would be far more practical to perform corrections based on the mass fraction remaining in the vial after each extraction.

To perform this mass fraction correction, Eq. 2.1 was formulated, where X_{adj} is the adjusted or corrected amount, X_n is the actual amount extracted at the n^{th} extraction, $\bar{x}$ is the average amount extracted over n runs, n is the number of extractions from the vial, and M_o is the initial, absolute amount of standard present in the vial. To employ Equation 2.1, an analyst would need record of the amount of analyte (in ng or moles) that had already been extracted from a given vial, and knowledge of the initial amount (in ng or moles) of standard that had been initially spiked into the vial.

$$X_{adj} = X_n + ((\bar{x} * n)\left(\frac{\bar{x}}{M_o}\right)) \qquad \text{Eq. 2.1}$$

Although performing corrections based on the absolute mass fraction extracted is not as exact as regression modeling, Figure 2.5 clearly demonstrates that a distinct effect is still attained when compared to the steeper slope of the uncorrected depletion rate. This can be further supported by the close agreement between the equation-corrected average nanograms extracted and initial extraction amounts, as presented in Table 2.5 The significance of such modeling is small when correcting for these minuscule 3% depletions, as signified by the meager 0.2% RSD improvements. However, if thousands of extractions were to be performed, Eq. 2.1 could be used to relate these older values to a new vial from an identical batch.

Table 2.5 Statistical data for depletion models and adjustment after 208 extractions.

Compounds	First 15 extractions (initial)			Unadjusted trend			Experimental trend adjusted			Mass fraction equation adjusted		
	Avg	SD	%RSD	Avg	SD	%RSD	Avg	SD	%RSD	Avg	SD	%RSD
Benzene	20.5	0.25	1.2	20.2	0.30	1.5	20.5	0.26	1.3	20.5	0.26	1.3
2-Pentanone	29.7	0.51	1.7	29.2	0.57	1.9	29.7	0.47	1.6	29.6	0.47	1.6
1-Nitropropane	58.1	0.94	1.6	57.6	1.0	1.7	58.1	0.91	1.6	58.1	0.92	1.6
Pyridine	20.6	0.33	1.6	20.3	0.39	1.9	20.6	0.35	1.7	20.5	0.35	1.7
1-Pentanol	41.5	0.63	1.5	40.9	0.75	1.8	41.4	0.63	1.5	41.2	0.66	1.6
Octane	15.1	0.31	2.1	15.0	0.37	2.5	15.1	0.37	2.4	15.0	0.37	2.5

Avg = Average SD = Standard deviation %RSD = percent relative standard deviation

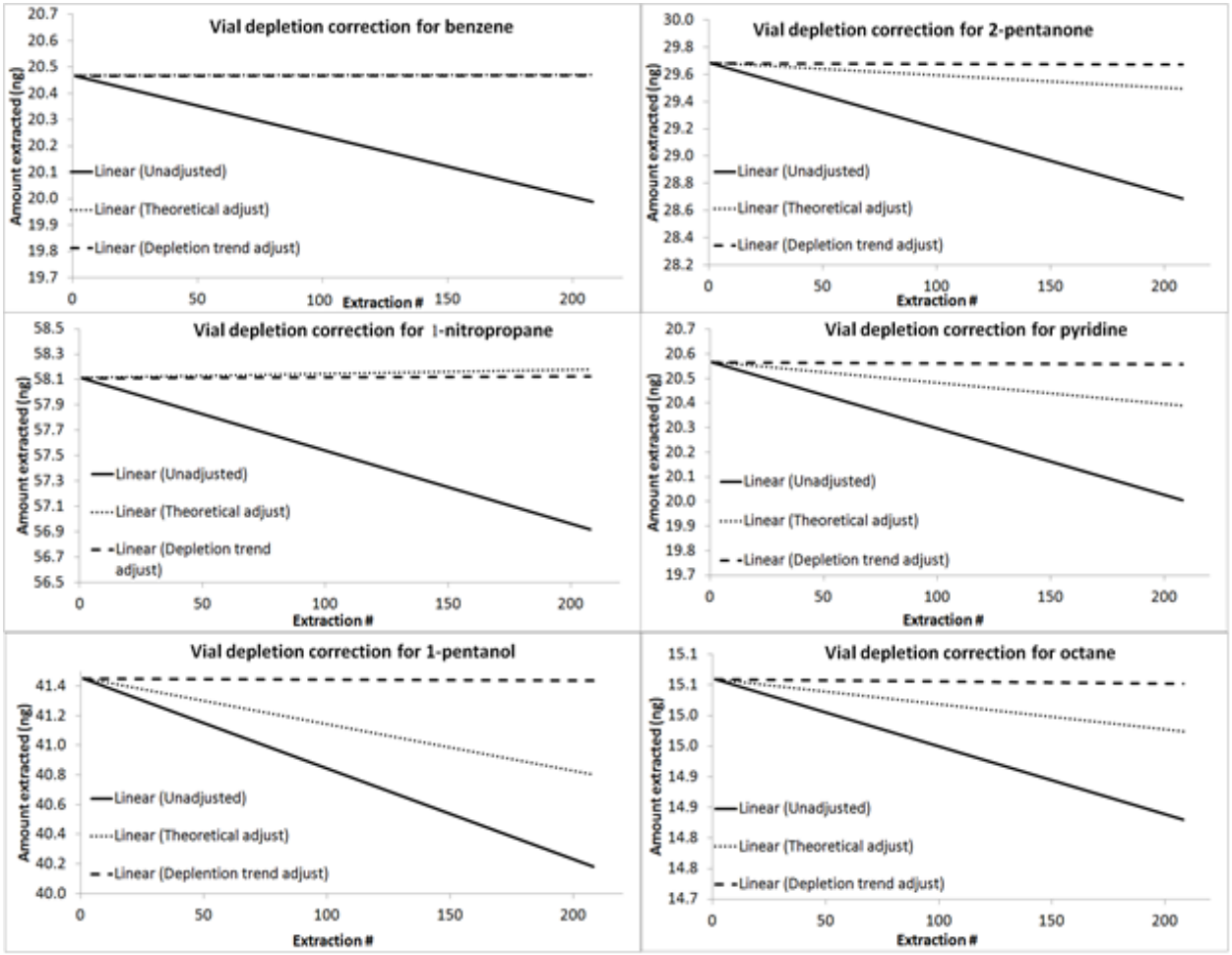

Figure 2.5 Adjusted depletion curves for a silicone oil–PS/DVB based standard gas generating vial corrected by experimental depletion trend and theoretical Equation 2.1 of the mass fraction extracted.

2.4 Conclusion and future directions

A silicone-oil based PD/DVB standard gas generating vial for performing instrument quality control and either internal standardization or standard addition by SPME is proposed within this study. Many benefits of developing these vials with silicone oil were demonstrated herein: they were shown to load much less analyte onto to the fiber than previous vial designs,[23] to possess a great degree of both intra-batch and inter-batch vial reproducibility, to be stable under a wide variety of storage conditions, and to deplete very slowly in a predictable fashion.

Results from the vial stability experiments indicate that amber vials should be used for the preparation of the standards and that vials should be allowed to equilibrate for 72 h at room temperature, prior to refrigeration in order to ensure maximum vial lifetime. Notably, the vials have been found to deliver a very repeatable amount of standard, as vial depletion was found to be less than 3.5% even after 208 extractions had been performed, as long as headspace is brought back to equilibria. Additionally, for applications that may require repeatable results after hundreds of extractions, it was shown that vial depletion could be corrected for by using the mass fraction removed from the vial.

In extension to quality control applications, these vials can be further used to perform on-fiber standard addition, internal standardization, and derivatization. These applications will be especially prominent for on-site applications,[76] particularly when combined with portable GC–MS instrumentation. Additionally, such vials would prove very useful for calibration of headspace analysis, instrumentation, sorbent traps, needle traps,[38] and many other techniques, as the production of standard mixtures would be readily achievable.

Chapter 3 Solid Phase Microextraction On-Fiber Derivatization Using a Stable, Portable, and Reusable Pentafluorophenyl Hydrazine Standard Gas Generating Vial

Preamble

The majority of the materials in this chapter have been published as a research article: Justen Poole, Jonathan Grandy, German Augusto Gómez-Ríos, Emanuela Gionfriddo, Janusz Pawliszyn; Solid Phase Microextraction On-Fiber Derivatization Using a Stable, Portable, and Reusable Pentafluorophenyl Hydrazine Standard Gas Generating Vial; *Anal. Chem.*, **2016**, 88(13), pp 6859-6866.

3.1 Introduction

Due to the broad range of organic compounds present in environmental and anthropogenic sample matrices, targeted analysis can be a difficult and often laborious task, requiring extensive and selective sample preparation. As a result, performing analysis of a particular class of compounds (e.g., aldehydes) requires the selection of an appropriate analytical method. Such targeted methods often consist of one or more analyte-specific steps that may impact different stages of the analytical process. Examples include the selective extraction of analytes by use of selective sorbents (e.g., molecularly imprinted polymers)[77,78] or through derivatization. Derivatization is of specific interest, as it can aid in improving both chromatographic separation and detector sensitivity of a given analyte while proving essential in the gas chromatography(GC) analysis of compounds with poor thermal stability. Additionally, derivatization affords the opportunity for functionalities to be

attached to certain analytes, such as halogens, which can then be targeted during instrumental analysis. The attachment of such functionalities then allows for the use of analytical instruments such as electron capture detectors (ECDs), which have been demonstrated to have remarkably low limits of detection. Additionally, selected ion monitoring mass spectrometry (SIM) for ions related to the derivatization reagent can also be employed, facilitating accelerated data processing.

Aldehydes and other carbonyl compounds are of particular environmental interest when considering their wide range of biogenic and anthropogenic sources.[79,80] Derivatization of carbonyl compounds can be accomplished in a variety of ways, and though not an exhaustive list, some applications include the following: (a) microfluidic chips, where a derivatization agent solution and an air sample are mixed in a microreactor;[81,82] (b) impingers, which operate on the same general principle, effectively scrubbing the sample gas of analyte by passing it through a solution containing a derivatization reagent; or (c) the use of conventional solid phase extraction (SPE), where a sorbent has been preloaded/impregnated with a derivatization reagent prior to sampling.[79,83] As an alternative, solid phase microextraction (SPME) can be applied toward derivatization through a process known as on-fiber derivatization, where the derivatizing agent is loaded onto the solid phase microextraction (SPME) fiber prior to, or after, the sample extraction. As SPME combines both sampling and sample preparation into a miniaturized, solvent-free format, it lends itself to greener sampling opportunities and, when coupled to portable instrumentation, rapid on-site sample analysis.[5,84,85] In order to fulfill the growing demand for instrument portability and on-site analysis, it is imperative that techniques and methods that can be easily taken into the field are continuously developed in order to facilitate comprehensive and quantitative on-site sampling and analysis. Though on-fiber derivatization for the sampling of carbonyl compounds is well documented in the literature,[71,86–99] as well as its various applications

for ozone,[100] organometallic compounds,[101] chlorophenols in water,[102] primary amines in sewage,[103] and pharmaceuticals in meat products,[104] these methods have not been particularly portable. Specifically, the absence of a portable and reusable derivatization agent standard, which is required to load the fiber with an appropriate derivatization reagent prior to sampling, has impeded both the automation and the portability of such methods.

To address this need, a portable pentafluorophenyl hydrazine (PFPH) standard headspace (HS) generating vial has been developed on the basis of the standard analyte generators previously described by Gomez-Rios *et al.*[23] and Grandy *et al.*[3] The aforementioned vials operate on the principle of thermodynamic equilibrium between an analyte-spiked composite sorbent, comprised of polystyrene-divinylbenzene (PS/DVB) resin particles and silicone oil, and an enclosed gaseous headspace resulting in a reproducible headspace concentration of the spiked analyte. These vials have demonstrated remarkable reusability owing to the high affinity of the analyte for the composite sorbent causing negligible depletion of analyte from the vial after extraction, while also providing reproducible SPME fiber loadings ($n > 200$). These vials are ideal for applications such as quality control and on-site/in-lab calibration though their ability to store reactive molecules was not investigated. The presented development of a gas generating vials application toward the storage of a highly reactive derivatization reagent, PFPH, demonstrates the first stable, portable, and reusable headspace standard of such a molecule.

In this work, the PFPH generating vial was successfully coupled to a portable GC-toroidal ion trap mass spectrometer (TMS), such that on-site, on-fiber derivatization was used to quantify formaldehyde from car exhaust. In addition, the vial was coupled with a two-dimensional gas chromatography (GCxGC) time-of-flight mass spectrometer (TOF/MS) using SPME and applied toward the monitoring of meat spoilage over time targeting aldehydes as markers of tissue

decomposition.[105] With this development, the standard gas generating vial will certainly begin to see expanded use in applications for on-site and in-lab calibration, QC, and storage of otherwise unstable gaseous standards.

3.2 Materials, instrumentation, and experimental methods

3.2.1 Materials and Reagents

Butanal, pentanal, hexanal, heptanal, octanal, nonanal, benzene, toluene, ethylbenzene, and xylene, along with PFPH and the 37 wt % formaldehyde solution used, were all purchased from Sigma-Aldrich (Mississauga, ON, Canada). Nanopure water was obtained using a Barnstead/Thermodyne generating system (Dubuque, IA, USA). The silicone oil was purchased from Kurt J. Lesker Company (Toronto, ON, Canada). 65 μm PDMS/DVB and 100 μm PDMS SPME fibers with stableflex cores were purchased from Supelco (Bellefonte, PA, USA), while the operated Tenax/Carboxen (CAR) 1001/CAR 1003 needle trap device (NTD) was provided by Torion Technologies of PerkinElmer (American Fork, UT, USA). Ground beef samples were purchased from a local grocery store. In order to ensure constant vial temperature, allowing for reproducible SPME fiber loadings, vials were heated in block heaters developed and fabricated at the University of Waterloo Science Shop. Each block-heater consisted of an electrical heater connected to a thermocouple and provided temperature accuracy of ±0.1 °C. As shown in Figure 3.1, a portable battery-operated block-heater was also assembled for on-site use of the analyte generating vials.

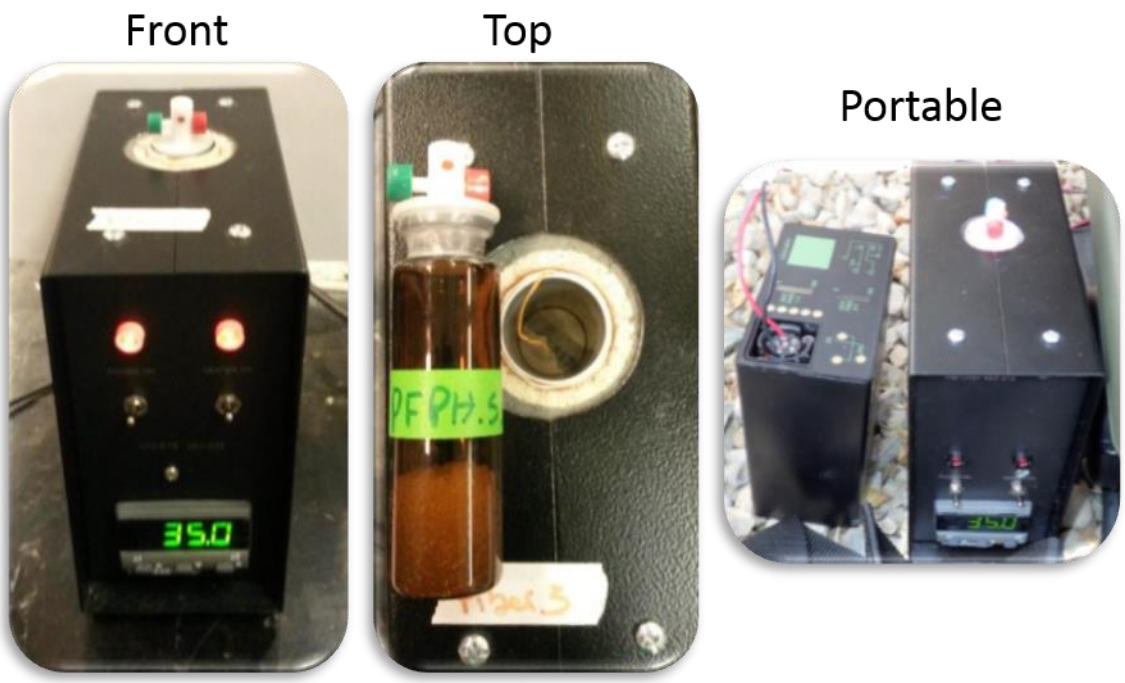

Figure 3.1 Block-heaters used to maintain constant vial temperature via an internal thermocouple. Front and top views are of the in-lab version, while the portable image shows a modified block heater plugged into an unmodified TRIDION-9 battery pack.

3.2.2 Instrumental analysis method (GC/FID and portable GC/MS)

All on-site analyses were performed using a TRIDION-9 portable GC-TMS (Torion Technologies of PerkinElmer, American Fork, UT, USA). Chromatographic separations were performed using a low thermal mass MXT-5 (5 m × 0.1 mm × 0.4 μm) Siltek (Restek, MA, USA) treated stainless steel column, with helium as carrier gas at a flow rate of approximately 0.3 mL min^{-1}. The column temperature was initially held at 50 °C for 10 s and then increased to 250 °C at a rate of 1.5 °C s^{-1} and held there for 15 s. Desorption of the DVB/PDMS fiber and tribed NTD was carried out under splitless conditions for 10 s at a temperature of 270 °C, followed by an opening of the 10:1 split valve for an additional 30 s. Ionization was performed using an electron-impact ion source (electron ionization), and the toroidal ion trap operated in a customized scan mode of 43−400 m/z.

Stability studies and vial validation experiments were conducted using an Agilent 5890 GC-FID (Santa Clara, CA, USA). Chromatographic separations were performed using an Agilent DB-5 column (30 m × 0.250 mm × 0.25 μm) (Santa Clara, CA, USA). The column temperature was initially held at 42 °C for 1 min, then increased to 250 °C at a rate of 20 °C min^{-1}, and was held there for 3 min. Desorption of the DVB/PDMS fiber was carried out for 2 min at a temperature of 260 °C in splitless mode.

Application of the PFPH standard gas generating vial to the semi-quantitative analysis of aldehydes as markers for meat spoilage was conducted using a GCxGC-TOF/MS Pegasus 4D (LECO Corp., St Joseph, MI, USA). The chromatographic system consisted of an Agilent 6890 GC oven containing a secondary oven and a quad-jet modulator, consisting of two hot-air jets and two cold nitrogen jets created by liquid nitrogen. The column configuration consisted of a Rtx-5SilMS (30m × 0.25 mm × 0.25 μm) (Restek Corp., Bellefonte, PA, USA) capillary column in the first dimension (1D) and a BP-20 (1 m × 0.1 mm × 0.1 μm) (SGE Analytical Science, Trajan Scientific Australia Pty Ltd.) in the second dimension (2D), connected by a SilTite μ-Union (SGE Analytical Science, Trajan Scientific Australia Pty Ltd.). A modulation period of 4 s was used, with a hot pulse duration of 0.6 s, and a cold pulse time of 1.4 s. The desorption of analytes from the SPME coating was performed in splitless mode at 270 °C for 10 min, using ultra-high purity helium as a carrier gas with a constant flow rate of 1.5 mL/min. The primary oven temperature was initially held at 50 °C for 1 min, followed by a temperature ramp of 20 °C/min until a final temperature of 250 °C was reached and then subsequently maintained for 30 s. The offset for the secondary oven temperature was set at 10 °C above the primary oven temperature. The modulator offset was set at +15 °C. The transfer line and ion source temperatures were set at 250 and 200 °C,

respectively. Electron impact ionization was performed at an energy output of 70 eV. A solvent delay of 60 s was employed. Mass range scanning was set at 35−600 m/z.

3.2.3 Formulation of the PFPH generating vial and n-aldehydes generating vial

In terms of the standard gas generating vial preparation the validated methodology previously described in Section 2.3 was used to prepare all further headspace generating vials throughout the study. However, the amount of the pure analyte standard(s) used may vary greatly depending on the intended application and volatility of a given analyte. As such, aldehydes C4 to C9 were spiked into the silicone oil at 0.005, 0.007, 0.009, 0.010, 0.013, and 0.015 wt %, respectively. Similarly, instrumental quality control vials were manufactured by spiking benzene, toluene, ethylbenzene, and o-xylene into silicone oil at 0.005, 0.007, 0.010, and 0.010 wt %, respectively. Finally, where the PFPH generating vials were applied for on-fiber derivatization a much greater amount of this reagent (1.19 wt%) is required per vial as to ensure significantly high fiber loadings while using minimal exposure times.

3.2.4 Derivatization scheme for PFPH aldehyde derivatization

When reacted with PFPH, aldehydes undergo a dehydration reaction, progressing through an alcohol reaction intermediate, and eventually resulting in the loss of a water molecule, forming a hydrazone.[106] As drawn in Figure 3.2 the formed hydrazone contains a double bond between the terminal nitrogen of the initial hydrazine functionality of the derivatization reagent and the carbon associated with the carbonyl functionality of the initial aldehyde or ketone. As expected, chromatographic separation confirmed such isomerization of all aldehydes, with the exception of formaldehyde (Figure 3.3). Upon analysis, the derivatized aldehydes were identified by examination of the resulting mass spectra and/or chromatographic retention times. In terms of mass spectral identification, PFPH has a molecular weight of 198 Da; however, once reacted with an

aldehyde, two hydrogen atoms from the PFPH and the oxygen of the aldehyde are eliminated as water. This results in a product molecular weight equal to the PFPH reagent (198 Da) plus that of the aldehyde in question, minus the molecular weight of water (18 Da). When performing electron impact ionization, hydrazones are cleaved at the double bond that was formed during the derivatization reaction, resulting in an ion with a mass-to-charge (m/z) ratio of 196. In addition, an ion with an m/z of 224 was also observed for all derivatized n-aldehydes larger than propanal. This ion corresponds to a McLafferty rearrangement of the reaction product after ionization. In this study, the molecular ion of the derivatization product could always be detected. Moreover, the proposed derivatization strategy could also be used with an Electron Capture Detector, allowing for greatly reduced limits of detection and quantification, as only halogenated compounds, such as the PFPH derivatization product, would demonstrate a detector response. However, as an operable ECD was not available in our laboratory at the time of this work, experiments were conducted using GC-FID and GC-MS instrumentation.

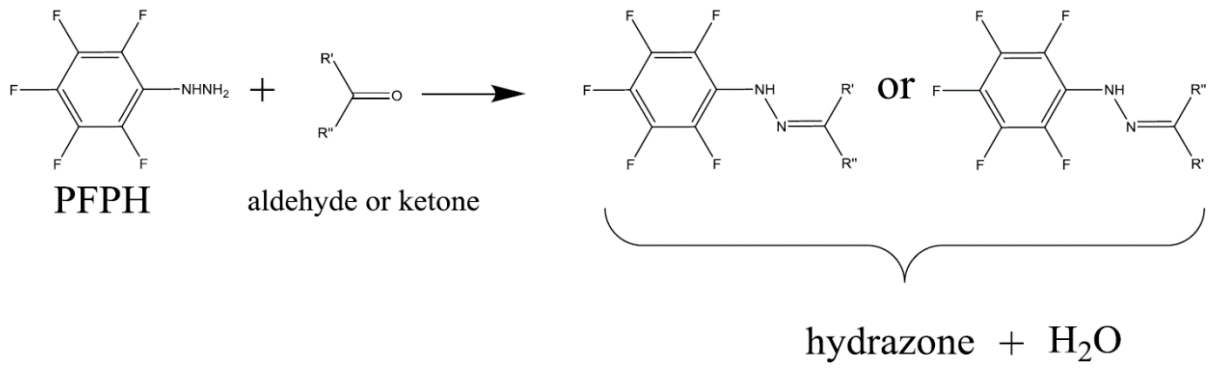

Figure 3.2 Schematic of the reaction between PFPH and an aldehyde or ketone, as described by Ho et al.[106]

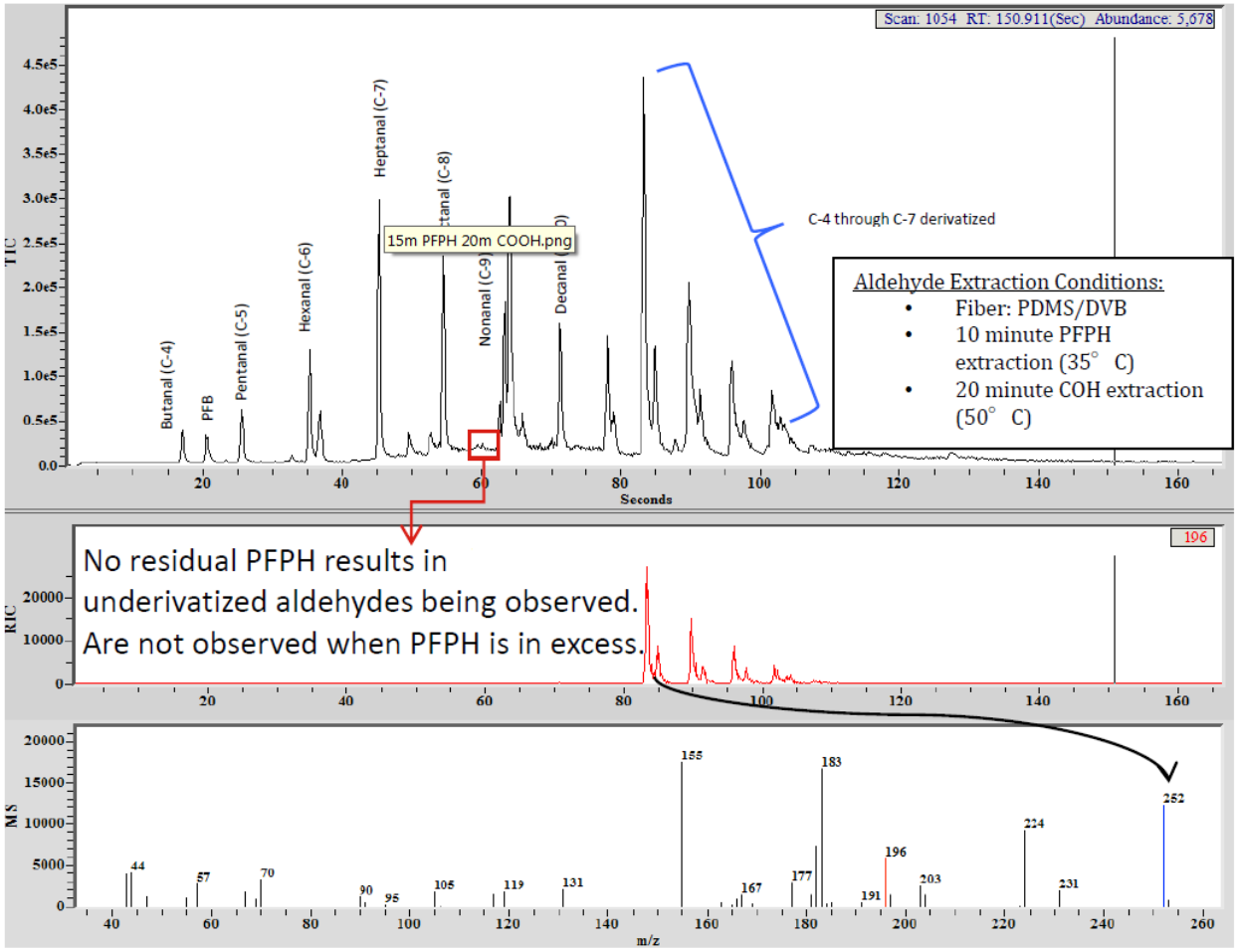

Figure 3.3 On-fiber derivatization using the standard gas generation vials to load both the PFPH derivatization reagent and aldehydes. Extractions from the PFPH gas generating vial were performed at 35 °C for 10 minutes prior to the exposure of the PFPH loaded fiber to the headspace on an aldehyde generating vial at 50 °C for 20 minutes.

3.2.4.1 Methodology of on-fiber derivatization

To perform the aforementioned on-fiber derivatization using the proposed standard gas generating vial, the following steps were implemented; first, the SPME fiber was preloaded with PFPH by performing a headspace extraction from the PFPH generating vial. Subsequently, the fiber was removed from the vial and then exposed to the sample matrix, where carbonyl compounds underwent a dehydration reaction with the PFPH. The steps involved can be visualized in Figure 3.4 while the reaction itself is described in Figure 3.2. Similarly, in Figure 3.3 an example

can be found of an obtained mass spectra. Finally, the fiber was thermally desorbed in the GC injection port for analytical separation and detection.

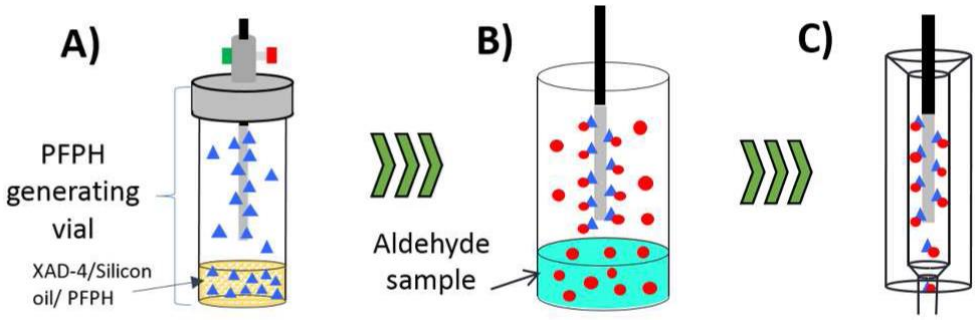

Figure 3.4 On-fiber derivatization procedure employing the new PFPH generating vial. A) PFPH loading of SPME fiber, B) PFPH-loaded fiber exposed to gaseous aldehydes, resulting in derivatization, and, C) thermal desorption of SPME fiber on the GC injection port.

3.2.5 Extraction conditions from the standard analyte generating vials

The standard gas generating vials containing PFPH and the BTEX QC were maintained at 35 °C throughout the experimentation, while vials containing linear aldehydes C4 through C9 were maintained at 50 °C in order to provide a higher headspace concentration of the heavier aldehydes. While not in use, vials were stored in a low light environment at room temperature (20 ± 1 °C). Prior to use, all vials were allowed to equilibrate to their experimental temperature for no less than 1 h prior to sampling. Similarly, after each extraction, vials were left to re-equilibrate for at least 10 min to ensure re-equilibrium was achieved between the headspace and the sorbent phase.[3] DVB/PDMS and PDMS SPME fibers were chosen for this study; however, DVB/PDMS fibers were used for the majority of the work presented as they have been previously shown to demonstrate a strong affinity for PFPH.[93] Extraction times from each vial varied between 10 s and 10 min, depending on the parameter under study. One minute quality control extractions were also performed from a BTEX-generating vial throughout the experiments, using a dedicated DVB/PDMS SPME fiber to monitor the stability of the analytical instrumentation used.

3.2.6 PFPH vial long-term stability

In order to ensure representative stability data, eight PFPH vials were formulated. Of these vials, four were capped using Mininert caps, while the remaining four were capped using conventional screw-on septa caps. Headspace volumes were verified to be the same in both formats. The Mininert cap was selected due to its capability to provide a better seal than that of a septa cap after multiple punctures. Given that an imperfect seal may allow for the introduction of atmospheric contamination of the headspace, resulting in eventual PFPH degradation or loss, the quality of the seal is considered a critical parameter. One vial of each cap type was placed in a fridge for storage at 5 °C, while the remaining six vials were placed in a dark cupboard at room temperature. This was done so that any differences in terms of storage temperature could be observed. Of the six vials stored in a dark cupboard, two of each type were sampled in triplicate at days 3, 7, 14, 30, and 77 after vial formulation. The remaining two vials and the two stored in the refrigerator were only sampled on days 30 and 77. This step was employed so as to observe whether any discrepancies could be observed between the vials that had been sampled previously and those that had not. All extractions, consisting of a 10 min exposure to the headspace of the PFPH gas generating vial, were performed under the same conditions. The GC-FID used for this study was calibrated for PFPH response by liquid injection, using standards prepared in hexane. Throughout the 77 day experiment, QC runs were performed in order to monitor instrumental variabilities. All data was quality control adjusted to the day of calibration, although the GC-FID used for the experiments remained within two standard deviations of the population mean of each QC standard for the duration of the experiment. A detailed outline of this experiment can be seen in Figure 3.5.

Cap type	Vial #	Storage	Day				
			3	7	14	30	77
Septa	1	Dark Cupboard (RT)				x	x
	2	Fridge (5°C)				x	x
	3	Dark Cupboard (RT)	X	x	x	x	x
	4	Dark Cupboard (RT)	X	x	x	x	x
Mininert®	1	Dark Cupboard (RT)	X	x	x	x	x
	2	Dark Cupboard (RT)				x	x
	3	Dark Cupboard (RT)	X	x	x	x	x
	4	Fridge (5°C)				x	x

**Note: Date of analysis denoted by an "x"

RT = Room temperature

Figure 3.5 Vial map for 77 days PFPH stability study, outlining storage conditions of light exposure and temperature of storage along with sampling schedule for all 8 vials.

3.2.7 Extraction of aldehyde spoilage biomarkers from ground beef

Ground beef samples were prepared by weighing 5 g of raw medium ground beef into 20 mL amber glass headspace vials and stored at room temperature. In order to increase the headspace concentration of semivolatile and volatile sample constituents, all samples were equilibrated for 1 h at 35 °C prior to extraction. Following a 5 min preloading of the derivatization agent, static headspace extractions of the beef samples were carried out for 30 min at 35 °C. In order to monitor the production of aldehydes during the meat spoilage process, extractions were performed in duplicate, with and without derivatization, on the day of vial preparation and 1, 5, and 7 days after sample preparation. All extractions were performed from previously unsampled vials to ensure cross-contamination from the PFPH did not occur.

3.2.8 Intra and inter-day stability of the portable GC-MS detector response following a cold start

The Tridion-9 GC-TMS has been designed to operate solely on battery power and a portable helium cylinder. Consequently, it is to be expected that the instrument will need to pump down vacuum and reach an operational state giving repeatable signal very quickly after being started. Therefore, using one of the aforementioned BTEX gas generating vials, continuous analyses were performed on the instrument for a period of 2 hours immediately following a cold boot of the instrument and then periodically over an additional 24 hour period. Extractions were performed using a DVB/PDMS fiber for 1 minute at a temperature of 35 ^{o}C. Desorptions on the portable GC/TMS were then carried out at 250 ^{o}C for 30 seconds with a 2-second splitless injection followed by an opening of the 1:10 split vent. The total peak area was then plotted on a control chart with the 2 standard deviation warning limit chosen to represent the stability of the instrument.

3.2.9 Application for on-site quantitation of formaldehyde in car exhaust

On-site samplings of formaldehyde from car engine exhaust were performed by first loading the derivatization agent onto the SPME fiber using a 10 min extraction from the headspace of the PFPH-generating vial. For the NTD samplings, 15 mL of the PFPH vial headspace was drawn onto the sorbent bed of the needle trap device. In order to facilitate this volumetric NTD extraction from the vial, a blank 22 gauge needle was also inserted through the vial septum to allow the headspace pressure to remain constant. Then, the PFPH-loaded sampling devices were positioned in the center of the vehicle exhaust. For NTD samplings 10 mL of sample was drawn from both hot and cold engine exhaust, while SPME fiber extractions were performed for 60 and 30 s, respectively. Prior to cold exhaust extractions, the catalytic converter was first verified to be cool to the touch. Next, the engine was allowed to idle for 30 s after ignition, followed by sampling.

For hot exhaust extractions, the vehicle was allowed to idle continuously, with sampling starting at 30 min after ignition. Cold car exhaust temperatures were observed to be equal to the ambient air temperature on the day of sampling, 16.3 °C while the hot car exhaust temperature was observed to equilibrate at 45.7 °C under engine idle conditions. To ensure stable instrument response, quality control extractions were performed from the BTEX generating vial on-site both before and after sampling in addition to the day of calibration. As it is infeasible to perform calibration by liquid injection on the portable GC/MS instrumentation due to the limited column capacity, a novel, NTD-based calibration technique was employed. To achieve this, an NTD was first preloaded with PFPH by successively extracting 10 mL from two separate septa-capped PFPH generating vials. Volumes of 0.1, 0.5, 1, 2, 4, and 6 mL were then drawn from the headspace above 10 mL of 0.04 wt % aqueous formaldehyde in a 20 mL headspace vial under 1500 rpm magnetic agitation. Extractions were verified to exhibit negligible depletion by performing a subsequent extraction from the same vial. The temperature dependent Henry's Law constant, as determined by Seyfioglu and Odabasi,[107] was then used to calculate the concentration of formaldehyde above such a solution, which was found to be 2.97 ng/mL. The obtained concentration was then used to determine the amount extracted by the needle trap with the use of Eq 3.1, shown here again, where n is the amount extracted, C is the headspace concentration, and V is the sample volume.

$$n = CV \qquad \text{Eq. 3.1}$$

Each point was analyzed in triplicate from freshly spiked formaldehyde solutions. The resulting response versus extracted mass (nanograms) calibration plot was observed to demonstrate a strong correlation ($R^2 = 0.9988$, Figure 3.6). However, the y-intercept for the line of best fit (19 816) was of similar magnitude to the response of the NTD extractions from hot car exhaust. As a result, the calibration plot was weighed by $1/x^2$, resulting in the relationship $y = 51\ 305x + 4145$, which was

then used to calibrate the SPME fiber and NTD on-site samplings.[108] Once the response relationship had been determined, further calibrations of the SPME extractions were performed using diffusion-based calibration, as described by Koziel et al.[109]

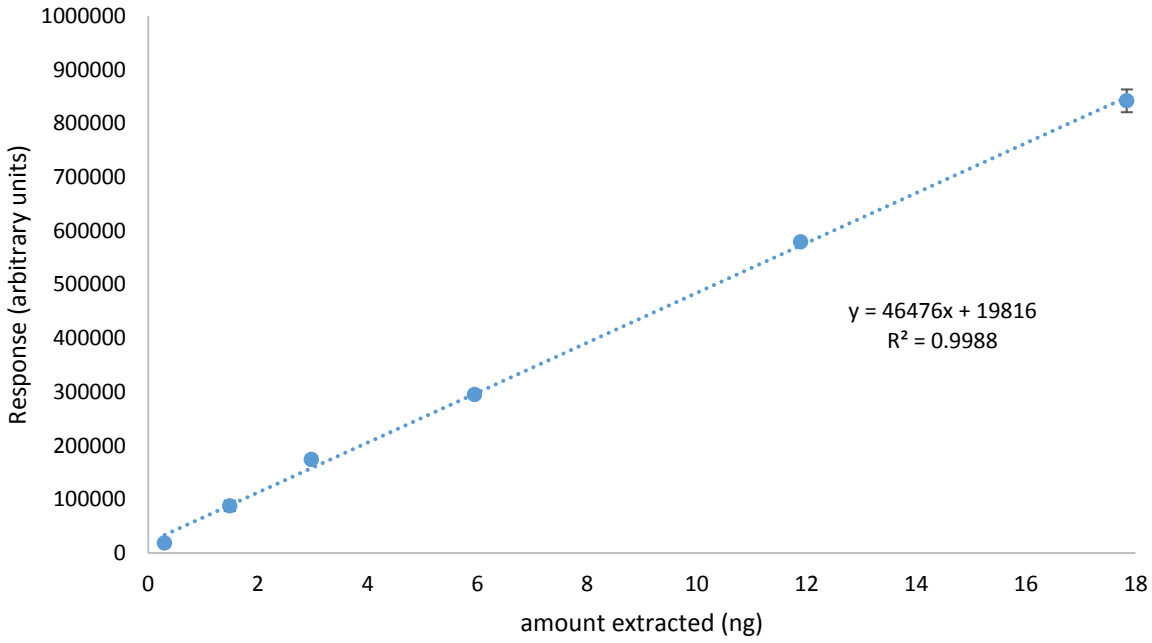

Figure 3.6 Calibration of gaseous formaldehyde employing on-fiber derivatization using a Tenax/Carboxen NTD. The NTD was loaded with PFPH by drawing 10 mL of headspace from two separate PFPH-generating vials. Subsequently, a varied volume from the headspace of a 0.04 wt% formaldehyde solution was drawn for extraction.

3.2.9.1 SPME fiber diffusion based calibration of formaldehyde

Calibration for the SPME car exhaust samplings was performed using the interface model of diffusion-based calibration described by Koziel et al., with Eq. 3.2 being applied due to the rapid sample flow rate (approx. 170 cm s^{-1}). The equations used in this calibration are given below, the first describing the gaseous concentration of the sample, as dependent on a range of variables described in Table 3.1 along with δ, the static boundary layer thickness. δ, in turn, is dependent on Re and Sc, the Reynolds and Schmidt numbers, respectively.

Eq. 3.1 $$C_g = 3\left(\frac{n}{t}\right)\left(\frac{\delta}{D_g 2\pi L b}\right)$$

Eq. 3.2 $$\delta = 9.52\left(\frac{b}{Re^{0.62}Sc^{0.38}}\right)$$

Where:

Eq. 3.3 $$Re = {2ub}/{v}$$

Eq. 3.4 $$Sc = {v}/{D_g}$$

Table 3.1 Variables and coefficients used in the diffusion-based calibration of formaldehyde in car exhaust for SPME fiber extractions.

Variable	**Meanings**	**Unit**	**Value used in this work**	
			Cold (T = 16.3 ºC)	**Hot (T= 45.7 ºC)**
C_g	Gaseous concentration	ng/m^3	calculated	
n	Mass extracted	ng	calibrated	
b	SPME fiber radius	m	0.00015	
D_g	Gaseous diffusion coefficient	m^2/s	$1.68 \cdot 10^{-5}$	$2.0 \cdot 10^{-5}$
L	SPME fiber length	m	0.01	
t	Sampling time	s	30	60
u	Linear velocity of sample	m/s	1.7	1.5
v	Kinematic viscosity	m^2/s	$1.75 \cdot 10^{-5}$	$1.48 \cdot 10^{-5}$

3.3 Results and discussion

3.3.1 PFPH vial long-term stability

Considering that current methods used in the generation of gaseous PFPH standards fail to provide a reusable headspace standard for extended periods of time, a requirement for on-site applications and standard storage, the long-term stability of PFPH within the standard gas generating vial was determined. As exemplified using a control chart at 2 standard deviations, shown in Figure 3.7, the vials were found to be stable over a 77-day period. This observation was further supported by having no vial which was sampled on days 3, 7, 14, and 77 exceeding a percent relative standard deviation (RSD) over 9% (Table 3.1). Similarly, storage conditions, sampling history, and cap type were found to have no impact on absolute fiber loadings as shown in Figure 3.8. Moreover, these results also indicated good inter-vial, intra-batch reproducibility for

PFPH fiber loadings with the pooled %RSD values for all vials tested on a given day providing %RSDs of 2, 5, 5, 5, and 9, for days 3, 7, 14, 30, and 77, respectively. Finally, and most impressively, when all extractions from all vials over the entirety of the stability study were considered, the average amount of PFPH loaded onto the DVB/PDMS SPME fibers was 2729 ± 196 ng, with an RSD of 7%. This observed reproducibility demonstrates the long lifetime of the vials which is due in part due to two main factors: (1) the negligible depletion of the vial after each extraction ensuring the headspace concentration remaining constant over time and (2) the enclosed headspace formed by the vial being successful at preventing the release of PFPH from the vial, or the introduction of impurities into the vial, which would otherwise result in a change in PFPH concentration.

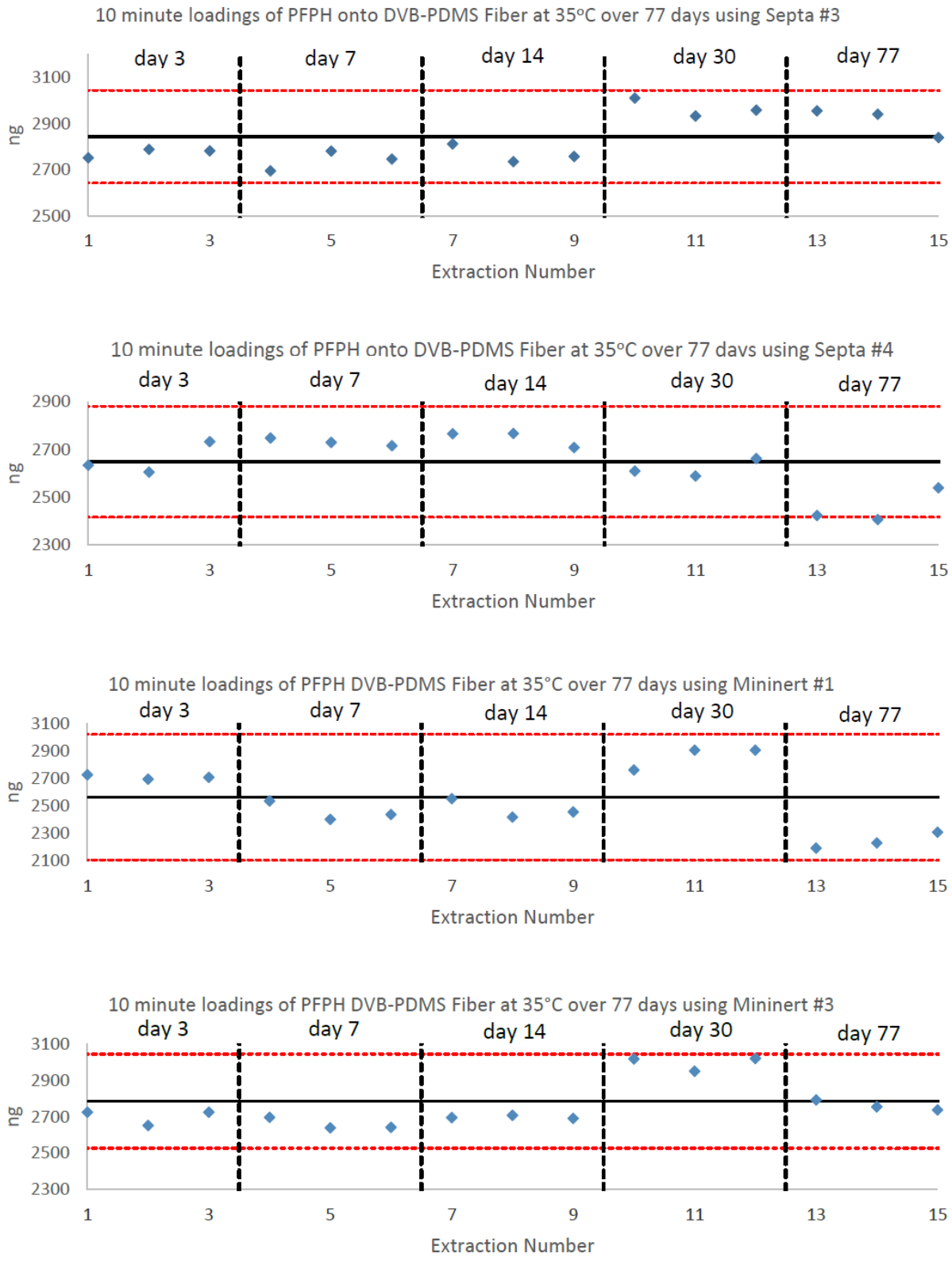

Figure 3.7 Amount of pentafluorophenyl hydrazine (PFPH) loaded onto a PDMS/DVB fiber over 77 days from all vials tested. Data were normalized by use of quality control experiments run daily.

Table 3.2.A: Intra-batch comparison of PFPH fiber loadings using the PFPH standard gas generating vials on days 3, 7, 30, and 77 of stability study, using a DVB/PDMS fiber for 10-minute extractions at 35 °C.

PFPH loading (ng)	Day 3			Day 7			Day 14		
Septa Vial 3	2752.2	2789.1	2782.6	2696.0	2780.5	2746.2	2811.7	2735.3	2758.0
Septa Vial 4	2633.3	2604.3	2732.6	2747.3	2729.4	2715.5	2766.1	2767.1	2707.4
Mininert Vial 1	2725.5	2695.0	2707.0	2535.0	2401.0	2437.6	2553.1	2418.0	2454.8
Mininert Vial 3	2724.5	2650.7	2724.5	2696.2	2638.3	2641.3	2693.6	2706.8	2690.5

Day average	2710.1	Day average	2647.0	Day average	2671.9
%RSD	2	%RSD	5	%RSD	5

Table 3.2.B: Intra-batch comparison of PFPH fiber loadings using the PFPH standard gas generating vials on days 3, 7, 30, and 77 of stability study, using a DVB/PDMS fiber for 10-minute extractions at 35 °C.

PFPH loading (ng)	Day 30			Day 77			% RSD*
Septa Vial 1	3114.2	3000.5	3048.1	2861.9	2796.7	2778.5	5
Septa Vial 2	2871.2	2883.7	2869.7	2756.8	2770.7	2893.8	2
Septa Vial 3	3010.9	2933.0	2958.4	2955.5	2941.1	2839.6	4
Septa Vial 4	2609.3	2588.6	2661.6	2423.0	2406.2	2539.4	4
Mininert Vial 1	2760.7	2905.8	2906.0	2193.0	2230.9	2308.7	9
Mininert Vial 2	2995.0	3011.7	3016.5	2403.3	2451.9	2417.0	12
Mininert Vial 3	3017.3	2948.8	3019.3	2791.3	2754.1	2736.9	5
Mininert Vial 4	2918.0	2858.9	2956.1	2609.6	2607.8	2553.5	7

Day average	2911.0	Day average	2625.9
%RSD	5	%RSD	9

* Percent relative standard deviation (%RSD) shown in the terminal column is calculated over all extractions from each respective vial over the duration of the stability study

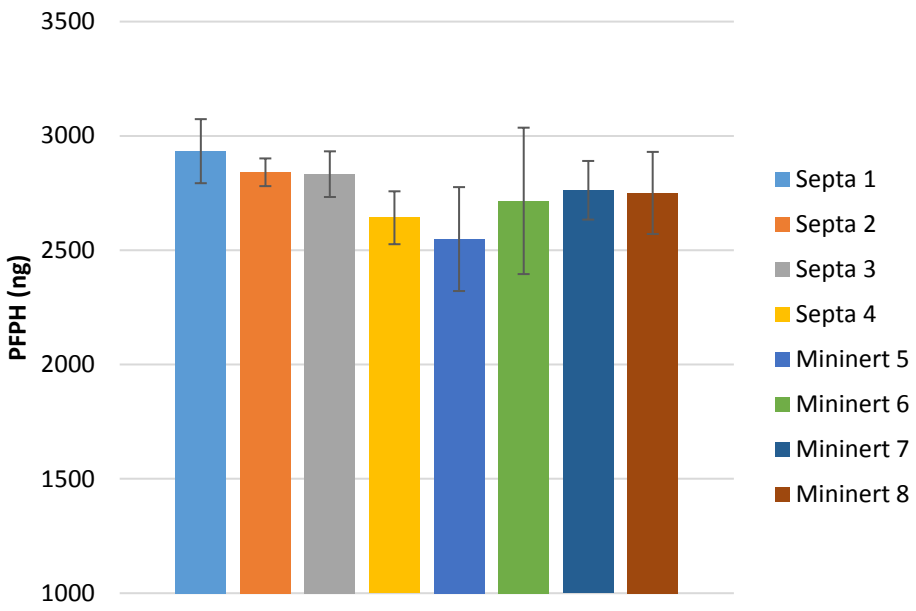

Figure 3.8 Quality control adjusted average PFPH fiber loadings over all extractions from all PFPH gas generating vials over 11 weeks, using a DVB/PDMS fiber for 10-minute extractions at 35 °C.

3.3.2 Reproducibility of the derivatization reaction

As PFPH fiber loadings were shown to be reproducible, we would expect that the derivatization reaction itself should also be reproducible. In order to confirm this, the reproducibility of the derivatization reaction was examined over a 7-day period. This validation was accomplished by using an aldehyde (C4−C9) standard gas generating vial in addition to the PFPH vial, with samplings being performed in triplicate at two-day intervals. Preloading of the SPME fiber with PFPH was performed for 5 min, followed by a 1 min exposure to the aldehyde-generating vial headspace. As demonstrated in Figure 3.9, the derivatization reaction was found to be very reproducible over the 7-day test period, with the response of the derivatized aldehydes remaining constant, as indicated by %RSD values of 4, 4, 4, 5, 5, and 9 for derivatized butanal, pentanal, hexanal, heptanal, octanal, and nonanal, respectively. The upward trend in %RSD with respect to molecular weight was thought to be a result of decreasing signals for these heavier aldehydes. This decrease in signal was likely due to a decrease in the headspace concentration of

the heavier aldehydes, as they possess a higher vial sorbent affinity and diffuse slower through the boundary layer of the fiber.[5]

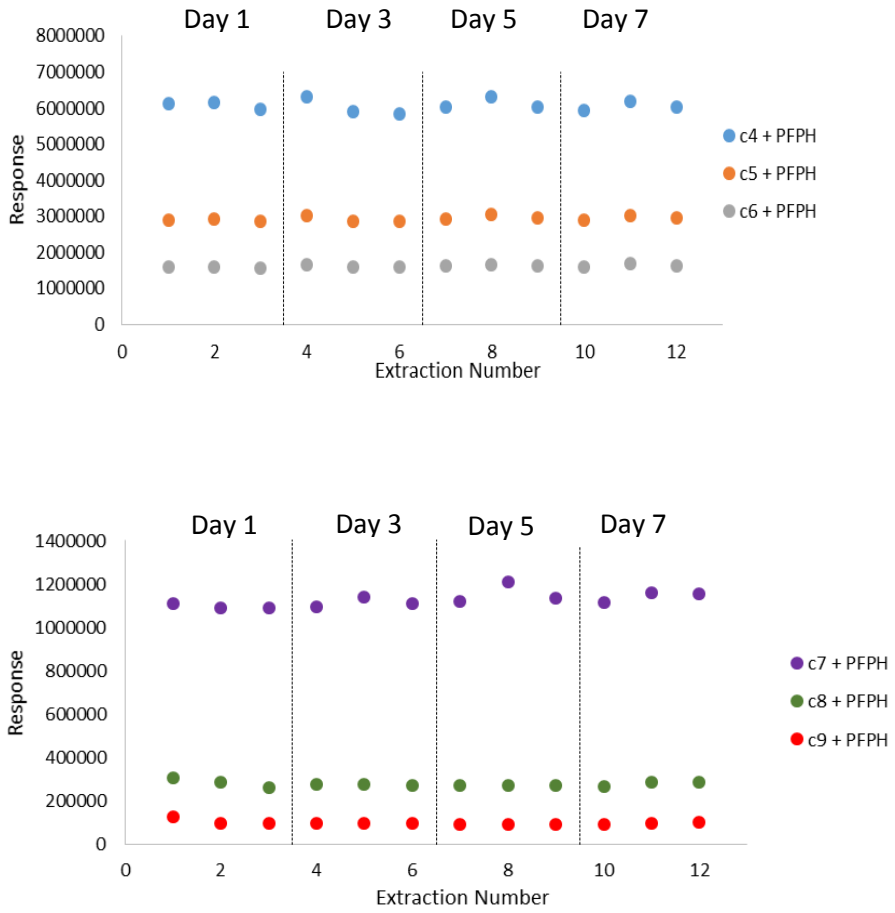

Figure 3.9 Reproducibility of derivatization of linear aldehydes (C4-C9) using PFPH standard gas generation vial reaction over time, using a DVB/PDMS fiber loaded with PFPH 5 minute extraction at 35 °C followed by a 1-minute extraction at 50 °C minute extractions at 35 °C.

3.3.3 Derivatization products extraction time profile

Although the derivatization reaction exhibited a good degree of reproducibility, even when performed repeatedly over 7 days, it was also important to ensure that the amount of derivatized product on the fiber could be predicted regardless of extraction time. Ideally, it would be expected that, as long as some residual PFPH remains on the fiber, aldehyde extraction should remain linear with a slope dependent on that aldehydes rate of diffusion across the fibers boundary layer. Hence,

a derivatization reaction time profile was conducted in order to confirm the linear uptake of the derivatization reaction products associated with the aldehydes studied. Using the aldehyde standard gas generating vial described previously, extraction times ranging from 10 s to 1 min were conducted while maintaining constant PFPH extraction conditions at 35 °C for 5 min.

As shown in Figure 3.10, all derivatized aldehydes exhibited a linear relationship between analyte response and aldehyde extraction time over the sampling interval tested. As the y-intercepts of some compounds are well above zero, two linear regions of analyte uptake are hypothesized to be present, though employing a sampling time of less than 10 s is not often practical.

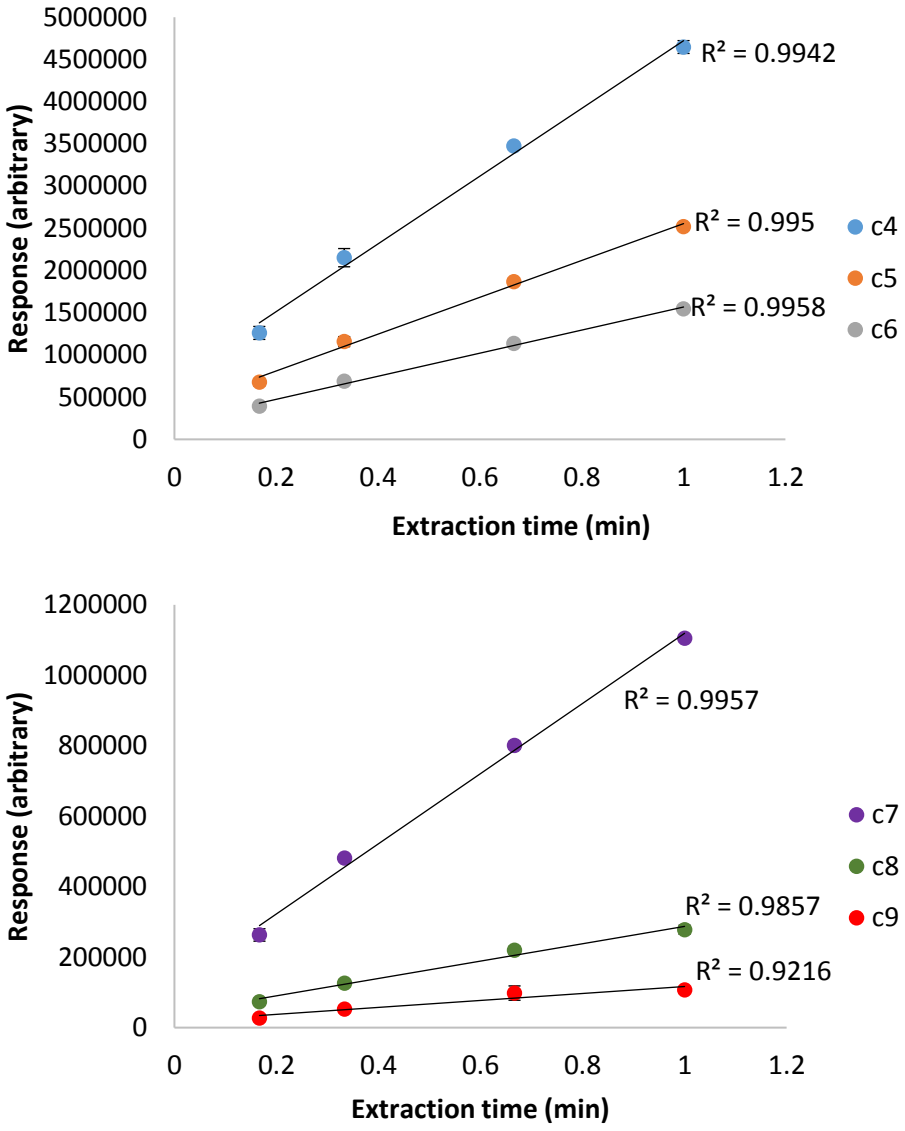

Figure 3.10 Extraction time profile of PFPH-derivatized n-aldehydes using a DVB/PDMS fiber and a 5-minute loading at 35 °C from a PFPH generation vial prior to an extraction of varied time from the headspace of a 0.04 wt% linear aldehyde solution.

3.3.4 Aldehyde concentration effect on response

Due to the wide range of aldehyde concentrations in environmental and anthropogenic matrices, it is imperative that reaction response is understood over a broad range of aldehyde concentrations. Furthermore, it would be advantageous if this response would exhibit a linear relationship, such that quantitation can be easily performed. In order to investigate whether the method demonstrates a linear response with respect to aldehyde concentration, samples containing

10−200 ppb of linear aldehydes C4 through C9 were formulated in aqueous solution. Prior to sample extraction, the SPME fiber was preloaded with PFPH for 5 min, followed by a 1 min exposure to the headspace of the aqueous standard. Each extraction was performed in triplicate. As clearly demonstrated in Figure 3.11 and Figure 3.12 which show the calibration plots for derivatized butanal, octanal, nonanal and pentanal, hexanal, octanal respectively the response of the proposed method demonstrated excellent linear correlation with sample concentration. No residual unreacted aldehydes were observed in any chromatogram throughout these concentration studies, thus confirming that the reaction between PFPH and the tested aldehydes is equally quantitative at room temperature as it was while using the aldehyde generation vial which was at 50 °C.

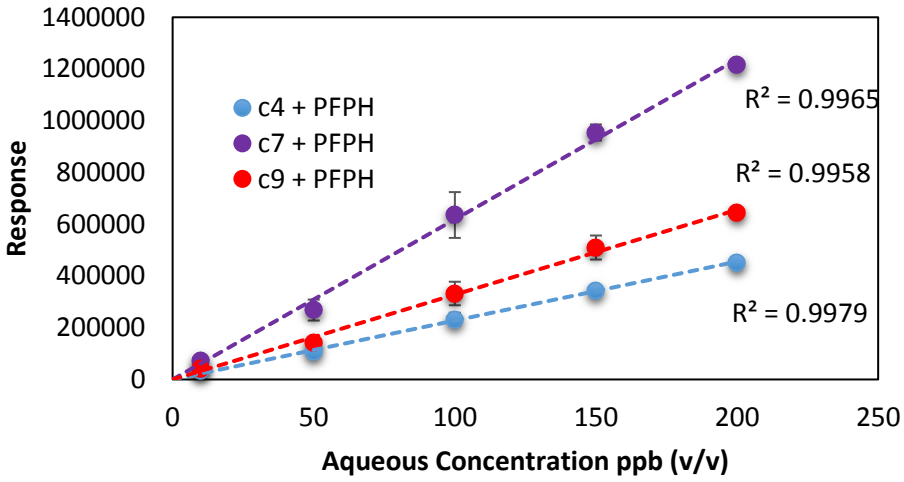

Figure 3.11 Demonstration of linear on-fiber derivatization response of butanal (c4), heptanal (c7), and nonanal (c9) for SPME headspace extractions above aqueous solutions ranging from 10 to 200 ppb (v/v) at room temperature, using a 1 min extraction.

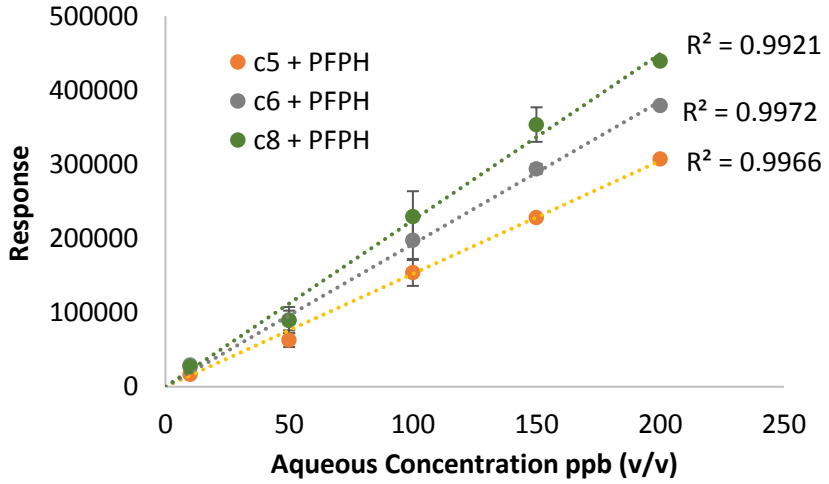

Figure 3.12 Demonstration of linear on-fiber derivatization response of pentanal (c5), hexanal (c6), and octanal (c8) for SPME headspace extractions above aqueous solutions ranging from 10-200ppb (v/v) at room temperature, using a one-minute extraction.

3.3.5 Extraction of aldehyde spoilage biomarkers from ground beef

With the confirmation of a reliable method, the versatility of the PFPH-generating vial was demonstrated by its application to the semi-quantitative analysis of aldehydes as markers for meat spoilage.[105] A range of aldehydes have been linked to the breakdown of fatty acids during the decomposition of meat products, particularly in beef and pork, and have been identified as contributing factors in the off-flavor and odor associated with spoiled meat.[110] A sample of medium ground beef, advertised as fresh, was obtained from a local grocery store. Identification of the derivatized aldehydes in the analyzed meat samples was performed by comparison of the retention times and mass spectra with those of derivatized standards of aldehydes (C4−C9). Figure 3.13 shows the bidimensional chromatograms obtained for aldehyde standards extracted with and without derivatization (a, b) and for extractions carried out on meat samples on the day of preparation (day 0) with and without derivatization (c, d). In addition, the isomerization of the derivatization reaction products was observed and could be resolved in two dimensions. A

magnified example of this can be seen in Figure 3.14 which shows the evolution of acetaldehyde resulting from the meat spoilage process.

The response of volatile aldehydes from the meat samples was generally observed to increase over time, though reproducibility was low between duplicate samples. This was likely a result of varying degrees of microbial activity in each sample, in part due to inhomogeneity of the meat sample.[110] Though ground beef was used, further homogenization would have likely provided more reproducible results. However, as a proof of concept, the application of the PFPH standard gas generating vial to the analysis of food products was a success. In particular, the sampling performed without derivatization only resulted in the detection of C7 through C10 aldehydes with very poor sensitivity, whereas derivatization allowed for the detection of a much broader range of aldehydes (C2 through C10).

In order to further test the applicability of the on-fiber derivatization approach, a 100 μm PDMS SPME fiber coating was also applied to the analysis of aldehydes from spoiled meat. This is particularly important, as PDMS coatings are more robust and have been applied to both ex vivo and in vivo samplings from tissues,[111] minimizing the occurrence of possible artifacts associated with the extraction process.[112] Due to the hydrophobic nature of the PDMS polymer, successful extraction of underivatized and short-chain aldehydes could prove to be difficult due to their polarity and relatively low concentrations. Consequently, the risk of losing important chemical information when sampling complex matrices with PDMS under underivatized conditions is high. By repeating the derivatization protocol with a PDMS 100 μm SPME fiber, C2, and C5−C9 derivatized aldehydes were observed, though lower responses were observed than those obtained for the DVB/PDMS coating. Considering what has been stated, it is evident that the PFPH standard

gas generating vial can be implemented in the monitoring of meat spoilage processes. However, the optimization of such a method is not within the scope of this work.

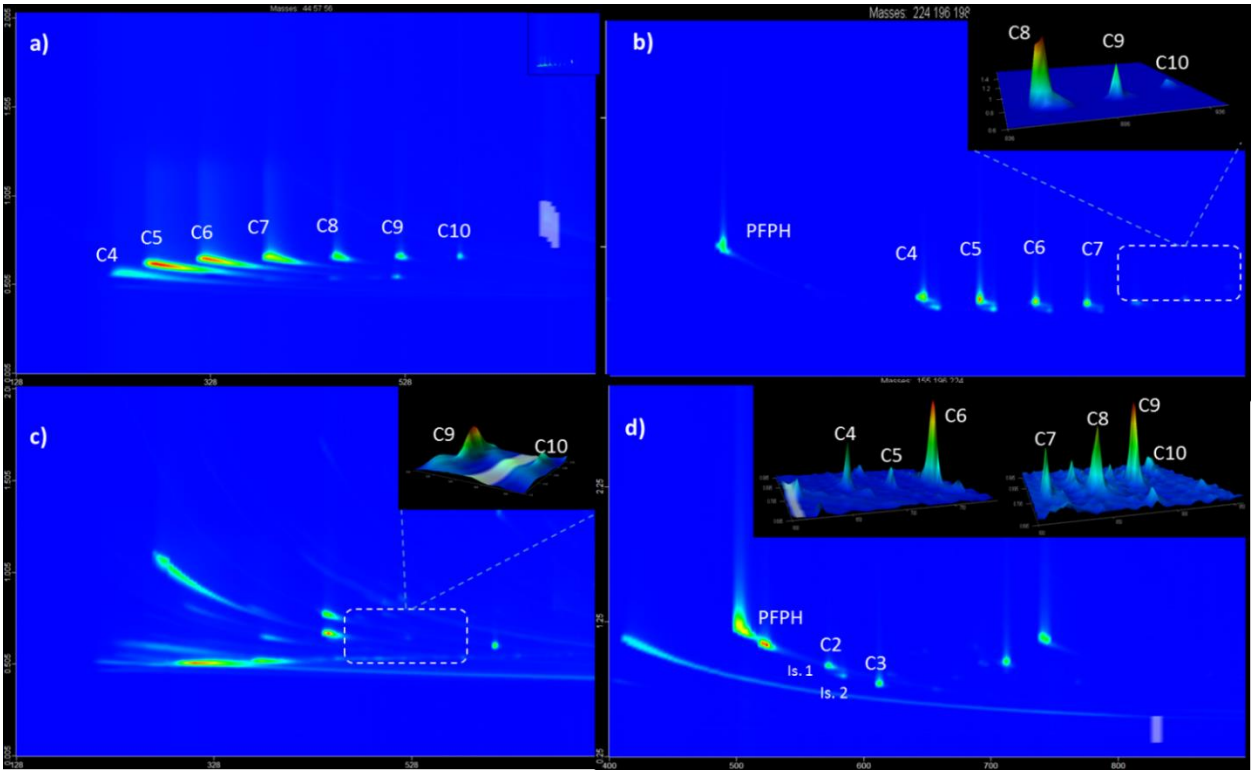

Figure 3.13 GCxGC-ToF/MS chromatograms of, A) underivatized, B) derivatized C4−C10 aldehydes standards, C) underivatized, and, D) derivatized aldehydes sampled from the headspace of freshly prepared ground beef meat samples.

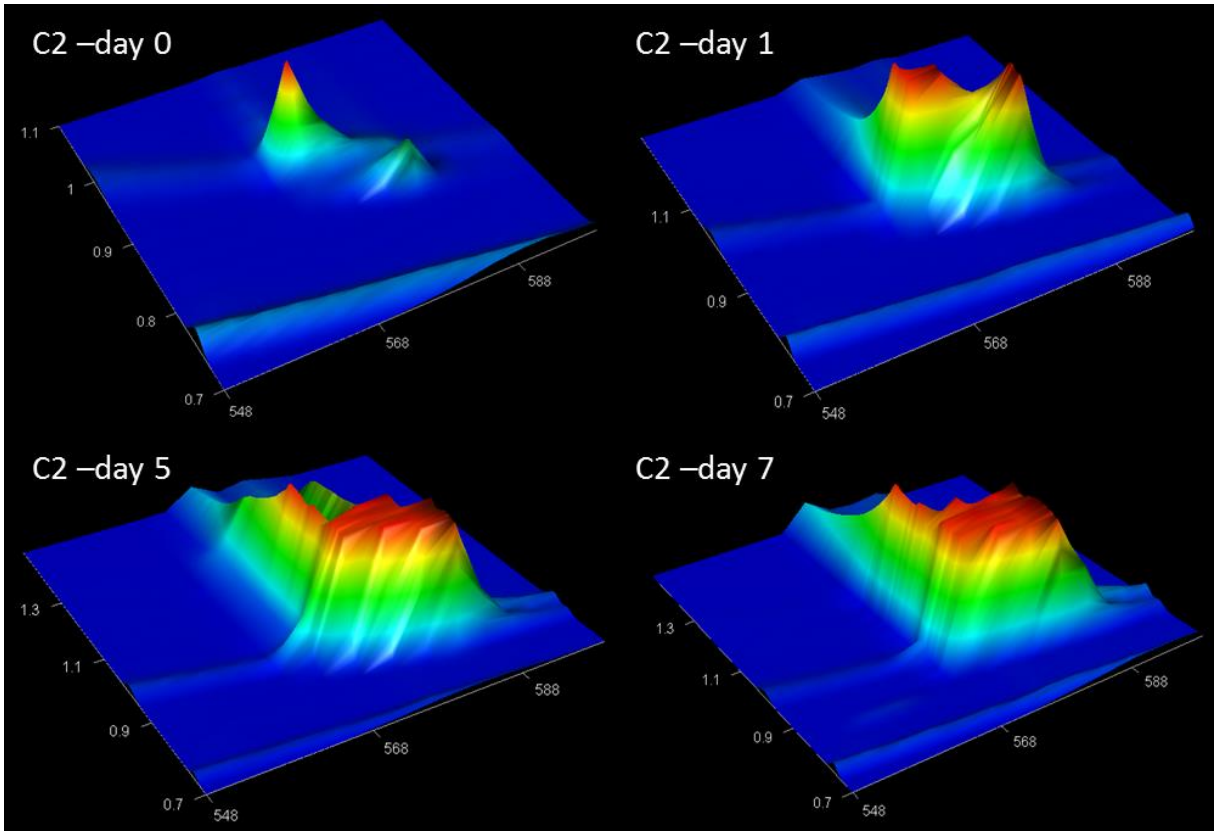

Figure 3.14 Observation of derivatized acetaldehyde over a period of 7 days resulting from meat spoilage, analyzed by on-fiber derivatization GCxGC-TOF/MS using a DVB/PDMS fiber loaded with PFPH for 10 minutes at 35 °C from a standard gas generating vial, followed by a 30 minute exposure to the headspace of 5 g of ground beef at 35 °C.

3.3.6 Intra and inter-day stability of the portable GC-MS detector response following a cold start

In order to generate reliable quantitative results with an on-site analytical methodology, it is imperative to first show that the related portable instrumentation is itself capable of providing consistent results. Furthermore, it is important to consider that, unlike traditional benchtop GC/MS instrumentation, hand-portable instruments need to be able to pump down and stabilize quickly following a cold start within the time limitations imposed by an on-site sampling environment and battery operation. As such it was demonstrated that the Tridion-9 portable GC/TMS was able to achieve repeatable detector response for a BTEX standard mixture 30 minutes following a cold start of the instrument. Furthermore, as shown in Figure 3.15 this response was shown to be stable

at 2 SD over a continuous 24 hour period. It is also important to note that the instrument was further shown to generate stable inter-day results after being continuously rebooted at various river-side sampling locations. These results, which were generated during a later study, can be viewed in Figure 5.6 of Section 5.3.3 of this thesis.

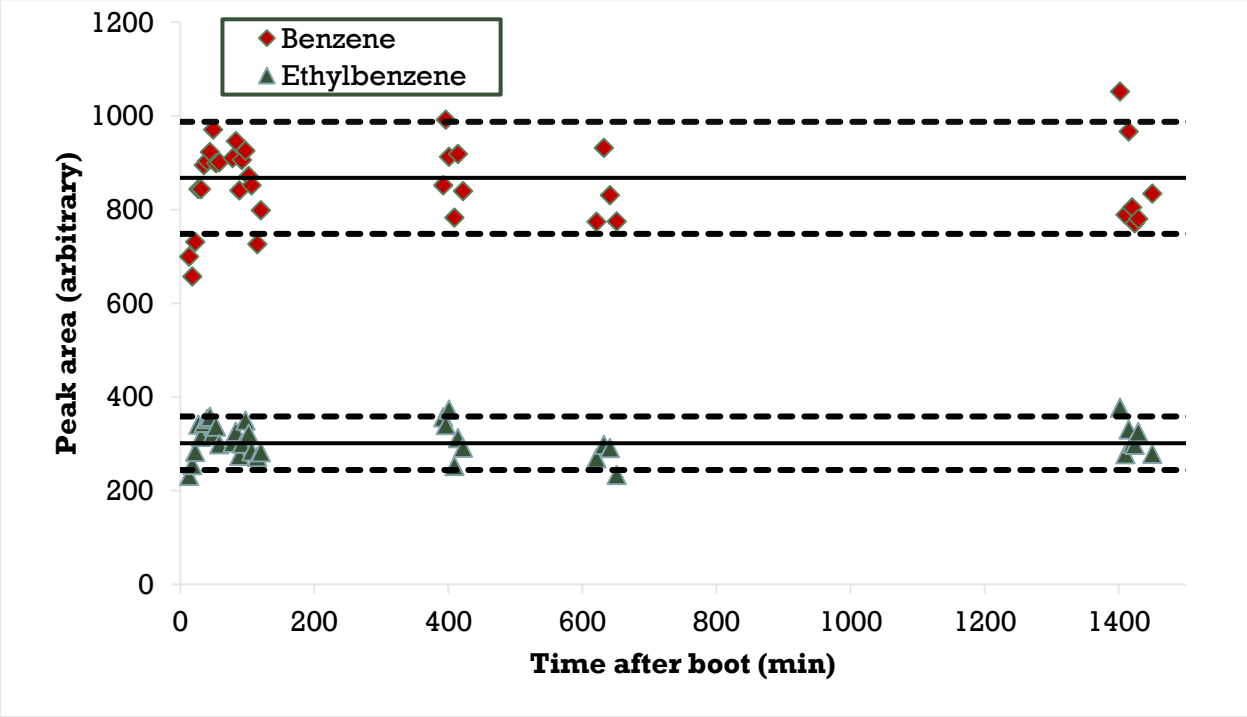

Figure 3.15 24 hour stability of the Tridion-9 GC/TMS following a cold start of the instrument. Control plot was plotted at 2 standard deviations of the mean. Extractions were performed using a DVB/PDMS SPME fiber from a BTEX standard gas generating vial at 35 °C for 1 minute. Desorption was carried out using a 10:1 split ratio.

* Toluene and o-xylene results omitted due to data overlap

3.3.7 Application for on-site quantitation of formaldehyde in car exhaust

As a final proof of concept, the portability of the PFPH-generating vial was confirmed by coupling the method to hand-portable GC/MS instrumentation for the quantitative on-site determination of formaldehyde from car exhaust. In order to compare the free and total formaldehyde concentrations before and after heating of the catalytic converter, both needle trap and SPME extractions were performed in triplicate from cold and hot car exhaust. These sampling

methods, namely, SPME and NTD, were selected because NTDs are able to extract both free and particulate-bound analytes in an exhaustive manner,[33] while SPME fibers are only sensitive to the gaseous, unbound analyte fraction. This allows the analyst to compare the free and total analyte concentrations by SPME and NTD, respectively, so as to characterize the fraction of particulate binding of a given analyte, in this case, formaldehyde. After extraction, both extraction devices were analyzed on-site using a portable GC/TMS. The derivatization product of formaldehyde was identified by the molecular ion of m/z = 210, and residual PFPH was verified to be present as described in Figure 3.3 to ensure PFPH excess. Instrument responses were calibrated to nanograms using the NTD calibration method, resulting in the relationship presented in Figure 3.7 ($y = 46476 + 19816$, $R^2 = 0.9988$) which was $1/x^2$ weighed to obtain $y = 51305x + 4145$ relationship which was used to convert response to nanograms extracted. For the needle trap extractions, the concentration of formaldehyde found in car exhaust was easily determined by the use of Eq. 3.1. However, as SPME is an open-bed equilibrium based extraction method, a diffusion-based calibration method was required.[109] The specifics of the employed diffusion-based calibration can be found in Section 3.2.9.1. As can be seen in Table 3.3, no significant differences were observed between the concentrations of formaldehyde determined using the SPME fiber or NTD from the hot car exhaust samples, though differences were observed in the cold car exhaust samples. With this in mind, it is possible to conclude that the vast majority of formaldehyde generated and subsequently vented via this particular exhaust system was in the gaseous fraction when the vehicle was running at its operational temperature. On the other hand, the results obtained for the cold car exhaust extractions indicate significant binding of formaldehyde to the particulate matter and aerosols generated and subsequently released by the vehicle immediately after engine ignition. Although we would typically expect the highly volatile formaldehyde molecule to preferentially

move to the free, gaseous fraction of the sample at ambient temperatures, the presence of water laden aerosol particles may have greatly increased the particulate bound concentration as formaldehyde would tend toward dissolution into the aqueous portion of the aerosol particle. This again highlights the strength of using both SPME and NTD to fully characterize the speciation of analytes in real systems.[33] Furthermore, another interesting observation could be made with regards to the effectiveness of the catalytic converter, as indicated by the reduction of total formaldehyde concentration by a factor of approximately 10 times when hot and cold car exhaust are compared. Most importantly, this experiment may very well outline the first instance where quantitative analysis of formaldehyde was successfully performed entirely on-site with GC/MS instrumentation. Moreover, these experiments have demonstrated just how portable SPME methods can be; among its many advantages, SPME allows for the on-site performance of repeated derivatizations of a target analyte from real samples when coupled to portable instrumentation.

Table 3.3 On-site determination of free and total concentrations of formaldehyde from car exhaust pre- and post catalytic converter ignition using a 10 min PFPH loading time for SPME extractions and a 15 mL sample volume for NTD from a PFPH generating vial at 35 °C.

Extraction Condition	Exhaust Temperature	Sampling Device	Formaldehyde (ng/mL-exhaust)
Pre-catalytic convertor ignition	16.3°C – Cold	NTD	0.37 ± 0.02
		Fiber	0.18 ± 0.02
Post-catalytic convertor ignition	45.7°C – Hot	NTD	0.042 ± 0.003
		Fiber	0.035 ± 0.005

3.4 Conclusion and future directions

A novel standard gas generating vial suitable for SPME on-fiber derivatization of aldehydes has been developed, while also demonstrating the ability of the standard gas generating vial to store gaseous standards of a highly reactive compound for extended periods of time. The application of this technology results in the use of no organic solvent while also reducing the

consumption of a toxic and highly reactive derivatization reagent, due to the reusability and stability of the compound in the vial developed. In addition, the PFPH generating vial was successfully shown to provide a means by which to perform derivatization from food matrices facilitating the targeted analysis of carbonyl compounds from a complex sample matrix. The PFPH generating vial was then applied to the completely on-site determination of formaldehyde from car exhaust, owing to the portable nature of the standard gas generating vial. The application of the in-vial standard gas generator for derivatization agents is expected to be expanded into a range of fields including clinical, food, environmental, and forensic analysis. Once fully realized, on-site sample derivatization and/or analysis owes itself to exciting new applications of sampling, particularly for analytes which may not be stable under storage or transport conditions to the laboratory.

Chapter 4 Development of a carbon mesh supported thin film microextraction membrane as a means to lower the detection limits of benchtop and portable GC/MS instrumentation

Preamble

The majority of the materials in this chapter have been published as a research article: Jonathan Grandy, Ezel Boyacı, Janusz Pawliszyn; Development of a Carbon Mesh Supported Thin Film Microextraction Membrane As a Means to Lower the Detection Limits of Benchtop and Portable GC/MS Instrumentation; *Anal. Chem.,* **2016**, 88(3), pp 1760-1767. Materials for all sections of this current Chapter, with the exception of Sections 4.2.6 and 4.3.3, are reprinted from this research article with the permission of Analytical Chemistry of the American Society of Chemistry (ACS). Copyright for this work remains the property of ACS publications and any further request for re-use of this information should be requested directly from them (**DOI:** 10.1021/acs.analchem.5b04008)

4.1 Introduction

Since being introduced in 1989, solid phase microextraction (SPME) sampling techniques have demonstrated steady growth in the field of analytical chemistry.[6–7,13] Of the many formats available today, the original SPME fiber-based geometry has been by far the most widely used worldwide, largely due to its miniaturized, easy-to-handle design that lends itself well to both high-throughput and on-site applications.[5,6,11] This has been prominently exemplified with a plethora of environmental, biological, industrial, food, and fragrance targeted analytical approaches, which are generally coupled to hyphenated gas chromatographic (GC) techniques.[11,21,113–117] However, standard fiber-based SPME is not without its limitations; the same miniaturization which allows the SPME fiber to be directly introduced into a GC injector inherently limits the surface area and volume of the sorbent coating.[29,48] A limited sorbent volume, in turn, fundamentally limits the

amount of a given analyte that can be extracted at equilibrium, as dictated by the fiber-sample partitioning coefficient, K_{fs}.[5,11,50] In addition, the small surface area available on a fiber directly controls the rate of analyte uptake and, consequently, method sensitivity during the linear pre-equilibrium regime of extraction.[5,11,22]

Hence, surface area becomes highly important when rapid, pre-equilibrium analyses of semi-volatile components, such as pesticides, are performed. To account for these shortcomings, recent work in microextraction technology has shifted toward the development of high surface area, membrane-based SPME samplers.[26,29,47,50,118]

Membrane SPME, also known as thin-film microextraction (TFME), is a relatively new avenue in microextraction techniques that have been successfully used for both GC- and high-performance liquid chromatography (HPLC)-based applications.[48,50] Membranes developed for GC applications have generally employed similar polymeric make-ups commercially used in standard SPME fibers, including polydimethylsiloxane- (PDMS), polydivinylbenzene (DVB), and Carboxen.[22,26,47,50] Initial works with TFME-GC techniques employed the use of premanufactured thin sheets (127 or 254 μm) of pure PDMS as an extraction phase.[49,50,119] Using this PDMS design, Qin et al. were able to demonstrate that a 10 cm^2 membrane provided approximately 10x the extraction efficiency for fluoranthene and pyrene when compared to commercially available PDMS sorptive stir bar technology (area = 1 cm^2).[47] Such a result was directly in line with what was expected theoretically, as shown in Eq. 4.1 below, where the amount of analyte extracted as a function of time (dn/dt) is directly proportional to the surface area (A) if all other factors are kept constant.[5,47,49] Despite this marked improvement, such preconstructed membranes are limited to PDMS in terms of available sorbent phases. Additionally, such large membranes required the construction of a supporting frame for direct immersion sampling with agitation.[47] Further works

in the area have explored the in-house preparation of particle-loaded PDMS membranes with and without the use of an inert supporting material.[26,47,118]

$$\frac{dn}{dt} = C_s\left(\frac{D_s A}{\delta}\right) \qquad \text{Eq. 4.1}$$

One such design, suggested by Jiang et al., utilized a platinum catalyzed PDMS preparation kit (SILGARD 184), such that macroporous DVB resin particles (diameter of 3−5 μm) could be suspended into the membrane.[26] The optimal DVB/PDMS ratio was found to be 20:100 (16.7%) w/w, with a compromise being made between extraction efficiency and the mechanical stability of the said membrane. Results from this study indicated that the composite membranes were much more efficient at extracting highly volatile and polar compounds such as toluene and benzaldehyde, respectively. However, without an appropriate support, these membranes proved to be very difficult for highly turbulent or agitated direct-immersion sampling. Additionally, experience has shown that inserting membranes greater than 6 mm in diameter into the thermal desorption unit (TDU) desorption tube commonly results in breakage. A final observation indicated that these membranes exhibited considerable siloxane bleed/background even after 10 h of thermal conditioning. Prior to the above-mentioned study, Riazi-Kermani et al. employed a similar polymeric mixture onto a thin fiberglass mesh to prepare the first-ever composite, supported TFME membrane.[47] These supported membranes were found to be much more physically stable than the composite TFME membranes introduced by Jiang et al., withstanding aqueous agitation rates of 800 rpm without folding, while surviving at least 50 consecutive injections. These 10 cm^2 membranes were also shown to extract between 46 to 117 times the amounts of analyte compared to traditional DVB/PDMS SPME fibers. However, one major limitation of this study was that it failed to address the likely presence of major siloxane bleeding that would occur when desorbing a composite membrane of this size. It is expected that if selected

ion monitoring (SIM) had not been used, background siloxane levels would have completely overloaded the detector, making such a membrane inappropriate for untargeted analysis. With this in mind, the choice of a more thermally stable PDMS for the preparation of a supported DVB/PDMS composite membrane would be ideal for untargeted analysis.

In the present work, one such membrane is proposed. By use of a high-density PDMS prepolymer in combination with DVB particles, spread onto a carbon-based mesh support, similar extraction efficiencies could be obtained while substantially lowering the inherent siloxane background. Furthermore, the carbon mesh was also found to provide some affinity for the analyte, which would provide an advantage over a comparable fiberglass-supported membrane in equilibrium conditions. These low-bleed membranes were also coupled with hand-portable GC-TMS technology, which allows for on-site detection limits well below what is currently thought possible.[52] Most impressively, these membranes are herein demonstrated to allow for sub-ppb detection of multiple organochlorine and organophosphorus pesticides from an aqueous matrix on the aforementioned portable GC-TMS instrument.

4.2 Materials, instrumentation, and experimental methods

4.2.1 Chemical and materials

2,4-Dichlorophenol, 2,4,6-trichlorophenol, carbofuran, atrazine, fonofos, chlorpyrifos, and parathion standards were purchased from Sigma-Aldrich (Mississauga, ON, Canada). Phorate D10 was purchased from CDN Isotopes Inc. (Quebec, Canada). HPLC grade methanol, isopropanol, hexane, and acetonitrile were obtained from Caledon Laboratories Ltd. (Georgetown, ON, Canada). Ultrapure water was obtained using a Barnstead/Thermodyne NANO-pure ultrapure water system (Dubuque, IA). The SYLGARD 184 silicone elastomer mix was acquired from Dow Corning (Midland, MI). The 5 μm diameter DVB particles and high-density PLOT PDMS were

provided by Supelco (Bellefonte, PA). The carbon fiber mesh weave (Panex 30) was provided by Zoltec Co. (Bridgetown, MO). The 250 mL Wheaton glass bottles were purchased from Thermo-Fischer Scientific (Ottawa, ON, Canada). Liquid nitrogen and ultrahigh-purity helium were supplied by Praxair (Kitchener, ON, Canada). Miniature helium cylinders (99.5%) were supplied by Torion Technologies Inc. (UT). The 65 μm divinylbenzene/polydimethylsiloxane (DVB/PDMS) SPME fiber assemblies and empty stainless steel (SS) sorbent tubes were provided by Sigma-Aldrich. The Tenax/CAR Custodian needle trap device and Calion-13 standard mixture (containing acetone, methyl tert-butyl ether, methylene chloride, heptane, methylcyclohexane, toluene D8, perchloroethylene, bromopentafluorobenzene, bromoform, 1,2-dibromo-tetrafluorobenzene, methyl salicylate, tetrabromoethane, and tetradecane, ordered by volatility) were supplied by Torion Technologies Inc. (American Fork, UT). The Twister sorptive PDMS stir bar (1.5 cm long) was supplied by GERSTEL Co. (Mülheim an der Ruhr, GE). The membrane conditioning unit was developed at the University of Waterloo Science Electronics Shop (Waterloo, ON, Canada). Stainless steel cotter pins were supplied by Spaenaur Inc. (Kitchener, ON, Canada). Teflon holders were created by the University of Waterloo Science Shop (Waterloo, ON, Canada). The Elcometer 4340 motorized automatic film applicator and coating bar (adjustable gap of 0−250 μm) were acquired from Elcometer Ltd. (Rochester Hills, MI). The Mastercraft Maxxam 18 V powerdrill was purchased from Canadian Tire (Waterloo ON, Canada).

4.2.2 Instrumental analysis method (benchtop GC/MS and portable GC/MS)

Analytical instrumentation used for separation and quantitation included an Agilent 6890 GC and a 5973 quadrupole MS (Agilent Technologies, CA) coupled with a Gertsel cooling injection system (CIS) 4, Twister thermal desorption unit (TDU), and a MPS2 autosampler for membrane desorption and injection (GERSTEL, Mülheim an der Ruhr, GE). Additionally, a

Torion Tridion-9 GC- toroidal ion trap MS coupled with a prototype high volume desorption (HVD) module (Torion Technologies Inc. UT) was used to evaluate and compare membrane sensitivity for on-site analysis.

Chromatographic separations on the Agilent 6890-5973n were performed on a 30 m × 0.25 mm i.d. × 0.25 μm SLB-5 fused silica column (Sigma-Aldrich, Mississauga, ON). Helium carrier gas was used at a flow rate of 1 mL/min. The column temperature was initially held at 40 °C for 2 min, ramped to 200 °C at a rate of 10 °C min^{-1}, then kept for 2 min. The MS detector transfer line temperature, MS quadrupole, and MS source temperature were set at 300, 150, and 230 °C, respectively. Gas phase ions were generated using electron impact ionization, and the quadrupole was operated in full scan mode in the ranges of 35−400 m/z.

Chromatographic separations for untargeted analysis on the Tridion-9 were performed using a low thermal mass (LTM) MXT-5 (5 m × 0.1 mm × 0.4 μm) Siltek-treated stainless steel column (Restek Co. Bellefonte, PA). Helium carrier gas was used at a flow rate of approximately 0.3 mL min^{-1}. Different oven methods were used depending on the experiment being performed and will hence be disclosed in their own section. To maximize sensitivity while preventing any needle carryover, desorption of the Tenax/CAR 19-gauge needle trap transfer device was carried out at 280 °C for 20 s in splitless mode, followed by opening of the 10:1 split for 10 s, and then further opening of the 60:1 split for a final 10 s. The ion-trap heater was set to 155 °C with a transfer-line temperature of 250 °C during analysis. Ionization was performed using an electron-gun EI ion-source, and the trap was operated in a reduced scan mode in the ranges of 43−325 m/z).

4.2.3 Operation of the high volume desorption modules

In order to perform membrane desorption on the Twister TDU, an inert glass bead was first placed into the tapered 5 mm i.d. glass desorption tube to prevent the flat membranes from falling

through the tube bottom. Desorption was carried out at 250 °C using a helium stripping gas flow of 60 mL min^{-1} for 5 min. The desorbed analyte was then cryo-focused at −80 °C within the CIS module for the duration of the 5 min desorption. Following desorption, the CIS was then ramped to a temperature of 270 °C at a rate of 10 °C s^{-1} so as to perform splitless transfer of the analyte onto the Agilent 6890 GC-column for separation and quantitation.

In order to perform membrane desorption on the portable HVD prototype, membranes were placed into empty 3.5 in. stainless steel sorbent tubes. Next, the tubes were placed into the conventional trap holder, which was then fit into the body of the HVD module. Following, an adapter was placed on top of the conventional trap holder, which creates an airtight seal between the 3.5 in. sorbent tube and the 19-gauge Tenax-CAR needle trap device (NTD). A pair of heated clamps placed within the HVD module was then secured onto the sorbent tube, allowing for the 250 °C thermal desorption of the contained membrane. Subsequently, helium stripping gas was passed through the sorbent tube and into the attached NTD for 5 min. This process, outlined graphically in Figure 4.1, allows analytes to be transferred from the thin film membrane and onto the commercially available 19-gauge NTD, which can then be injected directly onto the Tridion-9 portable GC-TMS for separation and analysis. The HVD prototype system was thoroughly tested to ensure complete transfer of the analytes from the membrane to the NTD, ensuring no membrane carryover or needle trap breakthrough was occurring.

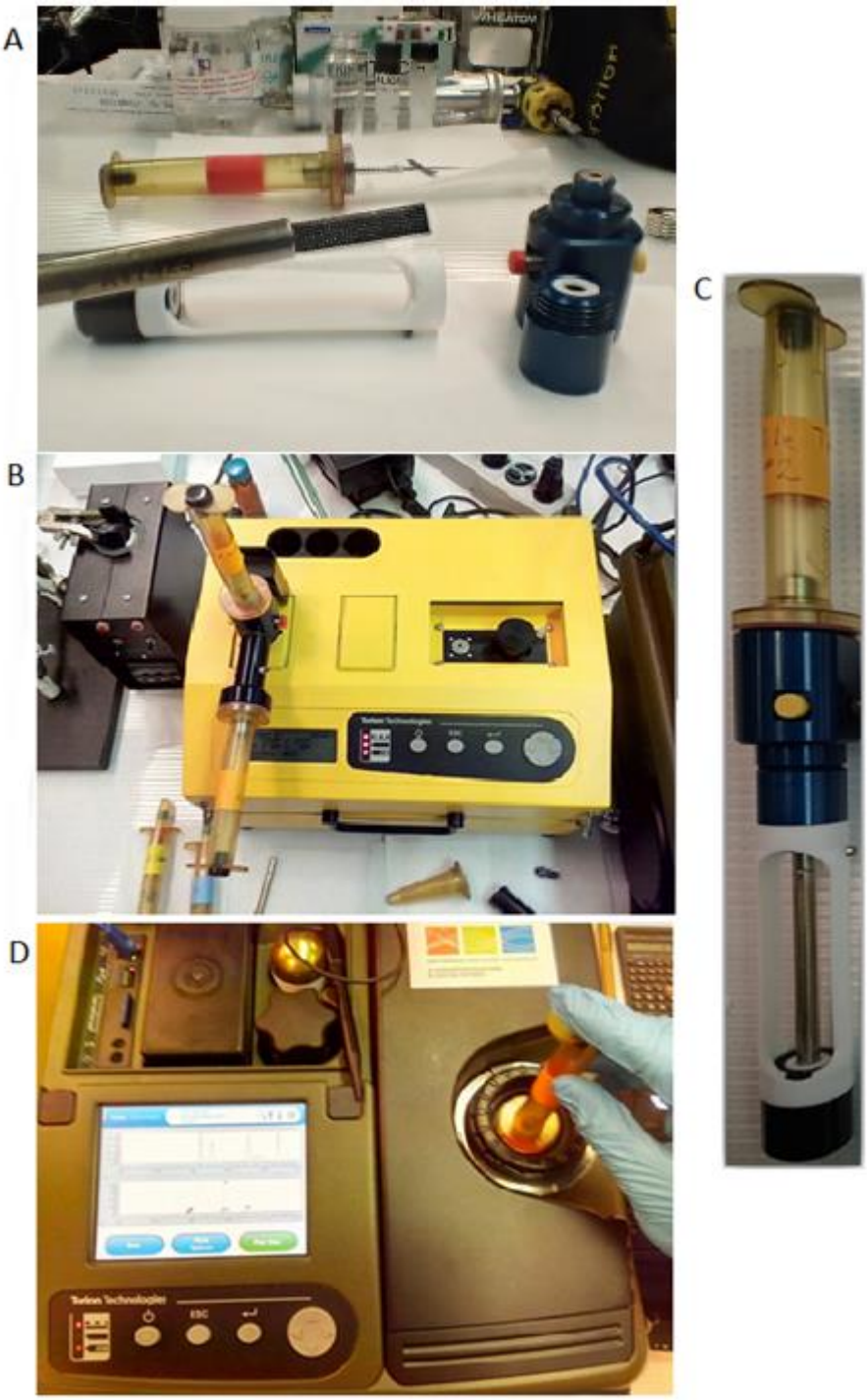

Figure 4.1. Desorption of TFME membranes onto the portable high-volume desorption module:
(A) Insertion of the membrane into 3.5“ sorbent tube, and into conventional trap holder.
(B) Transfer of analytes from TFME membrane to the needle trap using SPS-3 desorption unit (in breakthrough test configuration).
(C) Non-leaking linkage between the sorbent tube and 19-gauge needle trap device.
(D) Desorption of needle trap onto portable GC-TMS for separation and analysis.

4.2.4 Preparation of the carbon mesh particle-loaded membranes

Following the methodology described by Jiang et al., in order to first disperse the mesoporous 750 m^2 g, 5 μm DVB particles, a solvent was used to ensure homogeneous distribution of these particles.[26] To accomplish this, 0.450 ± 0.005 g of DVB particles were accurately weighed into a 20 mL headspace vial. A volume of 16 mL of hexane was then pipetted into this vial, and the mixture was vortexed for 1 min and then sonicated for 30 min. After mixing, 2.450 ± 0.02 g of the high-density PDMS pre-polymer was weighed into the same vial and vortexed for an additional 2 min, followed by 1 h of sonication. Most of the hexane was then volatilized from the mixture by purging the vial with nitrogen gas. Optimal viscosity was chosen subjectively when the mixture appeared to just barely flow when inverted in the vial. Future improvements upon this method could be made by weighing the mixture when this viscosity is achieved such that the same mass could be used in future preparations, lending to improved inter-batch reproducibility. Following these steps, 120 μL of the peroxide-based catalyst was pipetted into the mixture and manually mixed using a spatula for approximately 1 min.

Concurrently, a 25 cm × 60 cm (approx.) sheet of the carbon mesh was cut and secured to the Elcometer 4340 motorized film applicator. The coating mixture was then manually placed in a thin strip along the top of the carbon mesh sheet. The coating bar gap was adjusted to the thinnest setting available and then used to slowly spread the sorbent mixture across the carbon mesh surface. The coating was then cured inside a nitrogen-purged vacuum oven at a pressure of 15 torr (approximately), and at 190−200 °C for a period of at least 16 h. As the membranes are double sided, the entire process needed to be performed a second time to complete the membrane. Once both sides were cured, individual membranes were manually cut into two different, instrument-dependent sizes (2 cm × 4.85 mm for the Gerstel TDU and 4 cm × 4.85 mm for the prototype HVD

module). A brass template and sharp utility knife were used to make these cuts. It is important to note that it is essential to make a clean cut when preparing membranes so as to avoid the loss of small strands of carbon, which can block the injector during desorption. Coating the membrane edges in polytetrafluoroethylene (PTFE) was also found to further prevent this loss; however, this will not be further discussed herein, as it falls outside the scope of the current research.

Membranes were conditioned under nitrogen at 250 °C for 4 h using a membrane conditioning unit developed in-house by the University of Waterloo electronics shop. Once cooled, these membranes were washed in a 25:25:25:25 water/methanol/ isopropanol/acetonitrile v/v/v/v mixture for 2 h and then airdried on Kimwipes. Before use, all membranes were submitted to a final 30 min conditioning step at 250 °C inside the respective thermal desorption unit. In line with the standard SPME procedure, it is also recommended that this final conditioning step be re-performed whenever the membranes have been stored without use for long periods of time.

4.2.5 Comparison of membrane bleed and instrument background

To contrast the levels of detectable bleed, three of the DVB/PDMS/carbon mesh membranes described herein were compared with three DVB/PDMS unsupported membranes that were prepared using the method described by Jiang et al.[26] As membranes typically produce more bleeding after sitting for a greater period of time, a single blank desorption was performed 24 h prior to the comparative runs. Desorption and analysis were carried out on the Agilent 6890- 5973n instrument, with a GC runtime of 20 min.

4.2.6 Inter-batch reproducibility of the DVB/PDMS/Carbon Mesh supported TFME membrane

As to ensure the TF-SPME preparation procedure yielded statistically reproducible membranes, an intermembrane reproducibility study was also performed using a total of nine DVB/PDMS-Carbon mesh supported membranes selected from three unique batches. Extractions

were performed from a 250 mL McReynolds headspace generating jar at 55 ^{o}C for 10 minutes under static conditions. These conditions were specifically selected such that the volatile benzene was in near equilibrium with the membrane while the less volatile octane was still exhibiting near linear extraction kinetics thus, simultaneously testing for variances in sorbent volume and membrane surface area, respectively. All results were calibrated and presented in terms of nanograms by using a nanogram extracted versus response calibration curve generated by direct spiking of various volumes of liquid standards onto the TFME membranes. In order to confirm said reproducibility a total of nine membranes from three different batches were compared using a one-way ANOVA test at 95% confidence for each of the 6 McReynolds analytes. To avoid overloading of the MS detector while remaining in the calibration range, a 75:1 split injection was used. All extractions were randomized to account for any undetected drift of detector response while QC extractions were performed before and after the experiment.

4.2.7 Validation of the portable high volume desorption interface

To verify that the portable high volume desorption module was capable of completely transferring all of the analytes to the needle trap device, a series of membrane carryover and needle trap breakthrough tests were performed. 3-second TFME extractions were performed from the heavily concentrated Calion-13 standard tuning mixture at room temperature. Such short extraction times had to be used, as longer extractions would result in overloading of the portable GC-TMS instrument. Highly concentrated standards were chosen so as to represent a worst case scenario where NTD breakthrough and TFME carryover were most likely to occur. For this experiment, the GC column was initially held at 50 ^{o}C for 10 seconds, and then ramped to 270 ^{o}C at a rate of 2 ^{o}C s^{-1}.

In order to test for needle trap breakthrough, 2 NTDs were linked in series, as shown in Figure 4.2. Hence, if breakthrough of the more volatile analytes from the first needle were to occur, they would be trapped onto the second for detection. [33,38] Membrane carryover was evaluated by simply performing a second desorption from the same membrane. This allowed for confirmation as to whether any residual analyte remained from the first analytical run. Each step of the validation process was performed a total of 3 times to ensure reproducibility of the system.

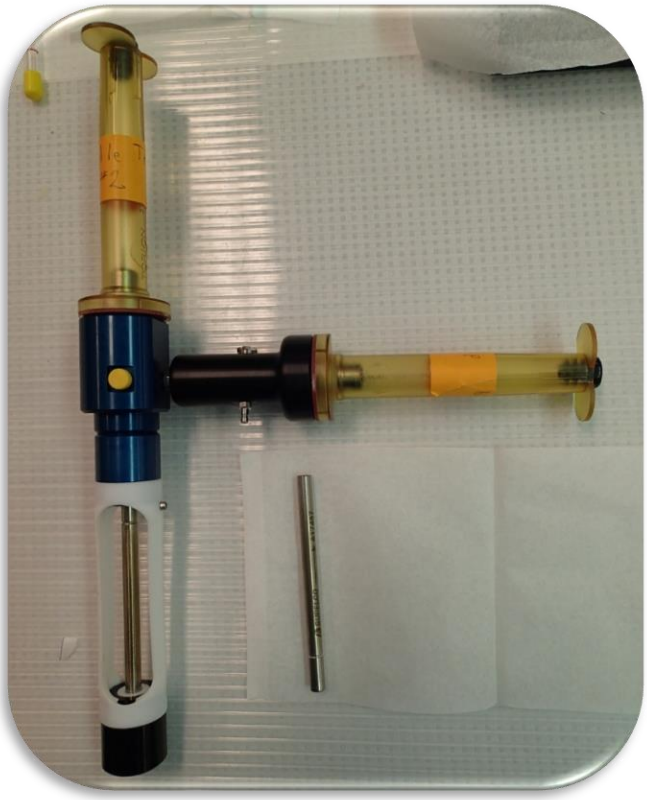

Figure 4.2. 19-gauge NTD Breakthrough test configuration for the desorption of thin film membranes.

4.2.8 Comparison of TFME extraction sensitivity using portable instrumentation

In order to determine the signal enhancement provided by the DVB/PDMS/carbon mesh TFME membrane for portable GC/MS instrumentation, aqueous samplings of various pesticides were performed using four different extraction materials. These sorbents included two separate DVB/PDMS/carbon mesh membranes (4 cm × 4.85 mm L × W), 1 DVB/PDMS unsupported

membrane (4 cm × 5.0 mm, L × W), 1 Gerstel PDMS sorptive stir bar (1.5 cm long), and a 65 μm DVB/PDMS SPME fiber. The 10 ppb aqueous pesticide test mixture consisted of 2,4 dichlorophenol, 2,4,6 trichlorophenol, phorate D10, carbofuran, atrazine, fonofos, chlorpyrifos, and parathion. Direct immersion extractions were performed at a magnetic stir rate of 1000 rpm from 300 mL of the 10 ppb pesticide standards, using the same sampling setup described by Riazi Kermani et al.[47] A relatively short extraction time of 15 min was chosen to more closely replicate a realistic time that could be allotted for sampling when performing analyses on-site under the constraint of battery power. Three replicate extractions were performed for each of the aforementioned samplers, and runs were randomized to account for any potential signal drift of the mass analyzer. For this experiment, the column temperature was initially held at 65 °C for 35 s, increased to 285 °C at a rate of 1.0 °C s^{-1} and then held for 60 s at this final temperature.

4.2.9 Untargeted on-site determination of water contaminants in an industrially-impacted lake

As a proof of concept, an entirely on-site TFME analysis of environmental lake water was performed at Silver Lake, located in Waterloo, Ontario. Water temperature was measured at 16.5 °C at the time of analysis. TFME extractions were performed for 10 min at approximately 350 rpm using a modified power drill attachment, as shown in Figure 4.3. After sampling, the membrane was blotted dry with a Kimwipe and immediately inserted into the 3.5 in. sorbent tube for desorption, which was undertaken with the use of the prototype HVD module. The portable GC/MS was operated out of the back of a car parked next to the sampling site, using an on-site configuration constrained by a miniature helium cylinder and battery power. For this experiment, the column temperature was initially held at 45 °C for 35 s, then increased to 285 °C at a rate of 1.5 °C s^{-1}, and held there for 60 s. For untargeted analysis, the signal was reported as the peak height of the respective quantitative ion. In addition to mass spectral matching with the NIST 2005

database, a linear retention index plot was also used to confirm the identity of the unknown compounds found in the real water samples. To generate this plot a novel standard gas generating vial was prepared by spiking C7-C20 n-alkane standards into an unmodified. One-minute TFME extractions were performed at 60 ^{o}C while the same GC-TMS desorption and analysis method was used.

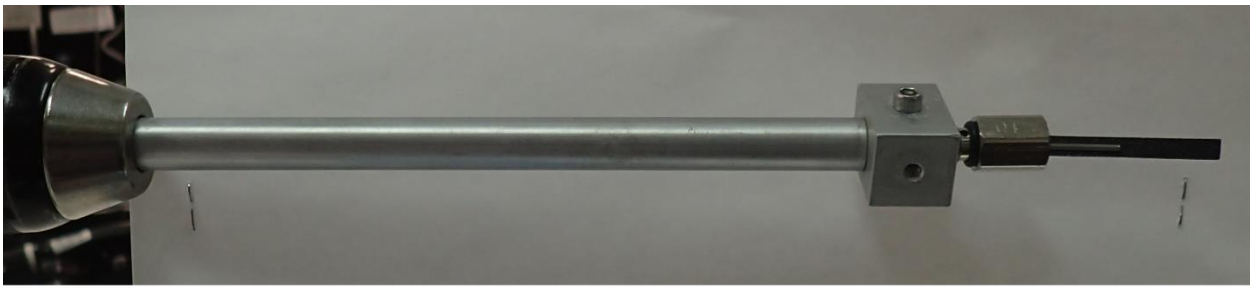

Figure 4.3 Modified power drill set-up holding a 4 cm x 5 mm DVB/PDMS/carbon mesh TFME membrane.

4.3 Results and discussion

4.3.1 Physical characterization of the DVB/PDMS/Carbon mesh thin film membrane

Sufficient physical strength and ease of handling are of utmost importance when considering the development and use of any new sampling device. If a membrane-based sampler is especially flimsy or fragile, it may prove inappropriate for the sampling of turbulent aqueous flows or when agitation is applied. Additionally, such a membrane would likely break after being submitted to a few desorptions. Furthermore, if any portion of the analytical operating procedure for the membrane is found to be exceedingly difficult or tedious, few analysts will be interested in adopting the technique, especially when nontechnical end users are concerned. In view of these requirements, the new DVB/PDMS/carbon mesh supported membranes were shown to exhibit great physical characteristics, while being much simpler to insert and remove from the desorption tubes than previous designs. The first thing to note when viewing the new membranes would be the rectangular 4.85 mm-wide design shown in Figures 4.4 and 4.5. This design is in stark contrast

to the 6 mm circular, and house-shaped membranes previously discussed in the literature.[26,29,47] By limiting membrane width to just under the 5 mm inner diameter of the desorption tubes, insertion, and removal of the samplers for analysis were made abundantly simpler. Conversely, even the small, 6 mm diameter membranes commonly proved difficult to desorb. Said membranes had a tendency to stick to the inside of the desorption tube, requiring a metal wire to be pierced through their surface, which could periodically lead to membrane breakage after prolonged use. It is worth noting nonetheless that the rollable house design possesses a surface area of 10 cm^2, which is markedly larger than the 3.88 cm^2 provided by the 4 cm long rectangular membrane. However, to make up for this size difference, an analyst could simply insert multiple rectangular membranes side by side into the same desorption tube. The combination of high-density PDMS with the carbon mesh support was found to be advantageous for a multitude of reasons. First, although initial trials involving the preparation of unsupported DVB/PDMS membranes with the new high crosslink density PDMS had shown a substantial decrease in the amount of siloxane background upon analysis by GC/MS, these membranes were found to be exceedingly fragile, often breaking after the first use. In addition to providing additional extraction phase, the incorporation of the carbon mesh support had a rebar-in-concrete-like effect on the membrane structure, making the structure incredibly resistant to impact, and without a propensity to elongate or bend under stress. This rigidity proved especially useful for aqueous sampling. As shown in Figure 4.6, the 4 cm DVB/PDMS/carbon mesh membranes were shown to resist bending when direct immersion sampling was performed at 1000 rpm. Moreover, this strength allowed the membranes to be attached to a modified power drill, such that agitation could be performed during on-site water analysis. In fact, upon testing of the membrane architectures of both unsupported and supported designs, only those possessing a carbon mesh support resisted wrapping around the

cotter pin when agitated at 1300 rpm, although the 4 cm long carbon supported membrane was observed to bend into a persistent "J" shape at these speeds. Furthermore, the only unsupported membrane to resist wrapping at 350 rpm was the smallest, 2 cm by 5 mm design. These results are graphically illustrated in Figure 4.7. Such physical stability is essential for a reliable environmental sampling of high-flow waterways such as river systems. Additionally, quicker extraction kinetics can be obtained by applying higher agitation rates; accordingly, this would allow for greater method sensitivity with shorter sampling times.[29,120]

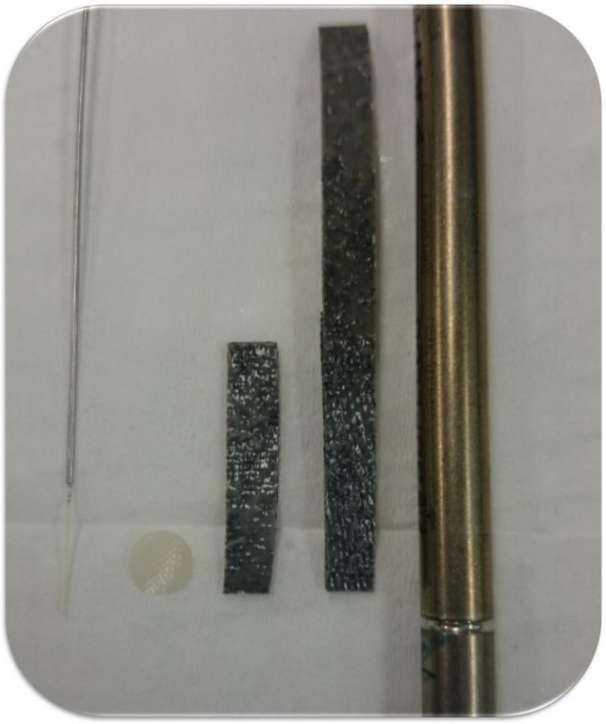

Figure 4.4 Evolution and design of DVB/PDMS extraction materials with, left-to-right: (1) a 65 μm DVB/PDMS SPME fiber, (2) an unsupported 6 mm diameter DVB/PDMS membrane, (3) a 2 cm × 4.85 mm DVB/PDMS/carbon mesh membrane, (4) a 4 cm × 4.85 mm DVB/PDMS/carbon mesh membrane, and (5) a standard 3.5 in. sorbent tube.

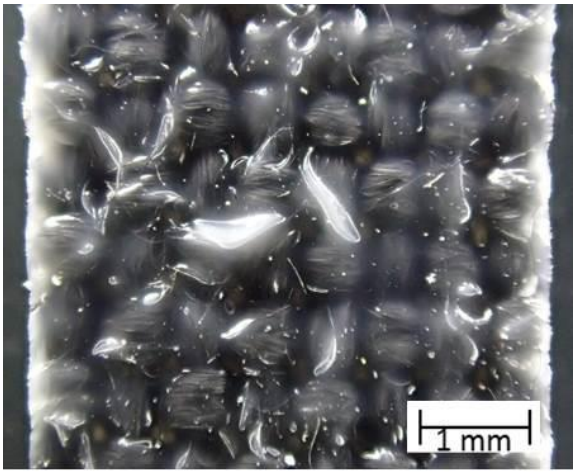

Figure 4.5 Surface of a DVB/PDMS-coated carbon mesh support with an optical magnification of 11x.

A B C

Figure 4.6 Direct immersion sampling of pesticides at 1000 rpm with, A) a 2 cm long, unsupported DVB/PDMS membrane, B) a 2 cm long DVB/PDMS/carbon mesh supported membrane, and, C) a 4 cm long DVB/PDMS/carbon mesh supported membrane.

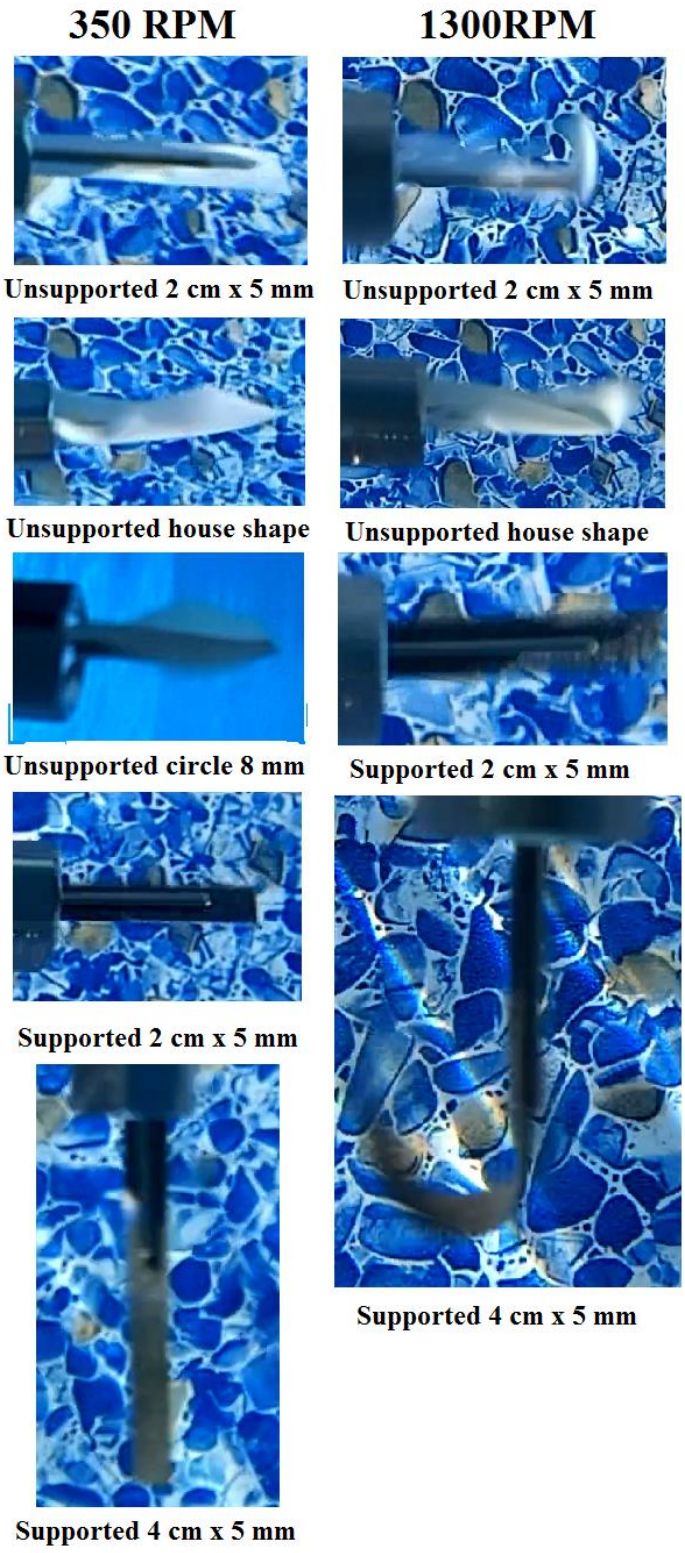

Figure 4.7 Direct immersion sampling of various TFME membrane designs using the modified drill sampler at 350 rpm and 1300 rpm.

4.3.2 Comparison of siloxane backgrounds using different TFME chemistries

As previously stated, the main motivation of this study was to minimize the amount of siloxane bleed occurring from TFME membranes upon thermal desorption. Although a small amount of background may be considered acceptable for most GC methods, if too much background occurs, it may become difficult to resolve which peaks are associated with the sample, versus those attributed to the background. This difficulty holds especially true when untargeted analysis is performed. Additionally, excessive background can also contaminate the electron impact ion source of the mass spectrometer, resulting in fluctuations in the ionization of target analyte and an overall reduction in the life of the source. With these facts in mind, background levels of blank desorptions from three different DVB/PDMS/carbon mesh membranes were compared with levels found for three DVB/PDMS unsupported membranes.

As demonstrated in Figure 4.8 below, the amount of bleed and associated background were substantially less when the high-density PDMS was used to prepare the TFME coating. Although it is difficult to comparatively quantitate background, a visual observation of the two stacked chromatograms clearly shows that the platinum catalyzed PDMS-based membranes exhibit a greater number of large bleed peaks than seen with the high-density PDMS-based design. Additionally, the height of these peaks was found to be much higher for the platinum catalyzed PDMS-based membranes. Hence, the newer membrane design was found to be far superior in terms of bleeding. In addition, considering that the larger 1.1×10^7 (height) siloxane peak obtained from the DVB/PDMS/carbon mesh membrane occurred so early in the chromatogram, this could be easily prevented by setting the solvent delay to 4 min.

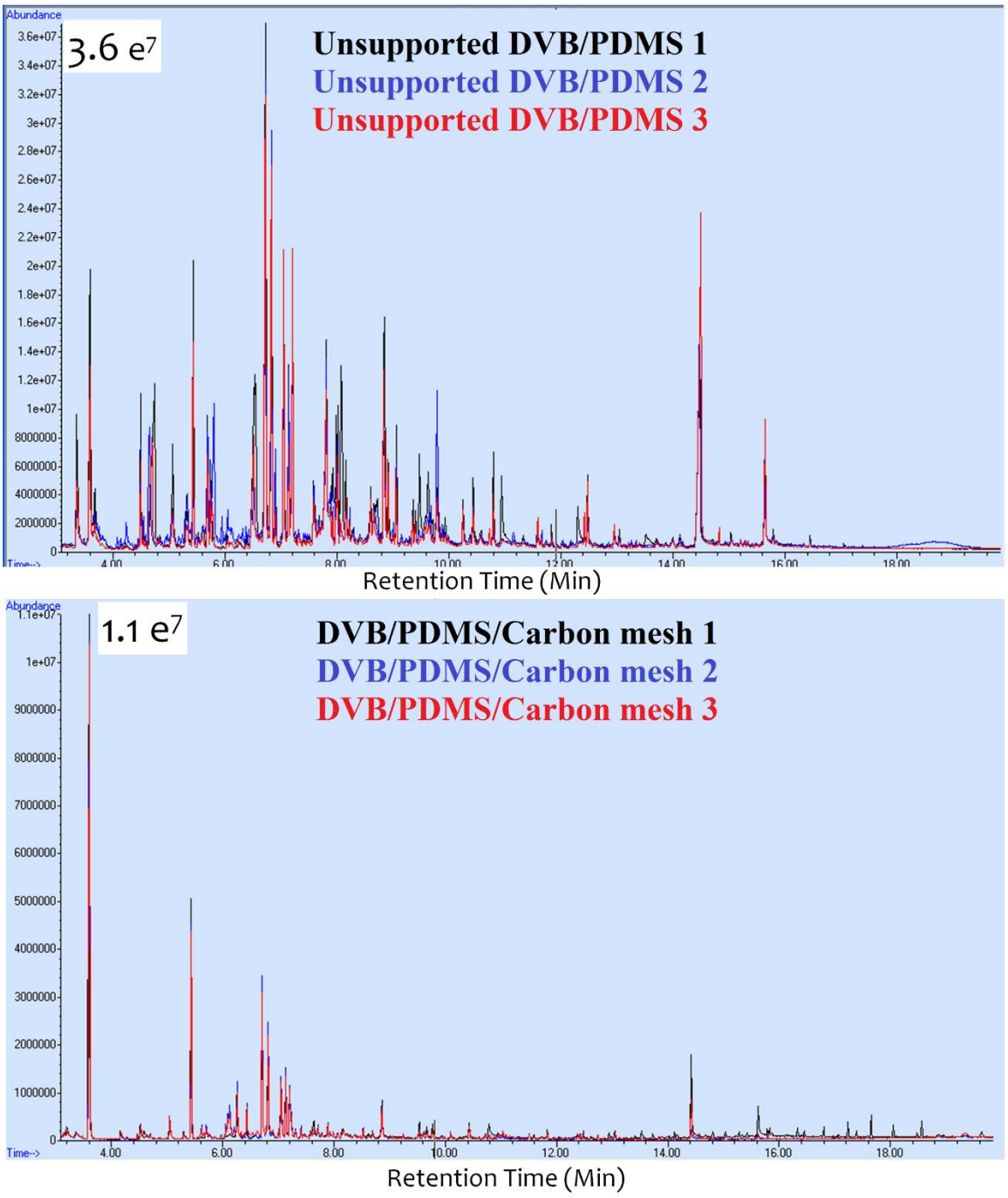

Figure 4.8 Comparison of membrane bleed and associated siloxane background for, A) three unsupported platinum catalyzed DVB/ PDMS membranes and B) three high-density PDMS DVB/PDMS/carbon mesh supported membranes. All membranes were of similar size and desorbed at 250 °C using 60 mL min^{-1} of helium for 5 min.

4.3.3 Inter-batch reproducibility of the DVB/PDMS carbon mesh membranes

A test for the inter-batch reproducibility of the prepared DVB/PDMS/Carbon mesh supported TFME membranes indicated very reasonable similarity between the three batches of membranes prepared. This inter-batch similarity is most notably demonstrated by the results of one-way ANOVA testing (Table 4.1) in which membranes prepared across all three batches were shown to be statistically similar regardless of the McReynolds probe being analyzed. Where extractions were carried out such that benzene, the most volatile analyte, and, octane the least volatile analyte were at near-equilibrium and near-linear extraction kinetics respectively, the similar results amongst batches also strongly indicated that these membranes were in-fact similar in terms of both total sorbent volume and membrane surface area. It is also worth noting that the error bars shown in Figure 4.9 give an indication as to the intra-batch repeatability as replicate extractions were performed using different membranes from the same batch. The related %RSD's which ranged from 6-12% was also considered quite reasonable for the chosen analytical methodology. Unfortunately, it was not statistically prudent to also perform 2-factor ANOVA testing as this data set fails the assumption that the absolute standard deviations must be similar between both factors tested, being membrane batch and analyte tested in this case

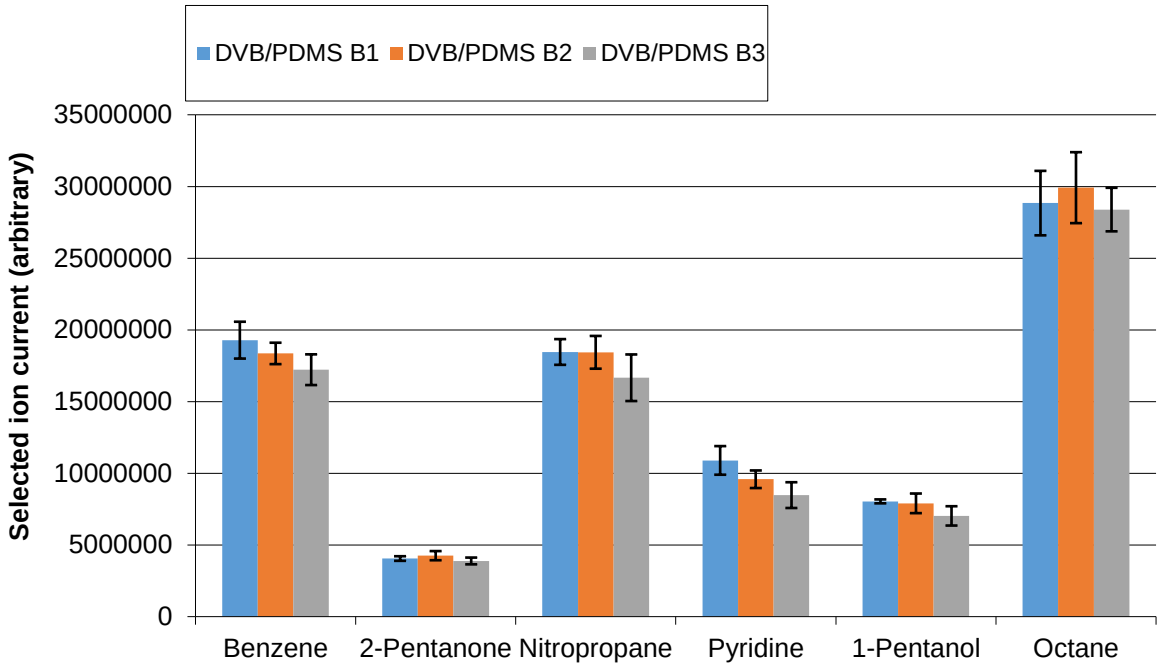

Figure 4.9: Inter-batch reproducibility of 3 separate carbon mesh supported DVB/PDMS TFME membrane batches. Extractions were performed from a McReynolds standard gas generating jar for 10 minutes at 55 ^{o}C as to achieve near equilibrium conditions for benzene and near linear extraction kinetics for octane.

Table 4.1 ANOVA testing at 95% confidence of inter-batch reproducibility of the DVB/PDMS/carbon mesh TFME. (F_{crit}=5.14)

Compounds	Benzene	2-Pentanone	1-Nitropropane	Pyridine	1-Pentanol	Octane
F_{TFME}	2.86	1.68	2.01	4.77	2.89	0.41
% RSD	7	6	7	12	8	6

4.3.4 Validation of the portable high volume desorption module

Achieving complete desorption and transfer of all compounds extracted using TFME techniques is of the utmost importance when considering any new high-volume desorption device. Hence, care was taken to ensure that minimal or no membrane carryover and needle trap breakthrough were observable from the portable HVD prototype. Generally speaking, one would expect membrane carryover to be most prominent with semi-volatile, heavier compounds while the lighter, more volatile compounds would be the first to break through a needle trap device.[12,23]

With this in mind, the acetone and tetradecane components of the Calion-13 standard were the most critical for the evaluation.

As demonstrated in Figure 4.10, no needle trap breakthrough was detected in any of the 3 replicate analyses performed. However, a very small amount (<2%) of tetradecane was found to carry over during one of the 3 runs performed. Considering that the levels of tetradecane extracted in this test were close to those required to overload the portable GC-TMS, this minuscule amount of carryover was not considered to be greatly significant. However, similar to precautions taken for standard SPME methods, it may be prudent to perform a carryover test on this system whenever a new type of sample is analyzed.

A more interesting point of discussion to be made from these results would be the poor chromatographic performance observed for early eluting analytes. This limitation is well known to occur with the Tridion-9 GC-TMS when highly volatile and concentrated compounds are analyzed using NTDs and, to a lesser extent, SPME while using a low-or-no split-flow. This occurs due to the relatively small amount of helium being passed through the NTD or past an SPME fiber as under splitless conditions, only 0.3 mL min^{-1} of helium passes through the injector and into the column during analysis. Hence, in splitless mode, any compound that is not completely refocused at the head of the GC column prior to oven ramping will have its peak width dictated by the time required to complete the desorption.

As mentioned, a similar effect may be observed even when a regular SPME fiber is used. The standard operating procedure for the portable GC/MS includes an opening of the 10:1 split anytime high concentrations of volatile organic compounds (VOCs) are analyzed. This effect is markedly worse when NTD injections are performed. However, it was found that by using a modified GC-method, decent chromatography could still be obtained for compounds as volatile as

benzene while performing splitless desorption. Additionally, good signal and chromatography were still attained for semi-volatile components, suggesting that these issues should not hinder pesticide analysis.

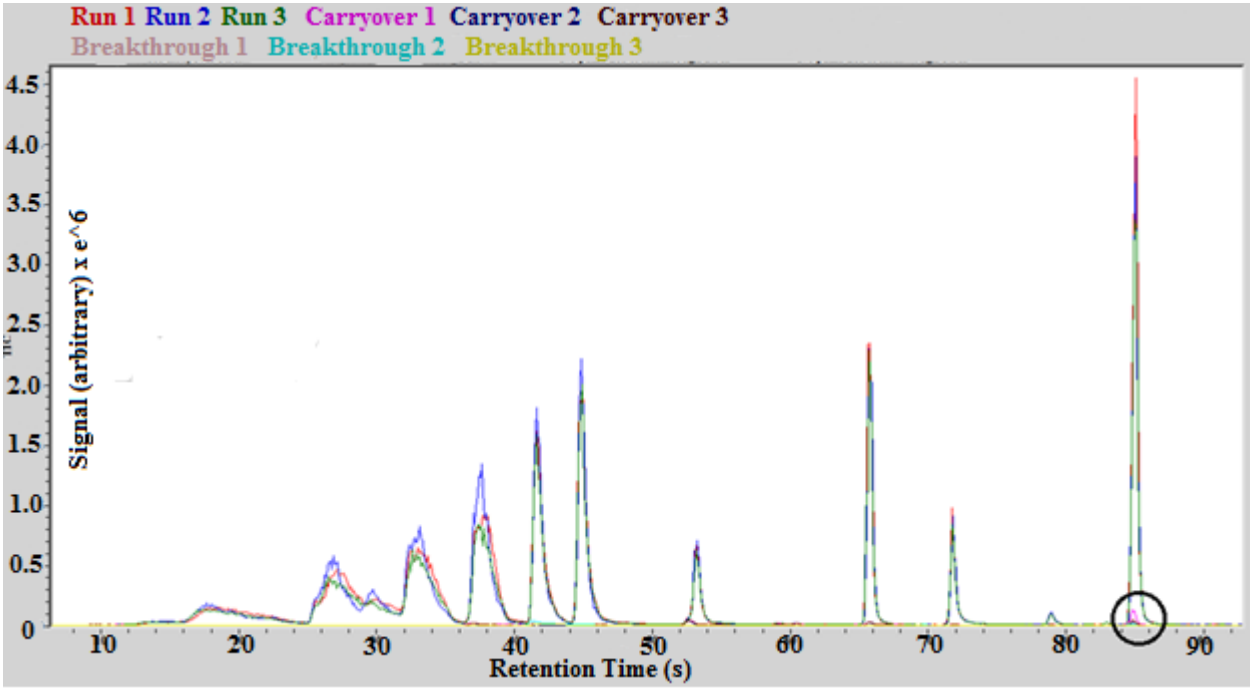

Figure 4.10 Examination of TFME membrane carryover and NTD breakthrough obtained with use of the portable high-volume desorption prototype. 3-second TFME extractions were performed at room temperature from a highly concentrated Calion-13 standard mixture, with a small amount (<2%) of tetradecane carryover detected for one of the 3 replicates.

4.3.5 Improvement upon the sensitivity of portable GC/TMS instrumentation by use of DVB/PDMS/Carbon mesh membranes to extract a mixed pesticide sample

As a demonstration of the advantages of the new DVB/PDMS/carbon mesh supported membranes, its extraction efficiency toward a pesticide mixture was directly compared with that of a standard 65 μm DVB/PDMS fiber, a 1.5 cm Twister PDMS sorptive stir bar, and an unsupported DVB/PDMS membrane of approximately the same size (4 cm × 5 mm). As the TFME membranes possessed a similar sorbent phase and dimensions, one would expect that they should extract a similar amount of analyte. Theoretically, this amount should be 25.3 times the amount

extracted via SPME at pre-equilibrium and 17.6 ± 2.2 times that amount once equilibrium had been achieved.

As shown in Figure 4.11 below, this result was accomplished with a surprising amount of congruency to this theory. With the exception of carbofuran, the 2 DVB/PDMS/Carbon mesh membranes were shown to extract a statistically identical amount of analyte as the unsupported DVB/PDMS membrane. However, standard deviations observed for the unsupported membrane were found to be much higher than any other sampler tested. As can be seen in Figure 4.12, this was likely due to the unsupported membrane flapping and folding during agitation at 1000 rpm. The amounts of 2,4-dichlorophenol, 2,4,6-trichlorophenol, Phorate D10, fonofos, chlorpyrifos, and parathion extracted by TFME were found to increase by factors of 21.2, 19.8, 18.5, 18,4, 26.8, and 23.7, respectively, when compared with a standard 65 μm DVB/PDMS fiber. Unfortunately, carbofuran and atrazine generated poor signals on the portable GC-TMS system, resulting in no detection for either compound when the SPME fiber and Twister sorptive stir bar were used. This result was a bit perplexing, as both compounds generated good signals when analyzed using benchtop GC/MS instrumentation. Additionally, when TFME was used, the signal for earlier eluting analytes was only found to increase by an approximate factor of 20, instead of 25.3. A potential explanation for this finding could be that more volatile analytes were beginning to approach equilibrium within the thinner membrane coatings (40 ± 5 μm per side). Conversely, the thicker 65 μm fibers would instead require a greater amount of time to begin exhibiting nonlinear extraction kinetics. Hence, equilibrium kinetics may explain why the factors for these more volatile analytes fell closer to the theoretical value of 17.6 ± 2.2 expected for an equilibrium extraction, where sorbent volume V_f, fiber constant K_{fs}, and sample concentration C_s determine the amount of analyte extracted, as shown in Eq 4.2.[5,22,113]

$$n = K_{fs} * V_f * C_0 \qquad \text{Eq. 4.2}$$

Additionally, to rule out nonlinearity of the toroidal-ion-trap detector, a rough calibration curve from 100 ppt to 50 ppb was prepared using the DVB/PDMS/carbon mesh membrane by applying the same extraction conditions as before. This plot can be found in Figure 4.12. As further shown in Figure 4.13 the obtained results demonstrated that 2,4-dichlorophenol, 2,4,6-trichlorophenol, Phorate D10, fonofos, chlorpyrifos, and parathion could all be detected using a selected ion chromatogram at 100 ppt. However, only 2,4-dichlorophenol, 2,4,6-trichlorophenol, and Phorate D10 gave a high enough signal-to-noise ratio at 100 ppt to be included in this calibration plot. It is worth mentioning that a test for membrane carryover was also performed at 10 ppb (Figure 4.14), confirming that there was no significant carryover originating from the TFME device or the transferring NTD.

Furthermore, in a later study performed using the benchtop TFME-TDU-GC/MS methodology, it was again confirmed that DVB/PDMS TFME membranes originating from the use of high-density PDMS and the carbon mesh support provided identical extraction efficiencies when compared to unsupported membranes prepared with the lower density, and higher bleed PDMS. It is worth noting however that the 23 pesticides investigated in this additional study remained in the pre-equilibrium regime of the extraction time profile at the chosen 30 minute of extraction time. Being in pre-equilibrium, and exhibiting near linear extraction kinetics would mean that surface area considerations would still dictate any observed changes in analyte uptake and total volume considerations would not play a role in relative extraction efficiencies. These results, shown in Figure 4.15 below, also show the importance of including DVB particles in the sorbent coating.

Unlike the DVB/PDMS composite, membranes prepared with pure PDMS come to equilibrium with the sample for the target pesticides very quickly during extraction. This quick

equilibrium for pure PDMS membranes, brought on by a lower analyte-sorbent affinity (lower K_{fs}), resulted in extraction amounts for most of the selected pesticides several orders of magnitude lower than that of the DVB/PDMS TFME counterparts.

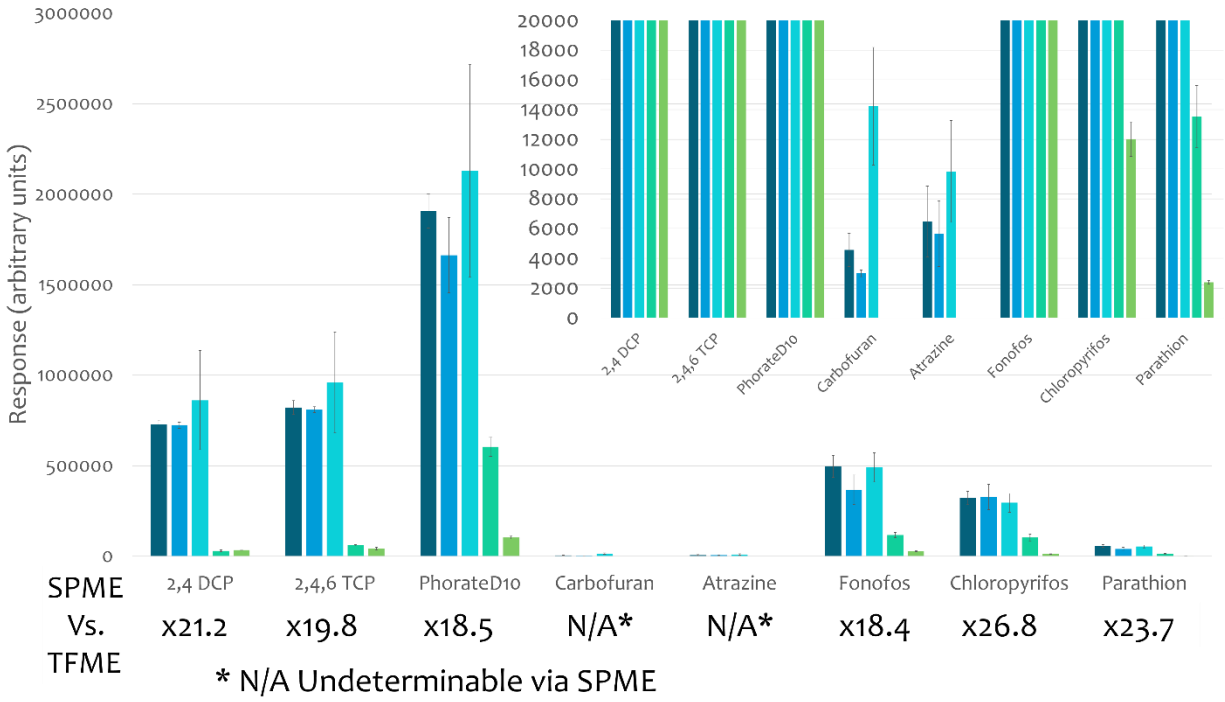

Figure 4.11 Comparative pesticide extraction efficiencies on portable GC-TMS instrumentation between two DVB/PDMS/carbon mesh membranes (3.88 cm^2), an unsupported DVB/PDMS membrane (4.0 cm^2), a 1.5 cm Twister PDMS sorptive stir bar, and a standard 65 µm DVB/PDMS SPME fiber. Direct immersion extractions were performed from 300 mL of a 10 ppb pesticide mixture for 15 min at room temperature and 1000 rpm agitation. Sensitivity improvement factors obtained with the use of a DVB/PDMS/carbon mesh in lieu of a standard DVB/PDMS fiber are also shown.

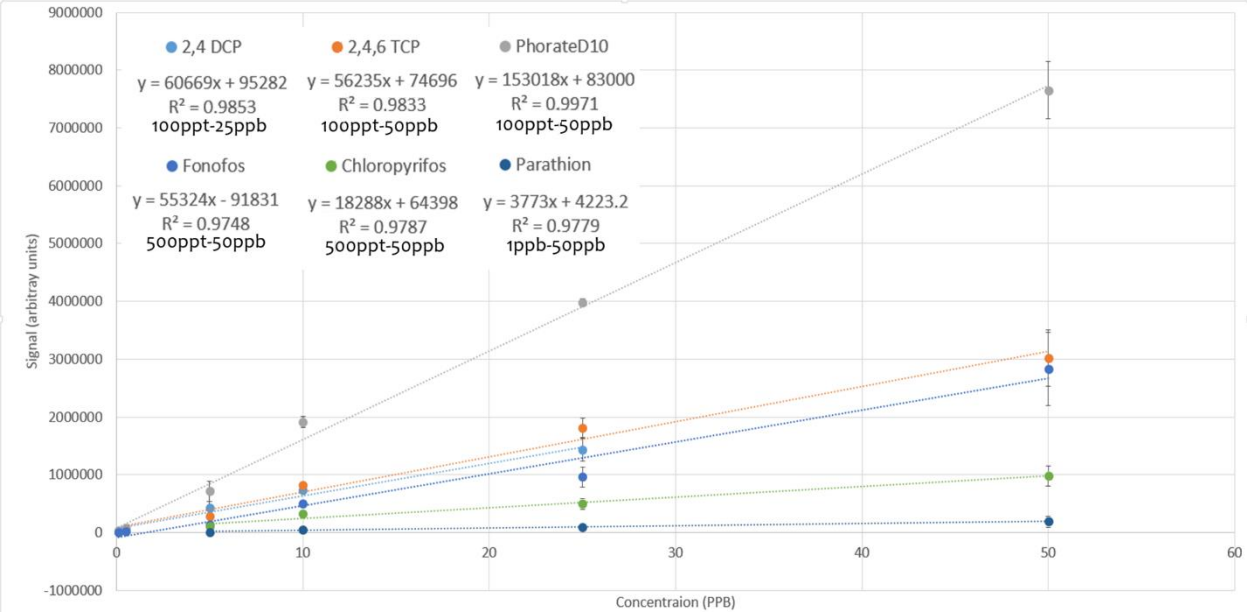

Figure 4.12 External calibration curve and linear range of the pesticide mixture using TFME on the portable GC/TMS instrument. Direct immersion extractions were performed with a DVB/PDMS/carbon mesh membrane (3.88 cm^2) from 300 mL of the appropriate concentration pesticide mixture for 15 minutes at room temperature while applying 1000 rpm agitation.

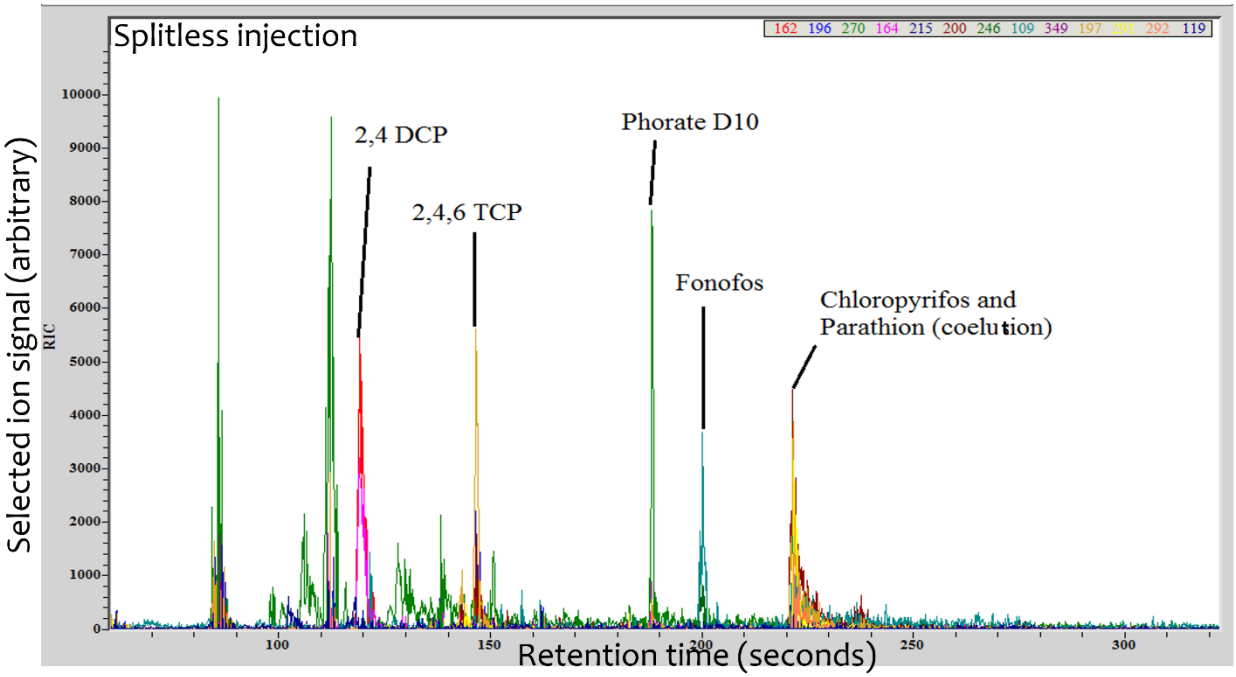

Figure 4.13 Selected ion chromatogram showing raw signal obtained on the Tridion-9 GC/TMS after a 15-minute extraction was performed at 1000 rpm using a DVB/PDMS carbon mesh supported TFME device from 300 mL of a 100 ppt aqueous pesticide solution.

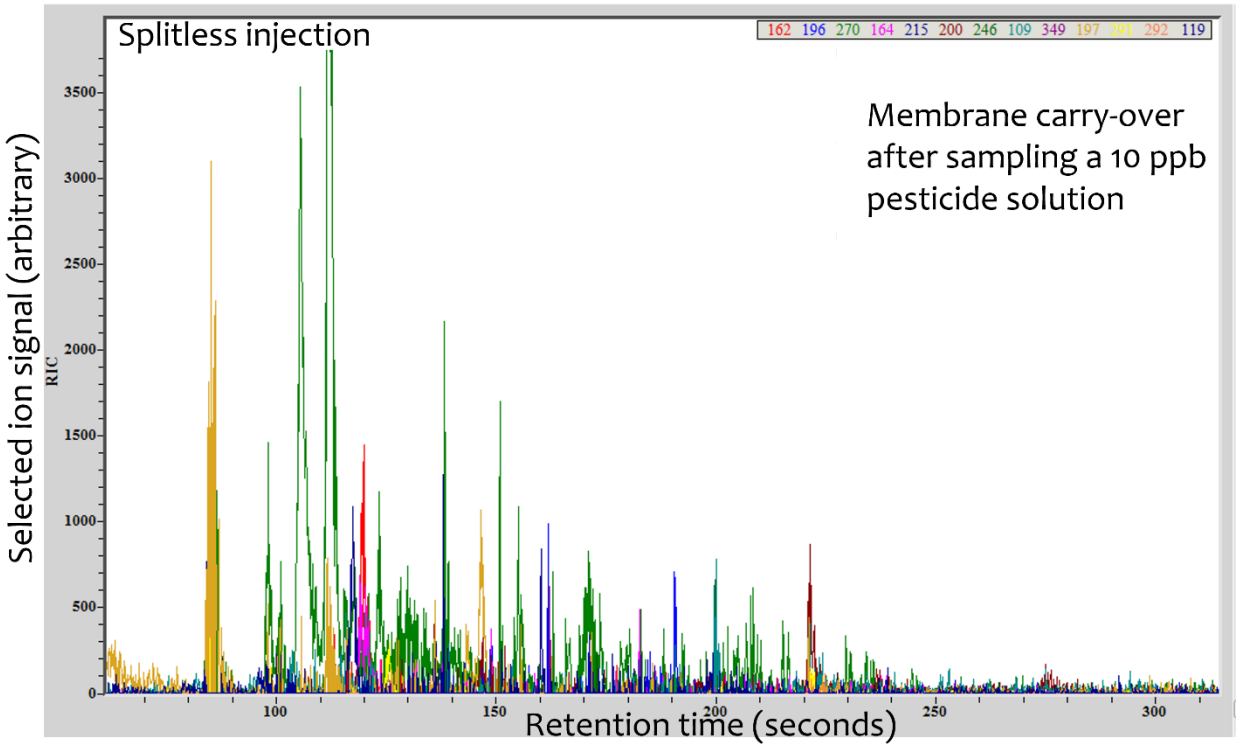

Figure 4.14 Reconstructed ion chromatogram showing raw signal obtained during a carry-over test (second desorption) after sampling a 10 ppb solution. Desorptions were carried out at 250 °C for 5 minutes using 35 mL min^{-1} of helium for the TFME desorption to the NTD. Results show no significant carry-over from the DVB/PDMS carbon mesh supported TFME device or the NTD used to transfer analyte.

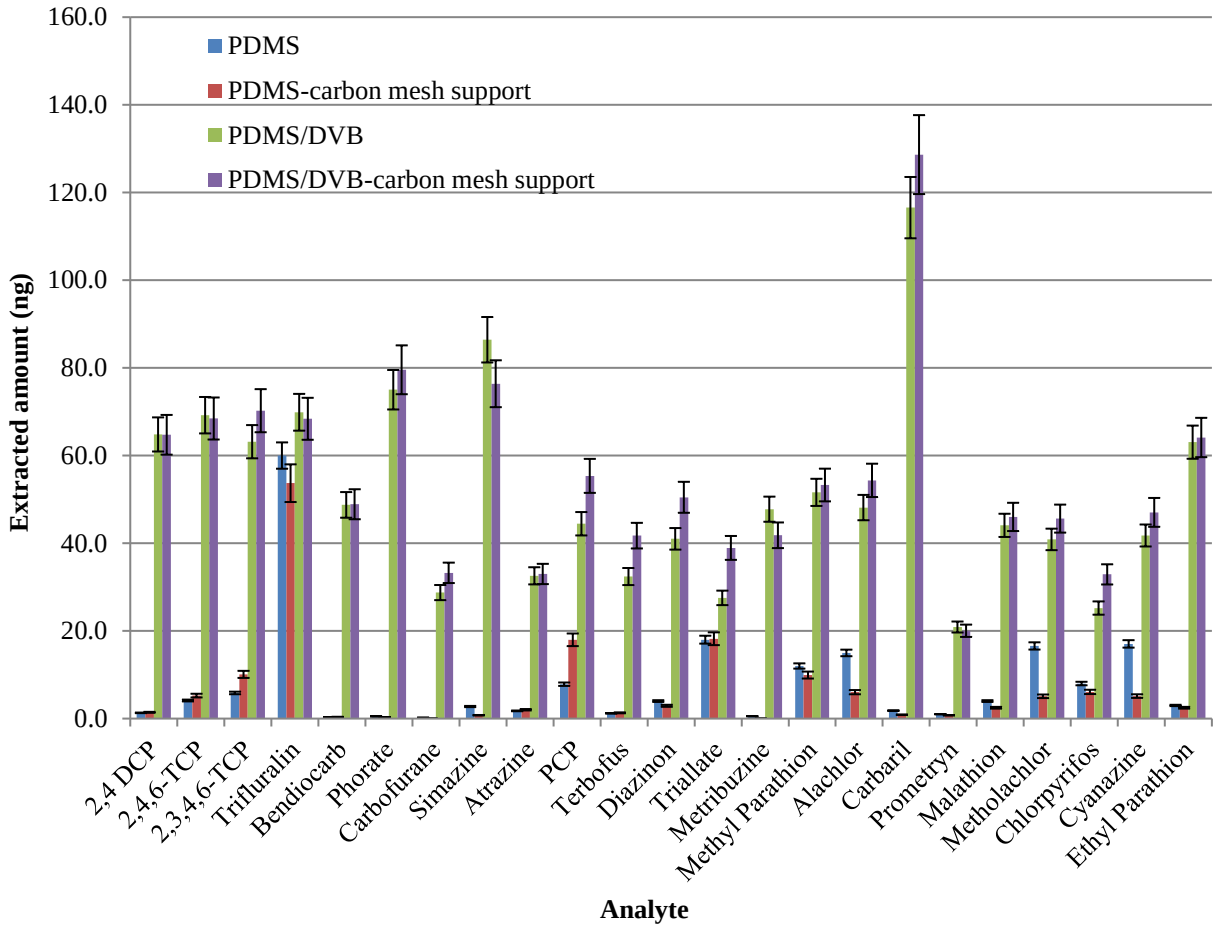

Figure 4.15 Comparison of the extraction efficiency of the various membrane chemistries with extractions performed from 300 mL of DI water spiked at 5 µg L^{-1} for 30 min extraction at 900 rpm and using 30 % NaCl, (n=3).

4.3.6 Untargeted on-site determination of water contaminants in an industrially-impacted lake

As a final proof of concept, it was important to show that the entire system could be employed entirely on-site. Henceforth, an untargeted analysis was performed for Silver Lake, situated in Waterloo, Ontario. This location was chosen because of concurrent construction of a light rail bridge at the inlet of the lake. The portable GC/MS was run on battery power alone; hence, only three replicate 10 min extractions were performed from the lake. Adding in the 5 min required for desorption and the 5 min needed for analysis, each run required 20−25 min in addition to 30 min required for the instrument to warm up and run performance validation. Recognizing

these shorter extraction times, it was very advantageous to be able to perform sampling with the modified power drill to improve the extraction kinetics and, consequently, method sensitivity.

Interestingly enough, a number of anthropogenic compounds that could be attributed to the ongoing construction were detected during analysis. These compounds, which are listed in Table 4.2 below, included toluene (T), ethylbenzene (E), xylene (X), 2,2,4-trimethyl-1,3-pentanediol diisobutyrate (TXIB), and tris(1-chloro-2-propyl)phosphate (TMCP). Identification of the unknowns was performed by comparing the generated mass spectra to those within the NIST mass spectrometry database, followed by confirmation using an n-alkane linear retention plot which was generated via analysis of highly re-usable C7−C20 n-alkane standard headspace generating vial.[3,23] The presence of TEX was not entirely surprising, considering that multiple gas-powered pumps were used to bypass the water around the railway bridge during construction. Hence, it is very likely that small amounts of gasoline may have been spilled into the waterway.

The detection of TXIB and TMCP proved to be a little bit more intriguing. These compounds, which are commonly used as a plasticizer and flame-retardant, respectively, were found to generate a considerable signal. Further investigation of the construction site indicated that on the day of sampling, workers were in the process of applying polymer-reinforced concrete to the bridge. It is possible that this polymer component may have contained the aforementioned compounds; however, this is purely speculation.

Regardless, for the purposes of this experiment, it could be concluded that the on-site method worked appropriately for qualitative untargeted aqueous sampling. Additionally, it was reassuring to see that the method response was, for the most part, reproducible even though only three runs were performed. This would indicate that if a target analyte were selected, it should be possible to perform semiquantitative analysis completely on-site using this system.

Table 4.2 Compounds detected in Silver Lake, Waterloo, Ontario, with likely anthropogenic origins.

Compound	RT(s)	Quant ion	Exp LRI	NIST LRI	Signal (AVG)	SD	%RSD
Toluene	55.80	91	779	794	1740	72	4
Ethylbenzene	72.59	91	873	864	7035	1151	16
Xylene	77.13	91	901	896*	1913	592	31
TXIB	152.94	71	1612	1605	35725	2476	7
TMCP	169.68	99	1827	1814	14157	2865	20

Extractions were performed directly from 16.5 °C lake water with a DVB/PDMS/carbon mesh membrane, using a modified power drill at 350 rpm for 10 min. Desorption and analysis were performed on-site using a portable GC/MS and desorption unit. Reported for ortho-xylene. TXIB 2,2,4-Trimethyl-1,3-pentanediol diisobutyrate. TMCP Tris(1-chloro-2-propyl)phosphate.

4.4 Conclusion and future directions

A novel carbon-mesh-supported DVB/PDMS TFME membrane based on a high-density PDMS prepolymer for the trace level detection of volatile and semivolatile organic compounds is proposed in this study. Many benefits over the previous TFME designs were demonstrated herein. Use of the carbon mesh support was shown to greatly enhance the physical strength of these membranes while limiting the membrane shape to a rectangle of width just under 5 mm allowed for easy operation and desorption. Furthermore, this design allowed for the direct immersion sampling of turbulent water systems without any major bending or twisting of the sorbent. More importantly, the use of a high-density PDMS was shown to drastically reduce the amount of siloxane bleeding observed during thermal desorption. Furthermore, it was shown that these TFME membranes could not only be used on standard benchtop instrumentation but could also be coupled to hand-portable GC-TMS instrumentation by use of a prototype high volume desorption unit and commercially available 19-gauge needle traps. It was demonstrated that no significant analyte loss could be detected from the HVD prototype, even when a large amount of a broad volatility multicomponent standard was used. This concept was further explored by performing an entirely on-site investigation of water contamination in a construction-impacted lake, where a number of anthropogenic compounds were detected. Most importantly, when short 15 min extractions were performed from a 10 ppb aqueous pesticide mixture, these membranes were shown to provide

upward of 26.8 times more signal than a comparable DVB/PDMS fiber. Hence, TFME can be used to perform much more rapid on-site sampling while still generating signals comparable to what could be attained from longer SPME extractions.

Ultimately, the work performed with these DVB/PDMS/ carbon mesh supported membranes could very well decrease the generally high detection limits associated with portable instrumentation to levels more in-line with those observed on benchtop GC/MS instrumentation. Furthermore, if coupled with these benchtop instruments, detection limits could be driven even lower than what is currently obtainable.

Chapter 5 On-site and inter-laboratory validation and comparison of TFME technologies

Preamble

A portion of the materials in this chapter has been published as a research article: Hamed Piri-Moghadam, Emanuela Gionfriddo, Angel Rodriguez-Lafuente, Jonathan J Grandy, Heather L Lord, Terry Obal, Janusz Pawliszyn; Inter-laboratory validation of a thin film microextraction technique for determination of pesticides in surface water samples; *Anal. Chimica Acta.,* **2017**, 964, pp. 74-84. All of the materials from Sections 5.2.1, 5.2.3, 5.2.4, 5.2.5 5.3.1 and 5.3.2 and some of the material from Sections 5.2.2 of this current Chapter are reprinted from this research article with the permission of Analytical Chimica Acta of Elsevier Publications. Copyright for this work remains the property of Elsevier publications and any further request for re-use of this information should be requested directly from them (**DOI:** https://doi.org/10.1016/j.aca.2017.02.014)

5.1 Introduction

Considering the impact of pesticide residues on the environment and human health, several priority lists comprising maximum contaminant levels (MCLs) have been established by the US environmental protection agency (US EPA) and EU regulations[121–124] to monitor the quality of drinking, surface, and groundwater. Today, several official techniques,[122,123] including liquid-liquid extraction (LLE) and solid phase extraction (SPE), are available for determination of contaminants (*e.g.* pesticides and polycyclic aromatic hydrocarbons, PAHs[122,123]) in water samples. Nonetheless, critical challenges still remain in as far as carrying out accurate quantitation of some groups of compounds (*e.g.* hydrophobic and labile compounds). In many analytical procedures involving the determination of compounds characterized by medium to high hydrophobicity, common sources of errors that result in poor accuracy in quantitation are often

associated with loss of compounds during the transfer of water samples from the sampling site to the laboratory. In such cases, compound loss may stem from the adsorption of target analytes to the surface of the sampling/collection bottle, and/or their degradation during transportation.

LLE is currently one of the most popular techniques used in contract laboratories for analyses of water samples.[122] Apart from being time-consuming and tedious, LLE uses toxic solvents for extraction of compounds, which subsequently generate hazardous waste.[8,122,125] Aiming to reduce the use of organic solvents, SPE has also become established as a well-known official method that is commonly used in contract laboratories for analysis of water samples. However, loss of hydrophobic compounds during transportation to laboratories, as well as the need for elution of the sample through the cartridge and filtration (if necessary for removal of suspended particles) are major drawbacks of this technique.[125] Further, the use of hazardous solvents and the generation of waste also limit the applicability of the SPE technique. Application of microextraction methodologies such as solid phase microextraction (SPME), which replaces organic solvent with a solid phase, is an alternative approach that moves towards green sample preparation.

Solid-phase microextraction (SPME) was developed in the early 1990s[126] as a promising and innovative solvent-free technique that eliminates the need for toxic solvents and simplifies the method of extraction and analysis for a wide range of applications.[1,127–137] Indeed, SPME has been demonstrated to provide similar accuracy and precision as that offered by the accredited method for water analysis.[8,25] Given the several features afforded by SPME, such as the various available geometries,[29,138,139] biocompatibility,[128] and open-bed extraction, SPME-based technologies have been used in several applications (*e.g.* in-vivo and on-site extraction) that could not be otherwise carried out by application of LLE and SPE techniques.[125,140–142] However, SPME and SPE share a

common limitation in regards to the analysis of hydrophobic compounds. While previous SPME-based studies have had some success in improving the accuracy of results for hydrophobic compounds,[143,144] the development of environmentally friendlier, simplified, and more universal methodologies that can be adopted for industrial applications is still highly demanded.

The goal of the current study encompasses the development of new green strategies to improve the accuracy of quantitation, particularly for hydrophobic compounds, by application of two new approaches, which utilize in-bottle TFME and on-site TFME. Aiming to provide a procedure that allows for the implementation of the entire analytical procedure on-field, a method based on drill-TFME for extraction of compounds from the river, followed by on-site portable GC/MS analysis was also designed.

5.2 Materials, instrumentation, and experimental methods

5.2.1 Chemical and materials

Pesticide mixtures, including triazines, organophosphorus pesticides (OPPs), and carbamates in acetonitrile (ACN), were purchased from AccuStandard (New Haven, CT, USA). Pure standards of chlorophenols, trifluralin, and methyl parathion were obtained from Sigma-Aldrich (Oakville, ON, Canada). Internal standards, including 3,5-dichlorophenol-d3, trifluralin-d14 and metolachlor-d6, and diazinon d-10 were prepared from CDN Isotopes (Pointe-Claire, QC, Canada). The solubility and polarity of the studied pesticides are provided in Table 5.1. DVB particles (5 µm diameter) and high-density PLOT PDMS, used in the preparation of the mesh supported membranes, were obtained from Supelco (Bellefonte, PA, U.S.A). The SYLGARD 184 silicone elastomer mix used in the preparation of the unsupported membranes was acquired from Dow Corning (Midland, MI, U.S.A.). Nano pure water was obtained using a Barnstead/Thermodyne Nanopure ultra-pure water system (Type 1 water grade) for method

development. A mixture of standards at different concentrations was prepared in ACN by diluting stock solutions for preliminary experiments, method development, and preparation of calibration levels.

Table 5.1 List of target pesticides and their physiochemical properties.

Analytes	Log P	Boiling point (°C)	Molecular weight (Da)	Henry's law constant (atm^{-3}/MOLE)	Water solubility at 25°C (mg L^{-1})
Metribuzine	1.3	312.4	214.28	1.81E-12	1304
Carbofuran	1.76	313.3	221.25	1.63E-09	320
Bendiocarb	1.86	298.8	223.08	6.58E-11	45.7
Cyanazine	2.19	442.4	240.69	1.86E-12	96.4
Simazine	2.28	365.8	201.65	3.37E-09	589
Carbaryl	2.4	329.3	201.22	3.14E-09	416
Atrazine	2.63	368.5	215.00	4.47E-09	214
Methyl parathion	2.78	334.7	263.2	1.68E-07	29.4
Alachlor	2.92	404	269.76	2.23E-08	18.7
Malathion	2.92	385.1	330.35	8.39E-10	78.5
Metolachlor	3.00	406.8	283.79	1.49E-09	50.9
2,4-dichlorophenol	2.99	210.0	163.00	2.94E-05	3282.1
Prometryn	3.44	401.1	241.35	9.09E-09	26.6
2,4,6 trichlorophenol	3.58	246.0	197.5	-	-
Phorate	3.67	296.0	260.37	1.58E-06	18.9
Diazinon	3.81	353.9	304.34	8.73E-08	6.4
Ethyl parathion	3.84	375	291.26	2.96E-07	3.4
2,3,4,6 tetrachlorophenol	4.17	267.7	231.89	1.69E-07	17.9
Terbufos	4.37	319.6	288.43	2.78E-06	2.1
Chloropyrifos	4.77	375.9	350.58	2.52E-06	0.4
Pentachlorophenol	4.78	309.5	266.3	1.25E-07	3.1
Trifluralin	5.41	369.1	335.29	2.12E-04	0.2
Triallate	6.18	322.1	304.66	10.39	1.4

5.2.2 Instrumental analysis method (benchtop GC/MS and portable GC/MS)

Analysis of the targeted pesticides on bench-top instrumentation was performed by the Agilent GC 6890A instrument with a 5973C Series MS detector (Agilent Technologies, CA, U.S.A.). For thermal desorption of the compounds from the membrane, a cooling injection system 4 (CIS 4) equipped thermal desorption unit (TDU) was used (GERSTEL, Mülheim an der Ruhr, GE). TFME devices were transferred into the TDU unit using the automatic injection multipurpose system 2 (MPS2) autosampler provided by GERSTEL. Chromatographic separation of the selected pesticides was attained with use of the DB-5.625 capillary column (length of 30 m, 0.25 mm ID, 0.25 µm film thickness), provided by Agilent J&W (Santa Clara, U.S.A). Helium at 99.999% purity provided by Praxair (Kitchener, Canada) was used as carrier gas, at a flow of 1.2 mL/min. For chromatographic separation of the target analytes, the temperature programming was applied under the following conditions: initial oven temperature set at 50 °C for 2 minutes, which was increased to 220 °C at 12 °C/min, and then increased to the final temperature of 280 °C at a 8 °C/min and held for 1 minute, for a total run time of 24.7 minutes. Injection of the compounds was accomplished in the solvent vent/splitless mode. Desorption of the compounds in the TDU unit was attained by temperature programming initially started at 40 °C for 30 seconds and then increased to final desorption temperature of 250 °C at 700 °C/min. Liquid nitrogen (Praxair, Kitchener, Canada) was used cryofocus the desorbed analytes in the CIS 4 at -80 °C, and after completion of desorption, the CIS was heated to 270 °C at 12 °C/s to transfer the compounds to the column. Selected ion monitoring (SIM) mode (with ion groups shown in Table 5.2) of mass spectrometry was used for detection of compounds with electron impact ionization at 70 eV with the transfer line temperature of 290 °C, the MS source temperature of 230 °C, and the MS quadrupole temperature of 150 °C.

The on-site portions of the current study were performed using a Tridion-9 portable GC-MS and a corresponding SPS-3 thermal desorption unit (Perkin Elmer, American Fork, Utah). Transfer of compounds extracted by the TFME membranes to NTDs was performed using the SPS-3 module at a temperature of 250 ^{o}C for 5 minutes, using a helium flow of 35 mL/min. Aiming to maximize sensitivity while preventing any needle carryover, injections of the NTD device onto the Tridion-9 were carried out at 280 °C for 5 s in splitless mode, followed by the opening of the 10:1 split for 5 s, and then further opening of the 50:1 split for a final 30 s. Chromatographic separations were performed using a low thermal mass (LTM) MXT-5 (5 m × 0.1 mm × 0.4 μm) Siltek-treated stainless steel column (Restek Co. Bellefonte, PA). For chromatographic separations, the column was initially held at 40 ^{o}C for 20 seconds and then ramped to 270 ^{o}C at a rate of 1.5 ^{o}C/s where it was held for 50 s. The ion-trap heater was set to 155 °C with a transfer-line temperature of 250 °C during analysis. Ionization was performed using an electron-gun EI ion-source, and the trap was operated in a full scan mode in the ranges of 43−500 m/z). The on-site stability of the Tridion-9 portable GC-TMS was also evaluated by use of a BTEX standard gas generating vial held at 35 ^{o}C using the battery operated heating block assembly (constructed at University of Waterloo Science Electronics Shop). All on-site TFME samplings were performed directly from the river water at 2000 rpm for 10 minutes using a custom built TFME sampling case (PAS technologies, Germany).

TFME devices were prepared using a bar coating method that incorporates the use of an Elcometer 4340 automatic film applicator (Elcometer Inc., Manchester, UK), in accordance with the procedure described in Section 4.2.4 of this thesis The 19-gauge Tenax/Carboxen needle trap device (NTD) was purchased from the Torion Technology division of Perkin Elmer (American Fork, Utah).

Table 5.2 SIM parameters of the selected pesticides.

Group	Group Start Time (min)	Ions in group (m/z)
2,4 Dichlorophenol	9.00	162, 164, 98
2,4,6 Trichlorophenol	9.70	196, 198, 200, 97
IS-3,5 dichlorophenol-d3	11.70	165, 167
Picloram	13.00	196, 198, 200
2,3,4,6 Tetrachlorophenol	13.60	230, 232, 234
IS-Trifluralin-d14	14.00	267, 315
Trifluralin &Bendiocarb	14.63	126, 151, 166, 264, 306
IS-Phorate-d10	14.82	99, 131, 270
Phorate	14.93	97, 121, 260
Carbofurane & Simazine & Atrazine	15.20	149, 164,173, 186, 201, 173, 200, 215
Pentachlorophenol	15.58	264, 266, 268
Terbufos & IS-Diazinon-d10	15.69	57, 231, 103,138,183,314
Diazinon	15.79	137, 179, 304
Triallate	16.00	86, 268, 270
Metribuzine	16.50	144, 198, 199
Methyl parathion & Alachlor	16.73	109, 125, 263,45, 160, 188
Carbaril & Prometryn	16.87	115, 116, 144, 184, 226, 241
Malathion	17.20	93, 125, 127, 173
IS-Metalachlor-d6 & Metolachlor & Chlorpyrifos & Cyanazine	17.41	166, 242,162, 238,197, 199, 314,225, 240
Ethyl parathion	17.61	97, 109, 291

*ions listed by relative peak height and group with ion isomers

5.2.3 LLE-GC/MS official method

A Standards Council of Canada (SCC) accredited method based on LLE and GC/MS was used at Maxxam to analyze the split samples. In summary, 800 mL of each sample was extracted sequentially with dichloromethane after pH adjustment to acidic, neutral, and basic conditions, the combined extracts were concentrated, and an aliquot injected onto a GC/MS instrument. Maxxam's

standard operating procedure used in this study is based on US EPA method 8270, with three main modifications: SIM mode was used instead of the full scan analysis as specified by the EPA method; liquid extraction was performed in the original glass bottle submitted, whereas the EPA method requires the water sample to be transferred into a separatory funnel prior to extraction; and the amount of dichloromethane used for extraction was 50 mL instead of the 60 mL specified in the EPA method.

5.2.4 Optimized extraction and analytical procedure using TFME-TDU-GC/MS

During method development, 30 mL of nanopure water was added to an amber glass vial (40 mL) and pH was adjusted to 2.5 (±0.1) by phosphate buffer to achieve higher extraction efficiency for chlorophenol pesticides.[8] 9 mg of NaCl was added and extraction was performed at 900 rpm for 30 min. The internal standard at 0.5 mg L^{-1} was added to the sample for validation. In order to compare the PDMS membrane with the PDMS/DVB membranes, 300 mL of sample was used to avoid the possibility of exhaustive extraction. After extraction, the membranes were transferred to a TDU tube followed by an automated injection using the Gerstel autosampler.

5.2.5 Preparation and distribution of double-blind split samples

Surface water samples were collected from the Grand River at different locations in Waterloo, ON, Canada. A complete characterization of the water samples was performed before the pesticide analyses. Samples were verified as "non-detect" for the selected pesticides, then spiked with the target compounds and internal standards at different concentration levels. The fortified samples were split, coded and submitted to Maxxam Analytics (Maxxam) and the University of Waterloo on a blind basis for non-biased analysis. Three batches of surface water samples (18 samples in total) were collected within 3 months and analyzed for quantitation of 23 pesticides. Results from the accredited LLE methodology performed by Maxxam and the new

TFME-TDU-GC/MS method were compared in terms of method limits of quantitation MLOQ's, analytical accuracy, and Eco-scale greenness relating to the environmental impact of the applied technique

5.2.6 Design and development of an on-site TFME sampling case and bottle sampling apparatus

Figure 5.1a shows the apparatus designed for the in-bottle TFME strategy, including a 1 L bottle equipped with a Teflon home-built adaptor, which was employed to hold the membrane in the bottle through the use of a disposable fluorocarbon thread (Berkely fishing line). A PDMS/DVB thin film coated onto carbon mesh fabric was used for evaluation of the developed methods. The bottle was filled (1 L) with nano-pure water for method development, while surface water was utilized in real sample analyses.

The second employed strategy consisted of on-site application of the TFME membranes using the designed portable sampling case, which was capable of controlling the speed and time of agitation, and was equipped with a head to hold the multi-TFME devices. Compared to a commercial drill, the newly designed sampling case provides higher agitation rates (up to 4500 rpm) with controlled sampling times, and a longer battery life that exceeded several hours, facilitating on-site extractions from river waters. Figure 5.1b shows the accessory and other instruments used for on-site TFME, including the sampling case, multi-TFME holder, portable GC/MS, needle trap device (used to transfer analytes into the instrument), and standard gas generation vial (used to run QC).

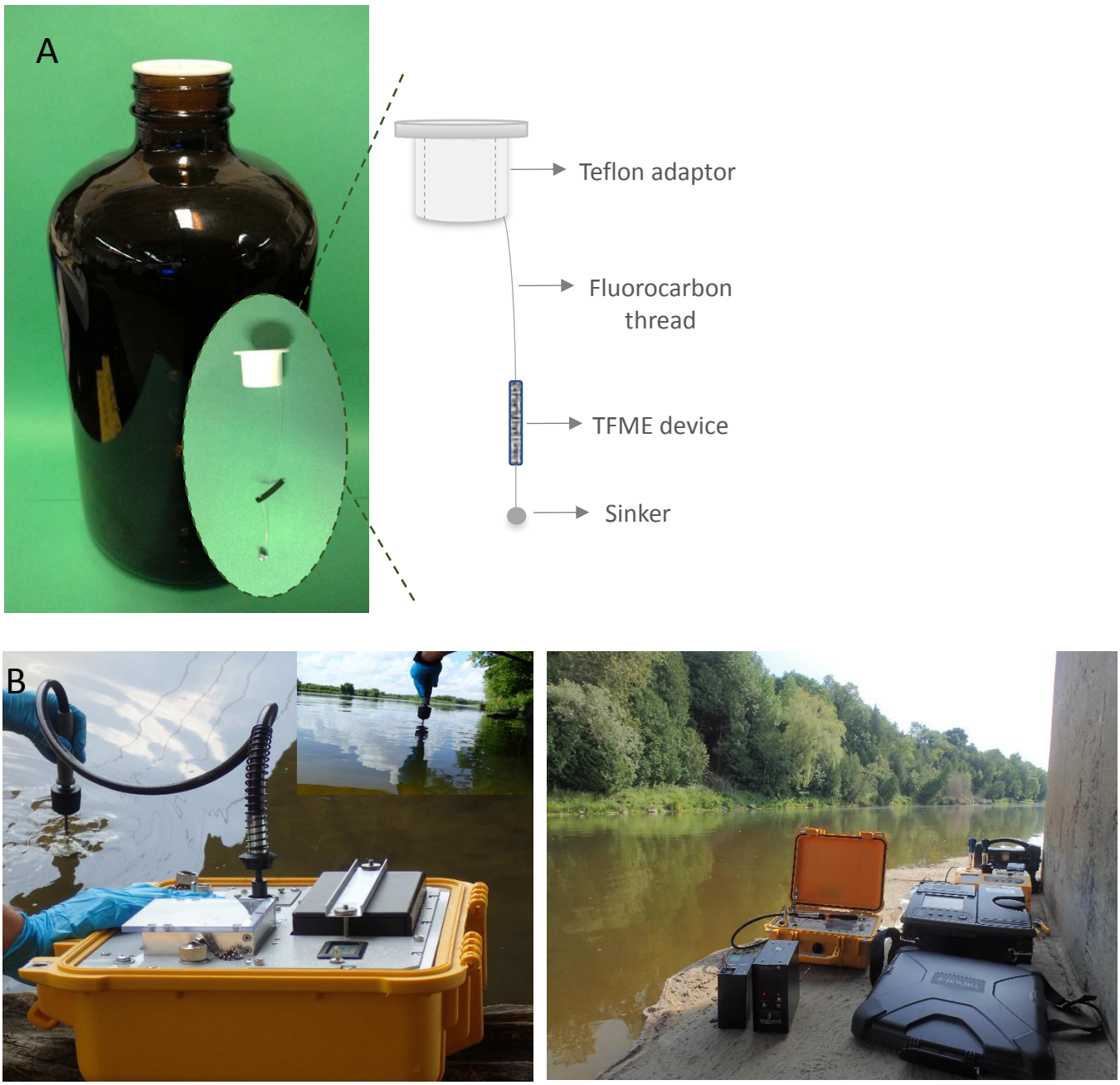

Figure 5.1 Developed sampling strategies based on, A) In-bottle TFME and, B) On-site TFME using drill accessories and a portable GC/MS instrument.

5.3 Results and discussion

5.3.1 Validation of analytical performance of the TFME-TDU-GC/MS method

The validation of the developed method was carried out under the optimized conditions described in Section 5.2.4. Blanks containing the selected internal standards were analyzed to determine noise levels for evaluation of the limits of detection (LOD) and limits of quantification (LOQ) defined as signal-to-noise ratio (S/N) equal to 3 and 10, respectively. As shown in Tables 5.3 and 5.4, The PDMS/DVB and PDMS/DVB carbon-mesh supported membranes show high and comparable sensitivity, resulting in low ng L^{-1} detection limits for most of the compounds studied. LODs in the range of 0.01-0.25 mg L^{-1} and LOQ between 0.025 and 0.5 mg L^{-1} for both membranes for the 23 pesticides tested. The linear dynamic range (LDR), also shown in Tables 5.3 and 5.4, was evaluated with 10-12 calibration points over 0.025-10.0 mg L^{-1} with all analytes showing good correlation to signal ($R^2 > 0.99$). With such a broad linear range, weighted linear regression ($1/x^2$) was applied in order to attain the best fitting data and to improve the accuracy of quantitation at lower concentration levels.[145] It should be noted that un-weighted linear least squares regression provides more weight to higher concentration points leading to poor fitting at lower concentrations. Tables 5.3 and 5.4 and summarize the method validation data obtained for both membranes. The detection limits for the developed method for all the studied pesticides not only meet the requirements reported by US EPA but for some compounds, are about 2 orders of magnitude lower than the dictated MCLs. The high extraction efficiency of the membranes is related to the larger volume and surface area of the extraction phase and therefore capacity and kinetics of the membrane extraction phase.[49] It is worth noting that these LODs were achieved with a 30 min (in pre-equilibrium regime) extraction time. LODs could be further decreased by using larger membranes, increasing the extraction time and/or using a larger amount of sample, assuming that

extraction was neither exhaustive nor negligible. On the other hand, in cases where faster analytical throughput is needed, shorter extraction times could be used, while still meeting or exceeding the US EPA MCLs. The accuracy of the method was evaluated at three levels of concentration including 0.06 mg L^{-1}; 0.6 mg L^{-1}; and 4 mg L^{-1}, representing low, medium and high concentration levels within the linear dynamic range. Each concentration level was analyzed in triplicate. As reported in Tables 5.3 and 5.4, all compounds showed good accuracy with reasonably good precision as indicated by RSD values in the range of 2-20%. Given the high stability of the membranes at the chosen experimental conditions, long membrane lifetime was also achieved.

Table 5.3 Method validation data summary for unsupported DVB/PDMS membrane.

Pesticides	**LOD (µg L^{-1}) (n=3)**	**LOQ (µg L^{-1}) (n=3)**	**LDR (µg L^{-1}) (n=3)**	**R^2**	**Slope**	**Intercept**	**Internal standard**	**Accuracy (n=3)**			**Precision (RSD %) (n=3)**		
								0.06 µg L^{-1}	0. 60 µg L^{-1}	4.0 µg L^{-1}	0.06 µg L^{-1}	0. 60 µg L^{-1}	4.0 µg L^{-}
2,4-DCP	0.025	0.050	0.050-10.0	0.996	0.00220	-0.0037	3,5-DCP-d3	90 %	104 %	93 %	9 %	8 %	4 %
2,4,6-TCP	0.010	0.025	0.025-5.0	0.996	0.00186	0.0027	3,5-DCP-d3	94 %	98 %	90 %	5 %	4 %	6 %
2,3,4,6-TeCP	0.010	0.025	0.025-5.0	0.991	0.00164	0.014	3,5-DCP-d3	87 %	99 %	107%	8 %	12 %	20 %
Trifluralin	0.025	0.05	0.050-10.0	0.998	0.00242	-0.039	Trifluralin-d14	101 %	74 %	88%	17 %	20 %	17 %
Bendiocarb	0.010	0.025	0.025-10.0	0.998	0.00228	0.00023	3,5-DCP-d3	97 %	106 %	96 %	6 %	6 %	3 %
Phorate	0.10	0.25	0.25-10.0	0.998	0.00106	0.22	Phorate-d10	ND	70 %	123 %	ND	18 %	10 %
Carbofurane	0.050	0.10	0.10-10.0	0.996	0.00134	0.052	3,5-DCP-d3	ND	123 %	90 %	ND	17 %	7 %
Simazine	0.075	0.25	0.25-5.0	0.997	0.000374	-0.0043	Metalachlor-d6	ND	89 %	122 %	ND	12 %	8 %
Atrazine	0.075	0.25	0.25-5.0	0.996	0.000975	0.057	Metalachlor-d6	ND	101 %	111 %	ND	10 %	5 %
PCP	0.050	0.10	0.10-5.0	0.991	0.00121	0.081	3,5-DCP-d3	ND	115 %	95 %	ND	16 %	9 %
Terbufos	0.10	0.25	0.25-5.0	0.997	0.00469	0.43	Diazinon-d10	ND	100 %	101 %	ND	12 %	9 %
Diazinon	0.025	0.050	0.05-10.0	0.999	0.00289	0.0065	Diazinon-d10	112 %	97 %	117 %	6 %	14 %	3 %
Triallate	0.025	0.050	0.05-10.0	0.991	0.00134	0.036	3,5-DCP-d3	82 %	123 %	91 %	11 %	22 %	13 %
Metribuzine	0.050	0.10	0.10-5.0	0.999	0.00187	-0.052	Diazinon-d10	ND	128 %	130 %	ND	3 %	13 %
Methyl parathion	0.25	0.50	0.50-5.0	0.987	0.00451	0.063	Diazinon-d10	ND	85 %	88 %	ND	22 %	12 %
Alachlor	0.025	0.050	0.050-10.0	0.998	0.00128	-0.0030	Metalachlor-d6	107 %	100 %	98 %	2 %	4 %	19 %
Carbaryl	0.050	0.10	0.10-10.0	0.991	0.00179	0.12	3,5-DCP-d3	ND	128 %	82 %	ND	17%	5 %
Prometryn	0.025	0.075	0.075-5.0	0.993	0.000690	0.032	Metalachlor-d6	ND	129 %	108 %	ND	20 %	4 %
Malathion	0.25	0.50	0.50-10.0	0.986	0.00302	0.99	Diazinon-d10	ND	98 %	103 %	ND	20 %	16 %
Metalachlor	0.010	0.025	0.025-10.0	0.999	0.00313	0.011	Metalachlor-d6	107 %	85 %	115 %	3 %	10 %	20 %
Chlorpyrifos	0.050	0.10	0.10-2.50	0.993	0.00208	0.069	Diazinon-d10	ND	87 %	99 %	ND	20 %	2 %
Cyanazine	0.050	0.10	0.10-10.0	0.999	0.000765	0.0033	Metalachlor-d6	ND	87 %	110 %	ND	9 %	20 %
Ethyl parathion	0.025	0.050	0.050-2.50	0.996	0.00318	-0.082	Diazinon-d10	123 %	101 %	-	17 %	14 %	-

LOD = limit of detection LOQ = limit of quantitation LDR = linear dynamic range

Table 5.4 Method validation data summary for the carbon mesh supported DVB/PDMS membrane.

Pesticides	**LOD (µg L^{-1}) (n=3)**	**LOQ (µg L^{-1}) (n=3)**	**LDR (µg L^{-1}) (n=3)**	**R^2**	**Slope**	**Intercept**	**Internal standard**	**Accuracy (n=3)**			**Precision (RSD %) (n=3)**		
								0.06 µg L^{-1}	0. 60 µg L^{-1}	4.0 µg L^{-1}	0.06 µg L^{-1}	0. 60 µg L^{-1}	4.0 µg L^{-1}
2,4-DCP	0.050	0.10	0.10-5.0	0.991	0.00198	-0.068	3,5-DCP-d3	ND	96 %	98 %	ND	20 %	2 %
2,4,6-TCP	0.025	0.050	0.050-5.0	0.992	0.00172	-0.013	3,5-DCP-d3	112 %	101 %	94 %	10 %	8 %	3 %
2,3,4,6-TeCP	0.01	0.025	0.025-10.0	0.994	0.00185	0.0064	3,5-DCP-d3	89 %	104 %	92 %	12 %	10 %	6 %
Trifluralin	0.025	0.050	0.050-10.0	0.994	0.00239	-0.0086	Trifluralin-d14	130 %	115 %	122 %	10 %	17 %	3 %
Bendiocarb	0.025	0.050	0.050-5.0	0.993	0.00230	0.0054	3,5-DCP-d3	95 %	110 %	96 %	7 %	13 %	8 %
Phorate	0.10	0.25	0.25-5.0	0.999	0.000946	0.27	Phorate-d10	ND	77 %	98 %	ND	15 %	10 %
Carbofurane	0.050	0.10	0.10-5.0	0.998	0.00163	0.070	3,5-DCP-d3	ND	129 %	87 %	ND	17 %	10 %
Simazine	0.075	0.25	0.25-5.0	0.998	0.000332	-0.018	Metalachlor-d6	ND	84 %	127 %	ND	17 %	6 %
Atrazine	0.025	0.075	0.075-5.0	0.999	0.000949	0.023	Metalachlor-d6	ND	96 %	120 %	ND	20 %	6 %
PCP	0.025	0.075	0.075-10.0	0.994	0.00145	0.061	3,5-DCP-d3	ND	130 %	82 %	ND	10 %	17 %
Terbufos	0.10	0.25	0.25-5.0	0.992	0.00387	0.59	Diazinon-d10	ND	124 %	122 %	ND	19 %	18 %
Diazinon	0.025	0.050	0.050-10.0	0.999	0.00283	0.018	Diazinon-d10	104 %	92 %	101 %	12 %	20 %	9 %
Triallate	0.025	0.050	0.050-10.0	0.989	0.00160	0.027	3,5-DCP-d3	92 %	122%	76 %	20%	17 %	15 %
Metribuzine	0.075	0.25	0.025-10.0	0.998	0.00154	-0.082	Diazinon-d10	ND	105 %	122 %	ND	4 %	10 %
Methyl parathion	0.25	0.50	0.50-5.0	0.995	0.00386	-0.12	Diazinon-d10	ND	81 %	95 %	ND	4 %	3 %
Alachlor	0.25	0.50	0.50-10.0	0.999	0.00126	-0.0043	Metalachlor-d6	115 %	97 %	99 %	2 %	13 %	4 %
Carbaryl	0.050	0.10	0.10-10.0	0.993	0.00222	0.12	3,5-DCP-d3	ND	124 %	71 %	ND	14 %	9 %
Prometryn	0.025	0.075	0.075-10.0	0.998	0.000666	0.042	Metalachlor-d6	ND	97 %	104 %	ND	8 %	10 %
Malathion	0.25	0.50	0.50-10.0	0.997	0.00316	0.14	Diazinon-d10	ND	113 %	98 %	ND	20 %	19 %
Metalachlor	0.025	0.050	0.050-10.0	0.997	0.00318	-0.0047	Metalachlor-d6	100 %	88 %	109 %	5 %	11 %	4 %
Chlorpyrifos	0.10	0.25	0.25-10.0	0.998	0.00210	0.092	Diazinon-d10	ND	126 %	117 %	ND	17 %	19 %
Cyanazine	0.050	0.10	0.10-10.0	0.997	0.000772	-0.0022	Metalachlor-d6	ND	88 %	105 %	ND	11 %	4 %
Ethyl parathion	0.025	0.050	0.050-50.0	0.997	0.00378	-0.024	Diazinon-d10	70 %	86 %	121 %	19 %	20 %	5 %

LOD = limit of detection LOQ = limit of quantitation LDR = linear dynamic range

5.3.2 Comparison of TFME-TDU-GC/MS methodology VS. LLE for real water samples

Many analytical laboratories use LLE for routine analysis of surface water samples as it is an established and US EPA approved method. The widespread use of LLE is mainly due to its simplicity, i.e., the interaction of the sample with an immiscible organic solvent in a separatory funnel. However, this sample extraction method requires relatively large sample volumes to achieve the sensitivity required to meet US EPA MCLs. Larger volumes of organic solvent and the need for specialized waste disposal of these solvents also increase the cost of this technique.[8,9]

The throughput for routine analysis can be laborious and tedious. In a previous study,[8] an extensive investigation was conducted comparing a fully automated SPME fiber method to LLE. In the present study, TFME was validated, and its performance compared to an LLE-based method, namely, US EPA method 8270. This LLE-based method was performed at Maxxam Analytics (Mississauga, ON). Maxxam maintains accreditation through the Standards Council of Canada (SCC) and the United States National Environmental Laboratory Accreditation Program (NELAP) among others.

Three batches of samples were collected over 3 months, with each batch containing 6 samples. Samples were fortified with the target analytes at different concentration levels by a third party then split and submitted to University of Waterloo and Maxxam on a blind basis. While the LLE method required 800 mL of sample, only 30 mL was used for the TFME extractions. Even though a lower volume of sample was used for the TFME method, lower detection limits were still achieved in comparison to LLE (Table 5.5). These lower detection limits were achievable because, unlike LLE, when SPME methods are used all the extracted amount is injected into the instrument giving higher sample pre-concentration. It should also be mentioned that, if the same volume of sample used for LLE were to be used for TFME, even lower detection limits would be attained, as

a 30 mL sample of water is known to be significantly depleted by TFME. Another difference between LLE and TFME lies in the quantitation approach: external calibration in case of TFME (based on microextraction methodologies)[22] and instrumental calibration by injection of the standard solutions for LLE (as an exhaustive method).

Table 5.6 compares the TFME and LLE results of the split sample analyses for the 18 surface water samples. Most of the studied pesticides were not detected by LLE at the sub mg L^{-1} level. These results indicate that with 414 data points for each method, 90% of the analytes were quantified by TFME, whereas only 53% of the compounds were detectable using the LLE method (Table 5.6). As previously mentioned, even with great sensitivity an analytical method is only useful if it can display a reliable degree of analytical accuracy. Hence, to compare the accuracy of the two described methods a blank was first run for each of batch of samples. Accuracy was calculated by dividing the concentration obtained by each method, LLE, and TFME, to the true concentration spiked into the samples. In Figure 5.2 the histograms show the accuracy of the results in the ranges of <50%, 50-70%, 70-130%, 130-150%, and >150% with non-detected results being excluded from the percentage. The TFME method was reasonably accurate for the real samples analyzed with approximately 70% of all results falling within the acceptable range of accuracy, 70-130%. This was also in good agreement with the LLE results as the reference method.

Table 5.5 Comparison of method detection limits for TFME and LLE methods.

Pesticides	**Units**	**TFME** (PDMS/DVB membrane**)**	**TFME** (PDMS-DVB-carbon mesh supported membrane	**LLE**
2,4-DCP	µg L^{-1}	0.025	0.050	0.25
2,4,6-TCP	µg L^{-1}	0.010	0.025	0.50
2,3,4,6-TeCP	µg L^{-1}	0.010	0.01	0.50
Trifluralin	µg L^{-1}	0.025	0.025	1.0
Bendiocarb	µg L^{-1}	0.010	0.025	2.0
Phorate	µg L^{-1}	0.10	0.10	0.50
Carbofurane	µg L^{-1}	0.050	0.050	5.0
Simazine	µg L^{-1}	0.075	0.075	1.0
Atrazine	µg L^{-1}	0.075	0.025	0.50
PCP	µg L^{-1}	0.050	0.025	0.50
Terbufos	µg L^{-1}	0.10	0.10	0.50
Diazinon	µg L^{-1}	0.025	0.025	1.0
Triallate	µg L^{-1}	0.025	0.025	1.0
Metribuzine	µg L^{-1}	0.050	0.075	5.0
Methyl parathion	µg L^{-1}	0.25	0.25	1.0
Alachlor	µg L^{-1}	0.025	0.025	0.50
Carbaryl	µg L^{-1}	0.050	0.050	5.0
Prometryn	µg L^{-1}	0.025	0.025	0.25
Malathion	µg L^{-1}	0.25	0.25	5.0
Metalachlor	µg L^{-1}	0.010	0.025	5.0
Chlorpyrifos	µg L^{-1}	0.050	0.10	1.0
Cyanazine	µg L^{-1}	0.050	0.050	1.0
Ethyl parathion	µg L^{-1}	0.025	0.025	1.0

Table 5.6 Results of blind split analyses of surface water samples by TFME and LLE.

Pesticides	SW 1 (Fortified at 0.067 µg L^{-1})			SW 2 (Fortified at 0.7 µg L^{-1})			SW 3 (Fortified at 0.40 µg L^{-1})			SW 4 (Fortified at 1.0 µg L^{-1})			SW 5 (Fortified at 3.0 µg L^{-1})			SW 6 (Fortified at 8.0 µg L^{-1})		
	TFME			TFME			TFME			TFME			TFME			TFME		
	PDMS / DVB	PDMS / DVB-Supp	LLE	PDMS / DVB	PDMS / DVB-Supp	LLE	PDMS / DVB	PDMS / DVB-Supp	LLE	PDMS / DVB	PDMS / DVB-Supp	LLE	PDMS / DVB	PDMS / DVB-Supp	LLE	PDMS / DVB	PDMS / DVB-Supp	LLE
2,4-DCP	0.087	< LOQ	ND	0.73	1.10	0.37	0.44	0.38	ND	1.1	1.4	0.49	4.9	4.1	1.6	11.0	13.0	3.9
2,4,6-TCP	0.087	0.13	ND	0.80	1.1	ND	0.47	0.67	ND	1.2	1.4	0.63	4.5	4.2	2.0	11.0	10.4	5.0
2,3,4,6-TeCP	0.078	0.10	ND	0.79	0.85	0.55	0.45	0.54	ND	1.2	1.2	0.74	4.9	3.5	2.3	12.4	9.6	5.8
Trifluralin	0.072	0.063	ND	0.60	0.63	ND	0.36	0.38	ND	0.95	0.93	ND	3.0	3.4	3.0	8.0	6.4	7.8
Bendiocarb	0.074	0.089	ND	0.68	0.83	ND	0.43	0.43	ND	1.0	1.1	ND	4.4	3.5	ND	10.0	5.3	ND
Phorate	ND	ND	ND	0.58	0.53	ND	<LOQ	<LOQ	ND	0.75	0.73	ND	3.0	3.2	1.1	8.3	9.9	3.0
Carbofurane	< LOQ	< LOQ	ND	0.88	0.94	ND	0.54	0.56	ND	1.3	1.2	ND	5.0	3.7	ND	11.3	9.1	6.8
Simazine	ND	ND	ND	0.49	0.58	ND	0.29	<LOQ	ND	0.80	0.75	ND	2.7	3.2	1.7	6.2	6.8	4.4
Atrazine	< LOQ	< LOQ	ND	0.7	0.80	ND	0.44	0.27	ND	1.1	1.0	0.56	2.8	3.1	2.1	6.3	6.4	5.2
PCP	ND	ND	ND	0.46	0.47	0.53	0.26	0.29	ND	0.72	0.73	0.72	2.5	2.1	2.2	6.7	7.1	5.6
Terbufos	< LOQ	ND	ND	0.60	0.47	ND	0.40	0.37	ND	0.90	0.76	ND	2.3	2.6	0.86	6.0	6.3	2.3
Diazinon	0.078	0.073	ND	0.70	0.72	ND	0.42	0.42	ND	1.0	1.0	ND	3.3	3.2	2.2	8.4	9.1	5.7
Triallate	< LOQ	0.058	ND	0.53	0.52	ND	0.32	0.34	ND	0.80	0.73	ND	2.0	2.0	3.0	5.5	6.6	7.4
Metribuzine	< LOQ	< LOQ	ND	1.10	0.14	ND	0.63	0.48	ND	1.4	1.3	ND	3.7	3.5	ND	8.8	8.0	5.3
Methyl parathion	ND	ND	ND	<LOQ	<LOQ	ND	<LOQ	<LOQ	ND	0.70	1.5	ND	1.2	1.7	2.6	6.8	7.0	7.0
Alachlor	0.083	0.082	ND	0.76	0.83	0.71	0.44	0.37	ND	1.1	1.2	0.95	2.6	3.0	2.7	6.2	6.2	6.6
Carbaryl	ND	ND	ND	0.43	0.37	ND	0.25	0.20	ND	0.60	0.52	ND	1.9	1.6	ND	6.8	6.3	ND
Prometryne	< LOQ	< LOQ	ND	0.70	0.59	0.65	0.35	0.18	0.35	1.0	0.86	0.86	1.8	2.2	2.4	5.5	7.6	5.5
Malathion	ND	ND	ND	0.80	1.0	ND	ND	ND	ND	0.78	1.3	ND	3.0	2.7	ND	8.2	6.7	ND
Metalachlor	0.11	0.11	ND	0.75	0.76	0.79	0.44	0.44	ND	1.1	1.1	1.0	3.0	2.9	2.8	7.3	7.3	7.0
Chlorpyrifos	ND	< LOQ	ND	0.35	1.3	ND	0.19	0.90	ND	0.48	1.9	ND	1.5	5.0	2.8	5.6	11.6	7.1
Cyanazine	0.12	0.13	ND	0.71	0.72	ND	0.43	0.42	ND	1.0	1.0	ND	2.7	2.6	1.8	7.0	6.7	4.7
Ethyl parathion	0.78	< LOQ	ND	0.65	0.50	ND	0.38	0.25	ND	0.94	0.77	ND	3.6	3.0	2.9	5.4	5.9	7.5

Table 5.6 (continued)

Pesticides	SW 7 (Fortified at 2.0 µg L^{-1})			SW 8 (Fortified at 7.5 µg L^{-1})			SW 9 (Fortified at 0.75 µg L^{-1})			SW 10 (Fortified at 9.0 µg L^{-1})			SW 11 (Fortified at 0.87 µg L^{-1})			SW 12 (Fortified at 4.5 µg L^{-1})		
	TFME		LLE	TFME		LLE	TFME		LLE	TFME		LLE	TFME		LLE	TFME		LLE
	PDMS / DVB	PDMS / DVB-Supp		PDMS / DVB	PDMS / DVB-Supp		PDMS / DVB	PDMS / DVB-Supp		PDMS / DVB	PDMS / DVB-Supp		PDMS / DVB	PDMS / DVB-Supp		PDMS / DVB	PDMS / DVB-Supp	
2,4-DCP	2.5	3.0	0.86	12.6	14.7	4.0	0.83	1.1	0.36	13.0	17.7	4.2	1.1	1.3	0.33	5.6	6.3	2.7
2,4,6-TCP	2.5	2.9	1.1	10.0	14.4	4.7	0.90	1.1	ND	10.0	16.2	5.4	1.1	1.2	ND	5.6	6.2	3.2
2,3,4,6-TeCP	2.5	2.4	1.5	10.5	13.0	6.1	0.93	0.88	0.65	10.3	13.3	6.9	1.1	1.1	0.62	6.4	5.6	4.1
Trifluralin	2.0	2.0	1.7	7.2	8.0	7.5.	0.80	0.74	ND	8.1	8.2	8.6	0.89	0.86	ND	4.7	4.9	5.1
Bendiocarb	2.1	2.3	ND	7.5	9.5	4.0	0.80	0.75	ND	9.6	8.7	4	0.93	0.90	ND	5.6	5.2	2.4
Phorate	2.0	2.2	0.93	11.2	12.3	4.4	0.68	0.80	ND	11.2	13.9	4.9	0.78	0.88	ND	5.3	5.6	2.9
Carbofurane	2.5	2.5	ND	11.6	10.4	7.4	0.94	0.92	ND	12.6	10.7	8.5	1.1	1.0	ND	5.9	4.8	5.1
Simazine	2.3	2.3	1.1	6.2	7.8	5.1	0.86	0.75	ND	7.6	8.3	5.7	0.98	0.92	ND	4.7	5.8	3.3
Atrazine	2.3	2.3	1.4	6.0	7.1	5.6	0.90	0.88	0.54	7.0	7.5	6.3	1.1	1.0	0.53	4.2	5.2	3.7
PCP	1.7	1.7	1.4	8.8	8.1	5.2	0.64	0.61	0.55	9.5	8.7	5.9	0.67	0.72	0.53	4.0	3.2	3.6
Terbufos	1.6	2.0	0.99	7.0	8.5	4.7	0.90	0.84	ND	8.9	8.6	5.3	1.1	1.3	ND	4.1	5.7	3.1
Diazinon	2.1	2.2	1.2	8.3	9.2	5.5	0.75	0.77	ND	10.0	10.3	6.2	0.94	0.94	ND	5.2	5.2	3.8
Triallate	1.5	1.8	1.6	7.3	7.4	7.1	0.68	0.69	ND	8.5	6.4	8.1	0.64	0.86	ND	2.4	2.8	4.8
Metribuzine	3.2	3.0	ND	8.7	10.9	ND	1.8	1.3	ND	11.6	13.7	5.3	1.9	1.7	ND	7.5	6.8	ND
Methyl parathion	1.5	1.4	1.5	3.5	4.7	6.7	1.4	0.52	ND	8.0	6.0	7.7	1.2	1.3	ND	3.1	2.7	4.5
Alachlor	2.4	2.5	1.8	6.3	6.3	6.2	0.95	0.93	0.75	7.8	7.3	7.1	0.93	1.1	0.74	3.6	4.3	4.3
Carbaryl	1.2	0.98	ND	8.0	7.5	7.8	0.46	0.49	ND	11.0	8.6	8.7	0.48	0.48	ND	4.0	2.3	5.2
Prometryne	2.7	2.5	1.4	8.2	8.5	6.1	1.4	1.3	0.63	10.7	9.0	6.3	1.2	1.4	0.69	5.3	5.5	4.3
Malathion	1.4	2.7	ND	8.7	8.0	5.2	ND	0.33	ND	11.5	10.0	6	1.2	1.3	ND	5.2	3.7	ND
Metalachlor	2.3	2.3	1.8	7.7	7.2	6.7	0.82	0.82	0.8	9.6	8.4	7.5	0.89	0.93	0.77	4.3	4.8	4.6
Chlorpyrifos	1.0	1.3	1.5	5.1	6.3	6.7	0.48	0.48	ND	7.5	6.0	7.7	0.58	0.57	ND	3.4	4.1	4.5
Cyanazine	2.1	2.1	ND	7.1	6.7	4.2	0.78	0.78	ND	8.9	7.8	4.6	0.86	0.89	ND	4.0	4.4	2.7
Ethyl parathion	2.4	1.9	1.6	12.8	11.2	7.2	0.81	0.64	ND	16.6	13.8	8.3	1.0	0.78	ND	8.1	6.0	4.9

Table 5.6 (continued)

Pesticides	SW 13 (Fortified at 0.6.0 ppb)			SW 14 (Fortified at 0.40 ppb)			SW 15 (Fortified at 2.5 ppb)			SW 16 (Fortified at 0.90 ppb)			SW 17 (Fortified at 7.5 ppb)			SW 18 (Fortified at 4.5 ppb)		
	TFME		LLE	TFME		LLE	TFME		LLE	TFME		LLE	TFME		LLE	TFME		LLE
	PDMS / DVB	PDMS / DVB-Supp		PDMS / DVB	PDMS / DVB-Supp		PDMS / DVB	PDMS / DVB-Supp		PDMS / DVB	PDMS / DVB-Supp		PDMS / DVB	PDMS / DVB-Supp		PDMS / DVB	PDMS / DVB-Supp	
2,4-DCP	0.84	0.36	0.31	0.54	0.55	ND	4.1	3.9	1.8	1.3	1.3	0.50	8.1	14.5	4.9	7.1	6.2	2.5
2,4,6-TCP	0.82	1.1	ND	0.54	0.58	ND	4.0	4.1	2.0	1.1	1.4	0.57	8.5	14.9	5.5	7.1	6.5	3.0
2,3,4,6-TeCP	0.74	0.87	ND	0.50	0.49	ND	4.1	3.6	2.4	1.1	1.1	0.68	9.0	12.3	6.2	7.3	5.8	3.5
Trifluralin	0.65	0.57	ND	0.42	0.40	ND	3.0	3.4	2.8	0.95	1.0	ND	8.7	7.9	7.8	4.9	5.3	4.3
Bendiocarb	0.51	0.35	ND	0.33	0.34	ND	2.6	2.6	ND	0.68	0.80	ND	6.2	5.7	ND	4.3	4.2	ND
Phorate	0.50	0.55	ND	0.30	0.34	ND	3.1	3.1	1.6	0.87	0.83	ND	7.3	11.5	4.3	5.5	5.5	2.3
Carbofurane	0.73	0.63	ND	0.46	0.42	ND	3.5	2.8	ND	1.1	0.98	ND	8.1	7.9	7.3	5.6	4.5	ND
Simazine	0.63	0.66	ND	0.31	0.35	ND	3.4	2.0	1.7	0.82	0.67	ND	7.3	8.5	5.2	5.1	6.2	3.0
Atrazine	0.80	0.87	ND	0.40	0.45	ND	3.0	2.4	2.1	0.98	0.80	0.56	6.8	8.2	5.9	4.6	5.4	3.5
PCP	0.53	0.30	ND	0.24	0.28	ND	2.1	1.7	2.1	0.55	0.56	0.62	5.6	7.1	5.6	3.5	3.0	3.2
Terbufos	0.78	0.54	ND	0.47	0.45	ND	2.8	3.1	1.5	0.88	1.0	ND	7.9	8.1	4.1	4.2	5.2	2.2
Diazinon	0.65	0.63	ND	0.43	0.43	ND	3.1	3.1	2.3	0.94	0.94	ND	7.9	8.6	6.1	5.2	5.2	3.5
Triallate	0.82	0.49	ND	0.42	0.37	ND	2.2	2.1	2.9	0.56	0.64	ND	5.9	7.5	7.7	3.4	3.0	4.4
Metribuzine	0.96	0.91	ND	0.64	0.62	ND	3.4	3.0	ND	1.4	1.1	ND	7.7	7.3	5.2	5.6	5.9	ND
Methyl parathion	0.40	0.27	ND	0.26	0.34	ND	1.4	1.3	2.5	0.55	1.6	ND	3.4	2.6	7.0	2.4	1.7	3.8
Alachlor	0.90	0.77	0.62	0.46	0.52	ND	2.3	2.2	2.6	0.89	0.76	0.90	6.4	7.1	6.9	3.6	4.0	3.9
Carbaryl	0.41	0.16	ND	0.21	0.19	ND	1.6	1.0	ND	0.43	0.31	ND	4.8	5.7	6.1	3.6	1.8	ND
Prometryne	1.4	1.1	0.55	0.64	0.68	0.39	3.9	2.5	2.1	0.57	1.1	0.92	11.2	13.8	6.3	7.2	7.1	4.0
Malathion	0.72	0.43	ND	0.48	0.73	ND	1.3	2.3	ND	0.96	0.84	ND	5.9	5.4	ND	3.4	2.4	ND
Metalachlor	0.65	0.66	0.62	0.38	0.43	ND	2.5	2.2	2.7	0.98	0.78	0.90	7.6	8.3	7.2	4.5	4.4	4.1
Chlorpyrifos	0.29	0.31	ND	0.18	0.81	ND	1.6	2.2	2.7	1.3	1.1	ND	5.9	5.5	7.3	3.0	2.5	4.1
Cyanazine	0.62	0.63	ND	0.40	0.50	ND	2.2	2.0	1.2	0.97	0.77	ND	6.9	7.7	4.4	4.0	4.0	2.6
Ethyl parathion	0.48	0.40	ND	0.34	0.29	ND	3.0	2.4	2.7	1.0	0.66	ND	9.2	8.1	7.4	6.1	4.3	4.2

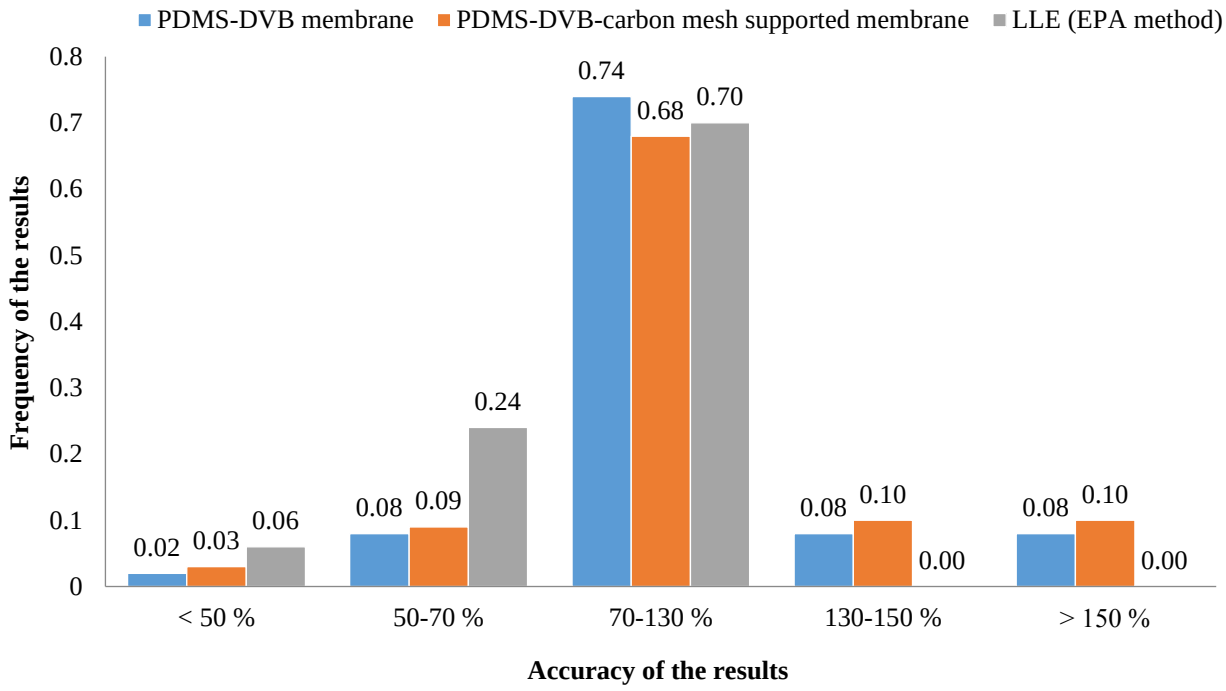

Figure 5.2 Accuracy of the TFME and LLE methods for the analysis of 18 surface water samples.

5.3.3 On-site application and comparison of various TFME based methodologies

At first, the drill-TFME method was optimized in the laboratory to evaluate influential parameters, including the extraction time profile and agitation rate of the drill. The agitation rate was the first parameter investigated, as it controls the thickness of the boundary layer, and affects the mass transfer of compounds to the coating. In the pre-equilibrium regime, improved sensitivity is expected to be achieved at higher agitation rates due to a decrease in the thickness of the boundary layer. Application of high agitation rates is beneficial for on-site extractions since a short extraction is preferred due to practical limitations (*e.g.* lifetime of the battery, the difficulty of sampling when the sample is not easily accessible). In view of this, agitation rates in the range of 500-3000 rpm were investigated in 1 L of nano-pure water spiked with the target pesticides at 1

μg L^{-1}. The highest sensitivity increases were observed for most compounds at 2000 rpm (Figure 5.3).

An extraction time profile was then obtained using the optimized stir rate of 2000 rpm in 1 L nano-pure water spiked at 1 μg L^{-1}. As shown in Figure 5.4, after three hours, all spiked compounds were shown to reach equilibrium. However, as previously mentioned, a shorter extraction time needed to be selected so as to simplify the on-site TFME procedure. Therefore, 10 minutes was selected as the extraction time for further evaluation of the methods.

For on-site analysis, the stability and repeatability of the portable GC/MS instrument are critical parameters that need to be frequently monitored by running an extensive quality control (QC) protocol. Unlike benchtop instrumentation, battery operated, portable GC/MS instruments must be powered off after each use. As such, a reusable standard BTEX gas-generating vial held carefully at 35 ^{o}C with a portable block heater was used to monitor the status of the instrument in the field.[3,4] In cases where the portable GC/MS was not directly equipped with the TDU unit, a secondary SPS-3 thermal desorption module was first used to transfer analytes from the TFME membranes to a needle trap device, which could then be directly introduced into the instrument.[1] All optimizations of the drill-TFME method were performed in a temperature-controlled laboratory at 22.5 ^{o}C. It is also important to note that if external calibration is to be used for real, on-site TFME experiments, the temperature of the sample matrix must match or be close to that of the external calibration experiment. Alternatively, the kinetic calibration[146] method, performed by loading internal standard on the coating, can be used to justify any temperature variation. However, a proper coating material needs to be selected to assure adequate desorption of the internal standard from the thin film that meets the adsorption-desorption symmetry.

Finally, analyses of real water samples along 4 sampling sites (2 affected and 2 low-impact) within the Grand River and Credit River (Ontario, Canada) were performed by three methods, including i) in-bottle TFME, ii) on-site TFME and bench-top GC/MS analysis, and iii) on-site TFME-portable GC/MS analysis. These sites included the small community of West Montrosse (clean) and downstream of multiple Kitchener/Waterloo golf courses (affected) within the Grand River, and both up and downstream of a covered dumpsite near Forks of the Credit Provincial Park. The temperature of the river was monitored using a thermometer and was found to be relatively consistent between the four sites, ranging from 22 ^{o}C +/- 1^{o}C for the Credit River sites, and 25^{o}C +/- 1^{o}C for the Grand River sites. Therefore, in the current study, there was no considerable temperature variation between the external calibration curve and real samples. For validation of the methods, one grab sample from each location was taken and submitted to Maxxam Analytics (Mississauga, ON).

Fortunately, in terms of river health, but unfortunately in terms of engaging scientific discussion, the levels of the targeted pesticide compounds in all rivers tested were well below the limits of detection of most of the methods being tested, as well as the reporting limit of the accredited method (US-EPA 8270) performed by Maxxam Analytics. However, some of these compounds could still be identified and quantified using the TFME bottle sampling method. These levels were found to be 19 and 3 ng L^{-1} for 2,4,6-TCP, trifluralin, and methyl-parathion on the Credit River dumpsite respectively, whereas 2,4,6-TCP, metolachlor, chlorpyrifos, and cyanazine were quantified at 9, 10, 11, 14 ng L^{-1} at the golf course site (Grand River), respectively. Many other compounds were detected using the TFME-bottle methodology, but were at levels just under the method LOQ; these findings can be viewed in Tables 5.7 and 5.8.

The toroidal ion trap of the portable GC-MS was run in full-scan mode (43-500 AMU), allowing for determination of the repeatability of the method, which was carried out by defining the identity of a select few of the unknown compounds that were extracted. In fact, the ability to quickly determine whether or not a target compound is present in a sample remains one of the key advantages of portable instrumentation. As such, 7 non-target analytes were identified and selected based on their molecular functional group from extracts obtained from the affected sites of both river systems, in terms of NIST mass spectra database matching and relative retention times (Figure 5.5, Figure 5.6). These results can be seen in Tables 5.9 and 5.10 for extracts obtained from the Credit River and Grand River sites, respectively. It was promising to see that relative standard deviation levels (n=5) for all compounds tested were around the +/- 20% range. This repeatability was further supported by favorable control chart data shown in Figure 5.7, where the instrument was demonstrated to maintain a stable signal, at 2 standard deviations of the mean, over the entire 1 month sampling period. This result was impressive considering the instrument had to be completely shut down and transported between the laboratory and each of the 4 sampling sites.

Although a direct comparison between the MLOQ's of the portable TFME-GC/TMS and contemporary benchtop methodologies was not directly performed during this study it is true that similar analytes were investigated and discussed in the results of Section 4.3.5 of this thesis. As such, these prior quantitation limits were demonstrated to be 100, 100, 100, 500, 500, and 1000 ng L^{-1} for 2,4-dichlorophenol, 2,4,6-TCP, phorate D10, fonofos, chlorpyrifos, and parathion respectively. Upon making this comparison it is impressive to see that these values were of similar magnitude to the sub-ppb levels reported for the accredited LLE methodology in accordance with the required MCLs.[10] In view of these findings, it is still possible to suggest that the field portable

analysis method can yield quick semi-quantitative results, and allow for absence-presence determination of target analytes at the required MCL level.

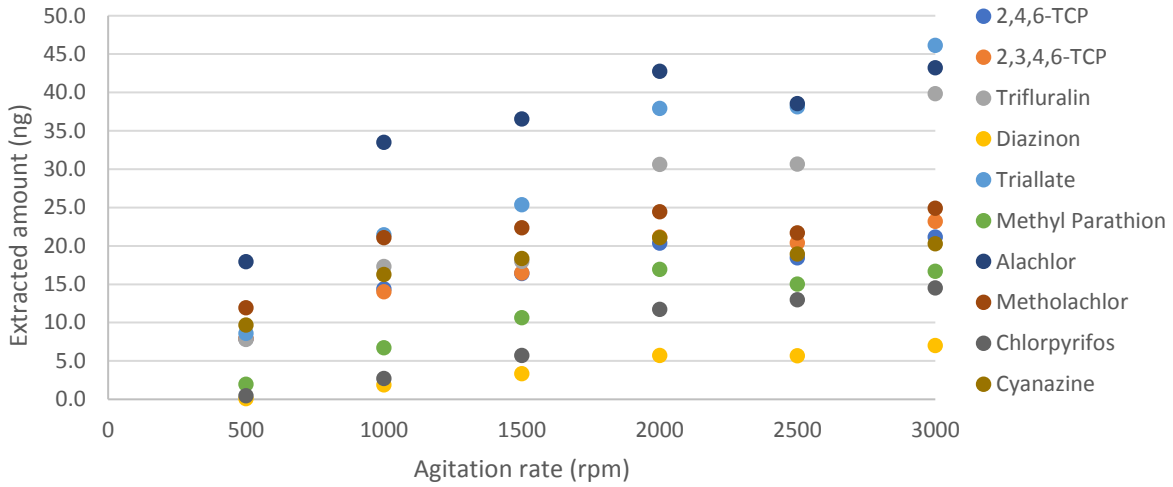

Figure 5.3 Optimization of agitation rate for drill TFME sampler using 1 L of nanopure water spiked at 1 µg L^{-1}. DVB/PDMS thin films were run on a TDU-GC/MS instrument.

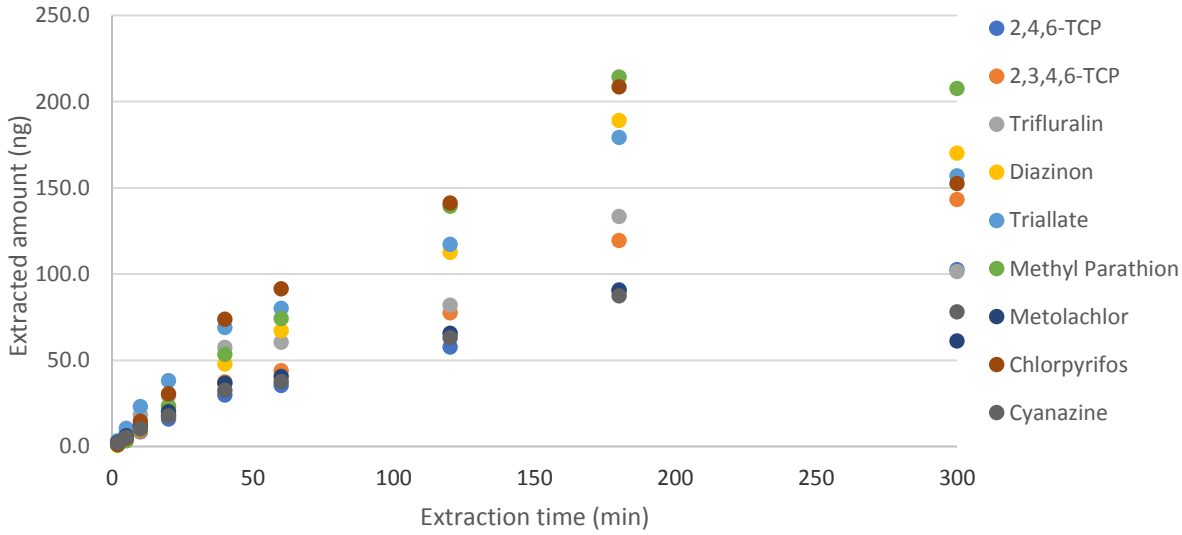

Figure 5.4 Optimization of extraction time profile of drill-TFME approach using 1 L of nanopure water spiked at 1 µg L^{-1}. DVB/PDMS thin films were run on a TDU-GC/MS instrument.

Table 5.7 Results of surface water analysis downstream of Credit River covered dumpsite.

Analytes	**Bottle sampling TFME** ($ng\ L^{-1}$)	**On-site extraction TFME** (Bench-top GC/MS) ($ng\ L^{-1}$)	**On-site extraction and analysis** (Portable GC/MS) ($ng\ L^{-1}$)	**LLE US EPA 8270** ($ng\ L^{-1}$)
2,4,6-TCP	19	ND	ND	ND
2,3,4,6-TCP	<LOD	ND	ND	ND
Trifluralin	3	ND	ND	ND
Diazinon	ND	ND	ND	ND
Triallate	<LOD	ND	ND	ND
Methyl Parathion	<LOD	ND	ND	ND
Alachlor	ND	ND	ND	ND
Metholachlor	<LOD	ND	ND	ND
Chlorpyrifos	<LOD	ND	ND	ND
Cyanazine	<LOD	ND	ND	ND

Table 5.8 Results of surface water analysis downstream of Kitchener/Waterloo golf courses.

Analytes	**Bottle sampling TFME** ($ng\ L^{-1}$)	**On-site extraction TFME** (Bench-top GC/MS) ($ng\ L^{-1}$)	**On-site extraction and analysis** (Portable GC/MS) ($ng\ L^{-1}$)	**LLE US EPA 8270** ($ng\ L^{-1}$)
2,4,6-TCP	9	ND	ND	ND
2,3,4,6-TCP	<LOD	ND	ND	ND
Trifluralin	ND	ND	ND	ND
Diazinon	<LOD	ND	ND	ND
Triallate	ND	ND	ND	ND
Methyl Parathion	<LOD	ND	ND	ND
Alachlor	<LOD	ND	ND	ND
Metolachlor	10	ND	ND	ND
Chlorpyrifos	11	ND	ND	ND
Cyanazine	14	ND	ND	ND

Table 5.9 Selected unknown identifications downstream of Credit dump site using completely on-site analytical methodology. Not shown are another 6 aliphatic hydrocarbons, 2-alkylbenzenes, 4 alcohols, 5 aldehydes, and 1 ester. (n=5)

Analyte	RT (s)	LRI	LRI (lit)	Average	SD	%RSD
Benzene	19.1	N/D	/	5464	1302	24
Ethylbenzene	62.7	863	864	5585	878	16
Benzaldhyde	76.5	966	965	4333	853	20
p-Cymene	83.8	1026	1025	7724	1573	20
Eucalyptol	85.3	1039	1035	4396	491	11
Nonanal	92.6	1103	1108	22826	4471	20
an alkylbenzene	144.0	1647	N/D	5634	737	13

RT = Retention time LRI = Linear retention index SD = Standard Deviation
%RSD = percent relative standard deviation

Table 5.10 Selected unknown identifications downstream of golf courses along the Grand River, using completely on-site analytical methodology. Not shown are another 2 aliphatic hydrocarbons, 4 alcohols, 8 aldehydes, and 3 chloroalkanes. (n=5)

Analyte	RT (s)	LRI	LRI (lit)	Average	SD	%RSD
Ethylbenzene	62.7	863	864	2347	323	14
o-Xylene	67.4	895	893	3799	826	22
Benzaldhyde	76.5	966	965	9472	2020	21
2-Nonanal	92.6	1103	1108	70283	9788	14
an alkylbenzene	144.0	1647	N/D	4601	648	14
1-chlorotetradecane	147.9	1695	1674	11302	2619	23

RT = Retention time LRI = Linear retention index SD = Standard Deviation
%RSD = percent relative standard deviation

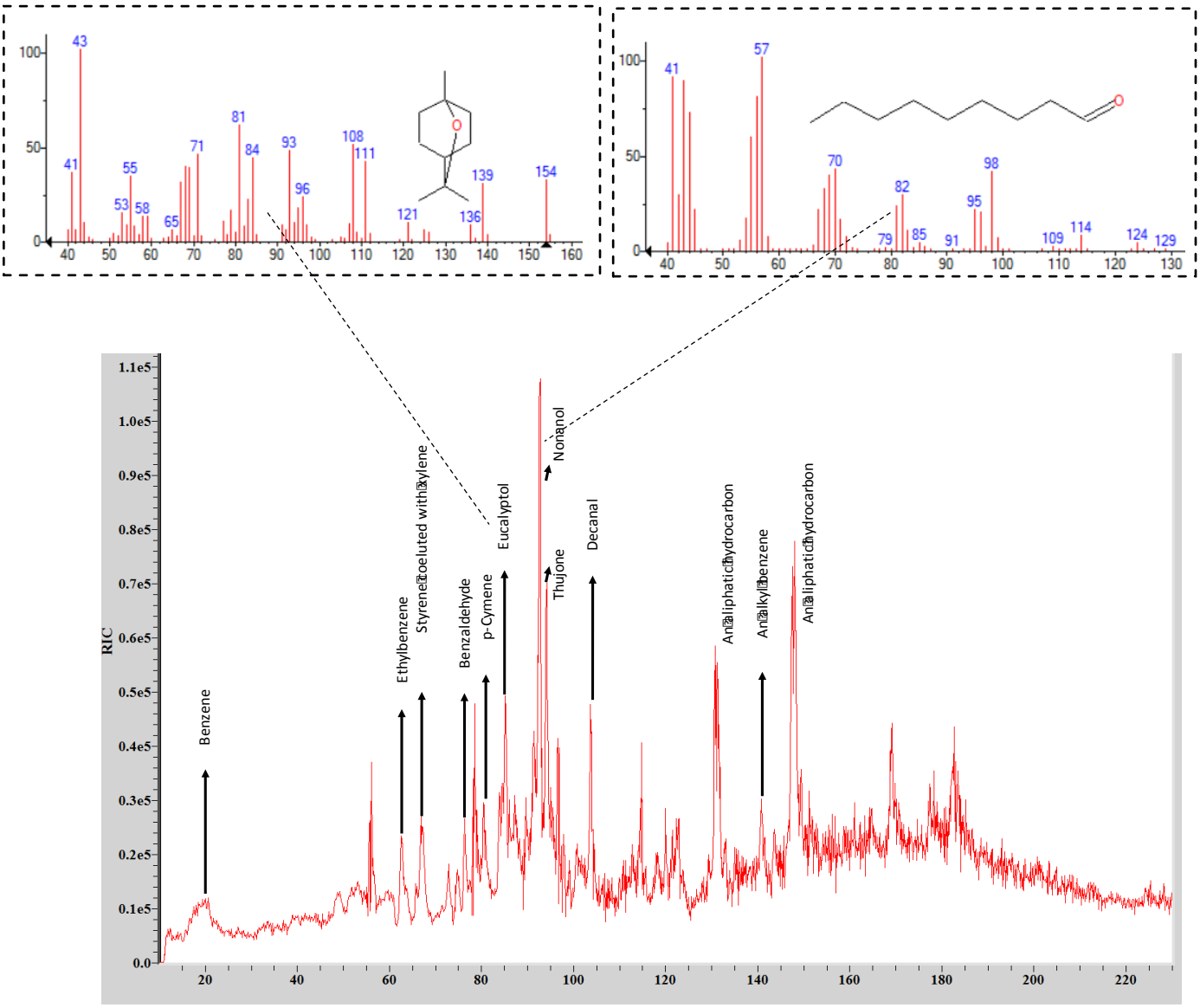

Figure 5.5 Untargeted water analysis using portable TFME-GC/MS downstream of Credit River dump site using completely on-site analytical methodology.

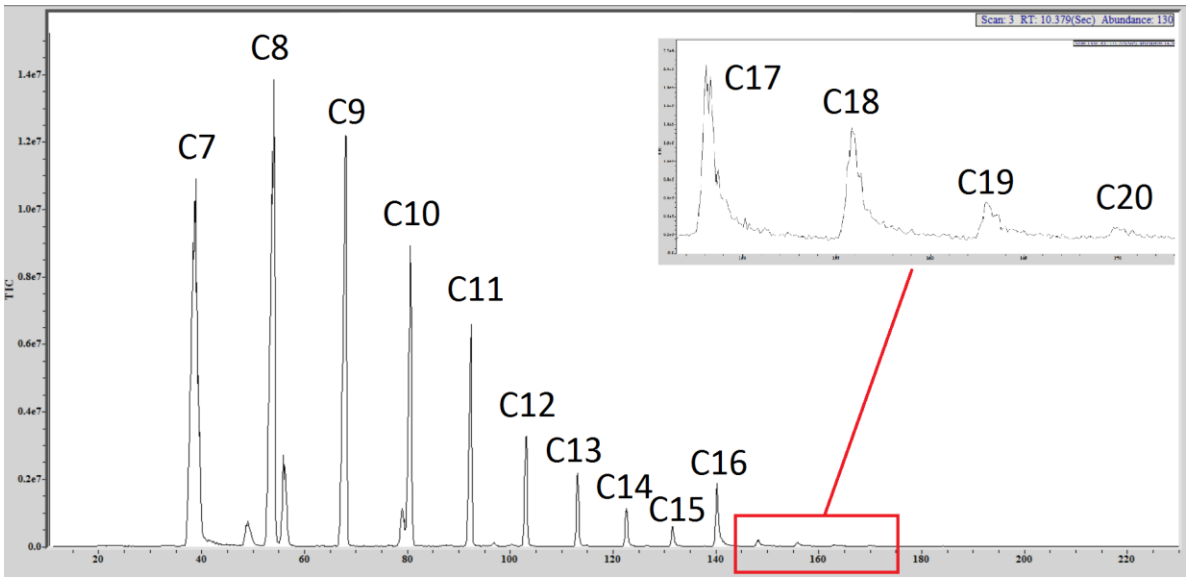

Figure 5.6 Linear retention index plot generated from C7-C20 n-alkanes standard headspace generating vial. 5 mL NTD extractions were performed at 65 ºC.

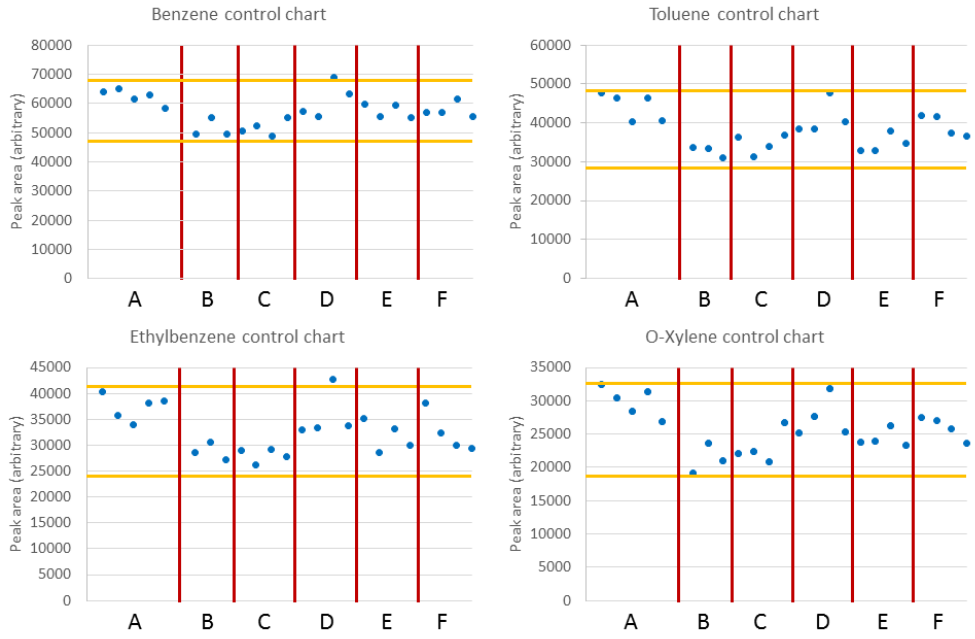

Figure 5.7 Control chart data for portable GC-MS instrument showing BTEX control data at 2 standard deviations (%RSD ≤ 14%) for, A) July 26th 2016, in-lab preceding on-site experiment, B) July 27th West Montrosse on Grand River, C) Aug 3rd Credit River upstream of dumpsite, D) Aug 8th Credit River downstream of dumpsite, E) Aug 19th downstream of golf courses on Grand River, F) Oct 12th Regular instrument check-up and tune post-sampling.

5.3.4 Comparison of the Eco-scale greenness of the developed methods

Nowadays, the development of green techniques and strategies that have minimal impact on the environment plays a vital role in current, trending research in analytical chemistry.[147–150] And indeed, it is widely acknowledged that in analytical chemistry, 'green chemistry' encompasses both separation science and sample preparation.[147] In this sense, green analytical chemistry techniques are focused on the "3R" and "4S" approaches.[147] The approaches are based on "Reduction, Replacement, and Recycling" of hazardous solvents and materials (3R) and the introduction of "Specific method, Smaller dimensions, Simpler methods, and Statistics"(4S).[147] To move towards green approaches, an ideal method would have to integrate several steps into one and preferably eliminate waste generation by performing the entire extraction and analysis on-site (or at least on-site extraction, with associated transportation of only the extraction device to the laboratory, rather than samples). With this in mind, several evaluations of the eco-scale greenness of methods have been introduced in different research areas, including analytical chemistry.[9] Such evaluations consider all the steps required for analysis of the samples, including sample collection, preservation, transportation, sample preparation, and analysis. Further, these evaluations are carried out by assigning penalty points based on the i) reagents used, ii) method, iii) energy consumption, and iv) waste production. In this regard, the main advantage of using SPME is that the extraction phase is constituted by a polymeric coating rather than a toxic organic solvent. While certain steps of the analysis workflow are inevitable (*e.g.* analysis by GC/MS, LC-MS/MS), penalty points can be reduced by eliminating the sampling step by on-site extraction and analysis. An evaluation of the greenness of the developed methods presented in this study, also including the standard US EPA 8270 method for comparison, is shown in Table 5.11. As can be seen, the TFME method is significantly greener as compared to the standard method (Eco scale 81

vs 57). While the TFME method incurs 5 penalty points for waste generation, significant differences exist between the TFME and LLE methods in terms of generation of waste. In TFME, the waste generated during sample preparation is only related to water samples that are spiked with an internal standard mixture. To eliminate this source of waste generation, the addition of internal standard can be avoided as long as there are no fluctuations in the instrument. In cases when internal standard is not added to the sample, the eco-scale greenness of the TFME method increases to 94. By development of on-site extraction and analysis strategies, the eco-scale for SPME techniques further increases to 99, becoming one of the greenest approaches in analytical chemistry, owing to the elimination of both sampling (transportation in the case of portable GC/MS analysis) and waste generation. It should be emphasized that penalty points associated with the establishment of the calibration curve, including standard solution, solvent and waste production, were not considered for this evaluation of the greenness of the method.[9]

Table 5.11 Evaluation of greenness of the developed methods and US EPA 8270.

Steps in the analytical process	**Analytical method**			
	In-bottle TFME	**On-site TFME** (Bench-top GC/MS)	**On-site TFME and on-site analysis** (Portable GC/MS)	**LLE (US EPA 8270)**
Sample collection	- Sampling: 1 - Transport: 1	- Transport*: 1	-	- Sampling: 1 - Transport: 1
Sample preparation	- ACN (100 µL) (Internal standard): 4 (0) - Isotopically labeled mixture: 4 (0) - Orbi-shaker: 1 - Waste production: 5 (0)	- Sampling case(drill): 1	- Sampling case(drill): 1	- Dichloromethane (50 ml × 2): 4×2 - ACN (Internal standard):4 - HCl: 4 - NaOH: 2 - Isotopically labeled mixture: 4 - Vortex: 1 - Tumbler: 2 - Turbovap: 2 - Occupational hazard: 1 - Waste production: 10
Analysis	- GC/MS with auto sampler: 3	- GC/MS with auto sampler: 3	- Portable GC/MS: 0 - Desorption chamber: 0	- GC/MS with auto sampler: 3
Penalty points (PP)	**19**	**5**	**1**	**43**
Eco-scale (100-PP)**	**81 (94)*** **	**95**	**99**	**57 (65)*** **

* Transport of the membrane (not the sample) after extraction

**Penalty points associated with the calibration curve were not considered for evaluation of the greenness of the methods[9]

*** Eco-scale without the addition of internal standard

5.4 Conclusion and future directions

A new method based on TFME was developed and validated through an inter-laboratory study of 23 pesticides in surface waters split between laboratories and submitted on a blind basis. The merits of using membranes were shown from several analytical aspects in comparison to conventional LLE methods. Agreement of the results between TFME and LLE methods demonstrate that TFME can be used for the routine analysis of selected pesticides in surface water

samples. TFME was shown to be an accurate method, providing much lower detection limits for many compounds, while eliminating the need for organic solvents and minimizing the amount of sample required. Based on these results, TFME might also be considered as an approach for on-site sampling for accurate and rapid quantification of compounds of interest. The improved sensitivity achievable by TFME would offset the lower sensitivity of portable instrumentation.

The goal of our research initiatives is to develop SPME techniques that are appropriate and suitable for use in a contract analytical laboratory environment. For adoption of an analytical technique in the industry as a well-accepted method, it is necessary to offer capabilities and advantages that are significantly different from existing approaches and improves the current limitations. While TFME has similar accuracy and precision as LLE (as an official US EPA method) it provides several benefits such as the need of small volume of sample, simultaneous analysis of acidic, basic and neutral compounds, rapidness, lower cost, and greenness. The data generated in this study support the potential application of TFME techniques in routine, production-oriented analyses.

The second approach investigated in this study, namely on-site extraction TFME and analysis facilitated by a home-built, drill-based sampling device, and field-portable GC/MS instrumentation opens other possibilities for rapid on-site screening and quantitation. In this approach, the transportation of samples to the laboratory is eliminated, thus showcasing this method as the ultimate green chemistry approach. Further, truthful quantification of labile compounds and elimination of analyte losses, as well or immediate decisions are facilitated by this approach. However, careful compensation for on-site temperature variations, and in cases where complex samples are analyzed need to be applied using in-coating calibration if good accuracy and precision are desired rather than just the gathering of screening information.

Chapter 6 Development of a hydrophilic-lipophilic balanced thin film solid-phase microextraction device for the balanced determination of volatile organic compounds

6.1 Introduction

Solid-phase microextraction (SPME) devices, particularly those used for gas chromatography based determinations have been well published in the literature since the early 90's.[6,126,151] Of these, most sorbent chemistries and commercial devices have been tailored to target non-polar volatile and semi-volatile organic compounds (VOC's, SVOC's) by extractions facilitated by primarily hydrophobic sorbents.[5,134,151] A notable exception would be the existence of the more polar compound oriented poly(ethylene glycol) (PEG) and polyacrylate (PA) SPME fibers which, much like polydimethylsiloxane (PDMS) may be considered a liquid-like sorbent with absorption being the primary mechanism of extraction.[5,10,11,15,151,152] In fact Naccarato *et al.* were able to demonstrate that when targeting polar, VOC's and SVOC's such as various benzothiazoles, benzotriazoles and benzosulfonamides, the polyacrylate-based fibers gave the broadest coverage even when compared to solid sorbents such as Carboxen (CAR/PDMS), divinylbenzene (DVB/PDMS) and DVB/CAR/PDMS fibers.[152] However, these liquid-like fibers still lack the broad spectrum sorbent strength exhibited by solid sorbent particles, giving a lower affinity for lower boiling VOC's and VVOC's.[5,10] Moreover, polar, absorptive coatings remain impractical for the determination of non-polar contaminants, much like how PDMS is unsuitable for polar compounds. [5,10] This limitation may leave a little to be desired in terms of simultaneous polar and non-polar analyte as even DVB/PDMS has a moderately high hydrophobic character.[153] Multi-polar Carboxen based SPME fibers have their limitations as well; although shown to give better coverage for both polar and non-polar compounds they are known to exhibit poor desorption characteristics making them only suitable for low boiling VVOC's.[5,10,151]

One possible solution may originate from recent developments in SPME-HPLC methodologies where researchers have begun using hydrophilic-lipophilic balance (HLB) materials to address these very same issues.[154,155] Exhibiting both hydrophobic interactions via a poly(divinylbenzene) backbone and the capability of hydrogen bonding and polar interactions at the N-vinylpyrrolidone group,[156] these HLB particles have seen growing use in SPE cartridges,[157] in-line SPE columns,[158,159] TF-SPME HPLC applications,[154,155] and even in various direct-to-MS configurations.[128,160–163] One recent approach, presented by Poole *et al.*, had shown that when used in-lieu of C-18, recessed SPME-needle devices prepared with HLB were able to extract 3-4 times the amount of polyunsaturated fatty acids from salmon tissue.[164] Moreover, in a very recent work by Gionfriddo *et al.* a HLB/PTFE SPME fiber was presented that could tolerate both thermal and solvent desorption allowing for parallel GC and HPLC based determinations.[135] In-fact, in an earlier work HLB particles had already seen use in the preparation of a GC-amendable TF-SPME.[165]

This 2015 study highlighted the use of HLB particles in the preparation of two TF-SPME devices, used in conjunction with GC/MS and HPLC/MS instrumentation respectively, for the *in-vivo* determination of prohibited substances in human saliva.[165] Although innovative, the HLB/PDMS membranes prepared were not without their limitations. At only 6 mm in diameter, the membranes were rather small compared to those used in other works.[1,25,47] This size may have been chosen to reduce the siloxane background associated with this PDMS. More recent works by Grandy *et al.* had demonstrated that using a more high-density PDMS is required to minimize such siloxane background.[1] Furthermore, as the commercial HLB particles chosen were intended for use in SPE cartridges they were considerably large at 60 µm in diameter; 12 x larger than that of the DVB typically used in SPME devices. As HLB is a solid sorbent the related sorbent strength

is directly related to the specific surface area which increases with decreasing particle size, and increases with pore volume. With these limitations in mind, the choice of smaller HLB particles, spread in combination with the aforementioned high-density PDMS would be ideal for the simultaneous balanced determination of both polar and non-polar analytes of varying volatility.

In the present work, various such membranes are explored. Using the carbon mesh supported high-density PDMS based membrane design[1], several HLB/PDMS/carbon mesh TFME devices were prepared using various types of lab-made, or commercial HLB particles. These membranes were shown to extract a substantially higher amount of mixed polarity VOC standards than the comparative DVB/PDMS composition while exhibiting a similar level of background bleed. Moreover, one of the homemade HLB chemistries exhibited equal or better performance to that of the top-tier 5 µm commercial HLB particle making this homemade HLB/PDMS/carbon mesh membrane the ideal choice for the untargeted determination of chlorination bi-products for hot-tub water.

6.2 Materials, instrumentation, and experimental methods

6.2.1 Chemical and materials

Benzene, 2-pentanone, nitropropane, pyridine, 1-pentanol, octane, toluene, divinylbenzene, N-vinylpyrrolidone and, 2-azobisisobutyronitrile were purchased from Sigma-Aldrich (Mississauga, ON, Canada). HPLC grade methanol, acetone, and acetonitrile were obtained from Caledon Laboratories Ltd. (Georgetown, ON, Canada). Ultrapure water was obtained using a Barnstead/Thermodyne NANO-pure ultrapure water system (Dubuque, IA). The 5 µm diameter DVB particles and high-density PDMS were provided by Supelco (Bellefonte, PA). The carbon fiber mesh weave (Panex 30) was provided by Zoltec Co. (Bridgetown, MO). Liquid nitrogen and ultrahigh-purity helium were supplied by Praxair (Kitchener, ON, Canada). The 65

μm divinylbenzene/polydimethylsiloxane (DVB/PDMS) SPME fiber assemblies and PS-DVB resin (XAD-4) was provided by Sigma-Aldrich. The commercial 5 μm HLB particles were provided by Waters Inc. The Twister sorptive PDMS stir bar (2 cm long) was supplied by GERSTEL Co. (Mülheim an der Ruhr, GE). KJLC 704 silicon pump fluid (tetramethyl tetraphenyl trisiloxane) was ordered from Kurt J. Lesker Company (Toronto, ON, Canada). The membrane conditioning unit was developed at the University of Waterloo Science Electronics Shop (Waterloo, ON, Canada). Cross locking grip tweezers with Stand were purchased from KW surplus store (Kitchener, ON, Canada). The Elcometer 4340 motorized automatic film applicator and coating bar (adjustable gap of 0−250 μm) were acquired from Elcometer Ltd. (Rochester Hills, MI). HLB-TFME and DVB-TFME membranes were prepared using the method reported in the literature.[1] Overhead stirrers with regulated speed controls were purchased from Scilogex LLC (Rocky Hill, Connecticut, USA). The 4 stage stir plate was purchased from Corning (New York, USA).

6.2.2 Instrumental analysis method (benchtop GC/MS)

In terms of analytical instrumentation, an Agilent 6890 GC and a 5973n quadrupole MS (Agilent Technologies, CA U.S.A.) was used for separation and quantitation while sample introduction was accomplished using a Gertsel, MPS2 autosampler to transfer the TF-SPME device to the thermal desorption unit (TDU1) cooling injection system (CIS4) (GERSTEL, Mülheim an der Ruhr, GE) for membrane desorption. Chromatographic separations on the Agilent 6890-5973n were performed on a 30 m × 0.25 mm I.D × 0.25 μm SLB-5 fused silica column (Sigma-Aldrich, Mississauga, ON, CA). Helium carrier gas was used at a flow rate of 1.2 mL/min. The column temperature was initially held at 40 °C for 2 min, ramped to 140 °C at a rate of 8 °C min^{-1}, then ramped to 250 ^{o}C at 40^{o}C min^{-1} and kept for 2 min. The MS detector transfer line

temperature, MS quadrupole, and MS source temperature were set at 300, 150, and 230 °C, respectively. Gas phase ions were generated using electron impact ionization at 70 eV, and the quadrupole was operated in SIM mode selecting ions 78, 86, 43, 79, 55, 85 m/z for benzene, 2-pentanone, 1-nitropropane, 1-pentanol and octane respectively, furthermore a reduced full scan method ranging from 35-300 m/z was used for the unknown determination of chlorination by-products.

To facilitate desorption of the 20 mm x 4.75 mm x 400 µm (L x W x T) TF-SPME membranes an inert glass bead was inserted into the tapered 5 mm I.D. glass desorption tube to prevent the membranes from slipping through the tapered bottom of the desorption tube which were designed to hold a wider cylindrical PDMS stir bar rather than a flat thin film. Desorption was carried out at 250 ^{o}C using a helium stripping gas flow of 60 mL min^{-1} for 5 minutes. The desorbed analyte was then cryo-focused at -130 ^{o}C within the CIS module for the duration of the 5-minute desorption. Following desorption, the CIS was then ramped to a temperature of 270^{o}C at a rate of 10 ^{o}C s^{-1} so as to perform transfer of the analyte onto the Agilent 6890 GC-column for separation and quantitation.

6.2.3 Preparation of the in-house HLB particles

Different in-house HLB particles polymerized, using either precipitation or suspension methodologies, were prepared with the intent to compare their extraction efficiency with commercially available sorbents. Precipitation polymerization was performed by reacting 4 mL of divinylbenzene with 1 mL of N-vinylpyrrolidone in 200 mL of acetonitrile with an addition of 30 mg of an azobisisobutyronitrile as an initiator. This mixture was then heated to 70 ^{o}C inside a 500 mL, three neck, round bottom flask which was kept under constant nitrogen purge and mixed at 100 rpm by use of an overhead stirrer for a period of 24 hours. Following polymerization, the

micro particles were washed twice in ethanol and separated from the supernatant solution by use of 10,000 rpm centrifugation for 15 minutes. Finally these particles were dried under nitrogen in a vacuum over at 80^{o}C for 24 hours.

The particles prepared using the suspension polymerization protocol were formulated to similar proportions to that of the precipitation methodology. Appropriately, 4 mL of divinylbenzene were reacted with 1 mL of N-vinylpyrrolidone in 200 mL of water with an addition of 30 mL of toluene to serve as the organic phase and porogen. 30 mg of azobisisobutyronitrile were still used to initiate the reaction. Furthermore, 250 mg of poly(vinyl alcohol) and 500 mg of methyl cellulose were used as stabilizers for the organic suspension. This mixture was then heated to 70 ^{o}C inside a 500 mL, three neck, round bottom flask which was kept under constant nitrogen purge and mixed at 700 rpm by use of an overhead stirrer for a period of 24 hours. The washing and drying procedure for the suspension polymerization method was the same as that described for the precipitation methodology.

6.2.4 Characterization of the sorbent particles and resulting membranes

Infrared spectroscopic data were collected on a Bruker Tensor 27, FT-IR spectrometer (Madison, WI USA) in powder form between 4000 and 450 cm^{-1}. The shape and size of the HLB particles and morphology of the HLB thin film membranes were determined by field emission scanning electron microscopy (FE-SEM Model No.) (Carl Zeiss, Germany). HLB particles were also characterized by transmission electron microscopy (TEM) (JEOL JEM-2010). The surface area of the HLB particles was determined using N_2 adsorption-desorption isotherms at 77 K. The samples were degassed at 100 °C for 24 h before adsorption measurements. The specific surface area was calculated by the Brunauere-Emmette-Teller (BET) method. Thermal stability of

synthesized membranes was evaluated by running a blank membrane analysis on the Agilent 6890-5973N GC-MS in full scan mode. Desorption was performed on a Gerstel TDU at 250 ^{o}C for 5 minutes using 60 mL min^{-1} of stripping He gas. Compounds were trapped by the CIS at -80^{o}C.

6.2.5 Preparation of the large volume McReynolds headspace generating jar

As McReynolds mixtures represent a varied class of inter-molecular interactions across a wide polarity range, a selection of benzene, 2-pentanone, 1-nitropropane, pyridine, 1-pentanol, and octane, which possess log[P] values from 0.84-4.78,[75] were used to prepare a large McReynolds standard analyte generating jar. The preparation of this spiked silicon oil-polystyrene-co-divinylbenzene resin was performed using the method described by Grandy[3], Gomez[75], Poole[4] *et al.* However, to ensure negligible depletion of the headspace standard when extracting with high capacity TF-SPME devices, a much larger gas generating jar was prepared. This 250 mL jar was composed of 30.0 g of PS-DVB resin and 80.0 g of spiked silicone diffusion pump fluid which itself was pre-spiked with 4 µL of benzene, 6 µL of 2-pentanone, 8 µL of 1-nitropropane, 6 µL of pyridine, 12 µL of 1-pentanol, and 12 µL of octane. Finally to allow the introduction of the TF-SPME membranes into the jar a small hole was drilled into the lid and a 2 mL disposable centrifuge tube whose bottom was cut was then glued into the hole. This headspace jar and corresponding TF-SPME introduction can be seen in Figure 6.1.

Figure 6.1: A 250 mL McReynolds standard headspace generating jar being sampled from with a TF-SPME device held by cross-locking tweezers.

6.2.6 Calibrating amount extracted by on membrane liquid injection

In order to calibrate the actual amount (in ng) of analyte extracted without having to remove the TDU-CIS and convert the injector to the GERSTEL septum-less head, or a standard split/splitless configuration, a novel calibration method, called on-membrane liquid injection, was employed. To execute this method the TF-SPME device was held in place by cross-locking tweezers while a gas-tight syringe was used to deliver 1-3 µL of methanolic McReynolds standard directly to the uncoated edge of the TFME device allowing for the standard to be wicked into the membrane. These membranes were immediately placed into the TDU desorption tubes pending analysis and each calibration level was run in triplicate (n=3). In addition to avoiding the need to change the injection system of the GC/MS, this method was found to exhibit additional advantages

in that a liquid calibration standard of a given concentration could be used for multiple calibration levels as the excess methanol was not found to overload the instrument. This outcome is likely because much of the volatile solvent was either lost from the membrane or, not trapped by the CIS during analyte transfer.

Where the calibration range was 200-10000 ng, spanning 2 orders of magnitude, the linear data shown in Figure 6.2 was transformed by the use of a $1/x^2$ weighing factor resulting in the calibration values presented in Table 6.1. This $1/x^2$ transformation was chosen as to avoid discrimination of any results that gave signal near that of the lower calibration points.[108] A 75:1 split ratio was used during calibration meaning of the 200-10000 ng injected, only 2.67-133 ng of the standard was actually reaching the detector. Furthermore, when a further 20000 ng injection was performed, the signal was shown to begin exhibiting non-linear behavior indicating saturation of the mass spectrometer.

Table 6.1 Calibration data for on-membrane liquid injection following $1/x^2$ weighing.

Compounds	Benzene	2-Pentanone	1-Nitropropane	Pyridine	1-Pentanol	Octane
Slope	13198	2706	4599	6115	1156	4928
Intercept	631760	154161	47465	39188	-3719	24433

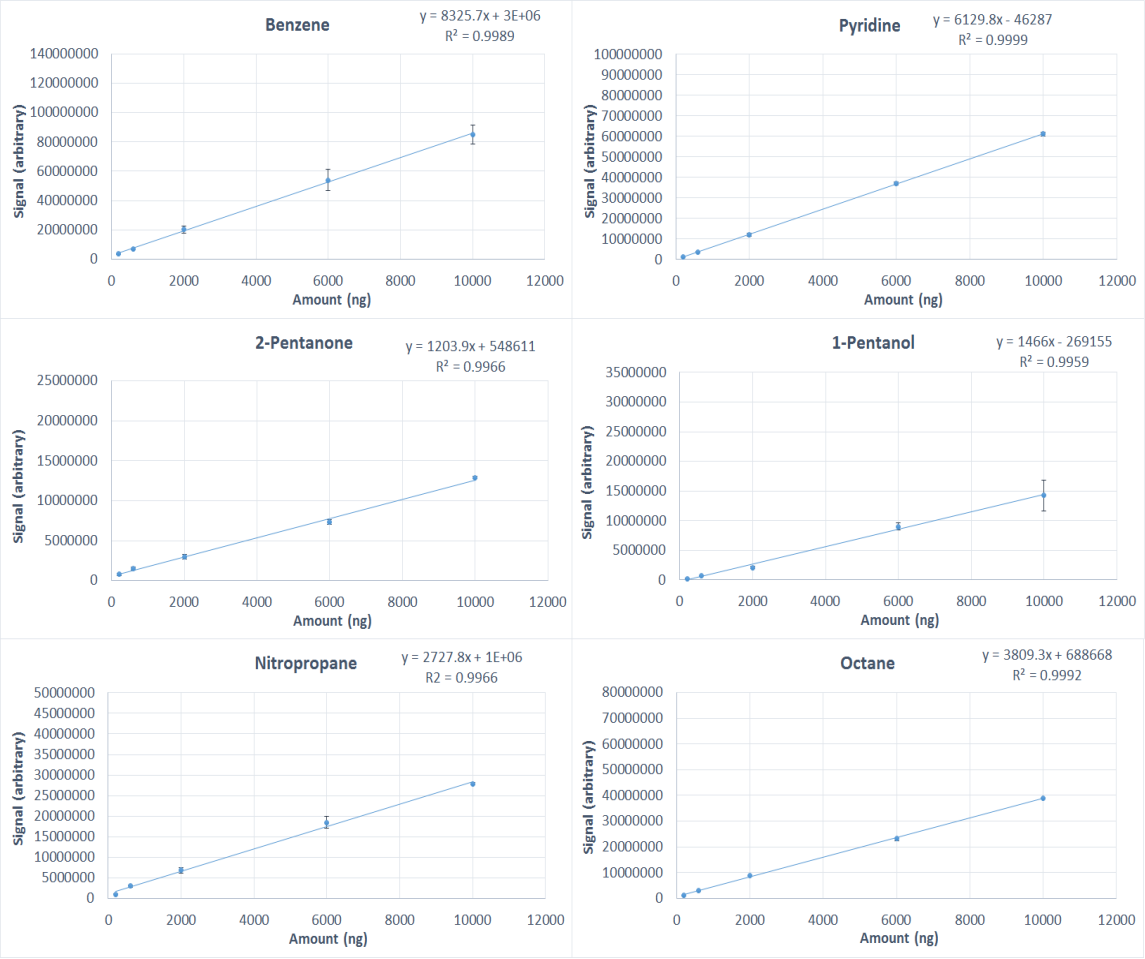

Figure 6.2 On-membrane liquid injection calibration curve for the modified McReynolds standards prior to performing $1/X^2$ weighing of the data.

6.2.7 Comparison of thin film extraction sensitivity using various sorbent particles

To compare the relative extraction efficiencies of the various TF-SPME sorbent chemistries, PDMS-Carbon mesh supported membranes prepared with 5 µm DVB, 5 µm commercial HLB, 1.3 µm precipitation polymerized HLB and 2 µm suspension polymerized HLB in addition to a 2 cm PDMS coated stir bar and a 65 µm DVB/PDMS SPME fiber were compared in terms of extraction amounts. These extractions were performed from the 250 mL McReynolds headspace generating jar at 55 ºC for 10 minutes under static conditions. In order to account for any intermembrane variability, 3 different membranes of each chemistry were analyzed 3 times

each (n=9 per membrane). All results were calibrated and presented in terms of nanograms. To avoid overloading of the MS detector while remaining well within calibration range, a 75:1 split, 10:1 split and splitless injection were used for the TF-SPME, SBSE, and SPME injections respectively. All extractions were randomized to account for any undetected drift of detector response while QC extractions were performed before and after the experiment.

6.2.8 Validation of volatile analyte stability on thin films stored in TDU tubes post extraction

To check the post-extraction stability of the McReynolds standards on the HLB thin film membranes, extractions were carried out at 55 ^{o}C for 10 min using TF-SPME devices prepared with the 1.3 µm HLB particles synthesized by precipitation polymerization. Post-extraction, membranes were stored in TDU tubes on the autosampler rack. Membranes were then analyzed immediately following extraction, 24 hours after extraction, or 120 hours after extraction. Extractions were performed in triplicate and analyzed on the GC-MS instrument. Desorptions were performed using a 75:1 split ratio at 250 ^{o}C for 5 min with 60 mL min^{-1} of stripping gas. Analytes were trapped within the CIS at -130 ^{o}C prior to GC injection.

6.2.9 Intermembrane analytical reproducibility of a modified McReynolds standard

As to ensure the TF-SPME preparation procedure yields statistically reproducible membranes an intermembrane reproducibility study was also performed using the data from the coating comparison experiment as such the same extractions protocols and membranes described in the aforementioned study were used. In order confirm said reproducibility the 3 membranes of each coating chemistry were compared using a one-way ANOVA test at 95% confidence for each of the 6 McReynolds analytes. Furthermore, the inter-batch reproducibility of the homemade HLB particles was also assisted by comparing two completely unique batches of HLB(P)/PDMS thin film membranes.

6.2.10 On-site thin film solid phase microextraction of chlorination by-products from a private hot tub

As a proof of concept, thin film membrane extractions were performed at a private hot tub. Headspace extractions were performed in triplicate by placing TFME in between the cross locking fiber grip tweezers at atmospheric pressure for 30 min. Direct immersion extractions were performed by filling 20 mL vials equipped with TFME holders to the brim with hot tub water. These extractions were performed for 30 minutes at a constant agitation of 1500 rpm using a magnetic stir bar on-site. The pH and temperature of hot tub water were measured to be 7.2 and 39.5 ^{o}C respectively, however, water was allowed to cool to near ambient temperatures (27 ^{o}C) prior to extraction. After extraction, the membranes were dried by dabbing with a Kimwipe and instantly stored in the 3.5-inch thermal desorption tubes with glass beads. The tubes were closed on both sides by using appropriate caps and transported back to the lab where analyses were performed immediately afterwards. Membranes were analyzed on the benchtop GC-MS (Agilent 6890-5973). Splitless desorptions were performed at 250 ^{o}C for 5 min with 60 mL min^{-1} stripping gas. Analytes were trapped in the CIS at -130 ^{o}C. For untargeted analysis signals were reported as peak areas in full scan mode (35-300 m/z).

6.3 Results and discussion

6.3.1 Physical characteristics of homemade sorbent particles and thermal stability of resulting thin films

HLB particles obtained after synthesis were characterized by FT-IR, SEM, TEM, and surface area analysis. The FT-IR spectrum of the HLB particle is shown in Figure 6.3. The peaks in the ranges of 3084–3018, 1642–1446, 795–708 and 2848–2921 cm^{-1} were respectively assigned to aromatic C=C-H, stretching, C-C stretching, aromatic C-H bending, and methylene C-H stretching. Furthermore, the signal at 1687 cm^{-1} was assigned to the C=O stretching vibration of

N-vinylpyrrolidone. These characteristic absorption peaks indicated the formation of poly(divinylbenzene-co-N-vinylpyrrolidone) resin.

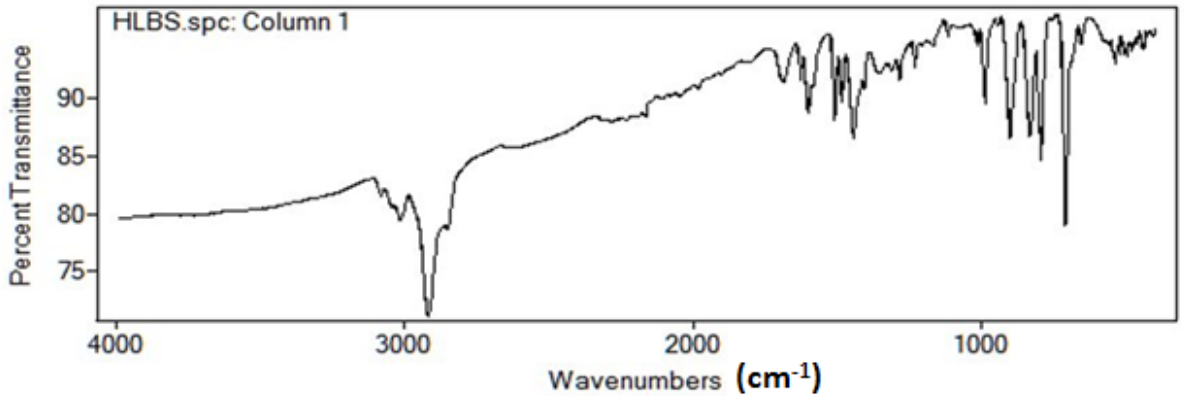

Figure 6.3 FT-IR spectrum of HLB particles synthesized by precipitation polymerization.

Following confirmation of poly(divinylbenzene-co-N-vinylpyrrolidone) resin formation, the morphological features of the particles were visualized by SEM and TEM. As can be seen in Figure 6.4, the particles obtained from precipitation polymerization were spherical, uniform and monodispersed. Particles were found to be approximately 1.33 µm using TEM analysis. Whereas the particles obtained by suspension polymerization were spherical but non-uniform and polydispersed with diameters ranging from 30-60 µm.

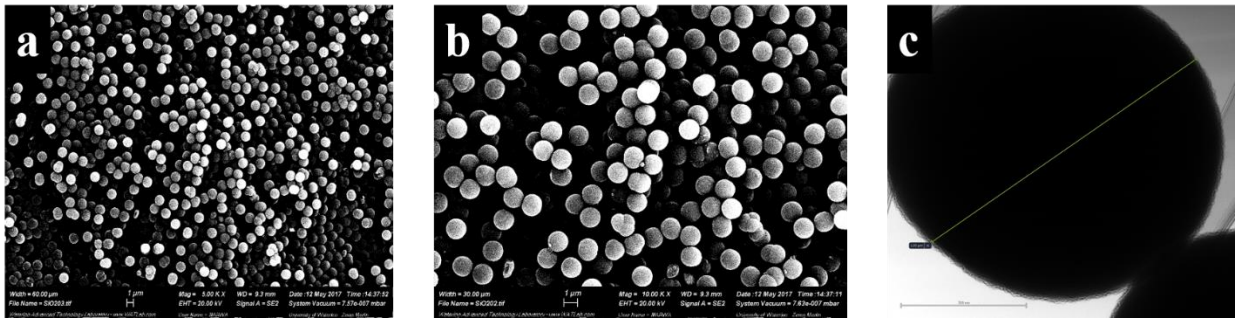

Figure 6.4: HLB particles synthesized by precipitation polymerization. SEM images, A) magnification 5000x at 20 kV, B) magnification 10,000x at 20 kV (scale 1 µm), and, C) TEM image recorded at 200 kV (scale 500 nm).

The specific surface area (SSA) of sorbent particles generally depends on the diameter and total porosity of said particle. As such it would be expected that the smaller 1.33 µm precipitation polymerized particles would have the higher SSA value. However, as can be seen in Table 6.2 this was not the case. The specific surface area of the HLB particles synthesized by precipitation polymerization was shown to be approximately half that of all other particles tested. Meanwhile, the SSA of all other particles tested, including the commercial DVB, commercial HLB, and the HLB prepared using suspension polymerization, were all found to be more or less the same. The SSA difference observed for the precipitation polymerized HLB is likely related to the lower pore volume and smaller pore size of these particles. Although purely speculative, these variations are likely due to the porogen chosen in the preparation of each particle type. For the precipitation-based HLB, acetonitrile was used in lieu of the toluene porogen that was employed for the suspension polymerization methodology. Toluene was also likely used for the commercial HLB particles as this is specified in the original HLB patent.[166] Despite having lower SSA the precipitation particles remain much more microporous with a pore diameter of only 12.99 Å. Such a microporous nature may have an inherent advantage for the extraction and retention of low boiling VOC's and VVOC's as these compounds generally have a much smaller molecular radius.[5,10]

Table 6.2: Comparison of the physical characteristics of the compared sorbent particles.

Material	SSA (m^2/g)	Pore size (Å)	Pore volume (mL/g)	Particle size (µm)
DVB (comm.)	750	400	1.54	5
HLB (comm.)	800	80	1.30	5
HLB Suspension	727	71	0.64	30-60
HLB Precipitation	335	13	0.20	1.33

Thermal stability testing of TFME membranes synthesized with commercial DVB and precipitation HLB particles were carried out via blank injections on the Agilent GC-MS. To

compare the levels of detectable bleed, three different DVB/PDMS/carbon mesh membranes were run with three HLB/PDMS/carbon mesh membranes. It can be perceived from the stacked chromatograms shown in Figure 6.5 that the backgrounds levels obtained from the HLB/PDMS membranes were comparable to that of the DVB/PDMS membranes. The peaks associated with the aromatic compounds bleeding of the DVB portion of the particles can be seen at retention time 6.5 to 9 min and appear to be slightly larger for DVB/PDMS. However, a few additional peaks can be seen within the first 3 minutes of the HLB/PDMS runs. These peaks remain unidentified but may be related to the N-vinylpyrrolidone portion of the HLB particle. Unsurprisingly, the 5 larger peaks associated with siloxane background are of similar magnitude regardless of device tested. Although any bleed may be considered undesirable it is important to remember that this background is still much less than previous designs and remains at a similar level to what is seen with other high volume PDMS devices such as the commercially available, Twister, 2 cm PDMS sorptive stir bar.

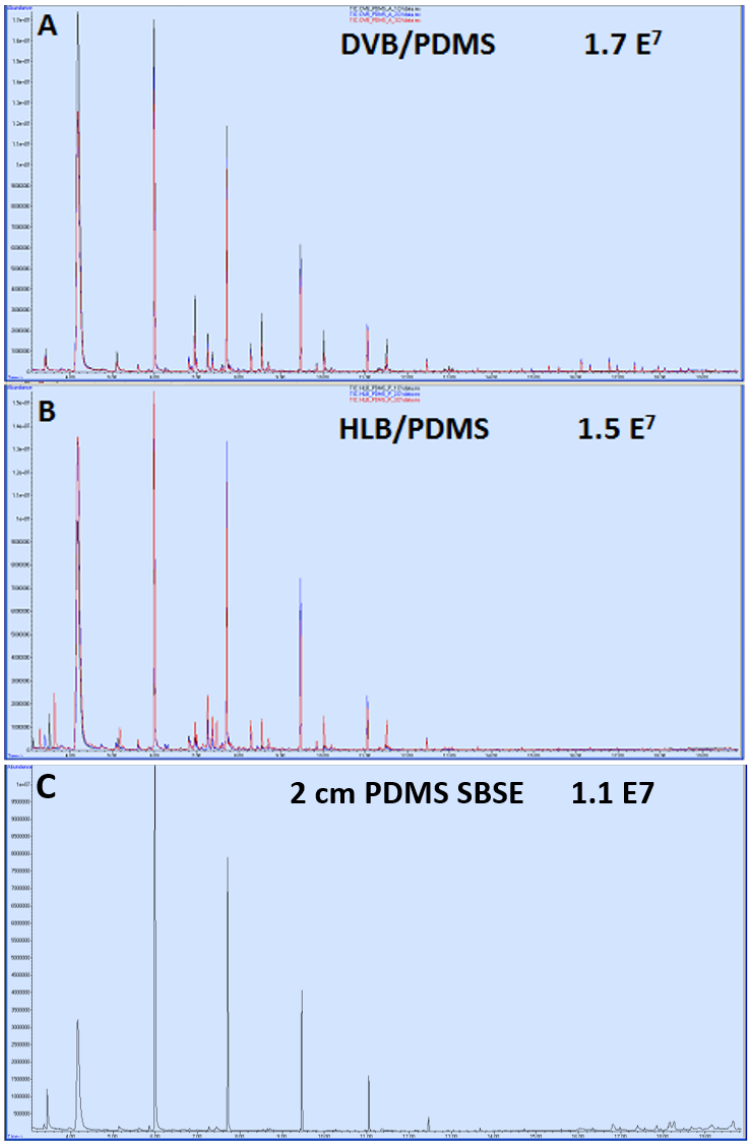

Figure 6.5 Comparison of membrane bleed and associated siloxane background for, A) three DVB/PDMS/carbon mesh supported membranes, B) three HLB/PDMS/carbon mesh supported membranes, and, C) commercial 2 cm pure PDMS SBSE. All membranes were of similar size and desorbed at 250 °C using 60 mL min^{-1} of helium for 5 min. desorption of the CIS was performed in splitless mode.

6.3.2 Improvement of TF-SPME affinity for polar VOC's using HLB loaded thin film membranes

As HLB based sorbents are designed to give a balanced coverage between both polar and non-polar analytes it was decided that a modified McReynolds standard comprised of benzene (log[P]= 2.13), 2-pentanone (log[P]= 0.98), , 1-nitropropane (log[P]= 0.94), pyridine (log[P]= 0.84), 1-

pentanol (log[P]=1.7) and octane (log[P]= 4.78) would be the most appropriate selection in terms of comparing the relative extraction efficiency of volatiles on a broad spectrum sorbent.[167] As shown in Figure 6.6 it was found that the 1.3 µm HLB particles prepared using the precipitation polymerisation method yielded the highest extraction amounts extracting a factor of 1.8x, 2.2x, 1.9x, 1.7x, 2.0x and 1.3x more benzene, 2-pentanone, 1-nitropropane, pyridine, 1-pentanol, and octane than the established DVB/PDMS based membrane respectively. In terms of the more established techniques, it was ubiquitously found that the DVB/PDMS SPME fiber offered the lowest extraction amounts, followed by the 2 cm PDMS SBSE stir bar due to the limited sorbent volume and lack of a broad polarity sorbent particle respectively. In fact, the DVB/PDMS TF-SPME device was found to extract on average, 35-75 times more analyte than the comparative SPME fiber. This is a great deal more than the 20 fold factor reported in our previous study where a membrane twice as large was used.[1] Such variation is almost certainly due to the fact that in the current study near equilibrium conditions were achieved allowing the entire volume of the sorbent to be used in extraction. Contrarily, pre-equilibrium conditions were chosen in the previously reported pesticide study as the goal was to show the benefits of having a high surface area extraction device for quick on-site analysis of semi-volatile water contaminants.[1] As previously alluded to, it is thought that the improved extraction efficiency offered by the precipitation polymerisation based sorbent particles is related to the improved polarity range of HLB, and the microporous surface structure of the particles. Particularly, when comparing the commercial HLB obtained from Waters and the precipitation particles it can be seen that despite the former having approximately double the specific surface area, the much more microporous precipitation polymerisation based particles, which used an acetonitrile porogen, still provide significantly

higher extraction amounts (2-tailed T-test at 95% confidence) for all of the analytes tested with a p= 0.00047 being the highest reported, for octane.

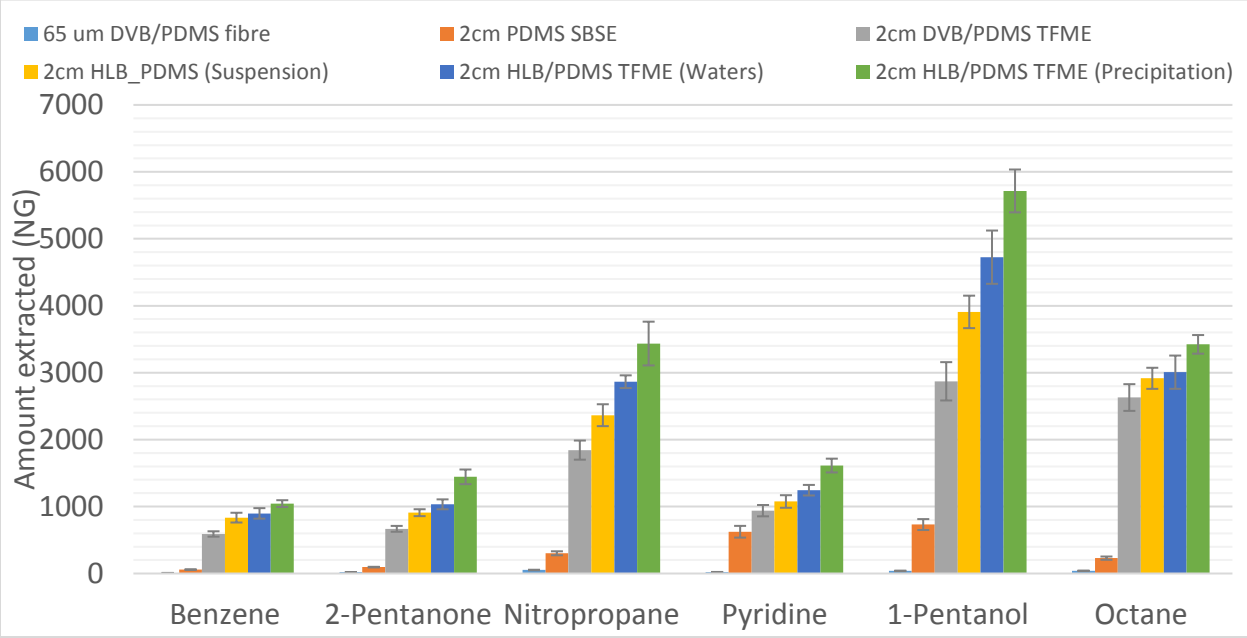

Figure 6.6 Relative extraction efficiencies of the studied McReynolds standards using: a 65 µm DVB/PDMS SPME fiber, a 2 cm PDMS SBSE stir bar, DVB/PDMS TF-SPME membranes, HLB/PDMS (suspension HLB) membranes, HLB/PDMS (commercial HLB) membranes, HLB/PDMS (precipitation HLB) membranes. Extractions were performed from the McReynolds standard headspace generating vial for 10 min at 55 ºC.

Table 6.3 Aggregated data of all extraction chemistries tested with results shown in nanograms.

	65 µm DVB/PDMS fiber			2 cm PDMS stir bar			DVB/PDMS TF-SPME		
	Average	SD	%RSD	Average	SD	%RSD	Average	SD	%RSD
Benzene	8	0.9	11	58	6	9	590	40	7
2-Pentanone	19	1.8	9	95	5	5	667	44	7
Nitropropane	52	4	8	302	30	10	1843	143	8
Pyridine	21	3	13	624	88	14	939	85	9
1-Pentanol	38	5	13	731	81	11	2871	286	10
Octane	39	4	11	229	25	11	2629	200	8
	HLB(S)/PDMS TF-SPME			HLB(C)/PDMS TF-SPME			HLB(P)/PDMS TF-SPME		
	Average	SD	%RSD	Average	SD	%RSD	Average	SD	%RSD
Benzene	834	73	9	898	78	9	1044	51	5
2-Pentanone	908	52	6	1033	74	7	1444	110	8
Nitropropane	2365	163	7	2865	95	3	3435	327	10
Pyridine	1076	94	9	1244	79	6	1613	103	6
1-Pentanol	3908	243	6	4725	398	8	5715	320	6
Octane	2916	158	5	3007	249	8	3423	139	4

6.3.3 On membrane storage stability of a modified McReynolds standard

To confirm the on-membrane stability of the modified McReynolds standards while being stored in the TDU tubes pending analysis, extractions were performed with the HLB(P)/TFME membranes. These membranes were then stored within the TDU tubes on the autosampler rack for 0, 24 and 120 hours. As validated via ANOVA at 95% confidence, giving F values from 0.001 to 3.64 ($F_{crit=}$5.14) for almost all the McReynolds probes analyzed stability was observed even after 120 hours of storage. The only exception to this observation was for pyridine (F = 27.25) which, as can be seen in Figure 6.7, exhibited a significant decrease after 120 hours of storage. This decrease is attributed to photo-degradation, as this result had been previously observed when McReynolds containing standard headspace generating vials were stored for 10 weeks at various conditions.[3] In this previous study, vials stored at room temperature with exposure to light were observed to exhibit looses for pyridine while those stored in a dark cupboard at room temperature did not.[3] As the thermal desorption tubes used to store the HLB/TFME membranes are comprised of clear glass this result was not surprising. However, it was surprising to observe such reproducible values for the highly volatile benzene even after prolonged storage. This stability is most likely due to the fact that when placed on the autosampler rack the TDU tubes remain relatively sealed with only a small hole with a long diffusion path at the top. Because the relative membrane volume and sorbent partition coefficient are so high in relation to the volume of static air remaining in the desorption tube, only a minuscule fraction of the total analyte extracted on the membrane must be desorbed to come to equilibrium with said remaining static air. Moreover, this study suggests that, as long as the TFME devices are capped and stored within the TDU desorption tubes, they should be suitably stable for transportation back to the lab for analysis after performing on-site samplings.

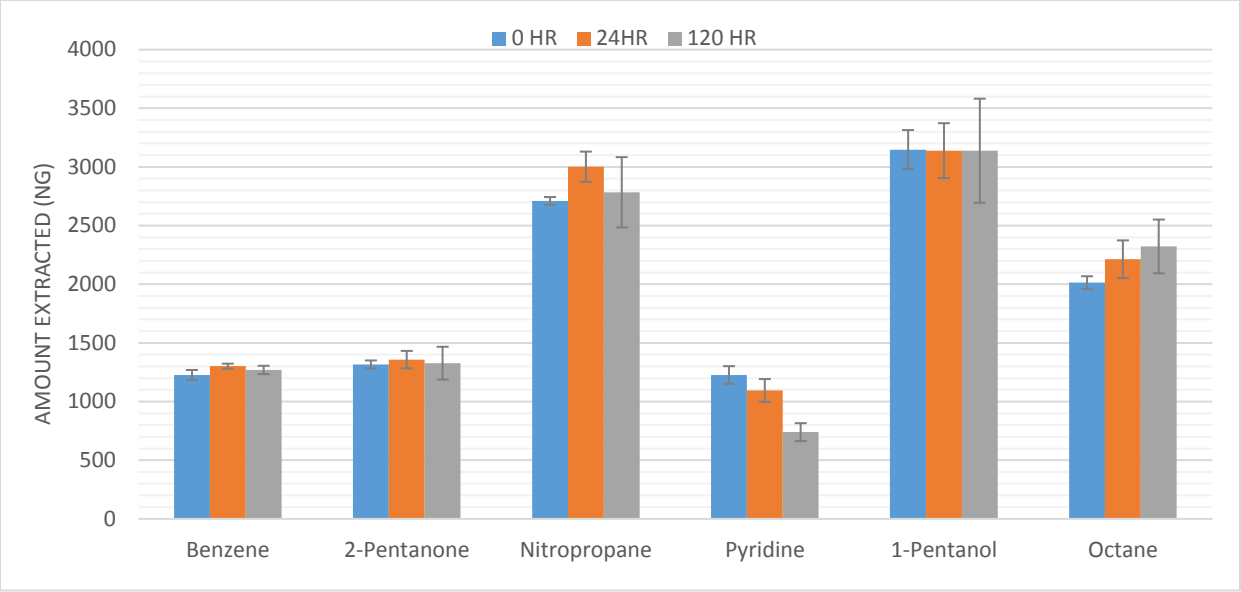

Figure 6.7: Stability of modified McReynolds compounds on the HLB/PDMS/carbon mesh membranes after, A) immediately following extraction, B) 24 hours of storage, and, C) 120 hours of storage.

6.3.4 Intermembrane analytical reproducibility of a modified McReynolds standard

In order to perform reliable sampling while using different TF-SPME membranes to represent different replicate analyses, it remains very important to confirm that they can be manufactured to be statistically reproducible or, at least within 10% variation of each-other. As such it was confirmed at 95% confidence that, for the most part, the prepared membranes were statistically similar when grouped by their corresponding sorbent chemistries. These 1-way ANOVA tests are summarized in Table 6.4 with the corresponding bar charts shown in Figure 6.8. Of the 24 one-way ANOVA tests performed the only exceptions to this agreement were found to be for 2-pentanone on the precipitation HLB based membranes and for 1-pentanol on the commercial HLB based membranes which exhibited F-values of 8.82 and 8.97 respectively (F-critical = 5.14). Such results are not uncommon when using ANOVA testing as one set of replicates with uncharacteristically low %RSD values can make even the smallest variations seem statistically significant. Upon viewing the data it was apparent that this happened to be the case as

the first and second membranes prepared using the precipitation-based HLB had %RSD values for 2-pentanone of 2% and 3% RSD respectively. Furthermore the second of the membranes prepared with commercial HLB was found to exhibit a minuscule %RSD of 1% for the 1-pentanol standard when considering most other values ranged between 5-10% RSD. Even so, if these values are to be considered statistically different their inter-membrane %RSD values for said compounds were still found to be 8% for both membranes.

A further test for the inter-batch reproducibility of the homemade HLB/PDMS/Carbon mesh supported TFME membranes indicated very good similarity between the two separate batches of membranes. This inter-batch similarity is most notably demonstrated by the results of the 2-tailed T-testing (Table 6.5) in which membranes prepared from two entirely unique batches of the homemade precipitation polymerized HLB particles were shown to be statistically similar regardless of the McReynolds probe being analyzed. Where extractions were carried out such that benzene, the least retained compound, and, octane the most retained analyte, were at near-equilibrium and pre-equilibrium extraction kinetics respectively, the similar results amongst batches also strongly indicated that these membranes were, in fact, similar in terms of total sorbent volume, sorbent strength, and membrane surface area. It is also worth noting that the error bars shown in Figure 6.9 give a further indication as to the intra-batch repeatability as replicate extractions were performed using different membranes from the same batch. The related %RSD's which ranged from 5-9% was also considered quite reasonable for the chosen analytical methodology.

Table 6.4 F-values corresponding to intermembrane variability generated from one way ANOVA testing performed at 95% confidence. Tested chemistries include DVB/PDMS TF-SPME membranes, HLB/PDMS (suspension HLB) membranes, HLB/PDMS (commercial HLB) membranes, HLB/PDMS (precipitation HLB) membranes. Extractions were performed from the standard McReynolds headspace generating vial for 10 min at 55 ºC.

	Benzene	2-Pentanone	Nitropropane	Pyridine	1-Pentanol	Octane	F Crit
DVB/PDMS	1.13	1.64	1.27	1.39	1.72	0.42	5.14
HLB(S)/PDMS	4.39	1.41	1.23	1.13	2.70	0.87	5.14
HLB(W)/PDMS	4.49	0.75	1.11	0.54	8.97	1.53	5.14
HLB(P)/PDMS	1.27	8.82	0.48	2.90	0.35	2.69	5.14

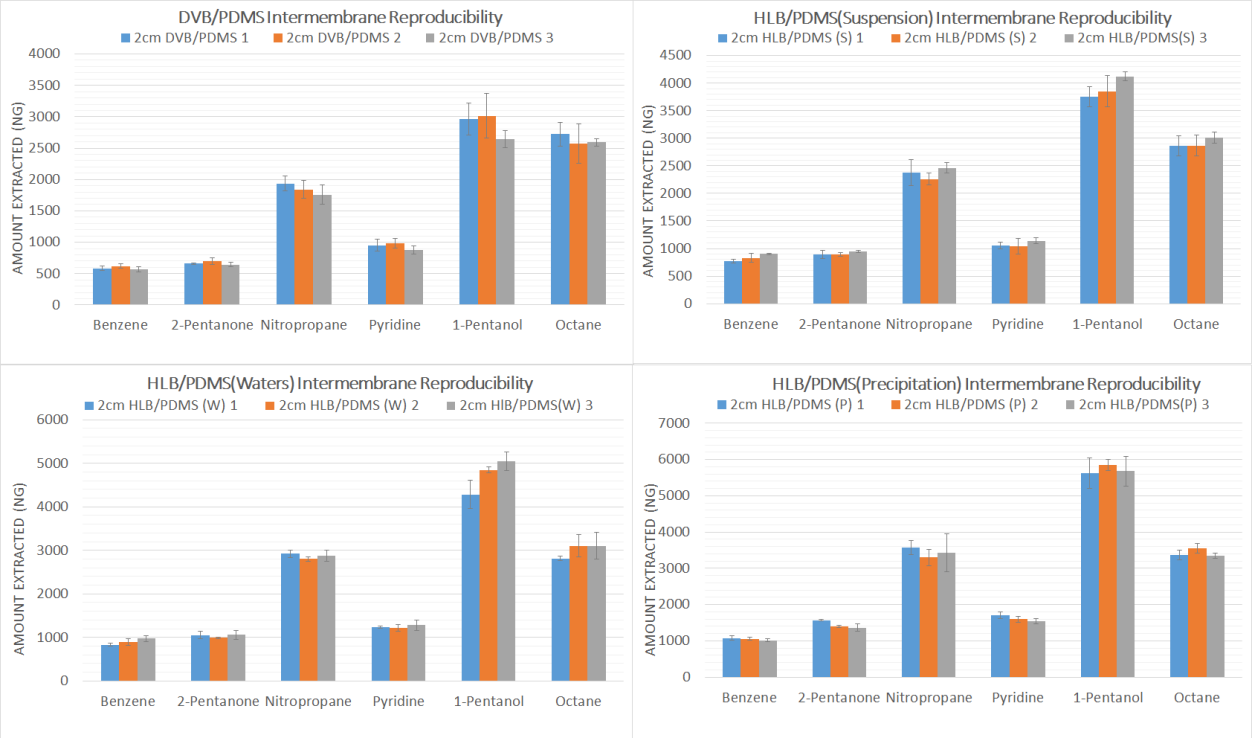

Figure 6.8 Intermembrane extraction amounts of the 4 TF-SPME chemistries tested including, A) DVB/PDMS TF-SPME, B) HLB/PDMS (suspension polymerization) TF-SPME, C) HLB/PDMS (commercial HLB) TF-SPME, and, D) HLB/PDMS (precipitation polymerization). Extractions were performed for 10 minutes at 55 ºC from the McReynolds standard headspace generating vial.

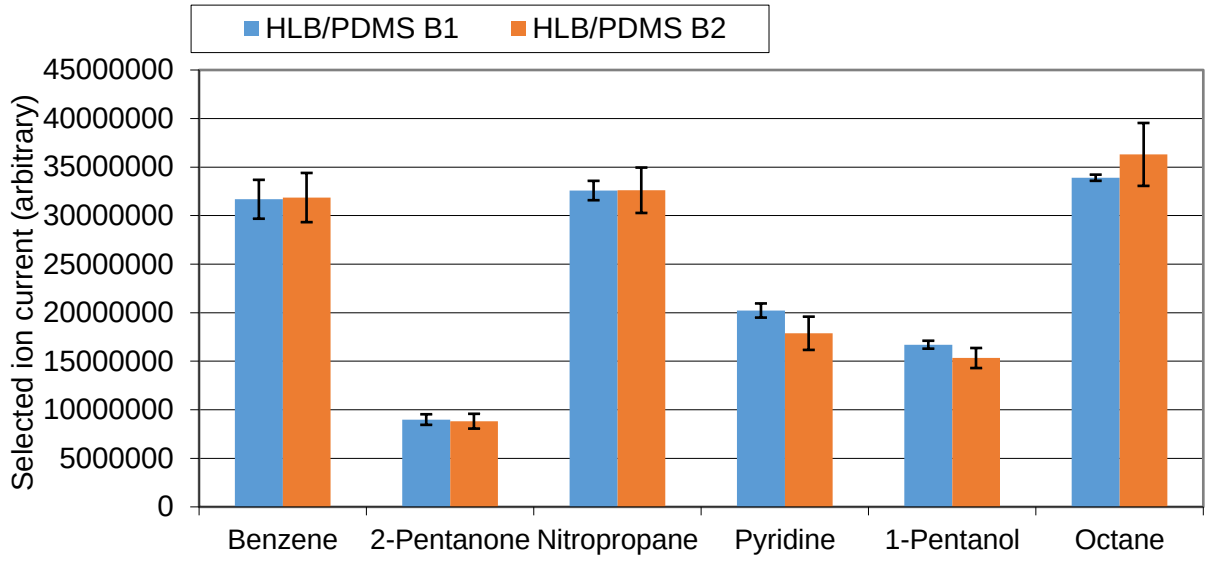

Figure 6.9: Inter-batch reproducibility of 2 separate HLB/PDMS(precipitation) TFME membrane batches. Extractions were performed from a McReynolds standard gas generating jar for 10 minutes at 55 ^{o}C as to achieve near equilibrium conditions.

Table 6.5 T-test at 95% confidence testing inter-batch reproducibility of the precipitation polymerization HLB/PDMS/carbon mesh TFME. (T_{crit}=2.78)

Compounds	Benzene	2-Pentanone	1-Nitropropane	Pyridine	1-Pentanol	Octane
T_{stat}	-0.09	0.32	-0.02	2.18	2.14	-1.28
% RSD	6	7	5	9	6	7

6.3.5 On-site thin film solid phase microextraction of chlorination by-products from a private hot tub

As a proof of concept, to show that the developed method and material (HLB based TFME) could be employed entirely on-site, extractions of chlorination by-products from a private hot tub were performed. Generally speaking, swimming pools and hot tubs use chlorine in the form of hypochlorous acid to disinfect the water. This chlorine reacts with organic compounds originating from human sweat, urine, and other bodily fluids. Because of the high levels of amines found in these bio-fluids (particularly urea) disinfection through chlorination may result in the formation of chloramines whose vapors are known to cause eye irritation and lung damage at high enough concentrations.[168]

Henceforth, on-site extractions were performed from the air directly above the surface of the hot-tub water while the aeration jets were engaged. Fortunately, no detectable chloramines were found in this air which is encouraging as this sampling was performed in the approximate location of a bathers head. However, when direct immersion extractions were performed three chlorination by-products were detected and identified as 3-chloro-1-propanamine, 2-chloroethylamine, and dichloroacetonitrile having retention time 3.53, 4.53 and 4.74 minutes respectively. Unfortunately, as these compounds have highly toxic vapors and considered unstable, it was decided to not handle their pure standards in our university laboratory and hence calibration was not performed. However, it was encouraging to see that the response of the developed methods was fairly reproducible having RSDs of 8-10 % and 3-9% for 3-chloro-1-propanamine and dichloroacetonitrile when extractions were performed using DVB/PDMS and HLB/PDMS membranes respectively. As shown in Tables 6.6 and 6.7, the response in the case of the HLB based TFME membrane was notably higher than that of the comparative DVB/PDMS. Once the unknown compounds were initially identified using the NIST mass spectral database, identities were confirmed using an n-alkane linear retention plot which was generated via analysis of a highly reusable C7−C20 n-alkane standard headspace generating vial. The retention time indices of 3-chloro-1-propanamine, 2-chloroethylamine, and dichloroacetonitrile were calculated to be 688, 788 and 811 which was close to their theoretical values 714, 790 and 806 respectively.

Table 6.6 Chloramine detections from hot-tub water using DVB/PDMS TF-SPME device.

Compounds	RT(s)	RTI	RTI(lit)	Average(sig)	SD	%RSD
2-Chloroethylamine	3.53	714	688	Detect	Detect	Detect
3-Chloro-1-propanamine	4.53	790	788	7.8E+07	6126876	8
Dichloroacetonitrile	4.74	806	811	1.5E+08	1.5E+07	10

Table 6.7 Chloramine detections from hot-tub water using HLB(P)/PDMS TF-SPME device.

Compounds	RT(s)	RTI	RTI(lit)	Average(sig)	SD	%RSD
2-Chloroethylamine	3.53	714	688	Detect	Detect	Detect
3-Chloro-1-propanamine	4.53	790	788	1.2E+08	1.1E+07	9
Dichloroacetonitrile	4.74	806	811	2.2E+08	7049678	3

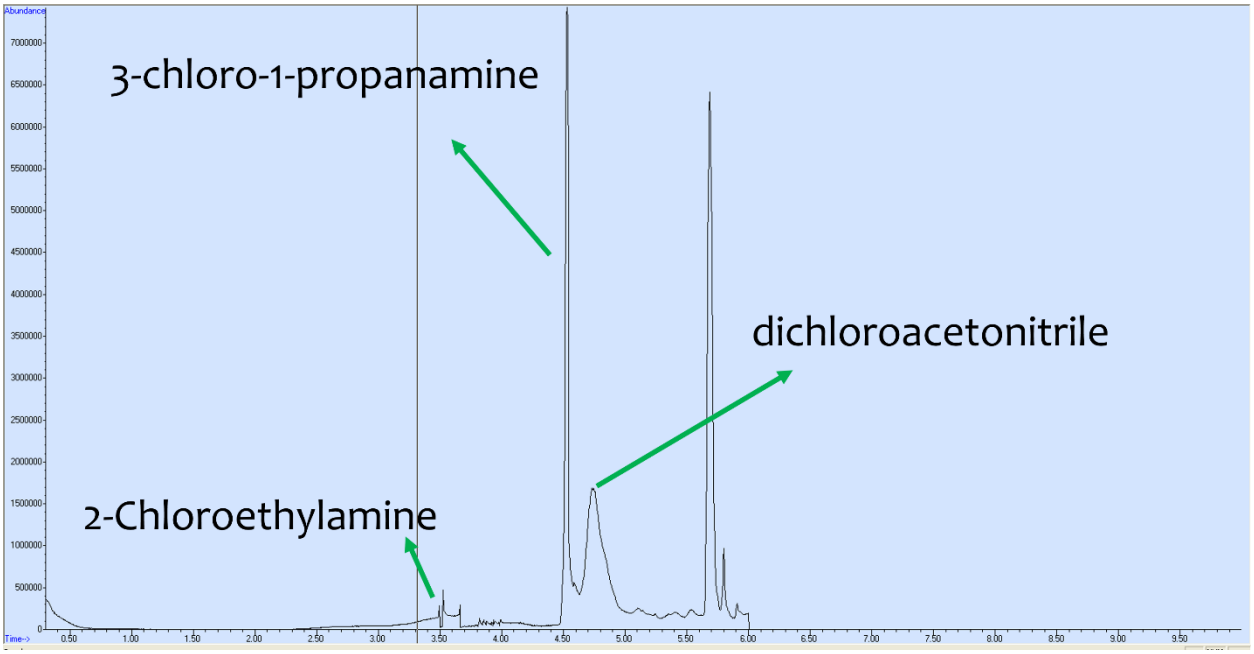

Figure 6.10: Total-ion chromatogram of the compounds detected by benchtop GC/MS after on-site extraction of chlorinated by-products were performed from a private hot tube. Extractions were performed from 20 mL of hot-tub water at a stir rate of 1500 rpm using the HLB/PDMS TFME membrane.

6.4 Conclusion and future directions

A new chemistry of TF-SPME involving the use of homemade hydrophilic-lipophilic balance (HLB) particles for the balanced detection of both polar and non-polar volatile organic compounds is proposed in this study. A considerably improved sensitivity, when compared to membranes prepared with DVB particles, was also demonstrated for the chosen compounds. Furthermore, the microporous, custom-made HLB prepared using a precipitation based polymerization technique was shown to significantly outperforming a comparable commercial mesoporous HLB particle for these volatile analytes. The background thermal stability for GC desorption was also determined to be comparable to that exhibited by the previous DVB/PDMS

based TF-SPME chemistry. Furthermore, the inter-membrane reproducibility was confidently validated within four different batches of membranes using the varying sorbent chemistries at a 95% level of confidence indicating that membranes could be prepared reliably. This reliability was further strengthened for the presented method by demonstrating that, when stored properly, even compounds as volatile as benzene remain stable on the membrane for at least 120 hours. Finally, the concept was proven to be effective in real-world applications by allowing for the precise determination of various chloramine compounds from a private hot tub.

As a result, the research undergone in the development of these homemade HLB particles, and the corresponding HLB/PDMS TF-SPME may very well offer a new and superior sorbent phase for the balanced coverage of volatile analytes typically reserved for gas chromatography applications in the future.

Chapter 7 Design and construction considerations of robust, self-sealing deep ocean samples for manual and robotic operation

7.1 Introduction

As analytical and exploratory scientists we strive to further the investigation of unique and otherwise unfamiliar environments. Time and again approaching these unexplored regions requires the development of new sampling devices and technologies to best address site-specific challenges.[76,164] Largely due to a miniaturized and easy-to-handle design, standard, fiber-based, solid phase microextraction techniques have been regularly employed for on-site sampling applications.[28,169,170] However, many fringe environments of interest exhibit conditions far too extreme for a common SPME fiber or other sampling devices to survive or be otherwise deployed.[164] As such, there still remain many environments that have been relatively unexplored particularly in terms of chemical or biochemical profiling.

One such fringe environment would be that of deep oceanic hydrothermal vents which remain as one of the few ecosystems on Earth that prosper entirely without sunlight. Remaining relatively untouched by humankind and the outside environment such locations have been theorized to be virtually unchanged since the advent of life and may provide a snapshot as to how some of the earliest known organisms survived.[171] Among other organisms, thermophilic extremophile bacteria located along these vents have evolved to survive in an anoxic environment devoid of solar energy.[171–173] To cope with such conditions these bacteria have developed many unique chemolithoautotrophic strategies to produce energy including the aerobic, microaerobic or anaerobic, oxidation or reduction of sulfates, sulfides, ammonia, nitrate, hydrogen, methane, and even iron-based compounds.[173] These metabolic pathways may provide many unique metabolites that have yet to be discovered and could provide clues as to the biochemical processes of some of the earliest organisms to ever exist. Classical sampling approaches for such investigations

generally involve whole volume grab-samples taken by large volume syringes onboard the ROV submersibles.[172,173] Once transported back to the surface vessel this water is either directly analyzed (following appropriate sample pre-treatment) or cultured to grow the microbiota of interest for further sampling.[171–173] Although simple in execution, grab sampling may not be without its downsides as it may be difficult to ensure the stability of the metabolites in the sample solution during transport back to the surface. This instability holds especially true when there remain continued biological activity and such vast changes in oxidation potential and pressure. It would, therefore, be preferential if sampling and sample preservation could be performed *in-situ* at the hydrothermal vent.

Accordingly, solid phase microextraction techniques have long been known as a reliable means for combining sampling and sample preparation into a single step.[10,11,151] As small organic molecules are extracted into the pore space of sorbent particles they can be removed from a given aqueous matrix.[10] Not only does this form of extraction eliminate the need to transport large volumes of water, it more effectively stabilizes an extracted compound preventing additional reactions; particularly further breakdown by biochemical processes.[151] However despite being portable, the standard fiber morphology of SPME is known to be rather fragile making it unsuitable for deep-sea sampling. Recent efforts by Poole *et al.* have presented a much more ruggedized SPME configuration.[164] Known as the SPME needle, this ruggedized device is designed such that the extraction phase remains recessed into the body of a solid stainless steel needle. In fact, these devices were even fabricated into custom ammunition to be shot from an airsoft gun at 91 $m \cdot s^{-1}$ for the in-vivo sampling of live fish tissue.[164] In addition to protecting the coating within the recession, the existence of a relatively thick solid steel core provided adequate rigidity which gave the SPME needle the strength required to puncture fish scale without breaking. Possessing a surface area 2.9

times greater than that of comparable SPME-HPLC fibers, these needles were also considerably more sensitive for the quick pre-equilibrium extractions used for live tissue sampling.[164] Fittingly, maximization of surface area has been the ongoing objective of many thin-film solid-phase microextraction (TF-SPME) approaches used for on-site sampling.[1,25,125,154] This is because when sampling times are short the amount of analyte extracted as a function of time ($\frac{dn}{dt}$) is directly proportional to surface area (A) and does not depend and sorbent volume or strength (Eq. 7.1).[1,5,66] It is important to clarify however that a weak sorbent will not remain in this linear, pre-equilibrium regime for as long as a stronger sorbent, hence a strong sorbent is still important to ensure this assumption remains correct.

$$\frac{dn}{dt} = C_s(\frac{D_S\, A}{\delta}) \qquad \text{Eq. 7.1}$$

Appropriately, this current work presents a new SPME sampling morphology comprising of high surface area stainless steel bolts which have had extraction phase recessed into their solid S.S. bodies. Furthermore, to facilitate easy handling by divers and deep sea ROV submersibles these SPME bolts were built into self-sealing PTFE bodied enclosures. This self-sealing design was shown to stabilize compounds originating from a wastewater treatment facility on the sorbent coating for up to 2 weeks when stored at ambient conditions. As a further proof of concept, the diver operable morphology was then used to differentiate significant features from sponge and coral organisms at an on-site location in Cuba. Finally, these devices were successfully deployed on two different ROV submersibles several kilometers deep at deep ocean hydrothermal vents along the Pacific Rim.

7.2 Materials, instrumentation, and experimental methods

7.2.1 Chemical and materials

For chromatographic separations and coating desorption the MS grade methanol, acetonitrile, and water were obtained from Fisher Scientific Canada (Ontario Canada), while formic acid and ammonium acetate were purchased from Sigma-Aldrich (Oakville, ON, Canada). The dimethylformamide (DMF), 150 kDalton polyacrylonitrile (PAN) and hydrochloric acid used to prepare the coated devices were also purchased from Sigma-Aldrich. The 18-8 stainless steel nuts, bolts, and springs were purchased from Spaenaur (Kitchener, ON, Canada). The Teflon coated springs (Swagelok model 177-R3A-K1-B) were purchased from Swagelock Inc. (Sarnia, ON, Canada). The rare earth magnets were purchased from Lee Valley Tools (Waterloo ON, Canada) The Teflon sampler bodies were sourced and constructed by the University of Waterloo Science Machine Shop (Waterloo ON, Canada) Plastic 300 μL vials and amber 2 mL glass vials along with pre-pierced PTFE/silicone septa used in puncture tests were purchased from Canadian Life Sciences (Peterborough, ON, Canada). The 5 μm, 800 m^2 g, hydrophilic−lipophilic balanced (HLB) particles used were obtained from Waters (Wilmslow, U.K.)

7.2.2 Instrumental and data-processing analysis method (High-resolution HPLC-orbitrap)

Analytical instrumentation used for the separation and detection of the untargeted analytes included a Thermo Acella autosampler-HPLC and an Exactive Orbitrap MS (ThermoFisher Scientific San Jose, California, USA). Chromatographic separations were performed using a Supelco Discovery pentafluorophenyl (PFP) HS F5 column, (2.1 mm × 100 mm, 3 μm) (Supelco, Millipore-Sigma Bellefonte, PA, USA). Mobile phase was pumped at a flow rate of 300 μL min^{-1}. Gradient elution was performed using a 2 component system consisting of mobile phase A,

99.9:0.1% water: formic acid v:v, and mobile phase B, 99.9:0.1% acetonitrile: formic acid v:v. Initial mobile phase conditions for the PFP column separation were 100% A from 0 to 3.0 min, followed by a linear gradient to 10% A from 3.0 to 25.0 min, and an isocratic hold at 10% A until 34.0 min. The total run time was 40 min per sample, including a 6 min column re-equilibration period.

The analyses were performed using both positive and negative electrospray ionization (ESI) using the PFP-HPLC method described. The injection volume for all methods was 10 μL and samples were stored at 4ºC on the autosampler while waiting for injection. All injections were run in randomized order, and both instrument QC's and pool QC's were run periodically to verify instrument performance. MS acquisition was performed using AGC = balanced (1 000 000 ions) with a 50 000 resolution at 2 Hz. The injection time onto the C-trap was 100 ms. Sheath gas (arbitrary units), auxiliary gas (arbitrary units), sweep gas (arbitrary units), ESI voltage (kV), capillary temperature (ºC), and vaporizer temperature (ºC) were (i) 30, 10, 5, 4.0 (-2.9 negative mode), 300, and 300 with an acquisition range of 100-1000 m/z, for the positive and negative ESI reversed-phase methods. External instrument mass calibration was performed every 48 h and was within 2 ppm for all ions. This HPLC-MS metabolomics was adapted from the methodology developed and employed by Reyes-Garces [174].

Data processing was performed by first converting the raw data files to a mzXML format using the free Proteowizard software MSconvert. Parameters used included an mz level=1 filter, a 64-bit binary encoding precision, and selection of the write index option. These converted files were then imported into the software MZmine 2 for furthering peak filtering and detection.[175] After import, scan-by-scan filtering was performed on the data using a 5 data point Savitzky-Golay filter. A mass peak list was then generated using exact mass detection with an m/z range of 99-1000 m/z

with a mass tolerance of 5.0 ppm. From this mass list, chromatogram builder was then used with a minimum peak height of 10 000 (arbitrary) and a minimum width of 0.017 min. Deconvolution of these rebuilt chromatograms was then performed using a Savitzky-Golay filter with a minimum peak height of 10 000 (arbitrary) and peak width setting of 0.017-1.0 minutes. The generated peak list was then filtered using an m/z-range of 99-1000, a RT range of 0.8-35 minutes and peak width of 0.017-1.0 minutes. A compiled aligned peak list table was then generated using a 5 ppm, mass tolerance, 5% retention time tolerance, and weighting values of 10 and 20 (arbitrary) for RT and m/z respectively. Finally, once peaks associated with the instrument and sampler blanks were manually removed, the peaks list rows filter was again used on the compiled aligned peak list but with the minimum peaks per row set to 3. This secondary filtering removed erroneous single detections which was considered statistically prudent as there were always 5-6 replicates per sample. The processed aligned peak list was then exported as a .CSV file which was then imported into SIMCA-14 multivariate data processing software. Principal component analysis (PCA) was then performed using Pareto scaling for the determination of significant features and testing of data fit for the various samples run. Features that were deemed significant were then preliminarily identified by exact mass matching using the METLIN Metabolomics database with a 5 ppm mass accuracy tolerance.

7.2.3 Preparation of the coated bolt SPME devices

The first coated bolts were prepared using a spray coating methodology adapted from a procedure first reported by Musteata *et al.* and Mirnaghi *et al.*[176,177] This procedure involves dissolving a 150 kiloDalton polyacrylonitrile (PAN) in dimethylformamide (DMF) at a 10% PAN weight percentage and then mixing 10 mL of the resulting solution with 1.0 g of 30 µm HLB particles and an addition 3 mL of DMF to prepare a sprayable slurry. The surface of the stainless

steel bolts was etched by hanging their coatable surface in an open beaker of concentrated HCl under sonication for 10 minutes. An Aldrich glass sprayer (Sigma-Aldrich, Oakville, ON, Canada) was used to apply approximately 10-12 coats of the slurry. Each coat was set in a modified GC oven at 150 ^{o}C. These coated bolts were then cleaned and conditioned in a 50:50 methanol: water solution.

For bolts prepared with a recessed extraction phase, etching was performed for 1.5 hours which resulted in a 30 µm indentation on the stainless steel surface. Dip coating was then performed using a programmable actuator such that the bolts could be immersed in the aforementioned PAN/HLB/DMF slurry up to the edge of the etched surface. Furthermore, due to the availability of the sorbent, a smaller and more strongly sorbing 5 µm HLB particle was used. When dip coating was performed only 2 coats of the slurry were applied with each coat being set in a modified GC oven at 150 ^{o}C. The excess coating was then removed from the head of the bolt using a utility knife and the coating was then cleaned and conditioned in a 50:50 methanol: water solution.

7.2.4 Desorption of large surface area coated screw device

Desorptions were carried out by placing the coated bolts in a narrow, high-density polyethylene (HDPE) centrifuge tube such that the coated side of the bolt was immersed in the solvent. 800 µL of desorption solvent, consisting of 50:50 ACN: H_2O, was used to desorb each of the devices. The tubes were then placed in a Benchmark Scientific Benchmixer XL multi-tube vortexer (Mandel Scientific, Toronto, ON) and agitated at 1200 rpm for 75 minutes. Following desorption, the solutions were then transferred to 2 mL amber glass vials for storage and analysis. Pool QC`s were then prepared by removing 100 µL of solution from each individual sample and

mixing them into a single 2 mL vial. Pending and post analysis, these solutions were stored at -80 ^{o}C to ensure analyte stability.

7.2.5 Assessment of room temperature real sample storage stability

In order to confirm that the self-sealing sampler design was capable of stabilizing extracted compounds on the sorbent coating for purposes of multi-variate identification, real samples were taken using 3 different devices (18 coated bolts total) and then stored under varying conditions for up 12 days. The real world samples were taken at the outflow pipe of the Galt Wastewater Treatment Facility on the Grand River (Cambridge Ontario). Ambient river temperatures were measured to be 6.5 ^{o}C while the temperatures at the outflow fluctuated slightly around 20 ^{o}C. As shown in Figure 7.1, samplers were deployed on-site via kayak and sampling was performed for 1 hour. Following sampling, the devices were then closed into their sealed position and transported back to the laboratory. Solvent desorption was then immediately performed on 4 of the 18 coated bolts while the remaining devices were stored within the self-sealing sampler bodies at A: room temperature for 3 days, B: room temperature for 12 days, and C: in the -80 ^{o}C freezer for 12 days.

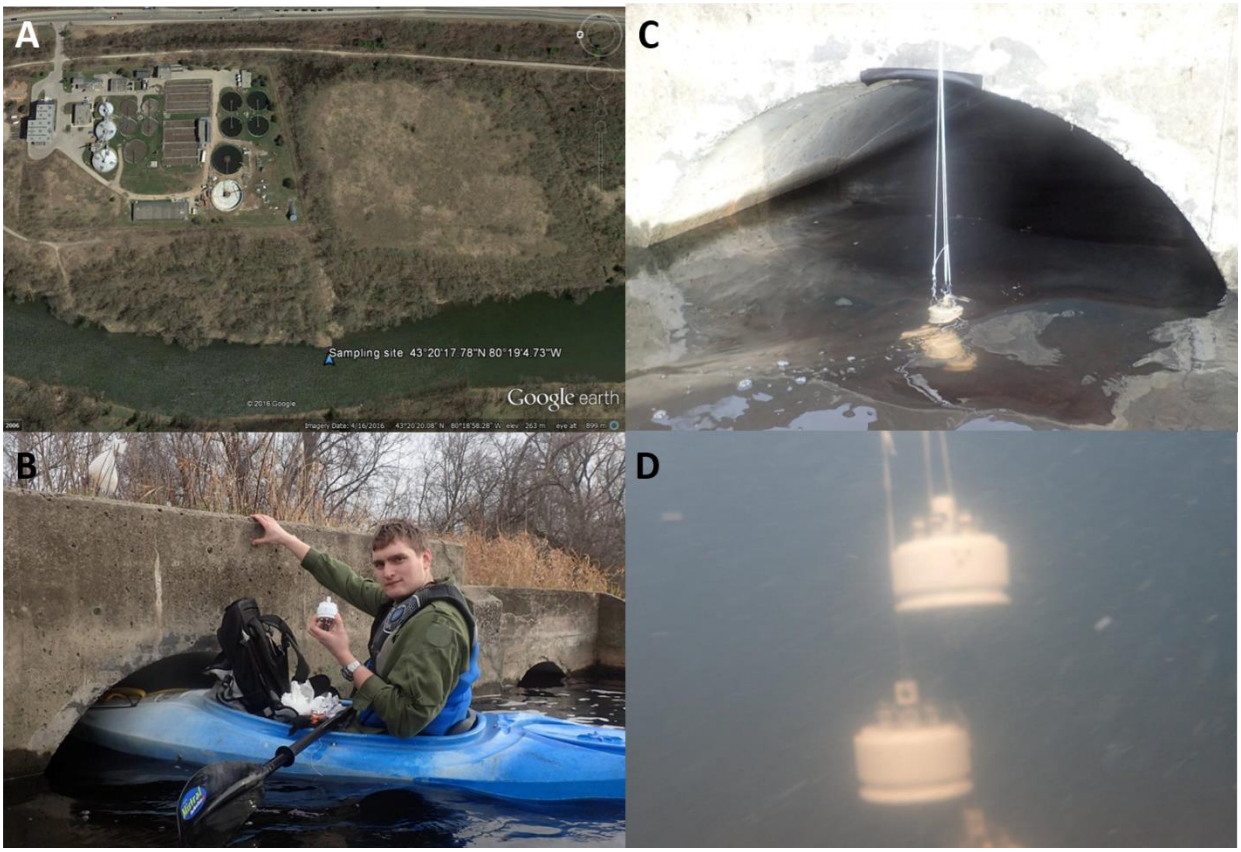

Figure 7.1 On-site deployment of the coated pin self-sealing samplers showing, A) Galt wastewater treatment facility outflow pipe sampling site (43°20’17.78”N, 80°19’4.73”W), B) kayak deployment of the samplers, C) centered position of samplers within the outflow pipe opening, D) underwater picture of the deployed samplers.

7.2.6 Deployment of diver operable samplers to differentiate significant features between Sponge and Coral samples

As a proof of concept, the diver operable self-sealing samplers were deployed on-site for the untargeted differentiation of compounds emitted from either sponge or coral organisms. A total of 4 samplers, each containing 6 replicate coated bolts, were deployed for approximately 1 hour each by a scuba diver along an unspecified Cuban beach. The first sampler was deployed as a control on a sandy substrate bottom where there were no proximate coral or sponge species. Samplers 2 and 3 were left at different locations along a single coral reef at positions where there were no sponges immediately nearby. The final sampler was then placed on top of an unknown

species of live sponge. Following sampling, the self-sealing devices were sealed, wrapped in aluminum foil and placed into individual clear polyethylene bags which were then transported back to Waterloo for desorption and analysis.

7.2.7 Multicomponent separation of various biomolecules from deep-sea hydrothermal vents

As a means to demonstrate the full robustness of the self-sealing coated bolt sampler design, various samplers were deployed on two separate dives for the on-site SPME extraction of hydrothermal vents. The first ROV sampling was performed at a depth of 1518 m on a hydrothermal vent located on the edge of the El Gordo seamount which, as shown in Figure 7.2, possessed a great deal of visible aquatic life. Three separate samplers were taken on the dive allowing for the sampling of A: an active hydrothermal vent B: Ambient ocean water to serve as a control and, C: an unused sampler to serve as a method blank. Unfortunately, due to a miss-communication between our research teams and the ROV crew, the sampler was only exposed for a total of 15 seconds in both the control location and active hydrothermal vent. The control sample (Figure 7.3) was taken just a few meters above the hydrothermal vent which was not considered ideal as some of the hydrothermal vent features to could have been also extracted by the control sampler. The ROV operators logged observation of the ROV-SPME samplings are listed in Table 7.1 below. Follow sampling, a given ROV-SPME device was then placed in an enclosed ROV "bio-box" for the remainder of the dive and ascent. Once shipside, these devices were then stored at -80 ^{o}C within the on-ship freezer for the remainder of the voyage. Finally, upon returning to port, the samplers were then shipped under dry-ice to the University of Waterloo for desorption and analysis.

Table 7.1: ROV-operator logging of ROV-SPME sampling event at El Gordo seamount hydrothermal vent.

Date and Time	Location	Coordinates	Depth
27/9/2014 06h11 UTC	ROPOS Perched on El Gordo vent	N 45 55.5713' W 129 58.7353'	1518 m

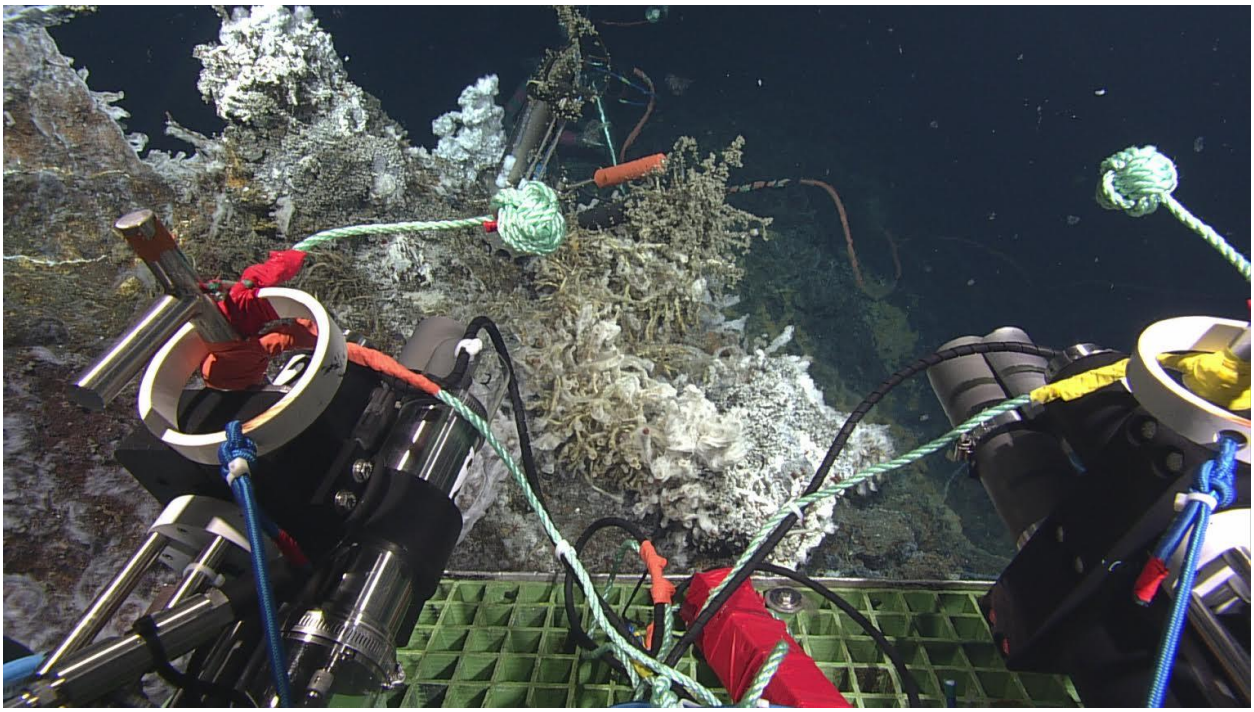

Figure 7.2: ROV-SPME sampling on-top of El Gordo hydrothermal site. Coated bolts were exposed for approximately 15 seconds

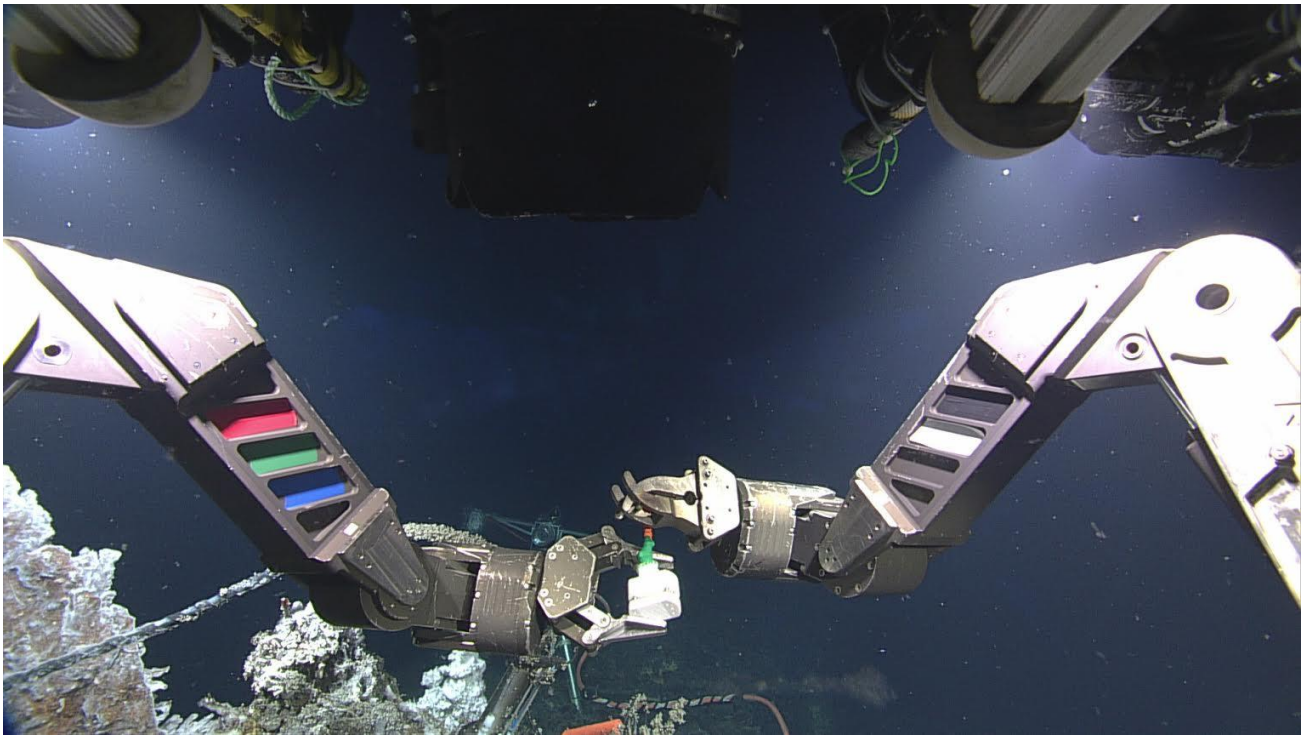

Figure 7.3 ROV-SPME control sampling above El Gordo hydrothermal site. Coated bolts were exposed for approximately 15 seconds.

The second ROV-SPME sampling was performed at a depth of 2929 m at an unspecified vent along the NW Rota dive site. The exact coordinates of this location are presented in the ROV operators log shown in Table 7.2. The sampling of the active vent site (Figure 7.4) was performed for exactly 6 minutes, 24 seconds with vent temperatures measured at 17.3 ^{o}C. The control extraction of the ambient seawater was performed during ROV ascent and lasted exactly 6 minutes with ambient water temperatures measured as 1.5 ^{o}C. Furthermore, much like the first ROV sampling, a third, unused, SPME device was carried onboard the submarine to serve as a method blank for the dive. Following sampling, a given ROV-SPME device was then placed in an enclosed ROV "bio-box", shown in the bottom left-hand corner of Figure 7.5, for the remainder of the dive and ascent. Once shipside, these devices were then stored at -80 ^{o}C within the on-ship

freezer for the remainder of the voyage. Finally, upon returning to port, the samplers were then shipped under dry-ice to the University of Waterloo for desorption and analysis.

Table 7.2: ROV-operator logging of ROV-SPME sampling event at NW Rota hydrothermal vent.

Time UTC	sample	type	site	J2- 801 Sample Comments - Urashima	latitude	longitude	Depth(m)
06:18	J801-SPME4-44	bio	Active Chimney - Ultra-no-chichi	SPME #4. (Solid Phase Micro Extraction). Sampler held overflow at an angle to maximally expose tubes to flow. Squeezed for six minutes in the flow. Stop 06:24.	12 55.3378	143 38.9521	2929
06:45	J801-SPME2-46	bio	ascent	Background SPME #2 sample during ascent. Ambient Temperature = 1.53C. Depth of squeeze: 2828-2667. Squeezed six minutes.	12 55.31	143 38.912	2828-2667

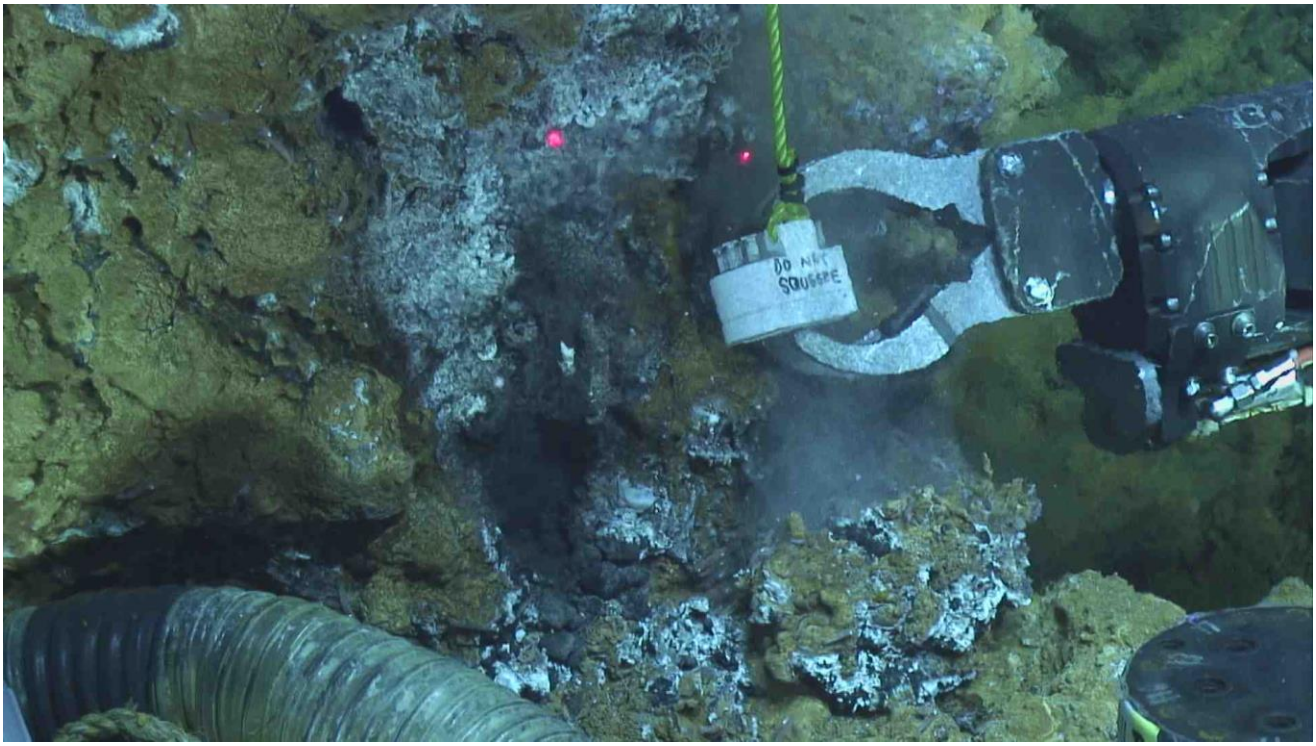

Figure 7.4: Location of the NW Rota ROV-SPME active vent site. Sampling was performed for 6 min, 24 seconds. The ambient temperature measured immediately before sampling was 17.3 ^{o}C.

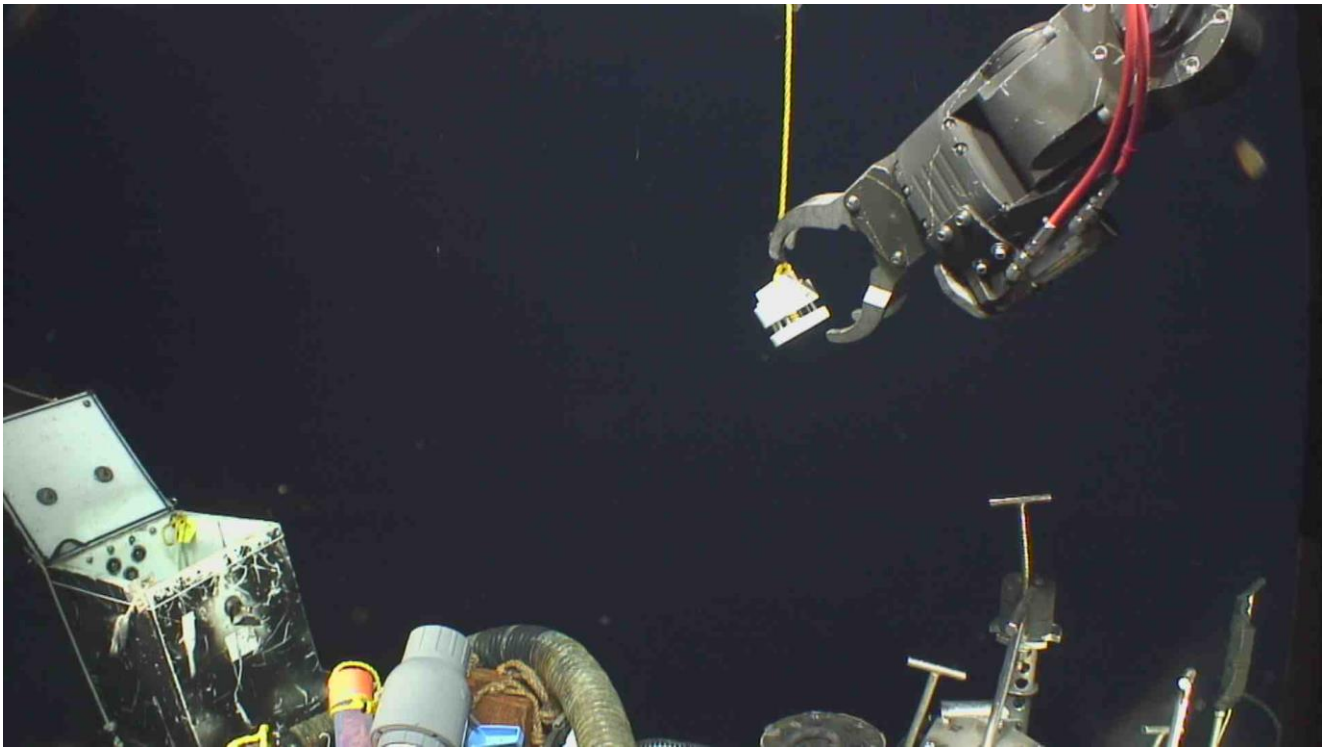

Figure 7.5: ROV-SPME control sampling taken during the ascent of the submarine. Ambient temperature was measured as 1.53 ºC while sampling was performed for 6 minutes. Bio-box storage location on the bottom left

7.3 Results and discussion

7.3.1 Design considerations and robustness of the coated bolt self-sealing sampler

In order to survive the harsh environment imposed by the deep ocean hydrothermal vent sampling regions many design considerations needed to be optimized during the construction of the ROV-SPME sampler. First and foremost the device needed to be designed in a way such that it could be easily understood by the ROV pilot and reliably handled using various ROV manipulators. Furthermore, it was essential that the device could withstand temperatures of superheated water well in-excess of 100 ºC, maintain a high degree of chemical resistance to the highly acidic plumes, and be able to equalize and withstand water pressure at depths exceeding 2 km (199 atm), Furthermore, it was important that the bolts could be exposed solely by the employment of a squeezing motion of the ROV manipulator.

Appropriately, the HLB/PAN coated screw ROV-SPME self-sealing sampler, as shown in Figure 7.6, was designed with all of these aforementioned requirements in mind. Firstly, in addition to having a solid, compression resistant body, no region on the sampler was designed to have tightly sealed void volumes ensuring the device could equalize to the ambient pressure at depth. Furthermore, by employing a solid PTFE shell and PTFE coated springs the sampler was designed to survive temperatures in excess of 300 ^{o}C and exhibit minimal extraction or modification by chemical species in the sampling environment. Another important aspect of the sampler was the spring assisted self-sealing design. As the ROV manipulator was limited to one axis of movement (squeezing) to toggle the device between the "open" (sampling) and "closed" (stowage) positions it was important that the device could be self-sealing such that the HLB-PAN coatings were protected from convection of the surrounding environment after sampling was completed. This design requirement was accomplished by positioning a heavy 115 kg cm PTFE coated spring at the center of the device which, upon releasing tension from the ROV manipulator, would force the two Teflon blocks apart, forcing the head of the coated bolts to sit flush against the top of the Teflon body effectively protecting the sorbent coating from convection and open bed diffusion. the incorporation of the six, large diameter, .635 cm thick, coated 18-8 stainless steel bolts directly within the sampler body was also advantageous. In addition to providing the sampler with superb physical strength under load, the diameter of the coated bolts also provided a major increase in the available surface area of the sorbent coating. As can be seen in Table 7.3 below out of all of the current SPME-HPLC morphologies, the coated screw format contains the largest amount of available sorbent and, more importantly, surface area. This large, 250 mm^2, surface area is needed to attain adequate sensitivity during the short sampling times available within the costly ROV dive time. As sampling times were expected to be 10 minutes or less it was expected that the

extraction of most analytes would be in the pre-equilibrium regime where sensitivity is dictated by surface area. As such, a factor of 22 times signal improvement was expected over a comparable HLB/PAN SPME fiber. Furthermore, with dimensions of 8 cm x 5 cm x 7 cm (W x D x H), this 6 replicate sampler was constructed to minimize the space requirements on the ROV submersible during the dive.

Following the successful construction and the first deployment of these ROV-SPME samplers this self-sealing design was slightly modified for the sampling of shallow waters by divers and light watercraft. This modified device, shown in Figure 7.7, incorporates a magnetic locking system such that the sampler can be held open during sampling (Figure 7.8A). Once sampling is complete the diver can simply press on the push rod such that the magnets are separated and the spring can hold the device in the closed position (Figure 7.8B). As pressure equalization considerations were not as critical, this embodiment was constructed much more tightly to further improve long-term storage of extracted compounds. Notwithstanding these modification other aspects of the diver operable sampler remain quite similar the ROV-SPME variant.

The coated bolts themselves can be considered a unique SPME morphology that required proper optimization. Initially, the SPME-bolts used in the first set of ROV-SPME samplers were prepared using an older spray coating method.[176,177] Although functional, it was later found that these coatings were prone to stripping when operated from within the SPME-ROV sampler body. This stripping was caused by the leading edge of the sorbent coating (Figure 7.9B) catching on the edge of the cylindrical walls of the PTFE sampler body when operated. To address this limitation it was decided to employ a recessed coating methodology which resulted in a coated surface possessing a diameter equal to or less than the unetched portions of the stainless steel bolt.[164] Partly due to the smaller 5 μm HLB particles, the recessed coating method was found to give a much

smoother and uniform coating. Furthermore, as the leading edge of the sorbent coating was protected within the recession it could no longer catch on the cylindrical edge of the PTFE sealing body. Although these coatings were much thinner, containing less volume than the previous design the available surface area was relatively identical. Hence, for the short extraction times used during ROV samplings extraction efficacy should not be affected.

Table 7.3 Comparative physical dimensions of coated HPLC SPME fibers, TFME blades, and the coated bolt sampler.

	Coated Dia.	Coating Thickness	Coating length	Coating Vol.	Coating S.A.
HPLC SPME fiber	0.27 mm	45 µm	1.5 cm	0.39 mm^3	11.1 mm^2
TFME blade	2.55 mm*	120 µm	2 cm	12.2 mm^3	102 mm^2
Coated bolt (spray)	6.65 mm	150 µm	1.2 cm	37.3 mm^3	251 mm^2
Coated bolt (recessed)	6.40 mm	25 µm	1.2 cm	6.2 mm^3	241 mm^2

*Coated width of blade

Dia. = Diameter Vol. = Volume S.A. = Surface Area

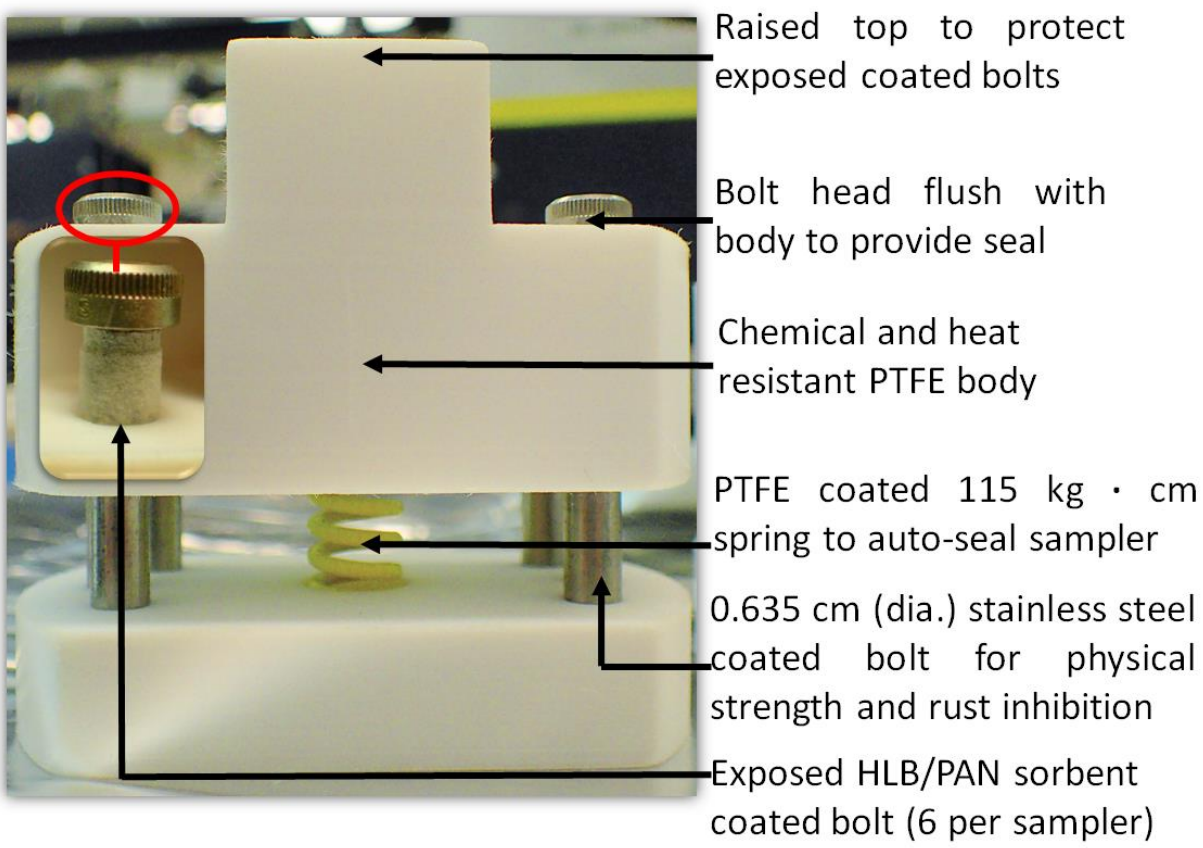

Figure 7.6 HLB/PAN ROV-SPME self-sealing coated bolt sampler. Older non-recessed coated bolt with 30 µm HLB particles is shown.

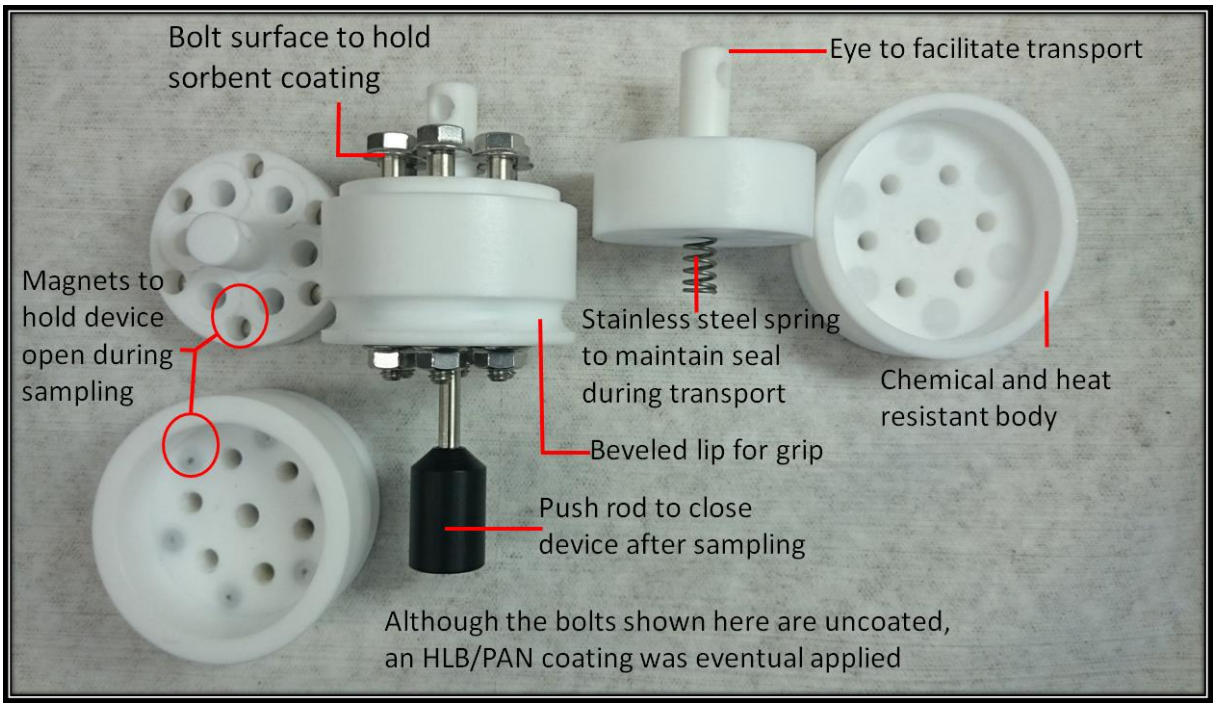

Figure 7.7 Breakdown of the magnetic and spring locking diver operable coated bolt SPME device.

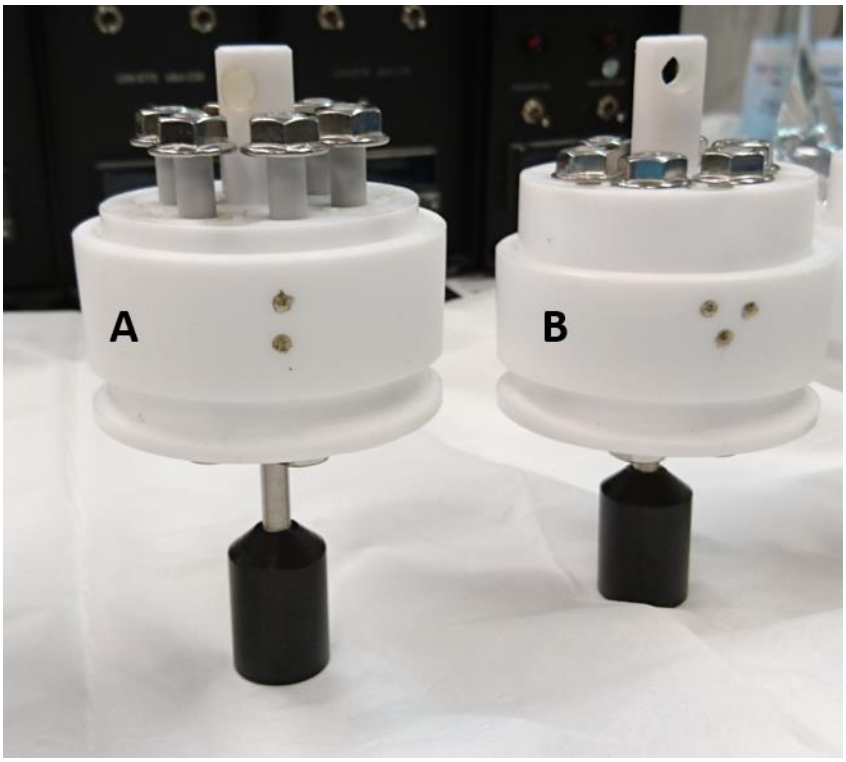

Figure 7.8 Magnetic and spring locking diver operable coated bolt SPME device shown in, A) sampling position, and, B) sealed position. Newer recessed coated bolt with 5 µm HLB particles is shown.

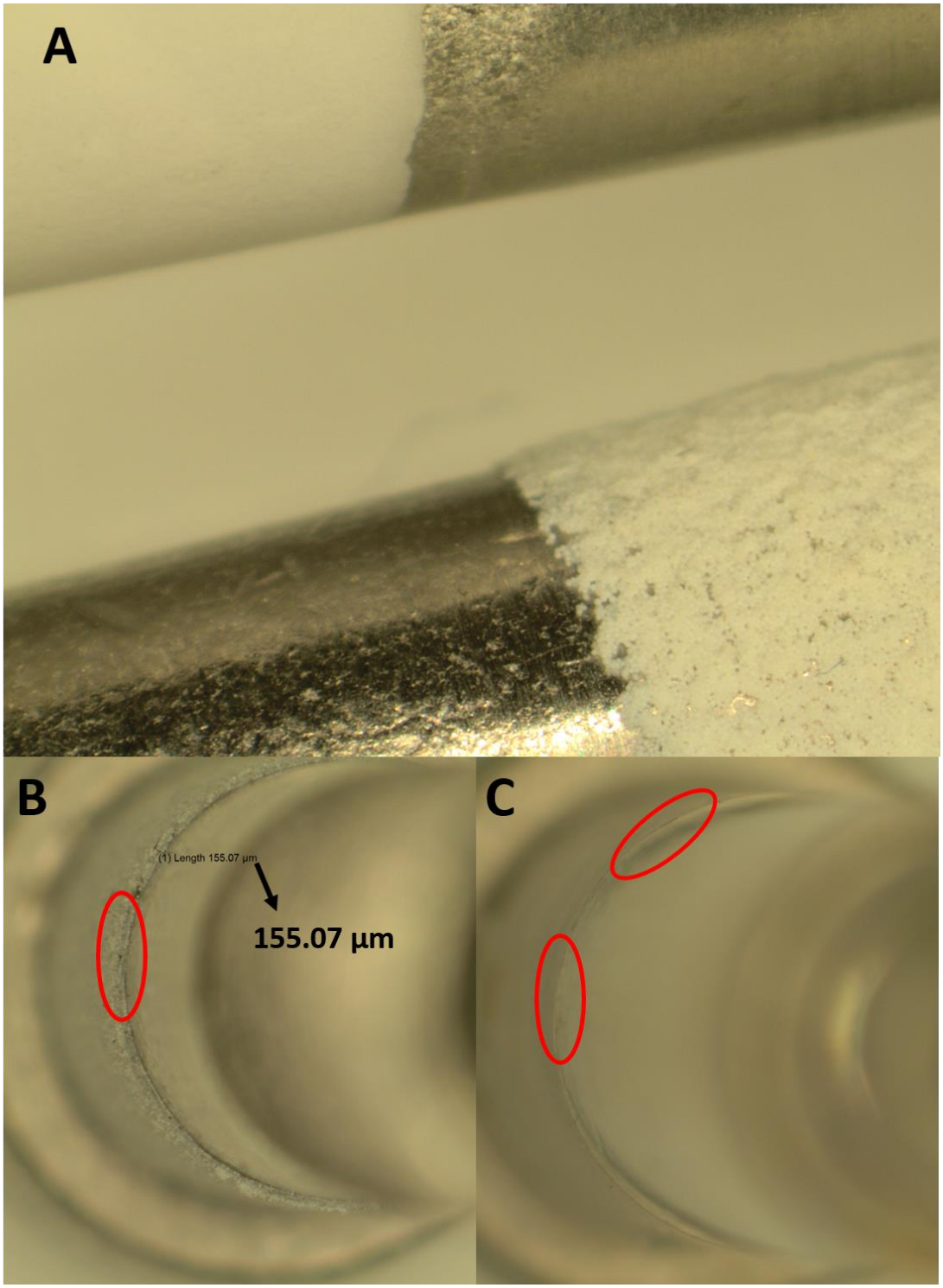

Figure 7.9 Comparison of the recessed Vs. non-recessed coated SPME bolt showing, A) side by side view of both devices, B) Top down view showing raised edge (155 µm) of the non-recessed device, (30 µm d. particle) and, C) top-down view showing the smooth edge of the recessed device. (5 µm d. particle)

7.3.2 Long-term real sample storage stability of Galt wastewater treatment facility outflow

As the coated bolt samplers were designed with the explicit purpose of stabilizing extracted compounds on the sorbent coating for extended periods at ambient conditions it was decided to perform identical real-world extractions from the outflow pipe of the Galt Wastewater Treatment facility with multiple devices that were then stored for varying amounts of time and conditions. This storage stability was validated using one-way ANOVA at a 95% level of confidence (Table 7.4) showing that for the 10 selected features there were no significant differences in the amount of analyte remaining on the sorbent coating, even following 12 days of room temperature storage. This is promising as even though these features were selected randomly, preference was given to compounds with lower molecular weight as these would likely be the most volatile and hence least stable on a given extraction phase. This result may also be viewed graphically in Figure 7.10 which additionally shows the relative signal of the response generated from the pooled QC sample. As the pooled QC was prepared by mixing a small portion from each extract, it was encouraging to see that it gave similar signal to that of the samples. However, as shown from the error bars of Figure 7.10 it was apparent that the pooled QC data, which is generated from 7 replicate injections from the same vial, gave noticeably less error than the pooled data from each of the individual coated bolts with %RSD's ranging from 5-12 % and 9-20% respectively. Although potentially indicating that there could be some variation in terms of inter-screw reproducibility, this variability is well within an acceptable range expected for on-site sampling methodologies. Furthermore, it is important to note that in most other TFME-HPLC studies where method reproducibility has been assessed, internal standards have typically been added to the sample solution during in-lab extractions.[176,178,179] This is not to say that internal standard correction is improper, in-fact, it is typically quite prudent to do so whenever possible as these corrections can account for any

unknown errors that could arise during desorption, liquid extract storage, instrumental analysis or variabilities between the SPME devices themselves.[176,178,179]

As to ensure that the noted reproducibility wasn't just associated with the 10 randomly selected features, principal component analysis was also applied to the dataset to see if any grouping could be observed between coated bolts from different storage conditions. Appropriately, no clustering was observed between samples in the related PCA-plot (Figure 7.11) indicating that any separation among samples was likely due to random background noise. This is to be expected as multivariate approaches base separation on the most significant features present in a given dataset. When no actual statistical differences exist between different samples the PCA algorithm will begin assigning random noise as the most significant driving factor for sample separation resulting in a randomly distributed PCA plot like that seen in Figure 7.11. Furthermore, because the samples were so similar, even the pooled QC data was found to exhibit poor grouping on the PCA plot, despite the good performance of instrumental QC data.

Although feature identification was not the focus of this study, the empirical molecular formula and likely compound class are also given in Table 7.4. The empirical formulas given were assigned based on exact mass matching on the Metlin database and all possibilities within +/- 5 ppm of the exact mass were listed. Exact identification for compounds is not possible based on exact mass matching alone, hence only likely compound type is presented herein. One interesting identification, however, was that of the most volatile analyte listed, the protonated xylene like compound with exact mass 107.0858. Although, very common water contaminants[180] these compounds are known to exhibit poor ionization efficient with electrospray ionization techniques (ESI) and are typically considered more GC-MS amenable. More interestingly, however, HPLC-MS methods have already been developed for the determination of various benzothiazoles and

benzotriazoles as common wastewater contaminants.[181,182] These classes of compounds were tentatively identified in this dataset. However, as previously mentioned, any of these tentative ID's are speculative without appropriate MS^n validation or standard confirmation but these results remain interesting nonetheless.

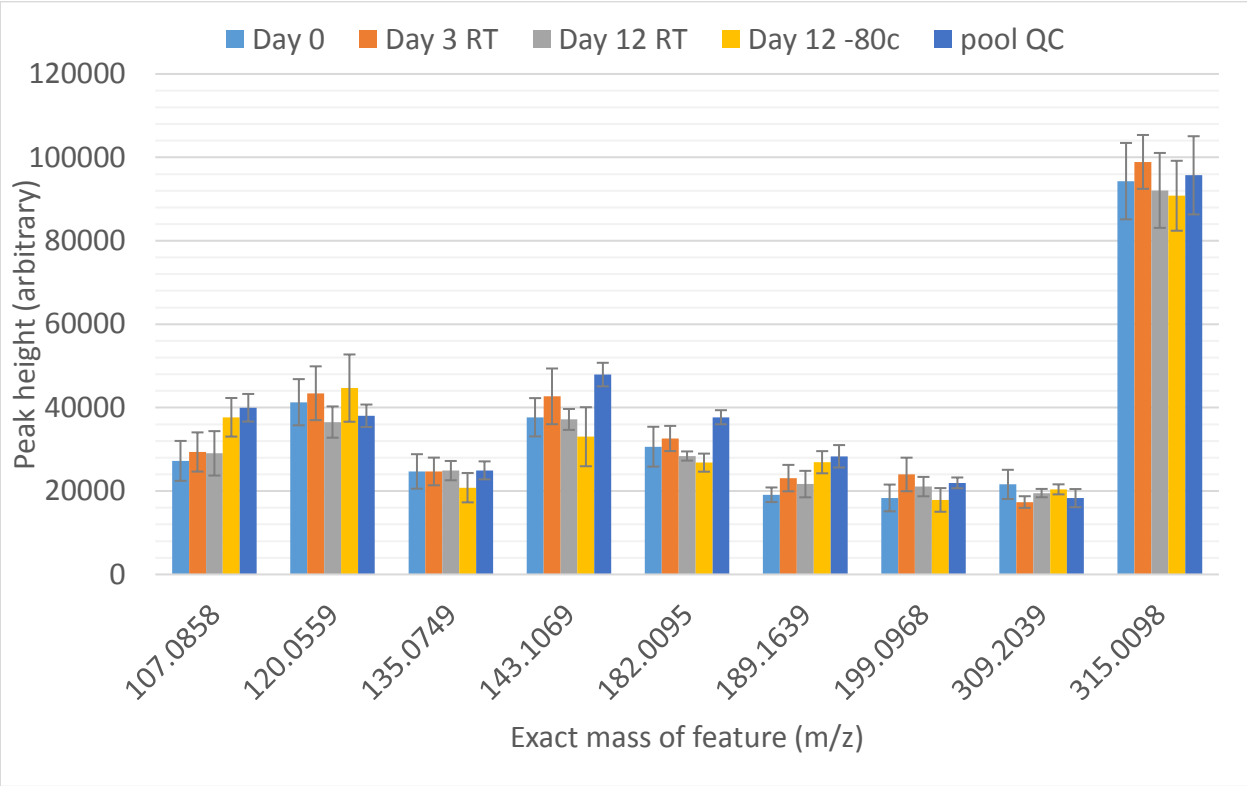

Figure 7.10 Stability of randomly selected volatile features on the HLB/PAN coated bolt SPME samplers, 2 hours following extraction, after 3 days of room temperature storage, after 12 days of room temperature storage, after 12 days of storage at -80 ºC. and, replicate extractions from the pooled QC.

Table 7.4 ANOVA testing at 95% confidence demonstrating 12-day room temperature storage stability of extracted compounds on the HLB/PAN coated bolt self-sealing sampler. (F_{crit} = 3.71)

Exact Mass	RT	Empirical formula	Tentative Compound class	F Value	%RSD
107.0858	19.93	C8H10	a xylene	2.08	20
120.0559	10.21	C6H5N3	benzotriazole or similar	0.92	16
135.0749	11.71	No match	No database match	0.77	16
143.1069	13.49	C8H14O2	a carboxylic acid	1.20	16
182.0095	16.92	C8H7NS2	a Methylthiobenzothiazole	1.47	13
189.1639	19.93	C5H6ClN3O	a Chloro-methoxypyrazin-amine	3.71	17
199.0968	11.59	C8H18O5	Tetra ethylene glycol	1.87	19
213.0429	18.84	C10H14O4	a carboxylic acid	2.03	16
309.2039	21.24	C7H16OS3 or C6H12O6S or C9H9ClN2O2		1.70	13
315.0098	21.63	N/D	Multiple possibilities	0.40	9

RT = retention time

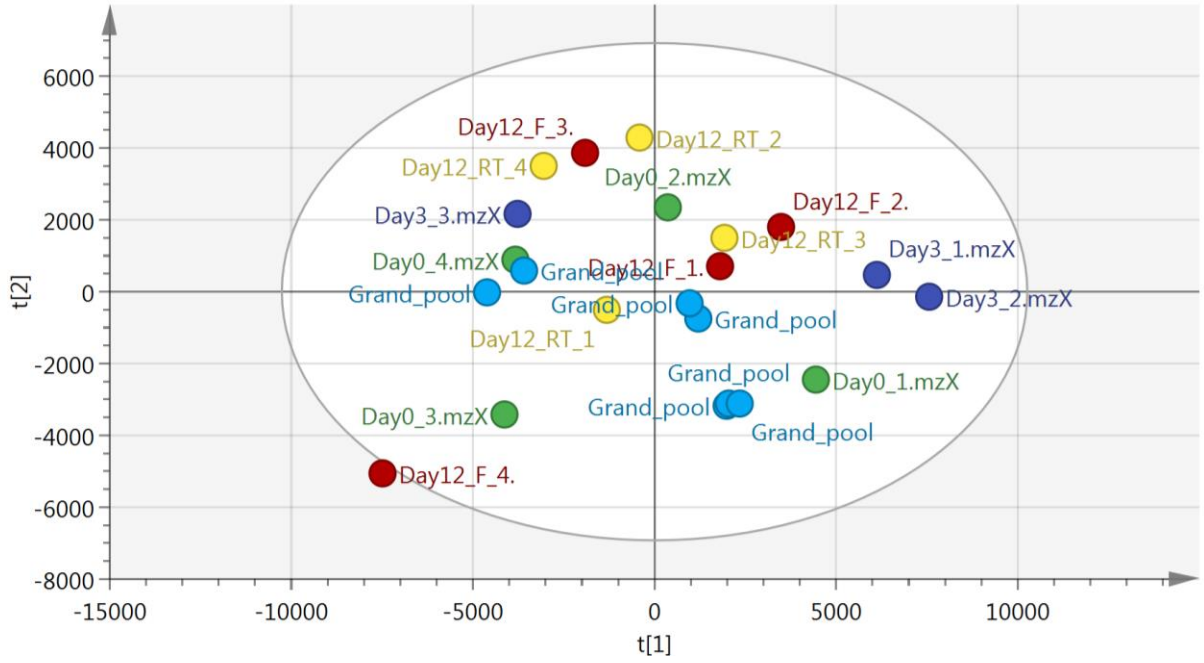

Figure 7.11 Multivariate comparison (PCA) of replicate samples corresponding to no long-term storage (GREEN), 3 days of room temperature storage (NAVY BLUE), 12 days of room temperature storage (YELLOW), 12 days of storage at -80 ºC (RED), and, the pooled QC injection (SKY BLUE). No separation patterns were observable, even for the pooled QC injection as all samples were nearly identical. Samples were run on the PFP column and ionized in positive mode. Separation is based on the exact mass peak height.

7.3.3 Differentiation of significant features originating from oceanic sponge and coral species

As an initial proof of concept to demonstrate that the diver operable coated bolt SPME sampler could stabilize extracts even when transported to and from distant countries, an on-site and untargeted determination of allelochemical compounds emitted from competing coral and sponge species was performed. Many species of sponge are known to directly compete with coral for space, effectively growing over and killing live corals.[183] During this competition both organisms emit various biomolecules theorized to assist in the destruction of their respective competitor in a process known as allelochemical interactions.[184] As reviewed by Thakur *et al.* many biological studies have been conducted identifying a plethora of species-specific allelochemicals emitted by sponges attacking coral.[185]

Hence, as an initial application, the diver operable morphology of the coated bolt samplers was fully deployed by having a diver place samplers on top of corals and a living sponge while visiting Cuba. As can be seen in Figure 7.12 adequate multivariate separation between the coral and sponge sample types could be achieved when Orthogonal Projections to Latent Structures Discriminant Analysis (OPLS-DA) statistical processing was used to group samples. It is important to note that OPLS-DA is considered a classed multivariate approach which discriminates separations based on user-defined groups.[186] It is therefore important to highlight that mild separation between these 2 groups was still observed when unclassed principle component analysis (PCA) was performed (Appendix Figure B.2). Moreover, as shown in Figure 7.15 when the samples were ionized in negative mode separation with superb clustering was observed for all three samples taken. As before, these classed OPLS-DA results were further supported by reasonable separation in a corresponding unclassed PCA plot (Appendix Figure B.5).[186] Further

breakdown and discussion of the various generated multivariate models generated in both PFP-positive and PFP-negative modes are presented in APPENDIX B of this thesis.

In terms of feature identification, only preliminary exact mass matching to an online metabolomics database (Metlin) was performed to date as the full biochemical interpretation of these results remains outside of the scope of this thesis. Further consultation with individuals knowledgeable in marine biochemistry is needed such that features can be narrowed down and an appropriate MS^n methodology or standards can be selected. In terms of feature selection, however, a features loading S-plot (Figure 7.13) that separates features based on the OPLS-DA separation shown in Figure 7.12 was first prepared. From this S-plot, features which are found to separate at the top right and bottom left of the main linear cluster were manually selected and listed in a table. Significant features can then be filtered in this list by using SIMCA's proprietary VIP algorithm with features possessing a VIP>1.000 to be deemed significant.[187] It is important to point out however that this algorithm has been considered as a "black box" by other users as Umetrics has kept related details secret.[187] Furthermore, it was found that VIP filtering may unnecessarily remove features that exhibit lower relative signal, but, exhibit an absence-presence relationship between 2 samples. Regardless, by using this methodology, a selection of significant features differentiating the biochemical profile of two coral samples from that of a competing sponge was accomplished. Although the biochemical interpretation of these features was not performed a list of potential exact mass identifications of said features may be viewed in Appendix B of this thesis.

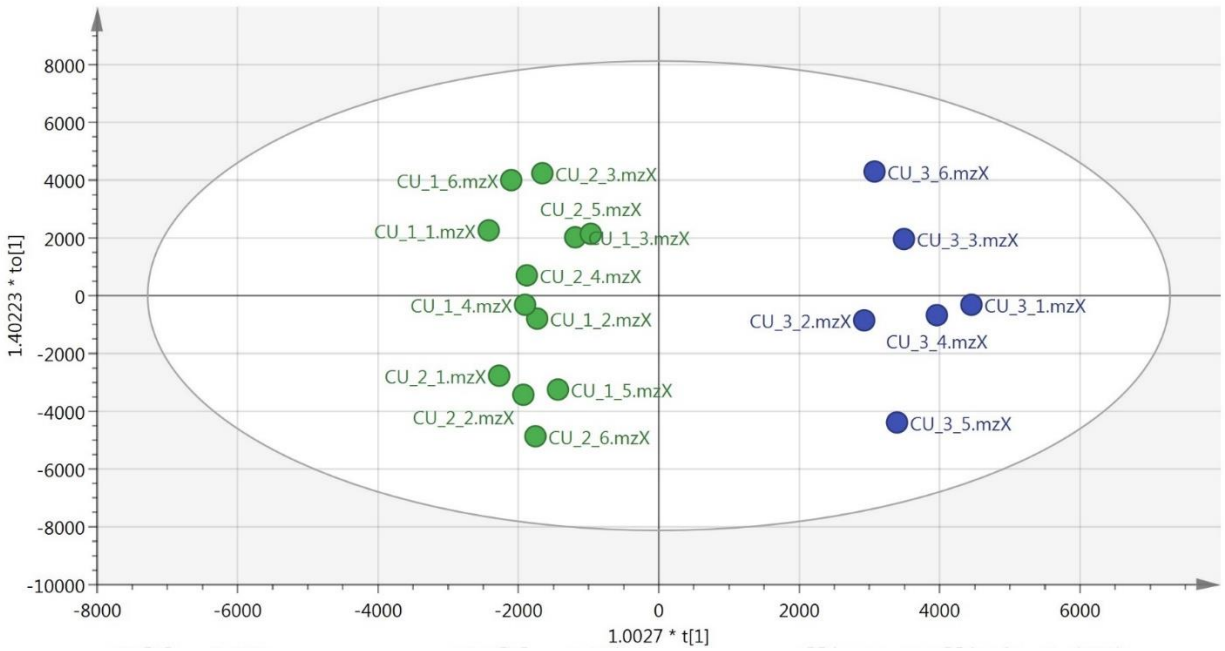

Figure 7.12: Classed multivariate separation (OPLS-DA) of replicate samples corresponding to extractions from the sponge sample (BLUE) and 2 different coral samples (GREEN). Samples were run on the PFP column and ionized in positive mode. Separation is based on the exact mass peak height.

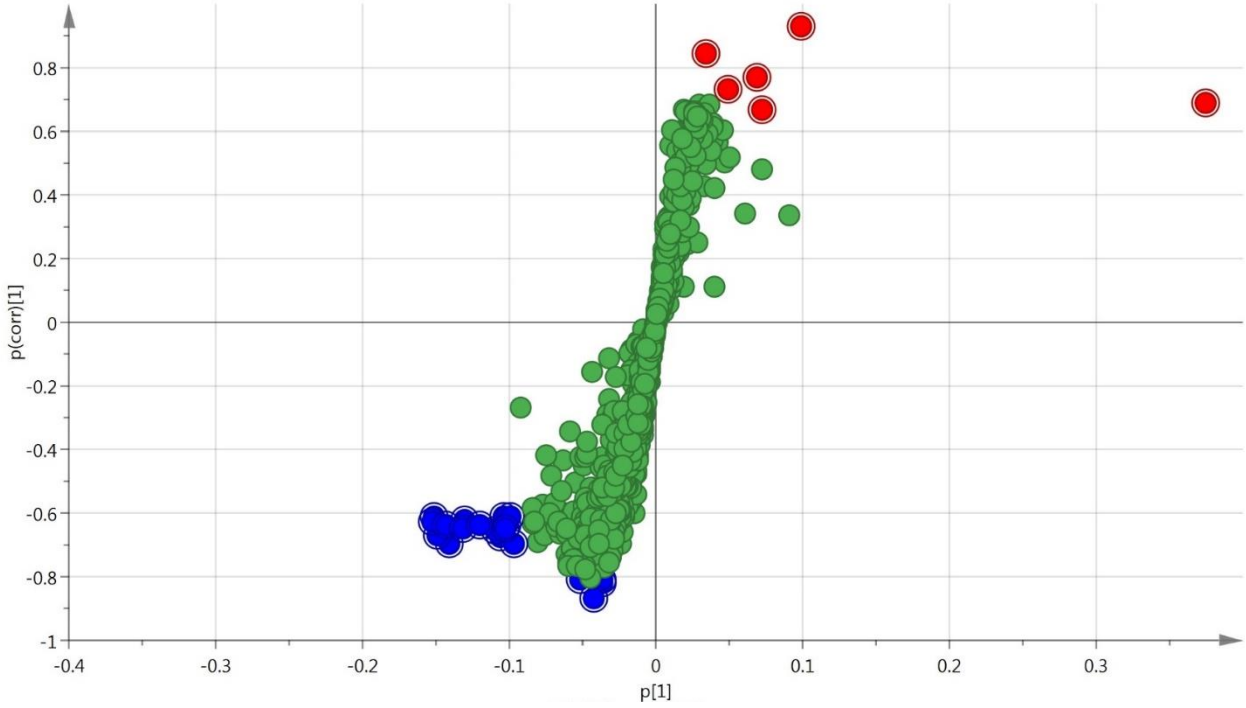

Figure 7.13: S-Plot generated from the classed multivariate separation shown in Figure 7.12 highlighting features in BLUE being statistically larger in the coral samples and features in RED being statistically larger in sponge samples.

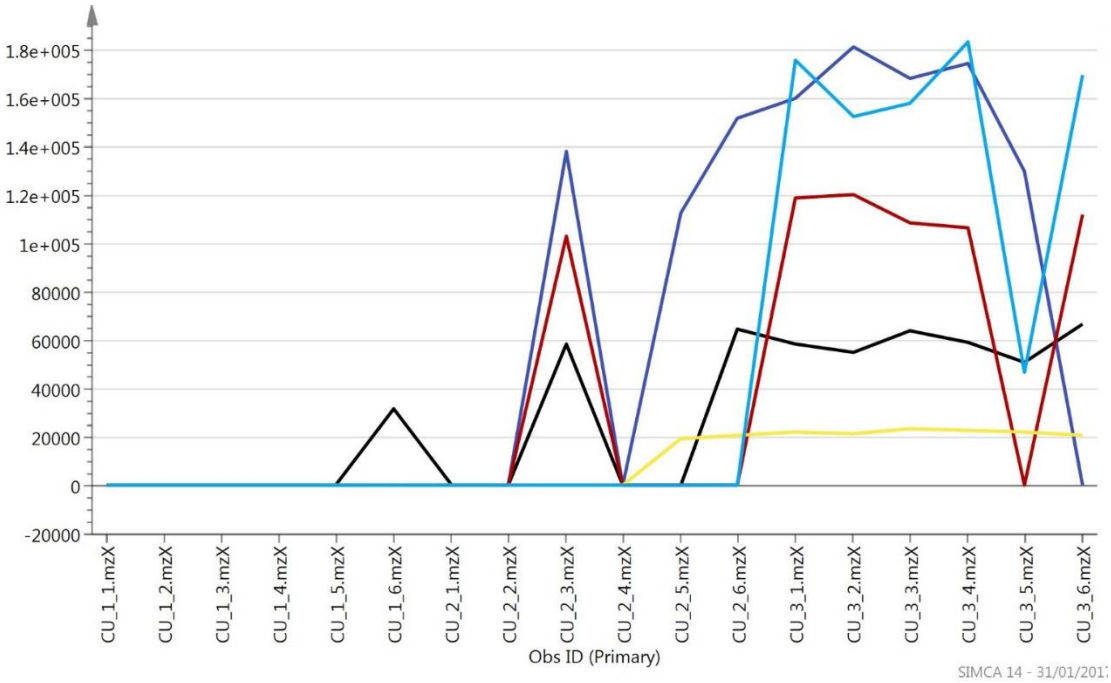

Figure 7.14: Distribution plot of significant features highlighted in RED from the sponge samples (CU_3_X) in Figure 7.13. Contrary to the coral samples, those features detected at the sponge site were nearly unique to that sample.

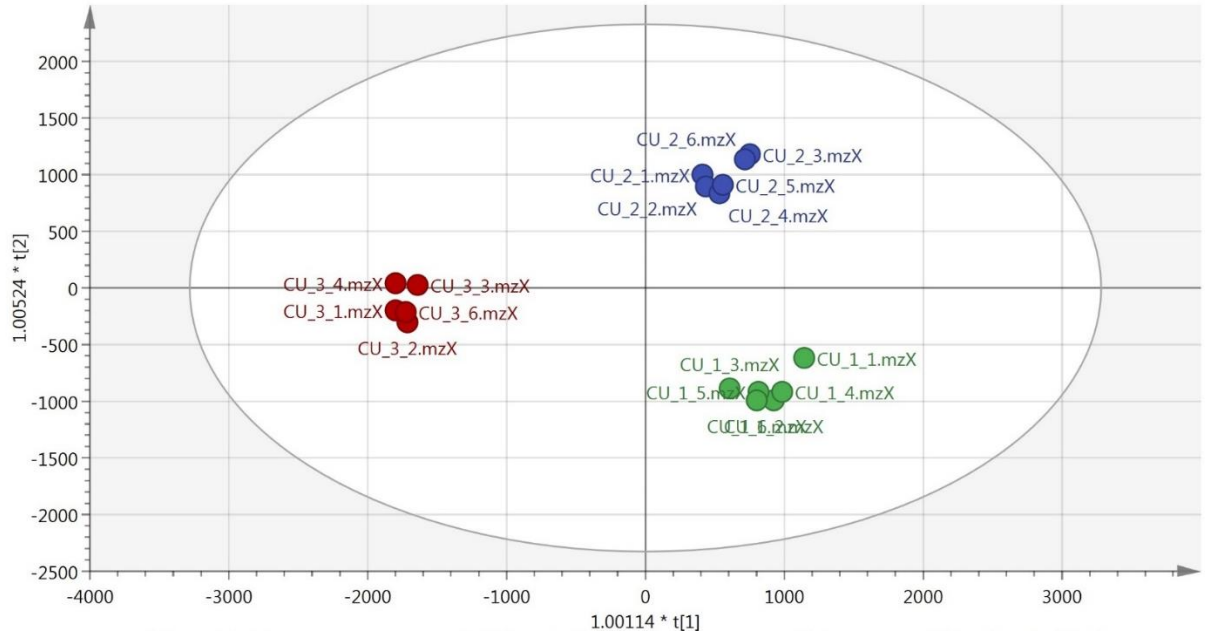

Figure 7.15 Classed multivariate separation (OPLS-DA) of replicate samples corresponding to extractions from the sponge sample (RED) and 2 replicate coral samples (BLUE and GREEN) showing superb clustering of data. Samples were run on the PFP column and ionized in negative mode. Separation is based on the exact mass peak height.

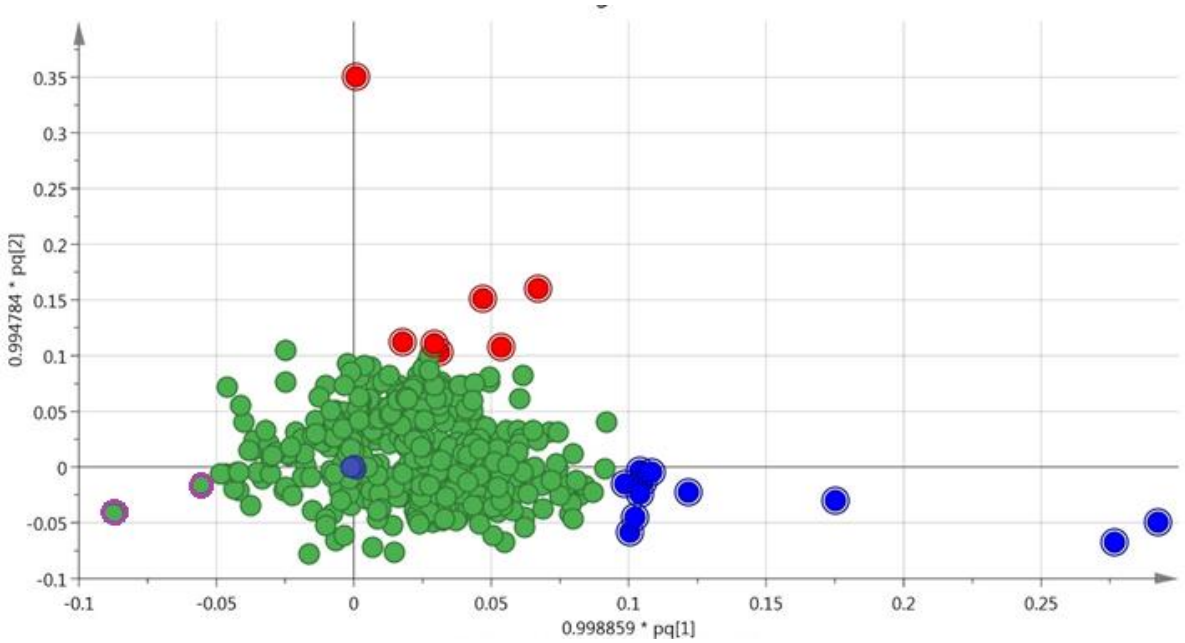

Figure 7.16 Loadings plot generated from the classed multivariate separation shown in Figure 7.15 highlighting features in BLUE being statistically larger in the first coral samples, features in RED being statistically larger in the second coral samples, and, features highlighted in PURPLE being larger in sponge samples.

7.3.4 Multicomponent separation of various biomolecules from deep-sea hydrothermal vents

As perhaps the most novel application of the coated bolt SPME sampler, multiple self-sealing ROV operable devices were prepared and deployed on 2 separate dives of ROV submersible submarines for the untargeted investigation of deep-sea hydrothermal vents. As previously noted, the first dive was performed at the El Gordo hydrothermal seamount 2.9 km deep in the Pacific Ocean. Unfortunately, due to a miscommunication between our joint team from the University of Waterloo, University of Victoria and the ROV operator team, the sorbent coating was only exposed to the vent and control samples for 15 seconds. Despite this incredibly short sampling time it was pleasantly surprising to see an excellent separation between the control and vent locations when unclassed principal component analysis was performed (Figure 7.17). This could be attributed to the large 250 mm^2 surface area of the coated bolts. Being 22.5 times larger than that of a classical SPME fiber, the response would theoretical be the same as if a 5.63-minute

fiber based extraction was performed instead. This result very much highlights just how important sampler design can be in saving an otherwise botched sampling opportunity. However, it is worth noting that only 5 of the 6 replicate samples from each site could be reliably plotted as 2 of the non-recessed coatings were found to be damaged as a likely result of scraping on the sampler body. It is for this reason that recessed coatings were used on future dives. After confirming reasonable unclassed separation of the samples, an OPLS-DA classed model (Figure 7.18) was then used to generate an S-plot and related VIP list to differentiate significant features from the samples. Significant features were then selected using the same methodology described in Section 7.3.3. Although discussion of the biochemical interpretation of these features is not contained within this thesis a list of the tentative exact mass identifications may be found in Tables C.1 and C.2 of Appendix C.

Much better communication was established between our research teams and the ROV crew during the second dive. Although this sampling did not necessarily give an ideal choice of the vent location due to constraints encountered by the ROV team, the samplings were performed properly, giving 6 minutes at both the control and vent site which had measured temperatures of 1.53 ^{o}C and 20.4 ^{o}C respectively. Furthermore, as seen in Figure 7.5, the control sampling was performed during ROV ascent, well away from the sampling site. The chosen vent site, shown in Figure 7.4, had very little visible life growing immediately around the hydrothermal plume, however, there was evidence of many shrimp living in proximity to this vent, likely feeding on microorganisms from this plume. In terms of multicomponent separation, the PCA plot, shown in Figure 7.21, still indicated good separation between the control and vent samples, however, grouping of the 6 vent samples was shown to be broad. Upon reviewing Figure 7.4 it was apparent that one side of the sampler was more directly inserted into the hydrothermal plume likely resulting

in this discrepancy. This can be further confirmed in consideration of the numbering scheme for the replicate bolts which relates to the crisscrossed order they were removed from the sampler body, as shown in Figure 7.24. Where bolts 2, 4 and 5 weren't in the high flow area of hydrothermal vent they extracted a similar amount of compound resulting in good clustering. However, bolt 3 on the other side of the sampler likely saw the highest flow rate as it would have been directly in front of the vent. As the fluid moved across the sampler flow velocities would have decreased and become more turbulent near the back-left side of the sampler (bolt 1). Furthermore, this variation can still be seen even when the samples were grouped by class using the OPLS-DA model. However, it is worth noting that despite this weaker clustering, samples could still be fully separated along the first principle component, T[1], of the OPLS-DA plot indicating that the loading of features on the generated S-plot shown in Figure 7.23 would still be reliable. A similar trend could be seen when the samples were instead ionized in negative mode. Figures corresponding to negative mode feature identification can be viewed in Appendix C. As before, the lists of tentative exact mass matches for these features are also included in Appendix C.

Despite lacking discussion on the biochemical importance of the various discovered hydrothermal vent features, the ability to differentiate these compounds from a control sample still manages to demonstrate that the design was effective thus fulfilling the scope and goal of this thesis. This is not to say that additional biochemical interpretation won't be performed later. In fact, a full understanding of these results could yet yield incredibly novel information regarding the earliest evolutionary state of life on Earth. Hence, interpretation of these results cannot be rushed, and much like the coral, sponge competition study, consultation with individuals knowledgeable in marine biogeochemistry will still be performed such that features can be narrowed down and an appropriate MS^n methodology or standards can be selected.

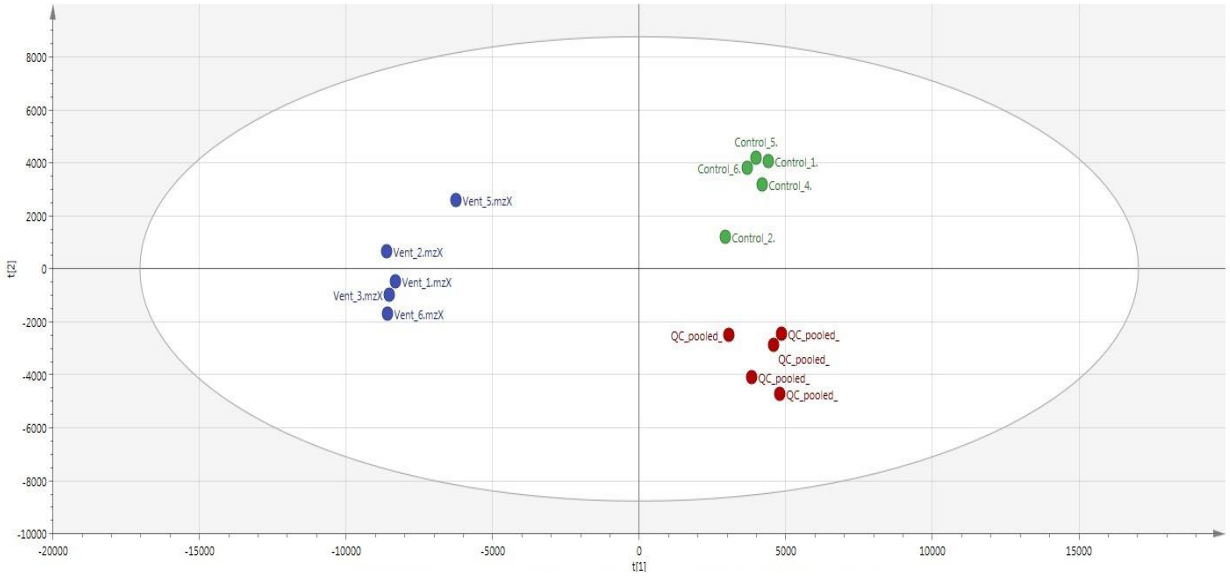

Figure 7.17 Multivariate separation (PCA) of replicate samples corresponding to extractions from the El-Gordo hydrothermal vent sample (BLUE), the control sample (GREEN), and, the validating pooled QC data (RED). Despite 15-second sampling excellent grouping and separation was observed for the samples. Samples were run on the PFP column and ionized in positive mode. Separation is based on the exact mass peak height.

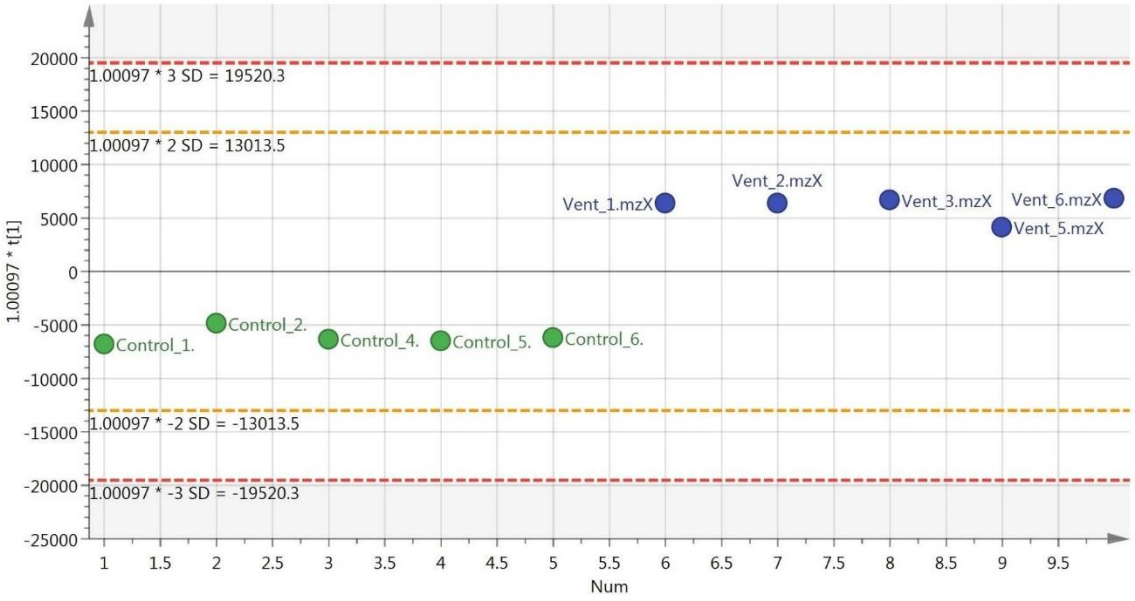

Figure 7.18: Single component classed multivariate separation (OPLS-DA) of replicate samples corresponding to extractions from the El-Gordo vent samples (BLUE) and ambient ocean control samples (GREEN). Samples were run on the PFP column and ionized in positive mode. Separation is based on the exact mass peak height.

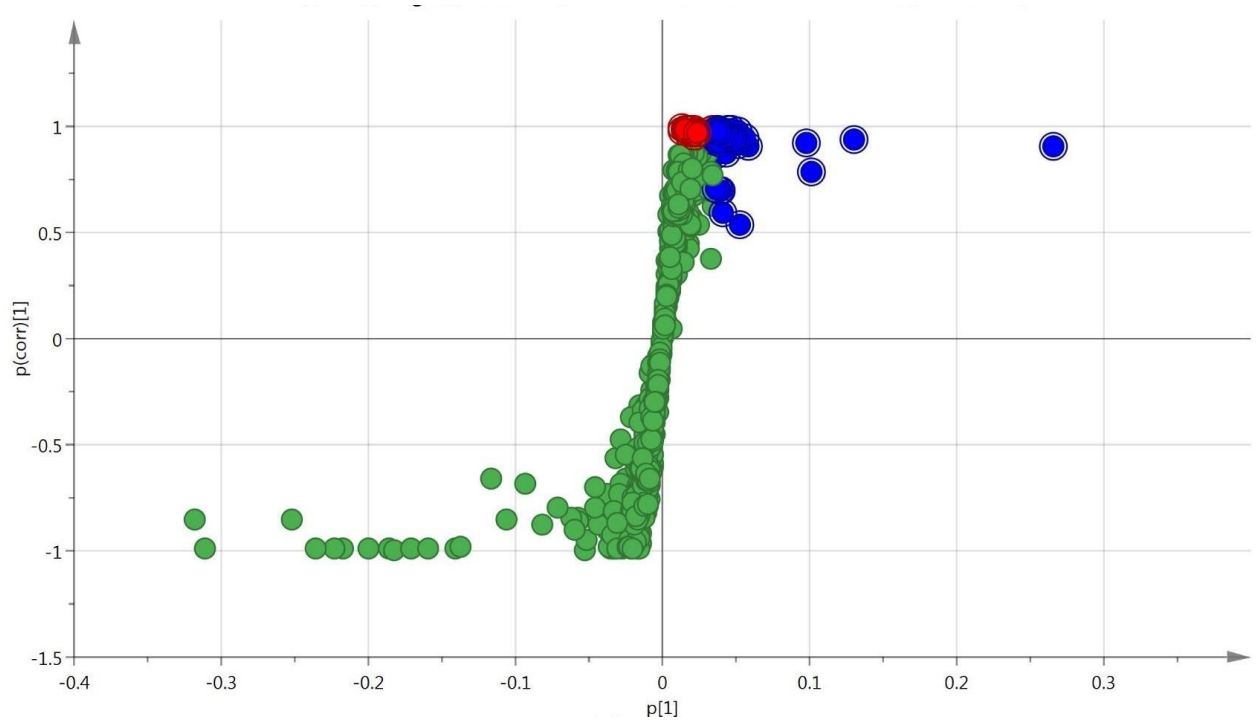

Figure 7.19: S-Plot generated from the classed multivariate separation shown in Figure 7.18 highlighting features in BLUE being statistically larger (VIP>1) in the vent sample and features in RED being exclusively present in the vent sample but with VIP<1.

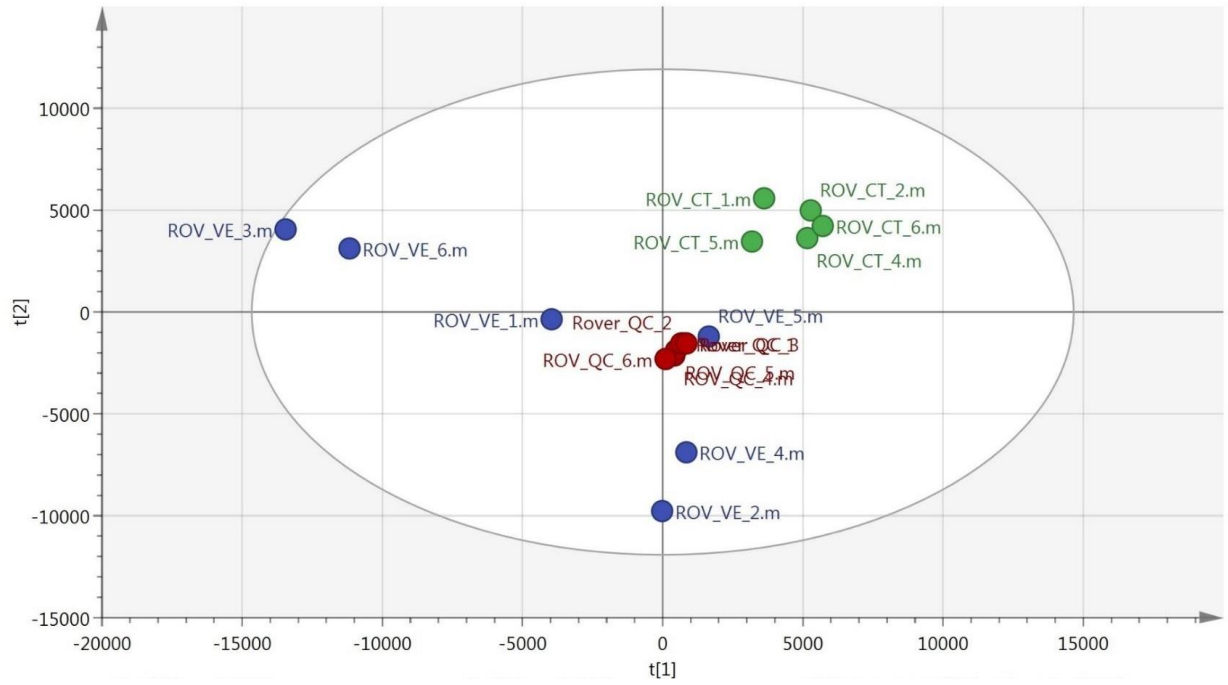

Figure 7.20 Multivariate separation (PCA) of replicate samples corresponding to extractions from the NW Rota hydrothermal vent sample (BLUE), the control sample (GREEN), and the validating pooled QC data (RED). Well grouped pool QC data indicates stable instrument performance. Samples were run on the PFP column and ionized in positive mode. Separation is based on the exact mass peak height.

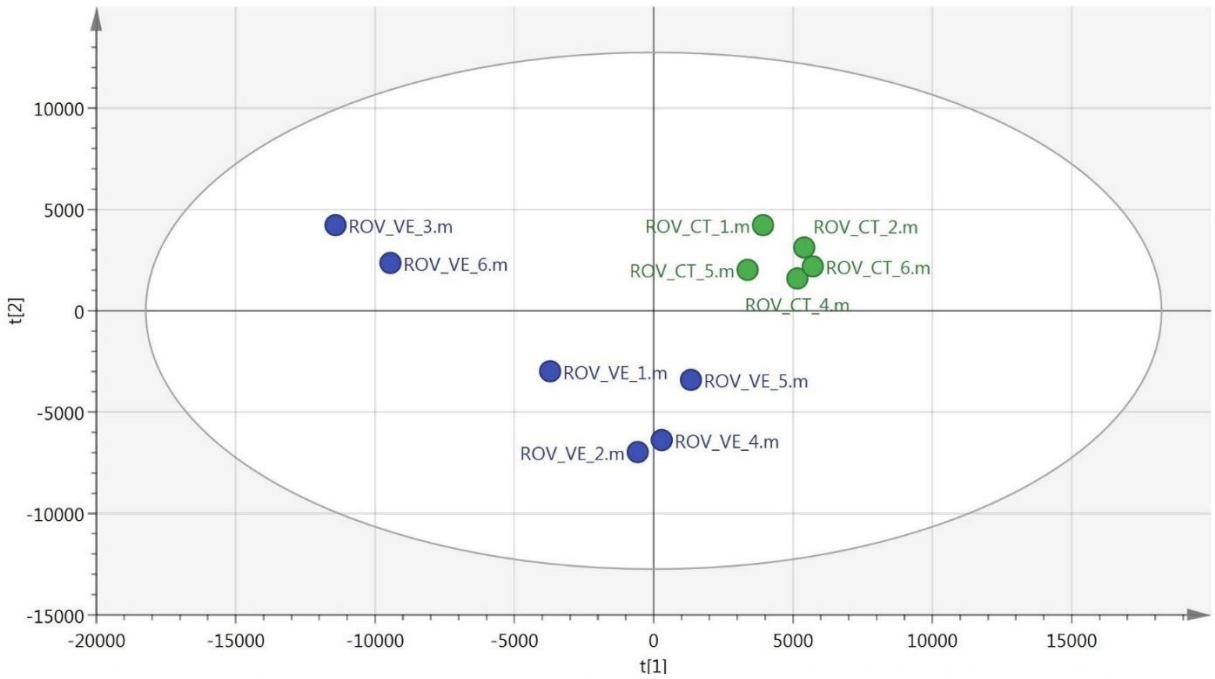

Figure 7.21 Multivariate separation (PCA) of replicate samples corresponding to extractions from the NW Rota vent sample (BLUE) and the control sample (GREEN). Pool QC's have been removed to better show clustering of ROV samples. Samples were run on the PFP column and ionized in positive mode. Separation is based on the exact mass peak height.

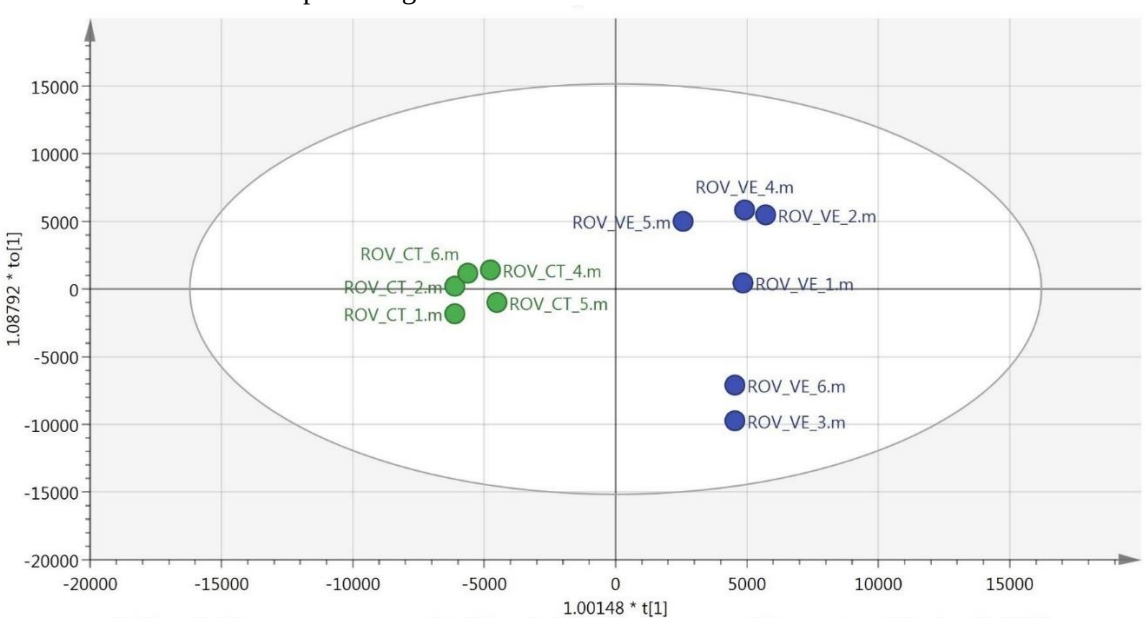

Figure 7.22: Classed multivariate separation (OPLS-DA) of replicate samples corresponding to extractions from NW Rota vent samples (BLUE) and ambient ocean control samples (GREEN). Samples were run on the PFP column and ionized in positive mode. Separation is based on the exact mass peak height.

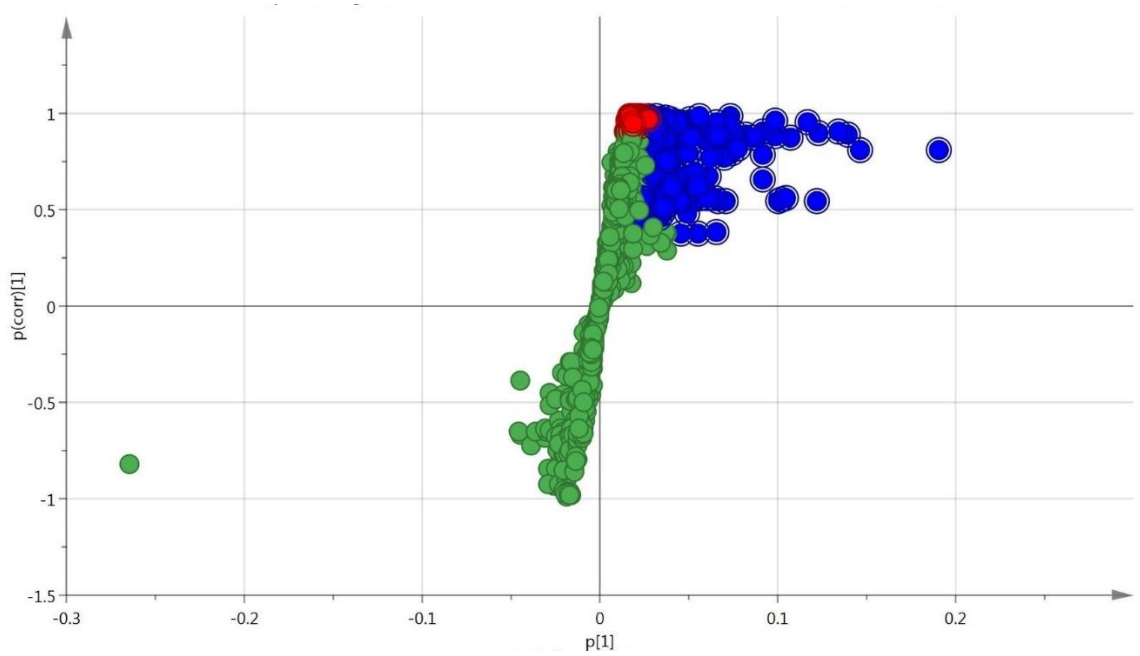

Figure 7.23: S-Plot generated from the classed multivariate separation shown in Figure 7.22 highlighting features in BLUE being statistically larger (VIP>1) in the vent sample and features in RED being exclusively present in the vent sample but with VIP<1.

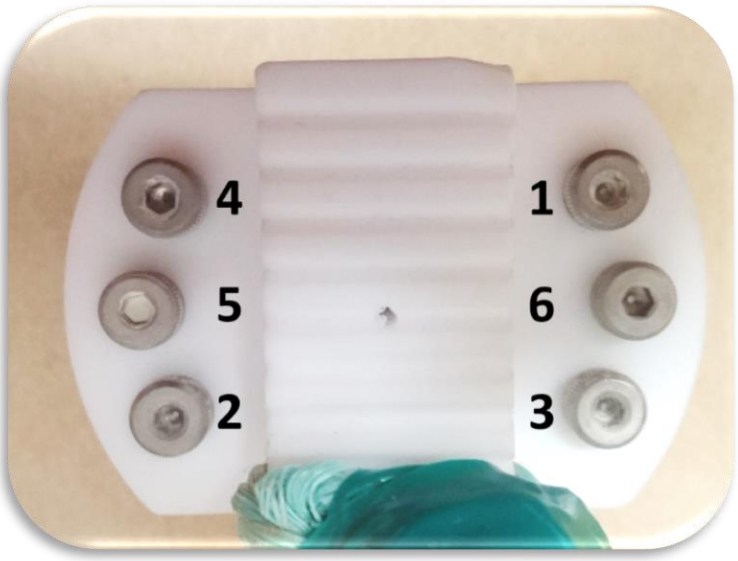

Figure 7.24 Crisscrossed bolt removal order from the ROV-SPME self-sealing sampler.

7.4 Conclusion and future directions

A new highly robust morphology of solid phase microextraction based on a high surface area recessed HLB/PAN coated bolt was demonstrated in this work. By enclosing these bolts in a

self-sealing Teflon body it was shown that analyte extracted from a real sample, such as wastewater effluent, could be stabilized on the coating for a period of at least 12 days. Furthermore, the enclosable design allowed samplers to be transported using unconventional means, such as with a traveling diver at ambient temperatures. In addition to providing the sampler physical rigidity, the large diameter cylindrical bolts also gave a high surface area to apply sorbent coating. This surface area was calculated to be more than double that of a comparable thin film blade device and 22 times more than an SPME-HPLC fiber. Particularly for the short sampling times used during the ROV-SPME extractions, this increased surface area is critical for ensuring maximum sensitivity. Although the biochemical interpretation of the ROV-SPME hydrothermal vent sampling remains to be investigated, the use of multivariate data analysis has indicated promising performance from these devices showing a strong statistical separation between those features extracted during control sampling and the hundreds of preliminarily identified compounds originating from the deep-sea hydrothermal vent sites.

For the purposes of this thesis, the works performed herein have shown how even the most difficult on-site samplings can be accomplished with appropriately designed sampling devices. However, further interpretation of the vast resulting dataset may yet yield undiscovered biochemical information pertaining to one of the harshest known ecosystems on our planet. As a result, this is a future work that cannot be rushed and appropriate collaboration must be established to make the most of this unique sampling opportunity facilitated by this robust sampler design.

Chapter 8 Summary and future perspective

8.1 Summary

As exploratory analytical scientists, we continue to expand upon the repertoire of available analytical approaches for the investigation of unique natural environments. Time and again approaching these underexplored regions requires the development of new sampling technologies to best address site-specific challenges. The recent advent of hand portable GC-MS instrumentation now provides a unique opportunity for the immediate determination of contaminants in such environmental systems. However, major limitations of these miniaturized detectors remain as they may lack the inherent stability of their unmoving, climate controlled benchtop counterparts while providing a significant loss of instrument sensitivity as a necessary trade-off for their power conserving, lightweight designs. When considering adaptable sampling approaches, solid phase microextraction (SPME) techniques have been well explored in terms of their applicability for on-site sampling and sample preparation. Accordingly, this thesis presented various novel morphologies and analytical methodologies based on the principles of solid phase microextraction as a means to improve the reliability and sensitivity of on-site environmental analysis.

Firstly, the developed silicone oil-PS/DVB based standard headspace generating systems were successfully shown to exhibit the necessary characteristics for performing instrument quality control and in-situ derivatization on-site. In addition to providing hundreds of repeatable SPME loadings of McReynolds probes from a single vial, it was shown that vials originating from completely different batches could deliver a statistically (95% confidence) identical amount of analyte. Furthermore, even when loaded with unstable, and reactive derivatization agents, such as PFPH, these headspace generators were proven to be stable at room temperature so long as they were protected from light in amber glass.

After establishing this reliable means for performing on-site quality control, thus accomplishing the first goal of the project, the focus was switched towards the preparation of a new TF-SPME device to improve detection limits for targeted and untargeted GC based analyses. Contrary to what was seen with prior membrane compositions, the new carbon mesh supported, high-density PDMS based TFME membranes exhibited low siloxane bleed and a much-improved signal-to-noise ratio. The addition of the carbon mesh support yielded superb physical characteristics allowing for stir rates approaching 4000 rpm when operated with the custom-built TF-SPME sampling case. When prepared with DVB/PDMS these membranes were found to be very sensitive, giving extraction amounts for aqueous pesticides of at least 20 times greater than that of a standard fiber morphology using identical sorbent. Furthermore, this extraction efficiency was then effectively doubled for polar VOC's by developing and incorporating a homemade microporous HLB particle which could be used in-lieu of DVB.

In terms of reliability, the improved TF-SPME devices were also shown to exhibit favorable intra and inter-batch reproducibility, regardless of the sorbent chemistry employed. With the help of our industrial partners at Maxxam and colleagues here at the University of Waterloo, a new TF-SPME method for the determination of multi-residue pesticides from surface waters was developed and compared to US-EPA certified LLE approaches. This comparison demonstrated that the novel TF-SPME approach gave similar accuracy to the accepted LLE method while providing additional advantages including higher sensitivity, small sample volumes, and faster throughput. Given these advantages, TFME was shown to be a great potential for adoption as a green alternative to LLE.

In addition to the improvements presented on benchtop instrumentation, these membranes could also be used to improve LOD's of our entirely on-site analytical approaches with hand

portable GC-TMS instrumentation. In fact, the high volume desorption unit involved was validated to successfully transfer all analytes from the TFME membrane to the portable GC-MS without any analyte carry-over detectable on the membranes or breakthrough of the transferring needle trap device. Beyond allowing for the in-lab sub-ppb detection of pesticides from surface waters on a hand-portable instrument, TFME-GC/TMS was fully deployed on-site at various riparian locations within Southern Ontario successfully screening for untargeted analytes in real river samples.

Finally, as a unique addition to this thesis, a pair of deep-sea sampling devices were designed to be deployed by divers and ROV submersibles respectively. Due to their self-sealing design, these samplers were shown to stabilize extracted analyte at room temperature for up to 12-days following sampling. Taking advantage of this stability, these devices were deployed on-site by a diver for the differentiation of significant features emitted by competing sponge and coral species and then transported back to Canada at ambient temperatures for desorption and analysis. As an ultimate testament to designing SPME devices for extreme environmental conditions, these samplers were then fully optimized for ROV deployment at deep-sea hydrothermal vents along 3 different regions of the Pacific Rim. Although the biochemical interpretation of the generated results is beyond the scope of this thesis, the ability to statically separate chemical features pertaining to such an inaccessible and harsh environment truly shows just how important the design and implementation of a proper sampler can be when investigating the worlds most unique natural environments.

8.2 Future perspective

The design, validation and on-site deployment of these various new sampling technologies present a bright future for the growing field of on-site environmental analysis. With their superior sensitivity, the presented thin film membranes really lend themselves well to further, and more

varied on-site method development with portable GC/MS instrumentation. As it stands most of the TFME-GC/TMS applications shown herein have successfully supported the concept of sensitive, entirely on-site analytical screening but have fallen short of more rigorous method development which may lead the way for on-site analytical approaches that go beyond initial screening. In terms of TF-SPME coating chemistries, new projects exploring the use of nano-carbon materials as sorbents have already been passed forward to a new generation of graduate researchers in our group. Other improvements such as PDMS or PFTE overcoating could also be explored allowing for matrix-compatible TF-SPME devices which could open a new avenue in the direction of food and consumer product sampling.

In terms of novelty, the hydrothermal vent application of the deep sea samplers remains an impressive feat. However, where much of this project remains outside the primary scope of this thesis, there is still likely much to be explored within the generated data. Proper bio-chemical interpretation of these features may very well yield additional discoveries regarding the microbiological life that has managed to survive in these dark ocean environments. Beyond what is presented herein further investigation will continue to be performed by the author of this thesis, colleagues, and our involved academic collaborators as to better understand this underexplored environment.

Ultimately though, this thesis has successfully displayed the development, validation and initial application for an assortment of novel SPME based technologies. Further work involving any of these devices will likely expand upon these initial applications turning them into fully developed methods and, hopefully, push the limits of what is possible for on-site environmental analysis.

Letter of Copyright Permission

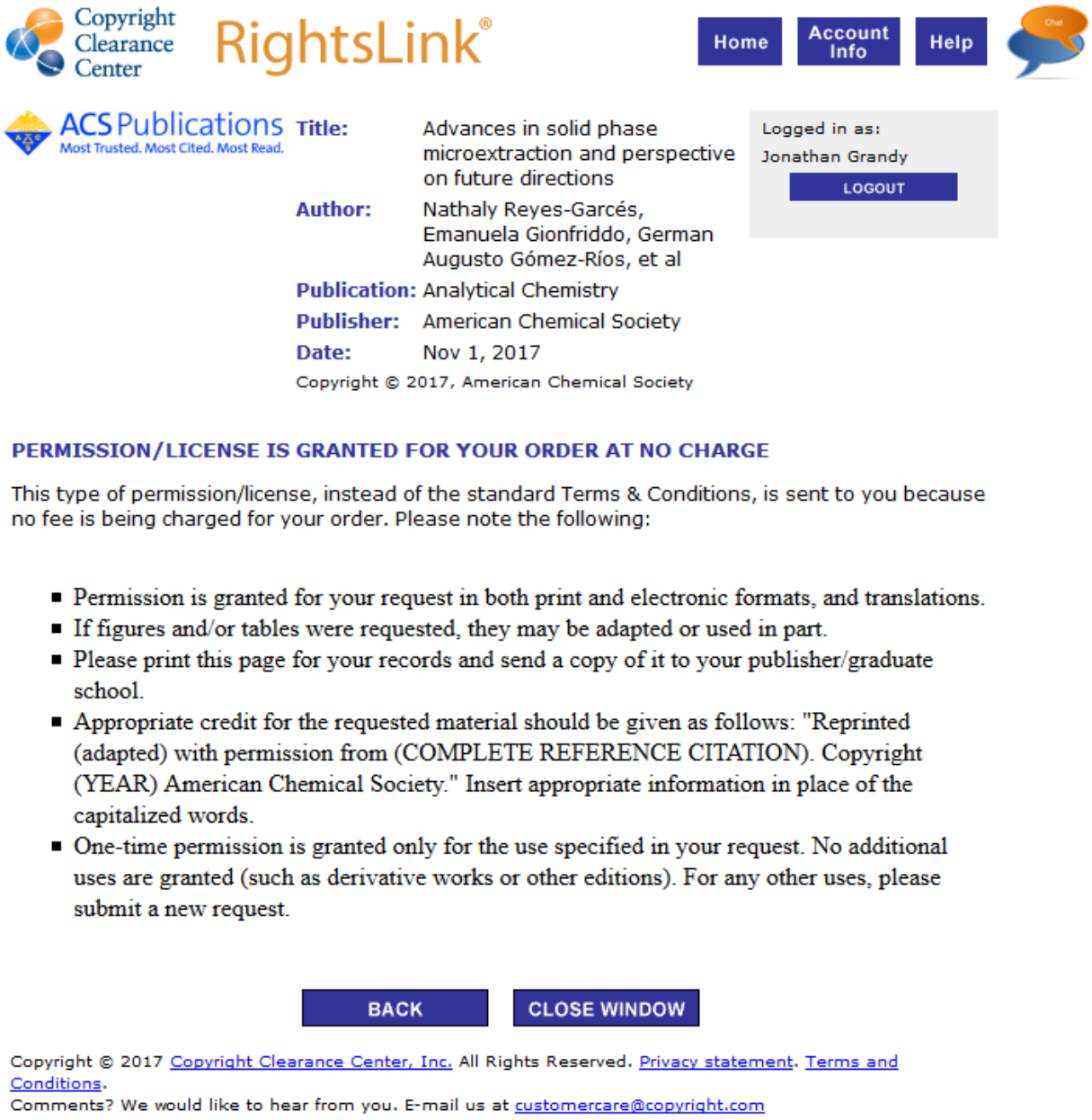

Copyright Clearance Center RightsLink®

Home | Account Info | Help

ACS Publications
Most Trusted. Most Cited. Most Read.

Logged in as:
Jonathan Grandy
LOGOUT

Title: Advances in solid phase microextraction and perspective on future directions

Author: Nathaly Reyes-Garcés, Emanuela Gionfriddo, German Augusto Gómez-Ríos, et al

Publication: Analytical Chemistry

Publisher: American Chemical Society

Date: Nov 1, 2017

Copyright © 2017, American Chemical Society

PERMISSION/LICENSE IS GRANTED FOR YOUR ORDER AT NO CHARGE

This type of permission/license, instead of the standard Terms & Conditions, is sent to you because no fee is being charged for your order. Please note the following:

- Permission is granted for your request in both print and electronic formats, and translations.
- If figures and/or tables were requested, they may be adapted or used in part.
- Please print this page for your records and send a copy of it to your publisher/graduate school.
- Appropriate credit for the requested material should be given as follows: "Reprinted (adapted) with permission from (COMPLETE REFERENCE CITATION). Copyright (YEAR) American Chemical Society." Insert appropriate information in place of the capitalized words.
- One-time permission is granted only for the use specified in your request. No additional uses are granted (such as derivative works or other editions). For any other uses, please submit a new request.

BACK | CLOSE WINDOW

Copyright © 2017 Copyright Clearance Center, Inc. All Rights Reserved. Privacy statement. Terms and Conditions.
Comments? We would like to hear from you. E-mail us at customercare@copyright.com

ELSEVIER LICENSE
TERMS AND CONDITIONS

Jan 12, 2018

This Agreement between Mr. Jonathan Grandy ("You") and Elsevier ("Elsevier") consists of your license details and the terms and conditions provided by Elsevier and Copyright Clearance Center.

License Number	4253280902314
License date	Dec 20, 2017
Licensed Content Publisher	Elsevier
Licensed Content Publication	Elsevier Books
Licensed Content Title	Comprehensive Analytical Chemistry
Licensed Content Author	Jonathan Grandy,Saba Asl-Hariri,Janusz Pawliszyn
Licensed Content Date	Jan 1, 2015
Licensed Content Volume	70
Licensed Content Issue	n/a
Licensed Content Pages	27
Start Page	209
End Page	235
Type of Use	reuse in a thesis/dissertation
Portion	excerpt
Number of excerpts	10
Format	both print and electronic
Are you the author of this Elsevier chapter?	Yes
Will you be translating?	No
Title of your thesis/dissertation	Development of Field Portable Solid Phase Microextraction Samplers for Performing On-site Environmental Analysis
Expected completion date	Feb 2018
Estimated size (number of pages)	220
Requestor Location	Mr. Jonathan Grandy 165 Erb St East Waterloo, ON N2J1M5 Canada Attn: Mr. Jonathan Grandy
Billing Type	Invoice
Billing Address	Mr. Jonathan Grandy 165 Erb St East Waterloo, ON N2J1M5 Canada Attn: Mr. Jonathan Grandy
Total	0.00 CAD

Order Completed

Thank you for your order.

This Agreement between Mr. Jonathan Grandy ("You") and Elsevier ("Elsevier") consists of your license details and the terms and conditions provided by Elsevier and Copyright Clearance Center.

Your confirmation email will contain your order number for future reference.

printable details

License Number	4280960725384
License date	Feb 02, 2018
Licensed Content Publisher	Elsevier
Licensed Content Publication	Analytica Chimica Acta
Licensed Content Title	A critical review in calibration methods for solid-phase microextraction
Licensed Content Author	Gangfeng Ouyang,Janusz Pawliszyn
Licensed Content Date	Oct 10, 2008
Licensed Content Volume	627
Licensed Content Issue	2
Licensed Content Pages	14
Type of Use	reuse in a thesis/dissertation
Portion	figures/tables/illustrations
Number of figures/tables /illustrations	1
Format	both print and electronic
Are you the author of this Elsevier article?	No
Will you be translating?	No
Original figure numbers	Fig. 5.
Title of your thesis/dissertation	Development of Field Portable Solid Phase Microextraction Samplers for Performing On-site Environmental Analysis
Expected completion date	Feb 2018
Estimated size (number of pages)	220
Requestor Location	Mr. Jonathan Grandy 165 Erb St East Waterloo, ON N2J1M5 Canada Attn: Mr. Jonathan Grandy
Publisher Tax ID	GB 494 6272 12
Total	0.00 CAD

ORDER MORE | CLOSE WINDOW

ACS Chemistry for Life®

Click here if you have difficulty reading this email >>

Dear Jonathan,

Your permission requested is granted and there is no fee for this reuse. In your planned reuse, you must cite the ACS article as the source, add this direct link <http://pubs.acs.org/doi/abs/10.1021/acs.analchem.5b04008>, and include a notice to readers that further permissions related to the material excerpted should be directed to the ACS.

Regards,

Jawwad Saeed

ACS Customer Services & Information

https://help.acs.org

Your help request has been resolved. If you have further issues regarding this matter, please let us know by responding to this email. Please note that this request will auto-close in 14 days. If you need to contact us after 14 days regarding this matter please submit a new help request and refer to this help request number.

How are we doing? Let us know!
Please click on your selection below to begin our two-question survey.

Based on this support interaction, how satisfied were you with the help provided?

Not at all satisfied *Completely satisfied*

0	1	2	3	4	5	6	7	8	9	10
○	○	○	○	○	○	○	○	○	○	○

E-mail Information:

Attachments	
cc	

Request Information:

Request #	9131-7921459
Date Created	12/07/2017 08:07 PM EST
Summary	Request for content reuse for PhD Thesis (DOI: 10.1021/acs.analchem.5b04008)
Details	Hello, I am writing to request the right to reuse the entirety of the material from an ACS AuthorChoice article published in Analytical Chemistry entitled, "Development of a Carbon Mesh Supported Thin Film Microextraction Membrane As a Means to Lower the Detection Limits of Benchtop and Portable GC/MS Instrumentation" (http://pubs.acs.org/doi/abs/10.1021/acs.analchem.5b04008) To which I am the primary author of. I wish to use this material for my PhD Thesis entitled " Development of Field Portable Solid Phase Microextraction Samplers for Performing On-site Environmental Analysis". The thesis itself will be approximately 200-250 pages and I wish to use the entire published article in question to comprise one thesis chapter. The thesis itself will be available by both print and electronically by the University of Waterloo Library holdings. Thank you for your time, Cheers! Sincerely, Jonathan J Grandy PhD Candidate and C2-162 Lab Manager Prof. Pawliszyn Research Group

References

(1) Grandy, J. J.; Boyaci, E.; Pawliszyn, J. *Anal. Chem.* **2016**, *88* (3), 1760–1767.

(2) Lee, C. W.; Tabor, D. G.; Cowen, K. A. *J. Mater. Cycles Waste Manag.* **2008**, *10* (1), 38–45.

(3) Grandy, J. J.; Gómez-Ríos, G. A.; Pawliszyn, J.; Gomez-Rios, G. A.; Pawliszyn, J. *J. Chromatogr. A* **2015**, *1410*, 1–8.

(4) Poole, J. J.; Grandy, J. J.; Go, G. A.; Gionfriddo, E.; Pawliszyn, J. **2016**.

(5) Pawliszyn, J. *Handbook of Solid Phase Microextraction*; Chemical Industry Press: Beijing, 2009.

(6) Belardi, R. P., Pawliszyn, J. B. *Water Qual. Res. J. Can.* **1989**, *24* (24), 179− 191.

(7) Arthur, C. L.; Pawliszyn, J. *Anal. Chem.* **1990**, *62* (19), 2145–2148.

(8) Rodriguez-Lafuente, A.; Piri-Moghadam, H.; Lord, H. L.; Obal, T.; Pawliszyn, J. *Water Qual. Res. J. Canada* **2016**, *51* (4), 331–343.

(9) Gałuszka, A.; Migaszewski, Z. M.; Konieczka, P.; Namieśnik, J. *TrAC - Trends Anal. Chem.* **2012**, *37*, 61–72.

(10) Pawliszyn, J. *Anal. Chem.* **2003**, *75* (11), 2543–2558.

(11) Bojko, B.; Cudjoe, E.; Gómez-Ríos, G. A.; Gorynski, K.; Jiang, R.; Reyes-Garcés, N.; Risticevic, S.; Silva, É. A. S.; Togunde, O.; Vuckovic, D.; Pawliszyn, J. *Anal. Chim. Acta* **2012**, *750*, 132–151.

(12) Cheng, W.-H.; Zhan, W.; Pawliszyn, J. *J. Chinese Chem. Soc.* **2013**, *60* (8), 1027–1032.

(13) Sample, , Pawliszyn. *75* (2003), 2543–2558.

(14) Potter, D. W.; Pawliszyn, J. *Environ. Sci. Technol.* **1994**, *28* (2), 298–305.

(15) Spietelun, A. *Talanta* **2011**, *87*, 1–7.

(16) Criado, M. R.; Pereiro, I. R.; Torrijos, R. C. *Talanta* **2004**, *63* (3), 533–540.

(17) Valencia, S.; Marín, J.; Restrepo, G. *Water Sci. Technol. Water Supply* **2013**, *13* (2), 499.

(18) Schüpfer, P. Y.; Huynh, C. K. *J. Occup. Environ. Hyg.* **2008**, *5* (8), 490–500.

(19) Zhou, J.; Han, Y.; Zhuang, H.; Feng, T.; Xu, B. *Food Anal. Methods* **2014**, *8* (7), 1661–1672.

(20) Fettig, I.; Krüger, S.; Deubel, J. H.; Werrel, M.; Raspe, T.; Piechotta, C. *J. Forensic Sci.* **2014**, *59* (3), 743–749.

(21) Jia, M.; Koziel, J.; Pawliszyn, J. *F. Anal. Chem. Technol.* **2000**, *4* (2), 73–84.

(22) Ouyang, G.; Pawliszyn, J. *Anal. Chim. Acta* **2008**, *627* (2), 184–197.

(23) Gómez-Ríos, G. A.; Reyes-Garcés, N.; Pawliszyn, J. *J. Sep. Sci.* **2013**, *36* (17), 2939–2945.

(24) Ouyang, G. *J. Sep. Sci.* **2008**, *31* (6–7), 1167–1172.

(25) Piri-Moghadam, H.; Gionfriddo, E.; Rodriguez-Lafuente, A.; Grandy, J. J.; Lord, H. L.; Obal, T.; Pawliszyn, J. *Anal. Chim. Acta* **2017**, *964* (July 2016), 74–84.

(26) Jiang, R.; Pawliszyn, J. *Anal. Chem.* **2014**, *86* (1), 403–410.

(27) Lord, H. L.; Zhan, W.; Pawliszyn, J. *Compr. Sampl. Sample Prep.* **2012**, *2* (1), 677–697.

(28) Kenessov, B.; Koziel, J. A.; Bakaikina, N. V.; Orazbayeva, D. *TrAC - Trends Anal. Chem.* **2016**, *85*, 111–122.

(29) Jiang, R.; Pawliszyn, J. *TrAC Trends Anal. Chem.* **2012**, *39*, 245–253.

(30) Jia, M.; Koziel, J.; Pawliszyn, J. *F. Anal. Chem. Technol.* **2000**, *4* (2–3), 73–84.

(31) Jonathan Grandy, Saba Asl-Hariri, J. P. In *Comprehensive Analytical Chemistry*; 2015; pp 209–235.

(32) Lord, H. L.; Zhan, W.; Pawliszyn, J. *Anal. Chim. Acta* **2010**, *677* (1), 3–18.

(33) Lord, H. L.; Zhan, W.; Pawliszyn, J. *Compr. Sampl. Sample Prep.* **2012**, *2* (1), 677–697.

(34) Cheng, W. H.; Jiang, J. R.; Lin, C.; Liou, J. J.; Wu, Z. H.; Hsu, Y. H.; Yang, Z. Y. *J. Air Waste Manag. Assoc.* **2014**, *64* (4), 488–493.

(35) Saito, Y.; Ueta, I.; Ogawa, M.; Jinno, K. *Needle-Trap Devices for Environmental Sample Preparation*; Elsevier, 2012; Vol. 3.

(36) Kędziora, K.; Wasiak, W. *J. Chromatogr. A* **2017**, *1505*, 1–17.

(37) Koziel, J. A.; Odziemkowski, M.; Pawliszyn, J. *Anal. Chem.* **2001**, *73* (1), 47–54.

(38) Asl-Hariri, S.; Gómez-Ríos, G. A.; Gionfriddo, E.; Dawes, P.; Pawliszyn, J. *Anal. Chem.* **2014**, *86* (12), 5889–5897.

(39) Silva, J. *1300* (2013), 193–198.

(40) Azari, M. R.; Barkhordari, A.; Zendehdel, R.; Heidari, M. *Microchem. J.* **2017**, *134*, 270–276.

(41) Baktash, M. Y.; Bagheri, H. *Microchim. Acta* **2017**, *184* (7), 2151–2156.

(42) Vallecillos, L.; Borrull, F.; Sanchez, J. M.; Pocurull, E. *Talanta* **2015**, *132*, 548–556.

(43) Kleeblatt, J.; Stengel, B.; Radischat, C.; Passig, J.; Streibel, T.; Sippula, O.; Rabe, R.; Harndorf, H.; Zimmermann, R. *Anal. Methods* **2015**, *7* (8), 3608–3617.

(44) Heidari, M.; Attari, S. G.; Rafieiemam, M. *Anal. Chim. Acta* **2016**, *918*, 43–49.

(45) Xie, X.; Dennis Tolley, H.; Lee, M. L. *J. Chromatogr. A* **2017**, *1502*, 1–7.

(46) Engler, K. N.; Lemley, A. T. *Environ. Toxicol. Chem.* **2013**, *32* (9), 1962–1968.

(47) Riazi Kermani, F.; Pawliszyn, J. *Anal. Chem.* **2012**, *84* (21), 8990–8995.

(48) Risticevic, S.; Niri, V. H.; Vuckovic, D.; Pawliszyn, J. *Anal. Bioanal. Chem.* **2009**, *393* (3), 781–795.

(49) Bruheim, I.; Liu, X.; Pawliszyn, J. **2003**, *75* (4), 1002–1010.

(50) Qin, Z.; Bragg, L.; Ouyang, G.; Pawliszyn, J. *J. Chromatogr. A* **2008**, *1196–1197* (1–2), 89–95.

(51) Jiang, R. *PhD Thesis* **2013**, *Strategies*.

(52) Contreras, J. A.; Murray, J. A.; Tolley, S. E.; Oliphant, J. L.; Tolley, H. D.; Lammert, S. A.; Lee, E. D.; Later, D. W.; Lee, M. L. *J. Am. Soc. Mass Spectrom.* **2008**, *19* (10), 1425–1434.

(53) Ouyang, Z.; Cooks, R. G. *Annu. Rev. Anal. Chem.* **2009**, *2* (1), 187–214.

(54) Smith, P. A.; Lepage, C. R. J.; Savage, P. B.; Bowerbank, C. R.; Lee, E. D.; Lukacs, M. J. *Anal. Chim. Acta* **2011**, *690* (2), 215–220.

(55) Smith, P. A.; Lepage, C. J.; Lukacs, M.; Martin, N.; Shufutinsky, A.; Savage, P. B. *Int. J. Mass Spectrom.* **2010**, *295* (3), 113–118.

(56) Smith, P. A.; Roe, M. T. A.; Sadowski, C.; Lee, E. D. *J. Occup. Environ. Hyg.* **2011**, *8* (3), 129–138.

(57) Snyder, D. T.; Pulliam, C. J.; Ouyang, Z.; Cooks, R. G. *Anal. Chem.* **2016**, *88* (1), 2–29.

(58) Zhang, M.; Kruse, N. A.; Bowman, J. R.; Jackson, G. P. *Appl. Spectrosc.* **2016**, *70* (5), 785–793.

(59) Visotin, A.; Lennard, C. *Aust. J. Forensic Sci.* **2016**, *48* (2), 203–221.

(60) Gałuszka, A.; Migaszewski, Z. M.; Namieśnik, J. *Environ. Res.* **2015**, *140*, 593–603.

(61) Smith, P. A.; Jackson, C. R.; Savage, P. B.; Bowerbank, C. R.; Lee, E. D.; Lukacs, M. J. *Anal. Chim. Acta* **2011**, *690* (2), 215–220.

(62) Contreras, J. a.; Murray, J. a.; Tolley, S. E.; Oliphant, J. L.; Tolley, H. D.; Lammert, S. a.; Lee, E. D.; Later, D. W.; Lee, M. L. *J. Am. Soc. Mass Spectrom.* **2008**, *19* (10), 1425–1434.

(63) Górecki, T.; Pawliszyn, J.; Belkin, M.; Caruso, J. *Anal. Commun.* **1997**, *34* (10), 275–278.

(64) Risticevic, S.; DeEll, J. R.; Pawliszyn, J. *J. Chromatogr. A* **2012**, *1251*, 208–218.

(65) Risticevic, S.; Lord, H.; Górecki, T.; Arthur, C. L.; Pawliszyn, J. *Nat. Protoc.* **2010**, *5* (1), 122–139.

(66) Chen, Y.; Koziel, J. A.; Pawliszyn, J. *Anal. Chem.* **2003**, *75* (23), 6485–6493.

(67) Risticevic, S.; Chen, Y.; Kudlejova, L.; Vatinno, R.; Baltensperger, B.; Stuff, J. R.; Hein, D.; Pawliszyn, J. *Nat. Protoc.* **2010**, *5* (1), 162–176.

(68) MacCrehan, W.; Moore, S.; Schantz, M. *Anal. Chem.* **2011**, *83* (22), 8560–8565.

(69) MacCrehan, W.; Moore, S.; Schantz, M. *J. Chromatogr. A* **2012**, *1244* (Supplement C), 28–36.

(70) Xie, X.; Truong, T. V.; Murray, J. A.; Contreras, J. A.; Tolley, H. D.; Lee, M. L. *Anal. Methods* **2013**, *5* (22), 6312.

(71) Wang, Y.; O'Reilly, J.; Chen, Y.; Pawliszyn, J. *J. Chromatogr. A* **2005**, *1072* (1), 13–17.

(72) Koziel, J. A.; Martos, P. A.; Pawliszyn, J. *J. Chromatogr. A* **2004**, *1025* (1), 3–9.

(73) Rajkó, R.; Körtvélyesi, T.; Sebők-Nagy, K.; Görgényi, M. *Anal. Chim. Acta* **2005**, *554* (1), 163–171.

(74) Daignault, S. A.; Noot, D. K.; Williams, D. T.; Huck, P. M. *Water Res.* **1988**, *22* (7), 803–813.

(75) Gómez-Ríos, G. A.; Reyes-Garcés, N.; Pawliszyn, J. *J. Sep. Sci.* **2013**, *36* (17), 2939–2945.

(76) Reyes-Garcés, N.; Gómez-Ríos, G. A.; Souza Silva, É. A.; Pawliszyn, J. *J. Chromatogr. A* **2013**, *1300*, 193–198.

(77) Caro, E.; Marce, R. M.; Cormack, P. A. G.; Sherrington, D. C.; Borrull, F. *J. Chromatogr. A* **2003**, *995* (1–2), 233–238.

(78) Chen, L.; Wang, X.; Lu, W.; Wu, X.; Li, J. *Chem. Soc. Rev.* **2016**, *45* (8), 2137–2211.

(79) Szulejko, J. E.; Kim, K.-H. *TRAC-TRENDS Anal. Chem.* **2015**, *64*, 29–41.

(80) Souza-Silva, E. A.; Gionfriddo, E.; Pawliszyn, J. *TrAC - Trends Anal. Chem.* **2015**, *71*, 236–248.

(81) Pang, X.; Lewis, A. C.; Rodenas-Garcia, M. *J. Chromatogr. A* **2013**, *1296* (SI), 93–103.

(82) Liu, C.; Choi, K.; Kang, Y.; Kim, J.; Fobel, C.; Seale, B.; Campbell, J. L.; Covey, T. R.; Wheeler, A. R. *Anal. Chem.* **2015**, *87* (24), 11967–11972.

(83) Herrington, J. S.; Hays, M. D. *Atmos. Environ.* **2012**, *55*, 179–184.

(84) Gorecki, T.; Pawliszyn, J. *F. Anal. Chem. Technol.* **1997**, *1* (5), 277–284.

(85) Reyes-Garces, N.; Gomez-Rios, G. A.; Silva, E. A. S.; Pawliszyn, J. *J. Chromatogr. A* **2013**, *1300*, 193–198.

(86) Stashenko, E. E.; Puertas, M. A.; Martinez, J. R. *Anal. Bioanal. Chem.* **2002**, *373* (1–2), 70–74.

(87) Stashenko, E. E.; Martinez, J. R. *J. Sep. Sci.* **2008**, *31* (11), 2022–2031.

(88) OJALA, M.; KOTIAHO, T.; SIIRILA, J.; SIHVONEN, M. L. *Talanta* **1994**, *41* (8), 1297–1309.

(89) Tsai, S.-W.; Kao, K.-Y. *J. Chromatogr. A* **2006**, *1129* (1), 29–33.

(90) Carrillo, G.; Bravo, A.; Zufall, C. *J. Agric. Food Chem.* **2011**, *59* (9), 4403–4411.

(91) Schmarr, H.-G.; Sang, W.; Ganss, S.; Fischer, U.; Koepp, B.; Schulz, C.; Potouridis, T. *J. Sep. Sci.* **2008**, *31* (19), 3458–3465.

(92) Bourdin, D.; Desauziers, V. *Anal. Bioanal. Chem.* **2014**, *406* (1), 317–328.

(93) Stashenko, E. E.; Puertas, M. A.; Salgar, W.; Delgado, W.; Martinez, J. R. *J. Chromatogr. A* **2000**, *886* (1–2), 175–182.

(94) Niri, V. H.; Mathers, J. B.; Musteata, M. F.; Lem, S.; Pawliszyn, J. *WATER AIR SOIL Pollut.* **2009**, *204* (1–4), 205–213.

(95) Rivero, R. T.; Topiwala, V. *J. Chromatogr. A* **2004**, *1029* (1–2), 217–222.

(96) Martos, P. A.; Pawliszyn, J. *Anal. Chem.* **1998**, *70* (11), 2311–2320.

(97) Koziel, J. A.; Noah, J.; Pawliszyn, J. *Environ. Sci. Technol.* **2001**, *35* (7), 1481–1486.

(98) Farajzadeh, M. A.; Nouri, N.; Khorram, P. *TRAC-TRENDS Anal. Chem.* **2014**, *55*, 14–23.

(99) Ma, J.; Xiao, R.; Li, J.; Li, J.; Shi, B.; Liang, Y.; Lu, W.; Chen, L. *J. Sep. Sci.* **2011**, *34* (12), 1477–1483.

(100) Lee, I.-S.; Tsai, S.-W. *Anal. Chim. Acta* **2008**, *610* (2), 149–155.

(101) Parkinson, D. R.; Bruheim, I.; Christ, I.; Pawliszyn, J. *J. Chromatogr. A* **2004**, *1025* (1), 77–84.

(102) Wang, X.; Chen, R.; Luan, T.; Lin, L.; Zou, S.; Yang, Q. *J. Sep. Sci.* **2012**, *35* (8), 1017–1026.

(103) Llop, A.; Pocurull, E.; Borrull, F. *J. Sep. Sci.* **2011**, *34* (13), 1531–1537.

(104) Jiang, Y.; Ni, Y. *J. Sep. Sci.* **2015**, *38* (3), 418–425.

(105) REINDL, B.; STAN, H. J. *J. Agric. Food Chem.* **1982**, *30* (5), 849–854.

(106) Ho, S. S. H.; Yu, J. Z. *Environ. Sci. Technol.* **2004**, *38* (3), 862–870.

(107) Seyfioglu, R.; Odabasi, M. *Environ. Monit. Assess.* **2007**, *128* (1–3), 343–349.

(108) Gu, H.; Liu, G.; Wang, J.; Aubry, A.-F.; Arnold, M. E. *Anal. Chem.* **2014**, *86* (18), 8959–8966.

(109) Koziel, J.; Jia, M.; Pawliszyn, J. *Anal. Chem.* **2000**, *72* (21), 5178–5186.

(110) Casaburi, A.; Piombino, P.; Nychas, G.-J.; Villani, F.; Ercolini, D. *FOOD Microbiol.* **2015**, *45* (A), 83–102.

(111) Bai, Z.; Pilote, A.; Sarker, P. K.; Vandenberg, G.; Pawliszyn, J. *Anal. Chem.* **2013**, *85* (4), 2328–2332.

(112) Gionfriddo, E.; Souza-Silva, E. A.; Pawliszyn, J. *Anal. Chem.* **2015**.

(113) Aranda-Rodriguez, R.; Cabecinha, A.; Harvie, J.; Jin, Z.; Marchand, A.; Tardif, R.; Nong, A.; Haddad, S. *J. Chromatogr. B* **2015**, *992*, 76–85.

(114) Souza-Silva, É. A.; Pawliszyn, J. *J. Agric. Food Chem.* **2015**, *63* (18), 4464–4477.

(115) Roberts, D. D.; Pollien, P.; Milo, C. *J. Agric. Food Chem.* **2000**, *48* (6), 2430–2437.

(116) Bicchi, C.; Iori, C.; Rubiolo, P.; Sandra, P. *J. Agric. Food Chem.* **2002**, *50* (3), 449–459.

(117) Sampson, M. M.; Chambers, D. M.; Pazo, Y.; Moliere, F.; Blount, B. C.; Watson, C. H. **2014**.

(118) Huang, J.; Deng, H.; Song, D.; Xu, H. *Anal. Chim. Acta* **2015**, *878*, 102–108.

(119) Jiang, R.; Cudjoe, E.; Bojko, B.; Abaffy, T.; Pawliszyn, J. *Anal. Chim. Acta* **2013**, *804*, 111–119.

(120) Pawliszyn, J.; Vuckovic, D.; Risticevic, S. In *Handbook of Solid Phase Microextraction*; 2012; pp 455–478.

(121) The European Parliament and the Council of the European Union. *Off. J. Eur. Union* **2008**, *L348*, 84–97.

(122) Barcelo, D. *J. Chromatogr.* **1993**, *643* (1–2), 117–1436.

(123) Hennion, M. C.; Pichon, V.; Barceĺ, D. *TrAC - Trends Anal. Chem.* **1994**, *13* (9), 361–372.

(124) Dolan, T.; Howsam, P.; Parsons, D. J.; Whelan, M. J. *Environ. Sci. Technol.* **2013**, *47* (10), 4999–5006.

(125) Piri-Moghadam, H.; Ahmadi, F.; Pawliszyn, J. *TrAC - Trends Anal. Chem.* **2016**, *85*, 133–143.

(126) Arthur, C.; Pawlyszin, J. *Anal. Chem.* **1990**, *62* (19), 2145–2148.

(127) Piri-Moghadam, H.; Lendor, S.; Pawliszyn, J. *Anal. Chem.* **2016**, *88*, 12188–12195.

(128) Piri-Moghadam, H.; Ahmadi, F.; Gómez-Ríos, G. A.; Boyaci, E.; Reyes-Garcés, N.; Aghakhani, A.; Bojko, B.; Pawliszyn, J. *Angew. Chemie - Int. Ed.* **2016**, *55* (26), 7510–7514.

(129) Gionfriddo, E.; Souza-Silva, E. A.; Pawliszyn, J. *Anal. Chem.* **2015**, *87* (16), 8448–8456.

(130) Risticevic, S.; Souza-Silva, E. a.; DeEll, J. R.; Cochran, J.; Pawliszyn, J. *Anal. Chem.* **2016**, *88* (2), 1266–1274.

(131) Mirabelli, M. F.; Wolf, J. C.; Zenobi, R. *Anal. Chem.* **2016**, *88* (14), 7252–7258.

(132) Nacham, O.; Clark, K. D.; Anderson, J. L. *Anal. Chem.* **2016**, *88* (15), 7813–7820.

(133) Xu, S.; Shuai, Q.; Pawliszyn, J. *Anal. Chem.* **2016**, *88* (18), 8936–8941.

(134) Bagheri, H.; Piri-Moghadam, H.; Naderi, M. *TrAC - Trends Anal. Chem.* **2012**, *34*, 126–138.

(135) Gionfriddo, E.; Boyacl, E.; Pawliszyn, J. *Anal. Chem.* **2017**, *89* (7), 4046–4054.

(136) Piri-Moghadam, H.; Alam, M. N.; Pawliszyn, J. *Anal. Chim. Acta* **2017**.

(137) Bagheri, H.; Bayat, P.; Piri-moghadam, H. *J. Chromatogr. A* **2013**, *1318*, 58–64.

(138) Li, J.; Wang, Y.-B.; Li, K.-Y.; Cao, Y.-Q.; Wu, S.; Wu, L. *TrAC Trends Anal. Chem.* **2015**, *72*, 141–152.

(139) Bagheri, H.; Piri-Moghadam, H. *TrAC - Trends Anal. Chem.* **2015**, *73*, 64–80.

(140) Bojko, B.; Reyes-Garcés, N.; Bessonneau, V.; Goryński, K.; Mousavi, F.; Souza Silva, E. a.; Pawliszyn, J. *TrAC Trends Anal. Chem.* **2014**, *61*, 168–180.

(141) Vuckovic, D.; Risticevic, S.; Pawliszyn, J. *Angew. Chem. Int. Ed. Engl.* **2011**, *50* (25), 5618–5628.

(142) Qin, Z.; Bragg, L.; Ouyang, G.; Niri, V. H.; Pawliszyn, J. *J. Chromatogr. A* **2009**, *1216* (42), 6979–6985.

(143) Ouyang, G.; Chen, Y.; Pawliszyn, J. *J. Chromatogr. A* **2006**, *1105* (1–2 SPEC. ISS.), 176–179.

(144) Ouyang, G.; Cui, S.; Qin, Z.; Pawliszyn, J. *Anal. Chem.* **2009**, *81* (14), 5629–5636.

(145) Almeida, A. M.; Castel-Branco, M. M.; Falcão, A. C. *J. Chromatogr. B* **2002**, *774* (2), 215–222.

(146) Ouyang, G.; Pawliszyn, J. *Anal. Chim. Acta* **2008**, *627* (2), 184–197.

(147) Koel, M. *Green Chem.* **2016**, *18* (4), 923–931.

(148) Tobiszewski, M.; Tsakovski, S.; Simeonov, V.; Namieśnik, J. *Green Chem.* **2013**, *15* (6), 1615.

(149) Pena-Pereira, F.; Kloskowski, A.; Namieśnik, J. *Green Chem.* **2015**, *17* (7), 3687–3705.

(150) Mokhtar, S. U.; Chin, S.-T.; Vijayaraghavan, R.; MacFarlane, D. R.; Drummer, O. H.; Marriott, P. J. *Green Chem.* **2015**, *17* (1), 573–581.

(151) Reyes-Garcés, N.; Gionfriddo, E.; Gómez-Ríos, G. A.; Alam, M. N.; Boyacı, E.; Bojko, B.; Singh, V.; Grandy, J.; Pawliszyn, J. *Anal. Chem.* **2018**, *90* (1), 302–360.

(152) Naccarato, A.; Gionfriddo, E.; Sindona, G.; Tagarelli, A. *J. Chromatogr. A* **2014**, *1338*, 164–173.

(153) Mester, Z.; Sturgeon, R. E. *Sample Preparation for Trace Element Analysis*; Comprehensive Analytical Chemistry; Elsevier Science, 2003.

(154) Ahmadi, F.; Sparham, C.; Boyacı, E.; Pawliszyn, J. *Environ. Sci. Technol.* **2017**, *51* (7), 3929–3937.

(155) Reyes-Garcés, N.; Bojko, B.; Pawliszyn, J. *J. Chromatogr. A* **2014**, *1374*, 40–49.

(156) Poole, C. F. *Principles and Practice of Solid-Phase Extraction*; Elsevier, 2012; Vol. 2.

(157) Moret, S.; Marega, M.; Conte, L. S. *4 . 14 Sample Preparation Techniques for the Determination of Some Food Contaminants (Polycyclic Aromatic Hydrocarbons , Mineral Oils and Phthalates)*; Elsevier, 2012; Vol. 4.

(158) Kataoka, H. *Column-Switching Sample Preparation Applications of Online SPE with Column Switching*; Elsevier, 2012; Vol. 2.

(159) Eisert, R.; Levsen, K. *J. Am. Soc. Mass Spectrom.* **1995**, *6* (11), 1119–1130.

(160) Gómez-Ríos, G. A.; Pawliszyn, J. *Angew. Chem. Int. Ed. Engl.* **2014**, *53* (52), 14503–14507.

(161) Gómez-Ríos, G. A.; Liu, C.; Tascon, M.; Reyes-Garcés, N.; Arnold, D. W.; Covey, T. R.; Pawliszyn, J. *Anal. Chem.* **2017**, *89* (7), 3805–3809.

(162) Gómez-Ríos, G. A.; Pawliszyn, J. *Chem. Commun.* **2014**, *50* (85), 12937–12940.

(163) Gómez-Ríos, G. A.; Gionfriddo, E.; Poole, J.; Pawliszyn, J. *Anal. Chem.* **2017**, *89* (13), 7240–7248.

(164) Poole, J. J.; Grandy, J. J.; Yu, M.; Boyaci, E.; Gómez-Ríos, G. A.; Reyes-Garcés, N.; Bojko, B.; Heide, H. Vander; Pawliszyn, J. *Anal. Chem.* **2017**, *89* (15), 8021–8026.

(165) Bessonneau, V.; Boyaci, E.; Maciazek-Jurczyk, M.; Pawliszyn, J. *Anal. Chim. Acta* **2015**, *856*, 35–45.

(166) Bouvier, E. S. P.; Meirowitz, R. E.; McDonald, P. D. Google Patents 1999.

(167) Gomez-Rios, G. A.; Reyes-Garces, N.; Pawliszyn, J. *J. Sep. Sci.* **2013**, *36* (17, SI), 2939–2945.

(168) Weinberg, H. S. *Philos. Trans. R. Soc. A Math. Phys. Eng. Sci.* **2009**, *367* (1904), 4097–4118.

(169) Poole, J. J.; Gomez-Rios, G. A.; Boyaci, E.; Reyes-Garcés, N.; Pawliszyn, J. *Environ. Sci. Technol.* **2017**, acs.est.7b03867.

(170) Xu, J.; Chen, G.; Huang, S.; Qiu, J.; Jiang, R.; Zhu, F.; Ouyang, G. *Trends Anal. Chem.* **2016**, *85*, 26–35.

(171) Baross, J. A.; Hoffman, S. E. *Orig. life Evol. Biosph.* **1985**, *15* (4), 327–345.

(172) Konn, C.; Charlou, J. L.; Donval, J. P.; Holm, N. G.; Dehairs, F.; Bouillon, S. *Chem. Geol.* **2009**, *258* (3–4), 299–314.

(173) Kato, S.; Nakamura, K.; Toki, T.; Ishibashi, J. I.; Tsunogai, U.; Hirota, A.; Ohkuma, M.; Yamagishi, A. *Front. Microbiol.* **2012**, *3* (MAR), 1–14.

(174) Vuckovic, D.; Pawliszyn, J. *Anal. Chem.* **2011**, *83* (6), 1944–1954.

(175) Olivon, F.; Grelier, G.; Roussi, F.; Litaudon, M.; Touboul, D. *Anal. Chem.* **2017**, *89* (15), 7836–7840.

(176) Mirnaghi, F. S.; Chen, Y.; Sidisky, L. M.; Pawliszyn, J. *Anal. Chem.* **2011**, *83* (15), 6018–6025.

(177) Musteata, M. L.; Musteata, F. M.; Pawliszyn, J. *Anal. Chem.* **2007**, *79* (18), 6903–6911.

(178) Strittmatter, N.; Düring, R.-A.; Takáts, Z. *Analyst* **2012**, *137* (17), 4037.

(179) Mirnaghi, F. S.; Mousavi, F.; Rocha, S. M.; Pawliszyn, J. *J. Chromatogr. A* **2013**, *1276*, 12–19.

(180) Bina, B.; Amin, M. M.; Rashidi, A.; Pourzamani, H. *Water Resour.* **2014**, *41* (6), 719–727.

(181) Reemtsma, T. *Rapid Commun. Mass Spectrom.* **2000**, *14* (17), 1612–1618.

(182) Asimakopoulos, A. G.; Ajibola, A.; Kannan, K.; Thomaidis, N. S. *Sci. Total Environ.* **2013**, *452–453*, 163–171.

(183) Aerts, L. A. M.; Van Soest, R. W. M. *Mar. Ecol. Prog. Ser.* **1997**, *148* (1–3), 125–134.

(184) Porter, J. W.; Targett, N. M. *Biol. Bull.* **1988**, *175* (2), 230–239.

(185) Thakur, N. L.; Singh, A. In *Marine Sponges: Chemicobiological and Biomedical Applications*; Pallela, R., Ehrlich, H., Eds.; Springer India: New Delhi, 2016; pp 37–52.

(186) Worley, B.; Powers, R. *Curr. Metabolomics* **2016**, *4* (2), 97–103.

(187) K Trivedi, D. *J. Chromatogr. Sep. Tech.* **2012**, *3* (6).

Appendix A Storage stability of PS/DVB standard gas generating vials

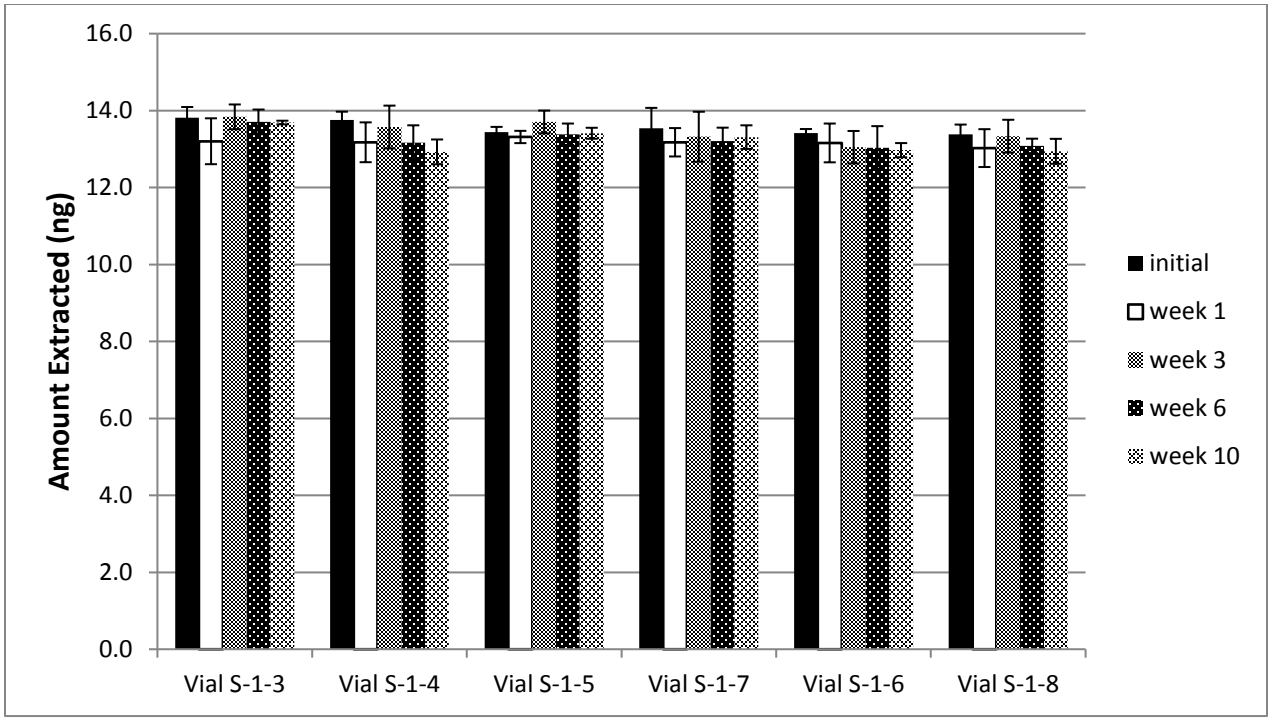

Figure A.1 10 week stability of benzene stored in a silicone oil-PS/DVB gas generating vials; extractions were performed at 35ºC with a DVB/PDMS fiber for 1 minute

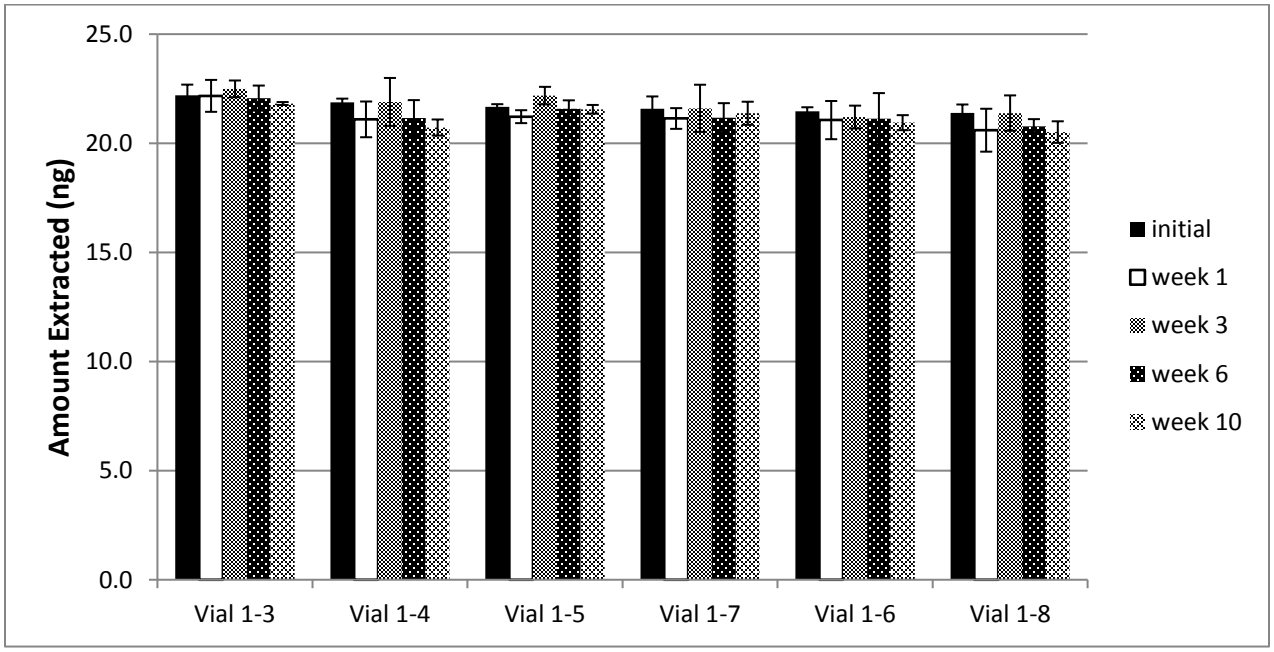

Figure A.2 10 week stability of 2- pentanone stored in a silicone oil-PS/DVB gas generating vials; extractions were performed at 35ºC with a DVB/PDMS fiber for 1 minute

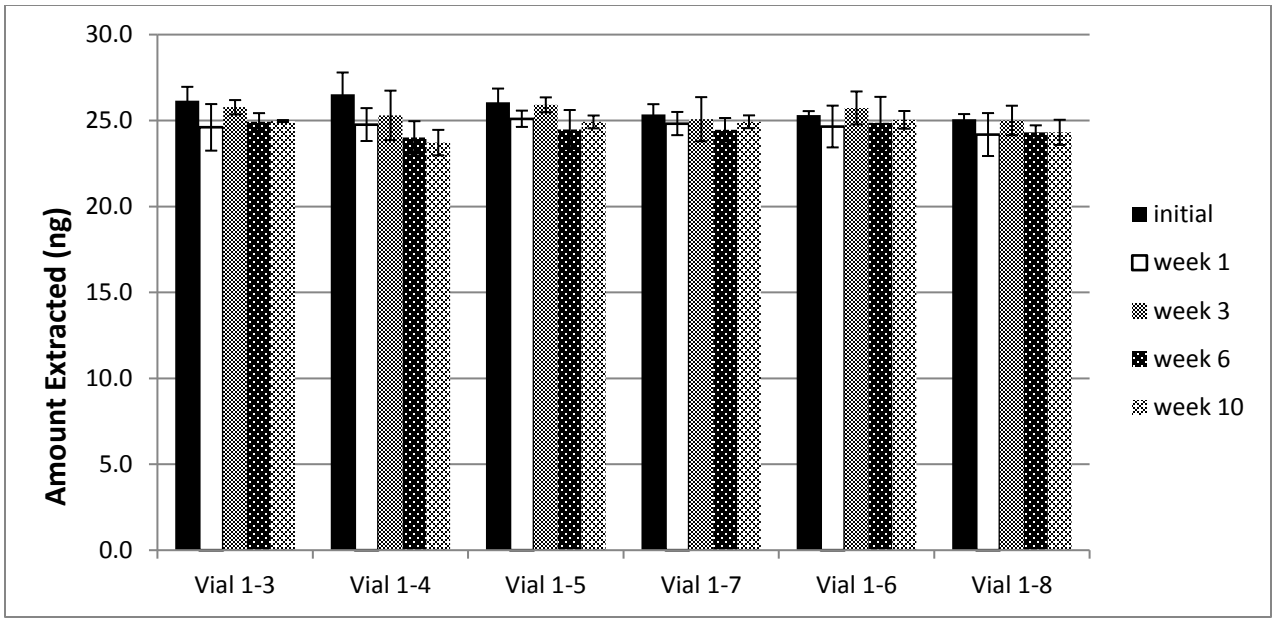

Figure A.3 10 week stability of 1-nitropropane stored in a silicone oil-PS/DVB gas generating vials; extractions were performed at 35ºC with a DVB/PDMS fiber for 1 minute

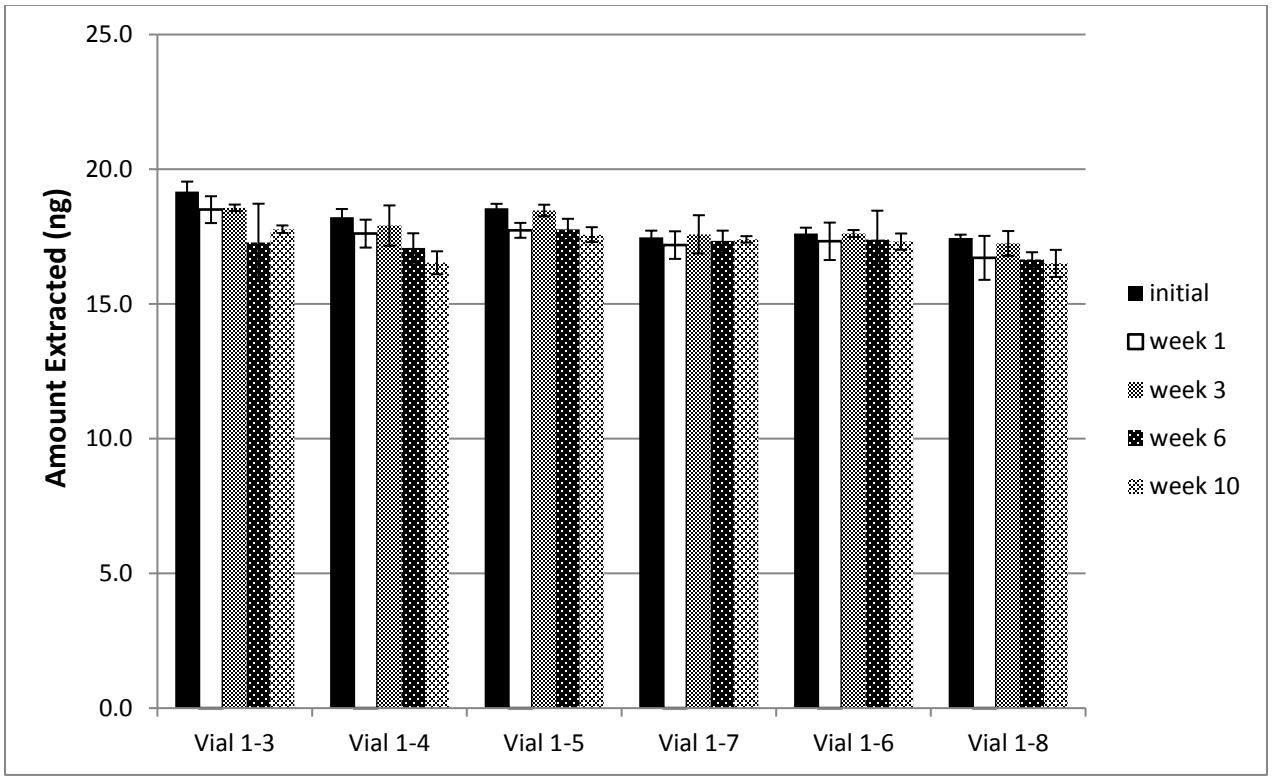

Figure A.4 10 week stability of pyridine stored in a silicone oil-PS/DVB gas generating vials; extractions were performed at 35ºC with a DVB/PDMS fiber for 1 minute

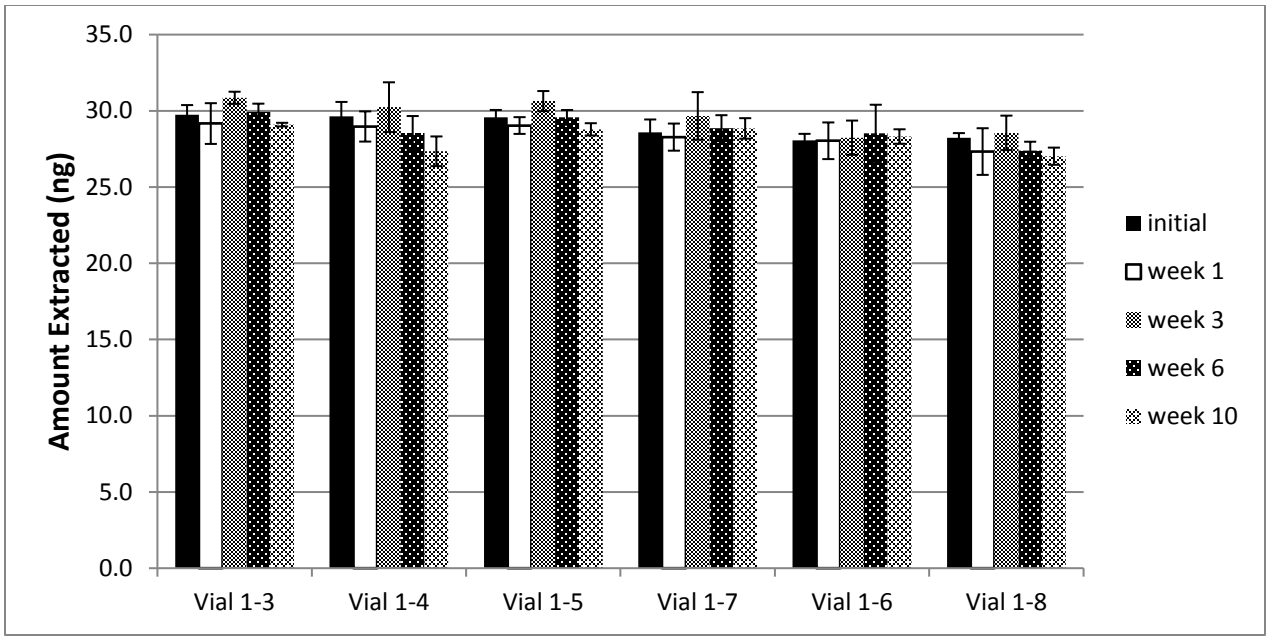

Figure A.5 10 week stability of 1-pentanol stored in a silicone oil-PS/DVB gas generating vials; extractions were performed at 35ºC with a DVB/PDMS fiber for 1 minute

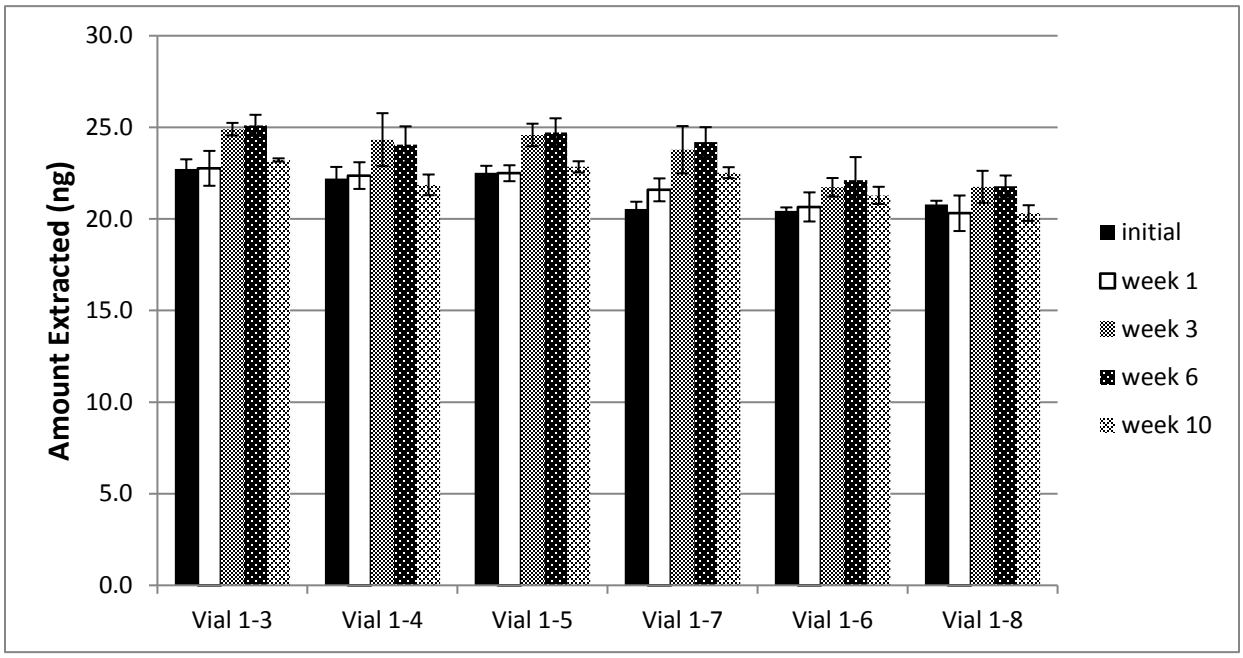

Figure A.6 10 week stability of octane stored in a silicone oil-PS/DVB gas generating vials; extractions were performed at 35 ºC with a DVB/PDMS fiber for 1 minute

Appendix B: Multivariate separation of significant features from coral and sponge study with preliminary exact mass matching of significant features.

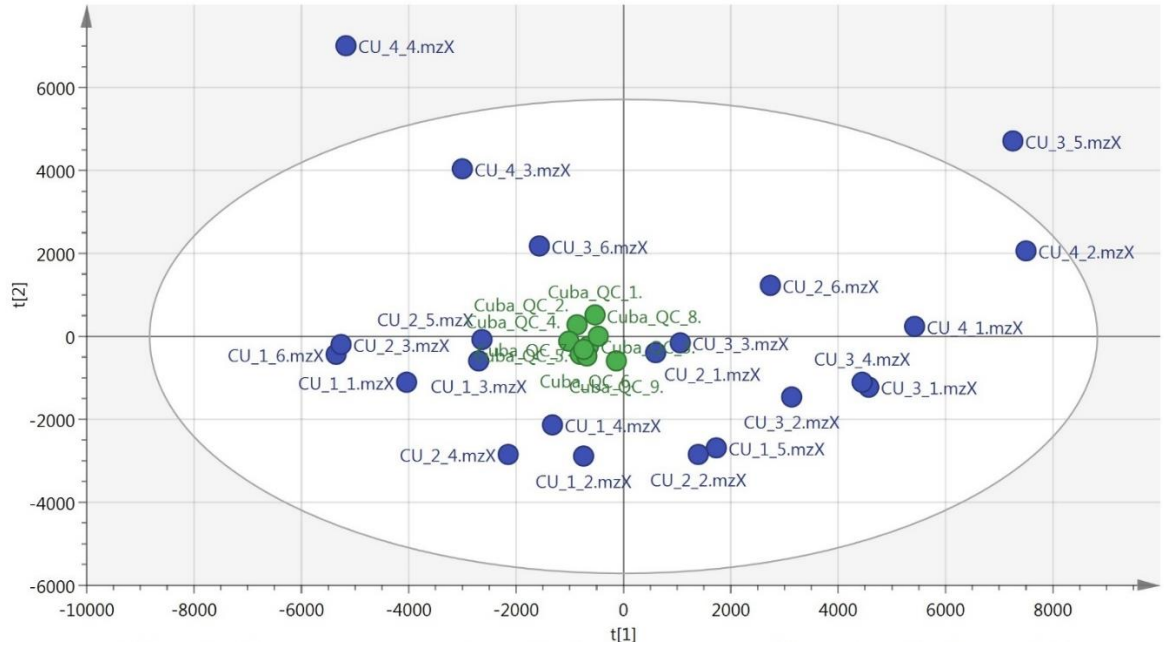

Figure B.1: Multivariate separation (PCA) of replicate samples corresponding to extractions from the sponge sample, 2 different Coral samples, and the control sampler. Clustering Pool QC data (GREEN) indicates stable instrument performance throughout the experiment Samples were run on the PFP column and ionized in positive mode. Separation is based on the exact mass peak height

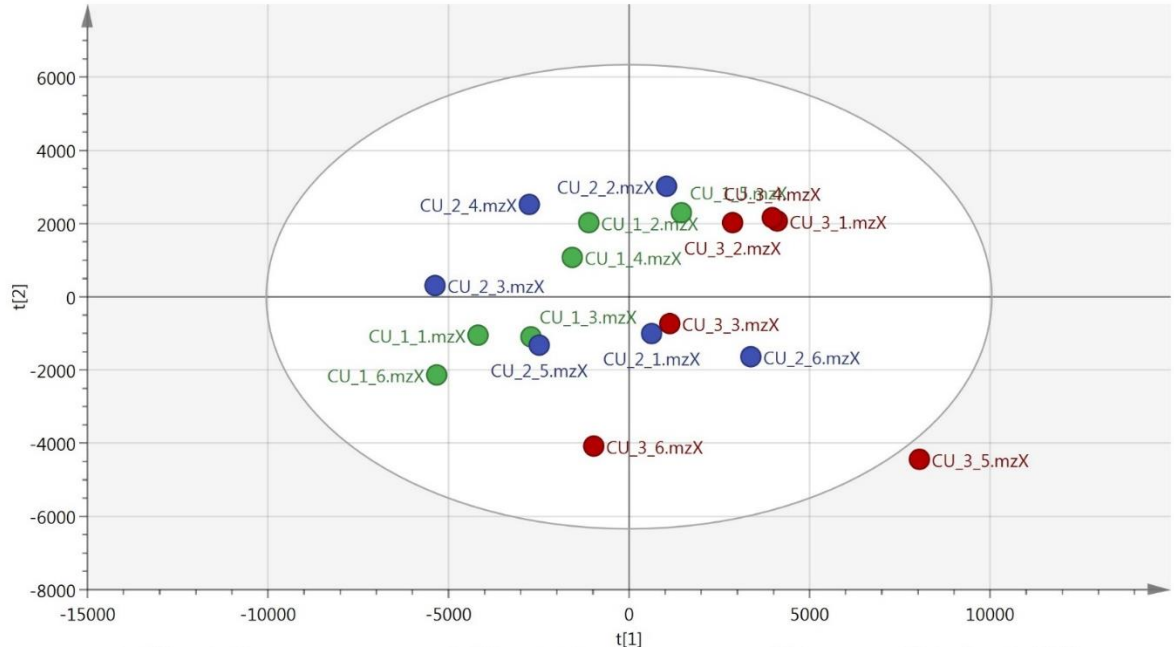

Figure B.2: Multivariate separation (PCA) of replicate samples corresponding to extractions from the sponge sample (RED), 2 different coral samples (BLUE and GREEN). Mild separation of the sponge and coral samples could be observed on the first principle component, t[1]. Samples were run on the PFP column and ionized in positive mode. Separation is based on the exact mass peak height

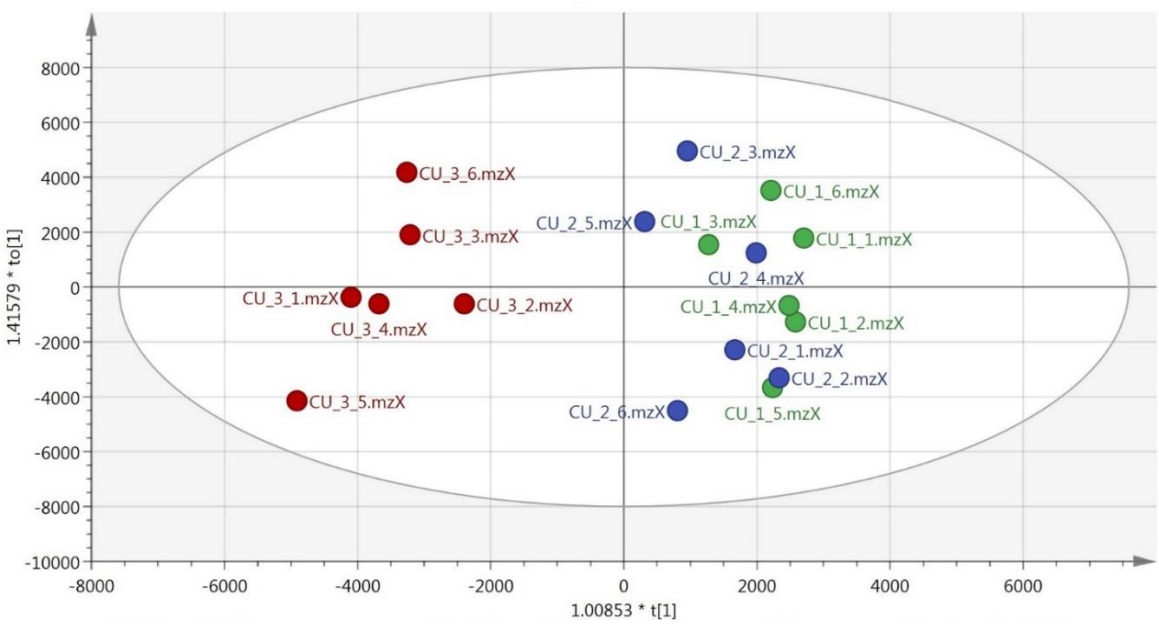

Figure B.3: Classed multivariate separation (OPLS-DA) of replicate samples corresponding to extractions from the sponge sample (RED) and 2 replicate Coral samples (BLUE and GREEN). Samples were run on the PFP column and ionized in positive mode. Separation is based on the exact mass peak height

Table B.1 Preliminary exact mass matching of features highlighted in BLUE from the Coral samples (CU_1_X, CU_2_X) in Figure 7.10. PFP-positive mode run. H+ Na+ NH4+ adducts were searched using METLIN on-line database and a mass accuracy +/-5 ppm

Feature ID	M/Z	P-value	Online Database Identification (Metlin) (Exact Mass only 5ppm)
1683	101.0532m/z	-0.818385	Diazomethyl-dimethylsilane (H+) or 3-Silylprop-2-enenitrile (NH4+)
1702	108.9489m/z	-0.80795	Fe(CN)2 (H+)
1789	138.5108m/z	-0.865418	No database match
1842	152.0362m/z	-0.675454	No database match
1848	153.0329m/z	-0.653664	Methylamino-methylimino-methanesulphonic acid or Imidazolidine-2-sulfonic acid (H+) or 1,2,5-Oxathiazolidine-4-carboxylic acid or Carbamic acid, sulfinyl-, ethyl ester or Propanoic acid, 3-(nitrosothio)- (NH4+)
1890	169.046m/z	-0.697574	28 possibilites: (23 H+), (4 NH4+) (1 Na+)
1943	197.041m/z	-0.697143	19 possibilites: (10 H+), (8 NH4+), (1Na+)
1983	218.984m/z	-0.668145	31 possibilities (12H+) (4 NH4+) (17 Na+) Sesquimustard (H+)
2033	241.9999m/z	-0.621784	3-chloro-2-fluoro-5-trifluoromethyl-benzamide (H+) or 6-Methyl-2,4-dioxo-1,2,3,4-tetrahydropyrimidine-5-sulfonyl chloride (NH4+) or Phosphoric triamide, N,N-bis(2-chloroethyl)- or Methyl 2-chloro-5-fluoro-6-methoxypyridine-3-carboxylate or 6-Isothiocyanato-2,3-dihydrophthalazine-1,4-dione (Na+)
2081	267.0133m/z	-0.809256	113 possibilities (49 H+), (31 NH4+), (33 Na+)
2320	532.895m/z	-0.638466	4(3H)-Quinazolinone, 6,8-dibromo-3-(2-chlorophenyl)-2-((propylsulfonyl)methyl)- (H+)
2347	566.8888m/z	-0.609132	2-tert-Butyl-4,6-dintro-2',4',6'-tribromodiphenylamine (NH4+)
2367	600.8825m/z	-0.609794	No database match
2380	634.8763m/z	-0.628868	No database match
2395	668.87m/z	-0.611834	No database match
2408	702.8638m/z	-0.636895	No database match
2434	770.8512m/z	-0.647258	No database match
2454	838.8387m/z	-0.639869	Cholesteryl triacontanoate (NH4+)
2468	906.8263m/z	-0.646205	No database match

Table B.2 Preliminary exact mass matching of features highlighted in RED from the Sponge samples (CU_3_X) in Figure 7.10. PFP-positive mode run. H+ Na+ NH4+ adducts were searched using METLIN on-line database and a mass accuracy +/-5 ppm

Feature ID	M/Z	P-value	Online Database Identification Metlin Exact Mass only (adduct)
615	151.0353m/z	0.6915	27 possibilities (8 H+), (16 NH4+), (3 Na+)
2826	148.976m/z	0.335381	(3-Chlorocyclopenta-2,4-dien-1-ylidene)methanone (Na+ only)
2882	147.9898m/z	0.733142	Dimethyl phosphate (Na+ only)
3848	104.5235m/z	0.666493	No database match
3850	107.9671m/z	0.767511	Thiocyanic acid, chloromethyl ester or Cyano(oxo)sulfanylphosphanium (H+)
3947	243.9421m/z	0.84686	2-Bromo-4-methoxy-1,3-benzothiazole (or similar isomer H+)
3989	126.9984m/z	0.93165	2-Chloroethyl methyl sulfoxide or Propane-1-sulfinyl chloride (H+)

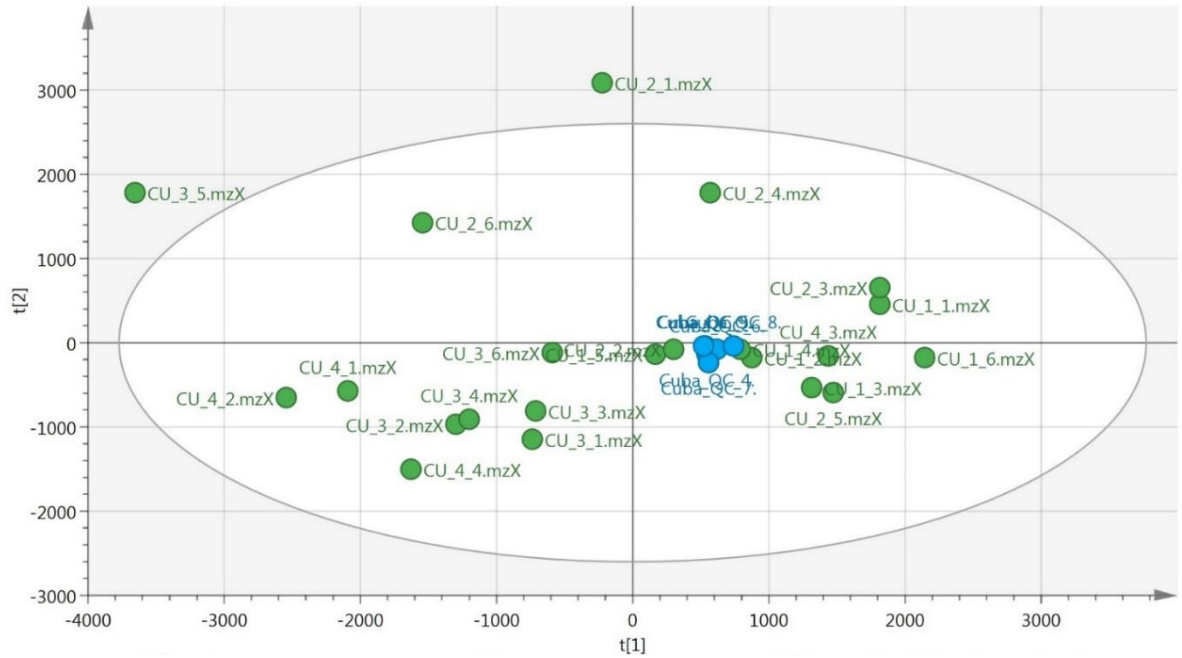

Figure B.4: Multivariate separation (PCA) of replicate samples corresponding to extractions from the sponge sample, 2 different Coral samples, and the control sampler. Clustering Pool QC data (BLUE) indicates stable instrument performance throughout the experiment Samples were run on the PFP column and ionized in negative mode. Separation is based on the exact mass peak height

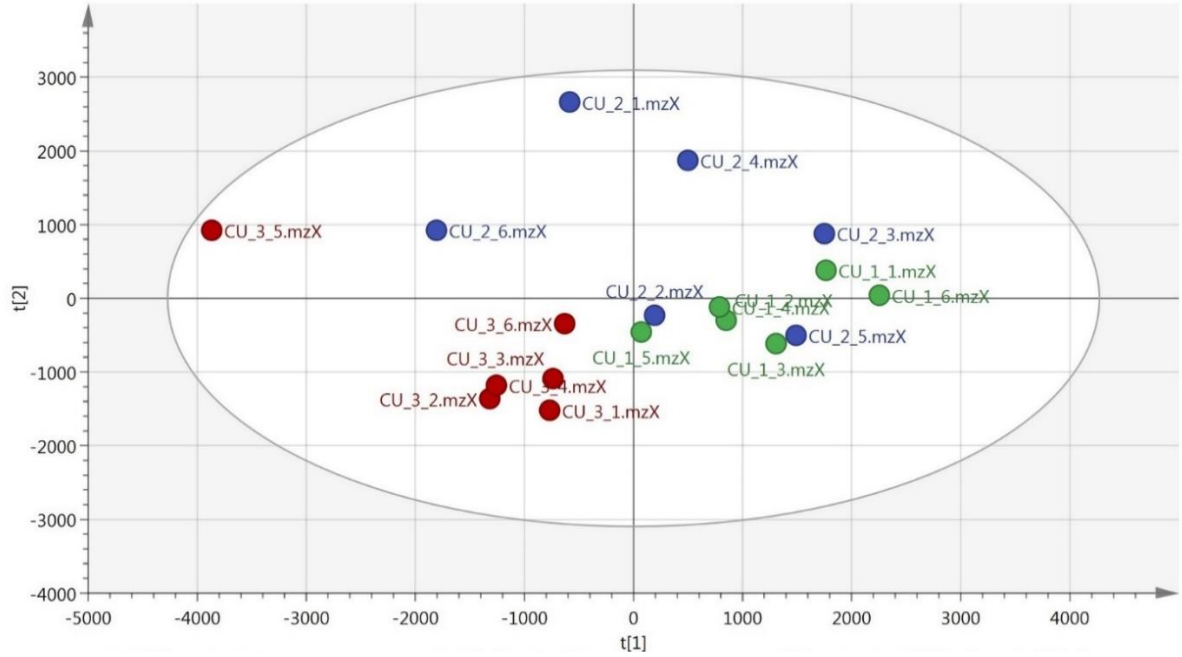

Figure B.5: Multivariate separation (PCA) of replicate samples corresponding to extractions from the sponge sample (RED), 2 different coral samples (BLUE and GREEN). With the exception of screw 3_5 reasonably good clustering of the could be in the negative quadrant of both the first and second principal component, Samples were run on the PFP column and ionized in negative mode. Separation is based on the exact mass peak height

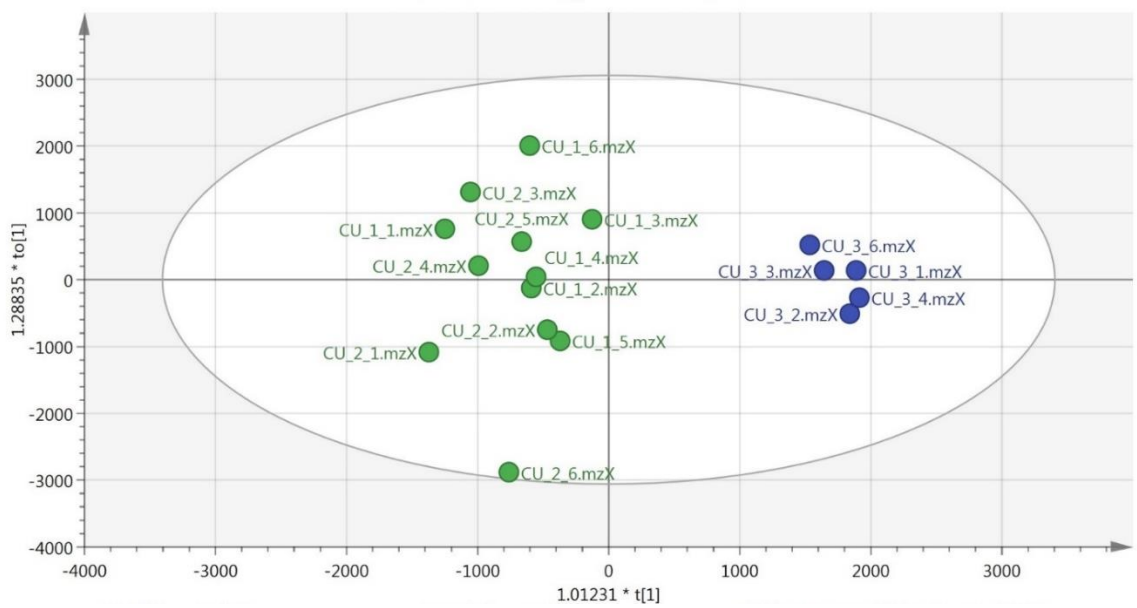

Figure B.6: Classed multivariate separation (OPLS-DA) of replicate samples corresponding to extractions from the sponge sample (BLUE) and 2 different Coral samples (GREEN). Samples were run on the PFP column and ionized in negative mode. Separation is based on the exact mass peak height

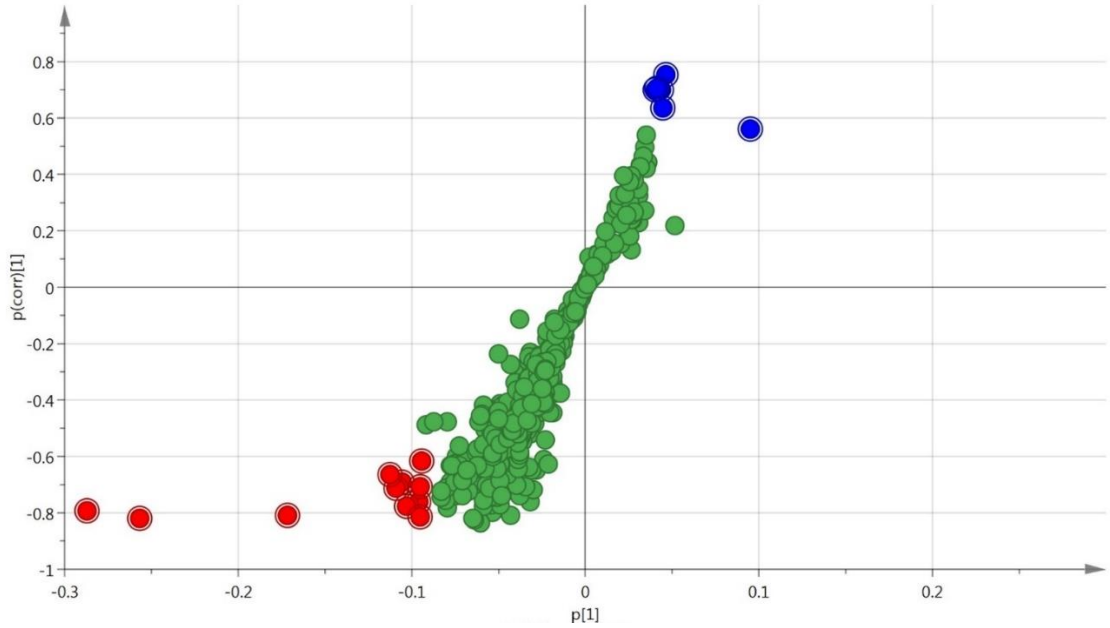

Figure B.7: S-Plot generated from the classed multivariate separation shown in Figure B.6 highlighting features in BLUE being statistically larger in the coral samples and features in RED being statistically larger in sponge samples.

Table B.3 Preliminary exact mass matching of features highlighted in RED from the Sponge samples (CU_3_X) in Figure B.6. PFP-negative mode run. H- Cl- adducts were searched using METLIN on-line database and a mass accuracy +/-5 ppm

ID	M/Z	Identity
1548	102.9561m/z	Phosphoric trifluoride (H-)
1557	114.988m/z	Phosphorohydrazidic difluoride (H-) or Carbonohydrazonic difluoride (Cl-)
1568	130.983m/z	Phosphinic fluoride, dimethyl- or 2-Chloro-1-fluoropropane or N,N-Difluorourea or 2-Chloro-2-fluoropropane (Cl-)
1596	158.9781m/z	20 metabolites all similar to: Benzal chloride (H-) or Bicyclo[4.1.0]hepta-1,3,5-triene, 3-chloro- or 4-Chloro-3-fluorobutan-2-one (Cl-
1760	288.9372m/z	81 possibilites (11 H-, 70 Cl-)
2078	404.9156m/z	1,8-Anthracenedisulfonic acid, 9,10-dihydro-9,10-dioxo- or 1,2-Bis(trichlorosilyl)decane or Bis(3-nitrophenyl)iodanium chloride (H-) or (7 possibilites Cl- such as 9H-Purine, 6-chloro-2-iodo-9-(phenylmethyl)- or 1-(4-bromophenyl)sulfonyl-3-phenylthiourea
2106	434.873m/z	Cervisol (H-)
2157	500.9211m/z	C10H13BaN4O7PS (PUBCHEM_54603515 H-)
2391	808.8366m/z	Cuprate(3-), [5-(acetylamino)-4-(hydroxy-.kappa.O)-3-[[2-(hydroxy-.kappa.O)-5-methyl-4-[[2-(sulfooxy)ethyl]sulfonyl]phenyl]azo-.kappa.N1]-2,7-naphthalenedisulfonato(5-)]-, trisodium (H-)
2423	894.8441m/z	Sampler body bleed (long chain polyfluoro compound)
2450	962.8316m/z	No database match

Table B.4 Preliminary exact mass matching of features highlighted in BLUE from the Coral samples (CU_1_X, CU_2_X) in Figure B.6. PFP-negative mode run. H- Cl- adducts were searched using METLIN on-line database and a mass accuracy +/-5 ppm

Var-ID (Primary)	**Var-ID (M/Z)**	**Identity**
1858	312.1731m/z	90 possibilities (31 H-, 59 Cl-)
2670	154.8981m/z	Sulfurous acid, potassium salt (Cl- unlikely!)
3316	198.9229m/z	1,2,4-Oxadiazole, 3-methyl-5-(trichloromethyl)- or 3-(Chloromethyl)-4-(dichloromethyl)-1,2,5-oxadiazole (H-) or 16 possibilities Cl-
3320	304.9145m/z	pd 150606 (H-) or 7 possibilities Cl- such as 6-Bromo-3-methyl-2-thioxo-2,3-dihydroquinazolin-4(1H)-one
3324	422.2312m/z	N-Palmitoyl-L-serine phosphoric acid or similar (H-)
3335	429.7601m/z	No database match

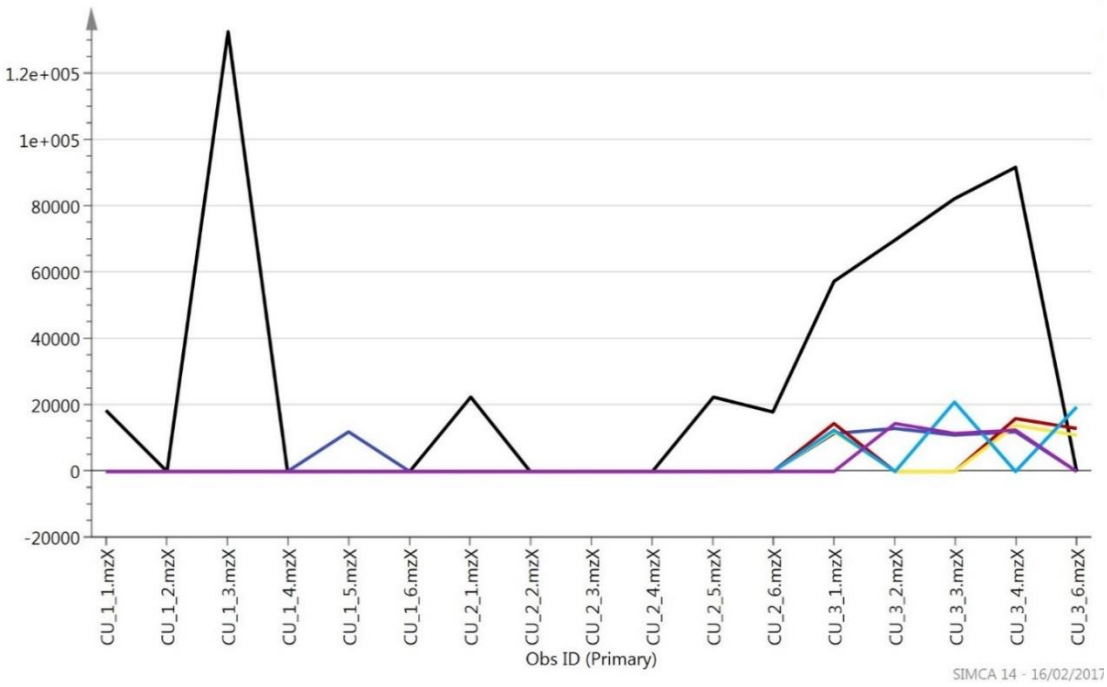

Figure B.7: Distribution plot of significant features highlighted in RED from the Sponge samples (CU_3_X) in Figure B.6. Contrary to the Coral samples, those features detected at the sponge were nearly unique to that sample

Appendix C: Multivariate separation of significant features hydrothermal vent study with the preliminary exact mass matching of significant features.

Table C.1 Preliminary exact mass matching of features highlighted in BLUE from the vent samples of the El Gordo ROV dive in Figure 7.16. PFP-Positive mode run. All adducts were considered when using the METLIN on-line database and a mass accuracy +/-5 ppm was used

Feature ID	M/Z	VIP-value	Online Database Identification (Metlin) (Exact Mass only, 5ppm)
721	128.0195(m/z)	7.51806	S-Methyl methanesulfinothioate (NH4)+
2060	167.0131(m/z)	3.67644	Bergaptol or similar $[M+H-2H2O]^+$
2190	156.0144(m/z)	2.86941	Cytosine $[M+2Na-H]^+$ or Ciprofibrate $[M+H+Na]^{2+}$
46	128.0196(m/z)	2.7863	S-Methyl methanesulfinothioate (NH4)+
2031	105.0037(m/z)	1.65938	Urea $[M+2Na-H]^+$ or N-nitrosomethanamine $[M+2Na-H]^+$
2047	146.0301(m/z)	1.57939	Glucoberteroin (3H3+) unlikely adduct
723	129.5602(m/z)	1.50513	No database match
2034	110.009(m/z)	1.47242	No database match
2041	129.0228(m/z)	1.44501	Asparaginyl-Glutamate (2Na2+) or Glutamyl-Asparagine (2Na2+)
2055	153.033(m/z)	1.41326	Glutamyl-Asparagine (2Na 2+)
2069	174.0251(m/z)	1.35896	S-Propyl thiosulfate or 2-(Methylthio)ethanesulfonate (NH4+)
2054	152.0363(m/z)	1.32046	3,4-Dehydrothiomorpholine-3-carboxylate (Li+)
1604	178.0563(m/z)	1.31237	sulfonated amino acid, multiple possible (Gly, Gly Cys, Pro) H+Na 2+
1533	130.0236(m/z)	1.25798	N-(7-Mercaptoheptanoyl)threonine 3-O-phosphate (3H3+)
1773	839.8423(m/z)	1.22073	No database match
2074	192.0622(m/z)	1.18021	Hydroxydopamine, Pyridoxine or similar multiple possibility (Na+)
1558	151.0091(m/z)	1.14841	No database match
1593	168.0163(m/z)	1.14588	1-[4,9-Dihydro-2-(methylthio)-1,3-thiazino[6,5-b]indol-4-yl]-2-propanone $[M+2Na]^{2+}$
1600	175.0258(m/z)	1.14225	1-(Ethylthio)ethyl methyl disulfide (Li+)
1981	171.0437(m/z)	1.12918	3-Sulfinoalanine (NH4+)
2063	169.0461(m/z)	1.11257	S,S,S,-tributylphosphorotrithioate (H+Na+)2+
2042	130.0171(m/z)	1.10603	Monomethyl sulfate $[M+NH4]^+$
1555	148.9759(m/z)	1.0856	Alpha-Chlorohydrin (K+), or Dimethyl hydrogen phosphite K+
2086	241.9647(m/z)	1.07795	No database match
1552	147.0333(m/z)	1.07209	No database match
1952	199.0387(m/z)	1.05866	Naphthalic anhydride (H+) or Thiocyclam (NH4+)
1671	255.9445(m/z)	1.02783	No database match
2040	129.0203(m/z)	1.02233	Thiocarbohydrazide (Na+) or Mercaptolactic acid (M+LI+)
2048	147.0309(m/z)	1.01825	Very large number of possibilities
1932	102.5359(m/z)	1.00399	No database match

Table C.2 Preliminary exact mass matching of features highlighted in RED from the vent samples of the El Gordo ROV dive in Figure 7.16. PFP-Positive mode run. All adducts were considered when using the METLIN on-line database and a mass accuracy +/-5 ppm was used

Feature ID	M/Z	VIP-value	Online Database Identification (Metlin) (Exact Mass only, 5ppm)
1705	332.9644(m/z)	0.97569	No database match
1948	194.0598(m/z)	0.94116	A peptide
1521	114.5586(m/z)	0.92913	No database match
1946	193.0631(m/z)	0.90935	ethyl-2-amino-4-methyl-Thiazole-5-Carboxylate (Li+)
1525	118.5489(m/z)	0.83549	Phenazopyridine or MelQX (H+Na) 2+
1628	204.0183(m/z)	0.82101	Benzoyl chloride or 4-Chlorobenzaldehyde (ACN +Na) +
1636	218.9486(m/z)	0.8109	No database match
1829	296.9712(m/z)	0.78267	Bis(2-methyl-3-furanyl)tetrasulfide (M+Li)+
1689	290.0037(m/z)	0.72056	MC-6063
1934	147.0334(m/z)	0.71672	9-Bromo-17beta-hydroxy-17-methylandrost-4-ene-3,11-dione (2Na + H)3+
1675	262.9564(m/z)	0.67676	Haloxydine (Na+ ACN)+
2107	442.8789(m/z)	0.66665	No database match
2062	169.0091(m/z)	0.61826	2-Ethyldihydro-3(2H)-thiophenone or very similar (M + K)+
2087	245.0449(m/z)	0.60444	1,3,5-Trihydroxyxanthone (H) or Phantasmidine (Na) or 3-(3'-Methylthio)propylmalic acid (Na
1810	209.0431(m/z)	0.60433	N-Isopropylammelide or N-Nitroso-N-morpholinoaminoacetonitrile (K)+
2071	175.9849(m/z)	0.574	No database match
1673	261.9704(m/z)	0.57051	4-Methyl-5-(2-phosphoethyl)-thiazole (K)+ or Trichlormethine (Na)+
1667	249.0029(m/z)	0.54697	Bromoisoquinoline (M+ACN
2085	240.066(m/z)	0.54503	Brassicanal B (Li)+ Crinasiadine (H)+ Dechloroethylcyclophosphamide (ACN+H)+ Methylthio 2-(propanoyloxy)propanoate (ACN+Na)+
1625	200.0425(m/z)	0.54035	Urea phosphate salt (likely adhered to coating)
1760	540.8818(m/z)	0.53296	No database match
1908	373.9556(m/z)	0.52542	No database match
1892	259.9818(m/z)	0.51084	No database match
2095	284.9865(m/z)	0.47007	Busulfan (M+K)+
2097	309.2834(m/z)	0.42658	No database match
2088	256.9194(m/z)	0.38857	No database match
1817	227.9831(m/z)	0.36713	Acephate (M+2Na-H) + or 2,4-Dichloro-2,5-dihydro-5-oxofuran-2-acetate (NH4)+

Table C.3 Preliminary exact mass matching of features highlighted in BLUE from the Vent samples of the NW Rota ROV dive in Figure 7.20. PFP-Positive mode run. All adducts were considered when using the METLIN on-line database and a mass accuracy +/-5 ppm was used

Feature ID	M/Z	VIP-value	Online Database Identification (Metlin) (Exact Mass only, 5ppm)
6647	132.0031(m/z)	7.03674	1,2-6-sulfonate
1808	146.0299(m/z)	5.56754	6-Methylthioguanine $[M+H-2H2O]^+$
1943	197.041(m/z)	5.29646	Diethylstilbestrol monosulfate (2NA2+) other possibilities
2347	566.8888(m/z)	5.07158	No database match
2380	634.8763(m/z)	4.88363	9,10,12,13-tetrabromo-stearic acid (K+)
6645	130.0167(m/z)	4.50695	Monomethyl sulfate (NH4+)
2408	702.8638(m/z)	4.46685	No database match
4304	218.9835(m/z)	4.32794	No database match
5958	416.2143(m/z)	4.23242	4 member amino acid/peptide
6674	169.0456(m/z)	4.22232	Pterostilbene Phosphate (2H2+), 3-Methylcyclohexanethiol (K+)
2434	770.8512(m/z)	3.90444	N/A
1308	418.2432(m/z)	3.78973	Peptide or nonaprenyl diphosphate
2454	838.8387(m/z)	3.61102	N/A
1820	148.0275(m/z)	3.58107	4-Pyrimidine Methanamine or similar (K+)
5263	218.1031(m/z)	3.38828	1-Isothiocyanato-8-(methylthio)octane (H+) or Pymetrozine
5485	508.3112(m/z)	3.3739	Amino acids/Peptide
5910	296.2579(m/z)	3.3691	A lipid or Long chain fatty acid
2367	600.8825(m/z)	3.33674	No database match
1848	153.0329(m/z)	3.1989	1-Fluorocyclohexadiene-cis,cis-1,2-diol
2395	668.87(m/z)	3.14419	beta-D-Glucosyl-1,4-N-acetyl-D-glucosaminyldiphosphoundecaprenol (2Na 2+)
2320	532.895(m/z)	3.1308	No database match
1842	152.0362(m/z)	3.00295	3,4-Dehydrothiomorpholine-3-carboxylate [Li+]
2468	906.8263(m/z)	2.98726	No database match
6694	220.9809(m/z)	2.85416	Glyceryl dinitrate (K+)
5491	513.2667(m/z)	2.79208	Amino acid/peptide
4310	234.961(m/z)	2.78633	2-Iodophenol methyl ether (H+)
2424	736.8574(m/z)	2.77059	No database match
2482	974.8138(m/z)	2.74854	Esterified long chain fatty acid
2446	804.8449(m/z)	2.73057	No database match
1698	106.0043(m/z)	2.68833	No database match
4496	273.2536(m/z)	2.65937	No database match
6662	150.1204(m/z)	2.62312	No database match
6668	158.0115(m/z)	2.61298	Sulfoacetic acid (NH4+)

6665	152.0383(m/z)	2.59946	(S)C(S)S-S-Methylcysteine sulfoxide (H+)
2462	872.8325(m/z)	2.58025	No database match
1951	199.9907(m/z)	2.49433	5-(1-Hydroxy-2-chloroethyl)-4-methylthiazole (Na+)
5834	336.2378(m/z)	2.48436	(-)-menthyl beta-D-glucoside or L-Citronellol glucoside (NH4+)
4283	157.0149(m/z)	2.46228	Thiodiacetic acid (Li+)
4319	257.977(m/z)	2.4223	Thallium (NH4+)
6713	265.0152(m/z)	2.4053	N-(3,4-Dichlorophenyl)-malonamate (NH4+) or Metobromuron(Li+)
2917	199.0383(m/z)	2.3565	Naphthalic anhydride (H+) Thiocyclam(NH4+) Hydralazine(K+)
2017	234.9614(m/z)	2.31663	2-Iodophenol methyl ether (H+)
2477	940.8201(m/z)	2.25733	No database match
1915	176.0223(m/z)	2.25693	Phosphocreatinine (H -H2O+) or 6-Aminonicotinamide or Isoniazid or Pyridylamide oxime (K+)
6850	434.2437(m/z)	2.24544	A peptide
1860	158.0118(m/z)	2.19499	Sulfoacetic acid (MH4+) or Citreovirone (H + Na2+)
3038	483.2493(m/z)	2.18282	A phospholipid (H+) (23S,25R)-25-hydroxyvitamin D3 26,23-peroxylactone / (23S,25R)-25-hydroxycholecalciferol 26,23peroxylactone (K+)
2271	464.9076(m/z)	2.1543	No database match
1909	175.0257(m/z)	2.14637	Methyl 1-(methylthio)propyl disulfide or Ethyl 1-(methylthio)ethyl disulfide (Li+)
1855	157.0151(m/z)	2.10725	Thiodiacetic acid (Li+)
5709	612.1627(m/z)	2.06936	Novclobiocin 104 (Na+) or a peptide (K+)
6644	129.0224(m/z)	2.06281	Ticarcillin (3H3+)
6580	281.2664(m/z)	2.02959	1-tetradecanyl-2-(8-[3]-ladderane-octanyl)-sn-glycerol (2H2+)
2065	257.9774(m/z)	2.02425	Thallium (NH4+)
6771	432.2375(m/z)	1.99122	A phospholipid
3901	273.9495(m/z)	1.94149	No database match
1999	227.9549(m/z)	1.91665	No database match
6500	851.3963(m/z)	1.89757	No database match
6703	243.9968(m/z)	1.88811	O-Phosphoryl-L-homoserine , O-Phospho-L-threonine, OPhosphoryl homoserine Iminoerythrose 4-phosphate (2Na – H+)
2381	635.378(m/z)	1.84923	Pandaroside B, Digitoxigenin bisdigitoxoside (H+) Cholestane-3,7,12,25tetrol-3-glucuronide (Na+) Lopinavir (Li+)
1856	157.0175(m/z)	1.83221	No database match
6702	243.0002(m/z)	1.82078	Treosulfan (H- 2H20+)
5417	423.1987(m/z)	1.81363	A Peptide
5996	476.2635(m/z)	1.79898	A Peptide

2396	669.3717(m/z)	1.78574	A Phospholipid or a Peptide
2368	601.3842(m/z)	1.78255	A phospholipid
2207	378.9004(m/z)	1.78048	Costatol (2Na –H+)
2942	316.1753(m/z)	1.77732	Alizapride (H+) or Sesamex or Neoilludin A or Toxin T2 tetrol or 3,7,8,15- Scirpenetetrol or Idebenone Metabolite (Benzenehexanoic acid, 2,5dihydroxy-3,4-dimethoxy-6-methyl-) ((NH4+) or a peptide
6741	313.1619(m/z)	1.77598	N6,N6-Dimethyladenosine (NH4+) or 1-Octen-3-yl glucoside (Na+) or a peptide
2348	567.3905(m/z)	1.76627	3-Hydroxypancuronium (K+)
1765	129.0226(m/z)	1.74465	5,7,3',4',5'-Pentahydroxy-3,6-dimethoxyflavone (2H+ Na 3+) or an isomer
2409	703.3655(m/z)	1.70574	Nostoxanthin sulfate (H+)
2090	273.9496(m/z)	1.70442	No database match
1955	202.0198(m/z)	1.68689	No database match
1936	192.062(m/z)	1.68302	A peptide
4302	216.9505(m/z)	1.67832	No database match
2322	533.3967(m/z)	1.65946	A Phospholipid
2371	608.8697(m/z)	1.63145	No database match
4312	239.9664(m/z)	1.62634	No database match
2425	737.3591(m/z)	1.62434	Septentrionine (Na+)
2429	744.8436(m/z)	1.62406	No database match
1910	175.0282(m/z)	1.62063	AMT (2Na-H +)
2328	540.8825(m/z)	1.61541	No database match
6648	134.9955(m/z)	1.61389	1,3-Dichloro-2-propanol (Li+)
5350	318.2398(m/z)	1.60595	A fatty acid
6506	492.8646(m/z)	1.60207	No database match
3784	658.5094(m/z)	1.60024	No database match
2498	114.5585(m/z)	1.59684	No database match
2456	839.842(m/z)	1.58626	No database match
2414	710.8507(m/z)	1.58551	No database match
6022	502.279(m/z)	1.57404	A Peptide
6632	112.0062(m/z)	1.57334	No database match
1846	153.0064(m/z)	1.56919	Fluorouracil (Na+) or Dihydrouracil or 3-Cyano-L-alanine or N- Methylhydantoin or Muscimol or 2,5-Dioxopiperazine (K+)
2385	642.8632(m/z)	1.56639	Stibogluconic acid (H+ -2H20+)
2435	771.3529(m/z)	1.56212	No database match
5616	223.0634(m/z)	1.54223	Phantasmidine or 2-(3'-Methylthio)propylmalic acid or 1-(1-Propenylthio)propyl propyl disulfide or 2,2,4,4,6,6-Hexamethyl-1,3,5trithiane or 2,4,6-Triethyl-1,3,5-trithiane (H+) or a Benzidine like compound (Na+)
2354	574.8758(m/z)	1.53757	No database match

4299	198.0415(m/z)	1.51816	Methyl phenyl disulfide (H+ACN+) Biapenem (2Na2+) Demethyltorosaflavone C or Tetracenomycin B3 or Prostalidin A (2H+)
2400	676.8567(m/z)	1.51762	No database match
2382	635.8794(m/z)	1.51604	No database match
5805	514.8778(m/z)	1.51434	No database match
2470	907.8295(m/z)	1.51236	A Triglyceride
2207	378.9004(m/z)	1.78048	Costatol (2Na –H+)
2942	316.1753(m/z)	1.77732	Alizapride (H+) or Sesamex or Neoilludin A or Toxin T2 tetrol or 3,7,8,15-Scirpenetetrol or Idebenone Metabolite (Benzenehexanoic acid, 2,5-dihydroxy-3,4-dimethoxy-6-methyl-) ((NH4+) or a peptide
6741	313.1619(m/z)	1.77598	N6,N6-Dimethyladenosine (NH4+) or 1-Octen-3-yl glucoside (Na+) or a peptide
2348	567.3905(m/z)	1.76627	3-Hydroxypancuronium (K+)
1765	129.0226(m/z)	1.74465	5,7,3',4',5'-Pentahydroxy-3,6-dimethoxyflavone (2H+ Na 3+) or an isomer
2409	703.3655(m/z)	1.70574	Nostoxanthin sulfate (H+)
2090	273.9496(m/z)	1.70442	No database match
1955	202.0198(m/z)	1.68689	No database match
1936	192.062(m/z)	1.68302	A peptide
4302	216.9505(m/z)	1.67832	No database match
2322	533.3967(m/z)	1.65946	A phospholipid
2371	608.8697(m/z)	1.63145	No database match
4312	239.9664(m/z)	1.62634	No database match
2425	737.3591(m/z)	1.62434	Septentrionine (Na+)
2429	744.8436(m/z)	1.62406	No database match
1910	175.0282(m/z)	1.62063	AMT (2Na-H +)
2328	540.8825(m/z)	1.61541	No database match
6648	134.9955(m/z)	1.61389	1,3-Dichloro-2-propanol (Li+)
5350	318.2398(m/z)	1.60595	A fatty acid
6506	492.8646(m/z)	1.60207	No database match
3784	658.5094(m/z)	1.60024	No database match
2498	114.5585(m/z)	1.59684	No database match
2456	839.842(m/z)	1.58626	No database match
2414	710.8507(m/z)	1.58551	No database match
6022	502.279(m/z)	1.57404	A Peptide
6632	112.0062(m/z)	1.57334	No database match
1846	153.0064(m/z)	1.56919	Fluorouracil (Na+) or Dihydrouracil or 3-Cyano-L-alanine or N-Methylhydantoin or Muscimol or 2,5-Dioxopiperazine (K+)
2385	642.8632(m/z)	1.56639	Stibogluconic acid (H+ -2H20+)
2435	771.3529(m/z)	1.56212	No database match

5616	223.0634(m/z)	1.54223	Phantasmidine or 2-(3'-Methylthio)propylmalic acid or 1-(1-Propenylthio)propyl propyl disulfide or 2,2,4,4,6,6-Hexamethyl-1,3,5-trithiane or 2,4,6-Triethyl-1,3,5-trithiane (H+) or Benzidine like compound (Na+)
2354	574.8758(m/z)	1.53757	No database match
4299	198.0415(m/z)	1.51816	Methyl phenyl disulfide (H+CAN+) Biapenem (2Na2+) Demethyltorosaflavone C or Tetracenomycin B3 or Prostalidin A (2H+)
2400	676.8567(m/z)	1.51762	No database match
2382	635.8794(m/z)	1.51604	No database match
5805	514.8778(m/z)	1.51434	No database match
2470	907.8295(m/z)	1.51236	A triglyceride
2716	626.1685(m/z)	1.50681	(C27H28O16) Luteolin 7-glucuronide-4'-rhamnoside or similar (NH4+)
1736	125.0115(m/z)	1.49977	N-Nitrosomethylvinylamine (K+)
4272	133.9989(m/z)	1.4897	No database match
2182	363.9298(m/z)	1.48834	Sodium L-ascorbic acid 2-phosphate (K+ unlikely as it is a salt)
2447	805.3466(m/z)	1.48717	No database match
2439	778.8382(m/z)	1.48631	No database match
2410	703.8669(m/z)	1.48026	No database match
6860	297.2612(m/z)	1.47931	A Diglyceride
2117	295.9423(m/z)	1.46874	No database match
3441	614.9109(m/z)	1.44931	No database match
2293	499.403(m/z)	1.44239	No database match
2258	446.8878(m/z)	1.43724	No database match
2450	812.8317(m/z)	1.43549	No database match
1390	614.4829(m/z)	1.43045	No database match
6722	280.9927(m/z)	1.41893	3-(Phosphoacetylamido)-L-alanine (K+) very likely metabolite
2469	907.3279(m/z)	1.41517	No database match
2459	846.8256(m/z)	1.41378	No database match
2283	481.9037(m/z)	1.4106	No Database Match
5808	580.4152(m/z)	1.40794	Rhodoxanthin (NH4+)
1977	216.9508(m/z)	1.40773	No possible database match
1204	590.426(m/z)	1.40215	A Peptide
1707	111.0097(m/z)	1.40164	Furosemide (NH4+) 4-phenyl-5-methyl-1,2,3-Thiadiazole (2Na 2+)
2455	839.3404(m/z)	1.39937	No Database match
5928	344.2064(m/z)	1.39638	Tributyrin (ACN + H+), Platyphylline, Nemorensine, Sarracine, 3,6-Ditigloyloxytropan-7-ol (Li+)
5911	299.1487(m/z) Found twice	1.39276	Neoilludin A, Toxin T2 tetrol, 3,7,8,15-Scirpenetetrol, Idebenone Metabolite: Benzenehexanoic acid, 2,5-dihydroxy-3,4-dimethoxy-6-methyl- (H+), p-Coumaroylagmatine(Na+), 10-Hydroxy-8-nor-2-fenchanone glucoside (H+ - H2O)

2463	873.3342(m/z)	1.37833	Mebhydrolin napadisilate (+MeOH +H)
5774	338.3413(m/z)	1.37657	N-Cyclohexanecarbonylpentadecylamine, Docosenamide (H+)
2437	771.8544(m/z)	1.37251	Ioversol (H+ - 2H2O) Metrizamide (H+ -H2O)
3184	548.8715(m/z)	1.36864	No Database Match
3315	582.3927(m/z)	1.36456	Valnemulin (NH4), Debenzoylzucchini factor B (Na+)
2181	363.0158(m/z)	1.3644	6-Thioxanthine 5'-monophosphate, Luteolin 3'-methyl ether 7-sulfate, Hispidulin 7-sulfate, Kaempferide 3-O-sulfate, Rhamnocitrin 3-O-sulfate, Tectorigenin 7-sulfate (H+ - H2O) or similar
6576	149.1186(m/z)	1.36188	A steroid (32 possibilities 2Na + H 3+)
6581	299.2769(m/z)	1.35604	A Diglyceride
2397	669.8723(m/z)	1.3527	No Database Match
6699	236.9584(m/z)	1.34968	No Database Match
5824	159.1379(m/z)	1.34806	C9 carboxylic acid (38 possibilities, H+)
2461	854.8128(m/z)	1.34567	No Database Match
1944	198.0418(m/z)	1.33492	Demethyltorosaflavone C, Tetracenomycin B3, Prostalidin A (2H2+)
2014	232.9283(m/z)	1.33103	No Database Match
2503	128.0707(m/z)	1.32992	D-1-Piperideine-2-carboxylic acid (GUVACINE) or an isomer (H+), 50+ other possibilities, only H+ is listed
1785	134.9958(m/z)	1.32707	S-methyl Isothiourea (-H + 2Na+)
3272	571.3862(m/z)	1.32645	2-(8-[3]-ladderane-octanyl)-sn-glycero-3-phosphocholine (CAN + H+)
5912	299.1484(m/z) Found twice	1.31236	Neoilludin A, Toxin T2 tetrol, 3,7,8,15-Scirpenetetrol, Idebenone Metabolite: Benzenehexanoic acid, 2,5-dihydroxy-3,4-dimethoxy-6-methyl- (H+), p-Coumaroylagmatine(Na+), 10-Hydroxy-8-nor-2-fenchanone glucoside (H+ - H2O)
2059	255.939(m/z)	1.31202	No Database Match
2478	941.3217(m/z)	1.31063	No Database Match
5839	379.2484(m/z)	1.30267	8-iso-16-cyclohexyl-tetranor Prostaglandin E2, F4-Neuroprostane, 1,9-dideoxyforskolin, Pleuromutilin, Annoglabasin F (H+), corticosterone or another steroid (MeOH+H+)
2419	718.8377(m/z)	1.30182	No Database Match
2484	975.8169(m/z)	1.29577	A triglyceride
1777	133.9991(m/z)	1.29481	No database match
2349	567.8919(m/z)	1.29404	MIPC(d20:0/26:0) (H+Na 2+
6678	175.9541(m/z)	1.27373	No database match
2850	780.5178(m/z)	1.26665	A phospholipid
3017	463.3421(m/z)	1.26481	Stoloniferone, Dolichosterone, Polyporusterone F (H+) or another steroid adduct
2118	296.9432(m/z)	1.26118	No database match
1771	130.9652(m/z)	1.25873	Calcium formate (H+) unlikely to ionize in this state
2246	431.9172(m/z)	1.25825	No database match

5699	520.1371(m/z)	1.25524	A Peptide
3000	441.329(m/z)	1.25492	thio-Miltefosine (NH4+)
2389	650.8503(m/z)	1.25333	No database match
1865	158.9661(m/z)	1.2532	Acetylenedicarboxylate (2Na-H+)
2483	975.3154(m/z)	1.25236	No database match
5749	219.1064(m/z)	1.25025	A Peptide
4956	619.6136(m/z)	1.24555	No database match
2241	423.9086(m/z)	1.24426	No database match
2295	499.9045(m/z)	1.23982	No database match
2502	128.021(m/z)	1.23933	N-Carbamoyl-2-amino-2-(4-hydroxyphenyl)acetic acid, or 5-aminosalicyluric acid (2Na 2+)
2006	230.9953(m/z)	1.23673	(Z)-[3-(Methylsulfinyl)-1-propenyl] 2-propenyl disulfide (Na+), Vanillic acid 4-sulfate (H+ - H2O), Luteolin 4'-methyl ether 7,3'-disulfate, Hispidulin 7,4'-disulfate (2 H+)
5353	323.3052(m/z)	1.22747	Clavepictine B (NH4+), Elaidamide (ACN + H+)
2360	582.8628(m/z)	1.21883	No database match
1753	128.0209(m/z)	1.21623	No database match
2273	465.4092(m/z)	1.21383	No reasonable database match
5077	214.1801(m/z)	1.2136	Aleprylic acid, dodecadienoic acid, Terpinyl acetate, Linalyl acetate, Bornyl acetate, octadienyl acetate, or similar (H+) (50 + metabolites)
1869	159.9675(m/z)	1.20686	No database match
2159	335.9655(m/z)	1.20652	A triglyceride
1776	133.0279(m/z)	1.20628	Ammonium sulfate (H+)
6146	551.3942(m/z)	1.20576	Ganoderic acid Mi (Li+)
2369	601.8848(m/z)	1.19687	No database match
5981	455.3444(m/z)	1.19528	No database match
2465	880.8187(m/z)	1.19329	No database match
6650	139.05(m/z)	1.18685	methyl 2-Pyrimidine Carboxylate, Urocanic acid, 4-Nitroaniline, Benzoquinone dioxime, (H+)
3896	250.9387(m/z)	1.18477	No database match
6001	477.3575(m/z)	1.1839	A steroid like: 11-acetoxy-3beta,6alpha-dihydroxy-9,11-seco-5alpha-cholest-7-en-9-one (H+)
4141	434.7886(m/z)	1.17959	No database match
5792	418.2433(m/z)	1.1764	Cincassiol B or a peptide (H+), nonaprenyl diphosphate (2 Na2+), Lasiocarpine (Li+)
2474	922.8003(m/z)	1.16579	No reasonable database match
6018	499.3707(m/z)	1.16575	No database match
2306	514.8753(m/z)	1.16517	No database match
2442	786.8252(m/z)	1.16139	No database match
2427	737.8598(m/z)	1.1577	No database match
6705	246.9782(m/z)	1.15638	No database match
3043	485.3552(m/z)	1.15483	No database match
2472	914.8132(m/z)	1.1524	A triglyceride

5836	356.9088(m/z)	1.1511	3,3-Dibromo-2-n-hexylacrylic acid, 9,9-dibromo-8-nonenoic acid (2Na-H+)
2184	364.9306(m/z)	1.14906	No database match
6032	507.3681(m/z)	1.14884	Theasapogenol A (H+)
5797	467.3008(m/z)	1.14728	A Peptide or steroid
6711	259.9744(m/z)	1.13826	No database match
6633	114.9876(m/z)	1.13817	No database match
5153	172.1331(m/z)	1.13709	Gabapentin (H+) nonadienoic acid or similar (Na+), Hexanoic acid (isomer) (ACN)
2039	244.9236(m/z)	1.13652	No database match
5702	526.4307(m/z)	1.13359	No database match
5969	433.3313(m/z)	1.13323	A steroid (100`s of possibilities)
3313	580.9173(m/z)	1.12907	No database match
1768	130.0235(m/z)	1.12127	Lofexidine (2+2+)
5627	264.0898(m/z)	1.12056	para-(Dimethylamino)azobenzene, Cyprodinil, ortho-Aminoazotoluene (K+), Methylthio propylmalic acid, Propenylthio propyl propyl disulfide (ACN+ H+) or another adduct of a peptide.
5416	423.1983(m/z)	1.12001	A Peptide
2323	533.8973(m/z)	1.11301	No database match
2485	982.8007(m/z)	1.1125	No database match
1693	103.0321(m/z)	1.1111	Ethylenethiourea (H+)
1132	223.989(m/z)	1.11106	Zinc Acetate (ACN +H+)
1812	147.0332(m/z)	1.102	9-Bromo-17beta-hydroxy-17-methylandrost-4-ene-3,11-dione (2Na + H 3+)
3840	699.5018(m/z)	1.09026	A phospholipid
2981	419.3159(m/z)	1.08666	A steroid
6551	461.8366(m/z)	1.08392	No database match
5614	220.0988(m/z)	1.07025	A Peptide
3868	151.0371(m/z)	1.06762	6-hydroxy-2-hexynoic acid, Dihydro-4,4-dimethyl-2,3-furandione, Dihydrophloroglucinol, or similar (Na+)
1763	128.0707(m/z)	1.06584	D-1-Piperideine-2-carboxylic acid (GUVACINE) or an isomer (H+), 50+ other possibilities, only H+ is listed
2277	472.8948(m/z)	1.06039	No database match
2480	948.8065(m/z)	1.05977	No reasonable database match
2249	432.918(m/z)	1.05883	No database match
2302	506.8883(m/z)	1.0559	No database match
5802	511.3271(m/z)	1.05463	A steroid, phospholipid, or peptide
2223	396.9201(m/z)	1.05327	1-Amino-2,4-dibromoanthraquinone (NH4 +)
2061	255.9443(m/z)	1.05011	No database match
2282	480.8365(m/z)	1.04976	No database match
6654	147.9895(m/z)	1.04299	D-Glyceric acid (2Na 2+)
6653	147.0329(m/z)	1.03988	No database match
2979	417.8107(m/z)	1.03977	Sulfobromophthalein (2 Na 2+)

6556	483.8497(m/z)	1.03923	A phospholipid
5900	282.2834(m/z)	1.03899	No database match
6714	267.0127(m/z)	1.03744	Chloromethiuron (K+) Flupyrsulfuron-methyl sodium (2 Na 2+)
2464	873.8347(m/z)	1.03403	No database match
6676	171.0431(m/z)	1.02663	3-Sulfinoalanine (NH4+)
4996	312.9426(m/z)	1.02536	3,3-Dibromo-2-n-hexylacrylic acid, 9,9-dibromo-8-nonenoic acid (H+)
5877	191.1641(m/z)	1.02274	methyl-octanoic acid or similar (MeOH + H+)
2448	805.8473(m/z)	1.01996	No database match
82	163.0754(m/z)	1.01678	15 H+ adducts Naphthalene dihydrodiol example or 100`s of other possibilities
2457	840.8433(m/z)	1.01043	No database match
1917	176.9362(m/z)	1.00956	No database match
2941	300.1521(m/z)	1.00814	Likely a small peptide
2487	997.4759(m/z)	1.00277	Asiaticoside or similar (K+)

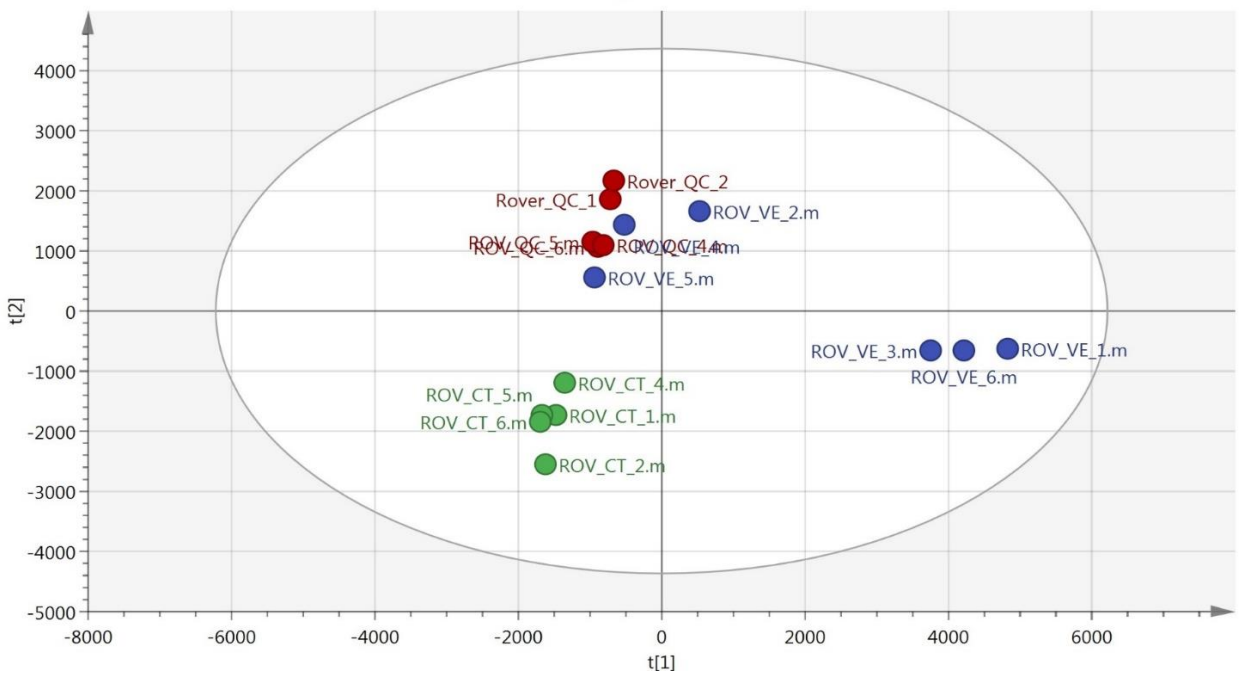

Figure C.1 Multivariate separation (PCA) of replicate samples corresponding to extractions from the NW Rota hydrothermal vent sample (BLUE), the control sample (GREEN) and the validating pooled QC data (RED). Well grouped pool QC data indicates stable instrument performance. Samples were run on the PFP column and ionized in negative mode. Separation is based on the exact mass peak height

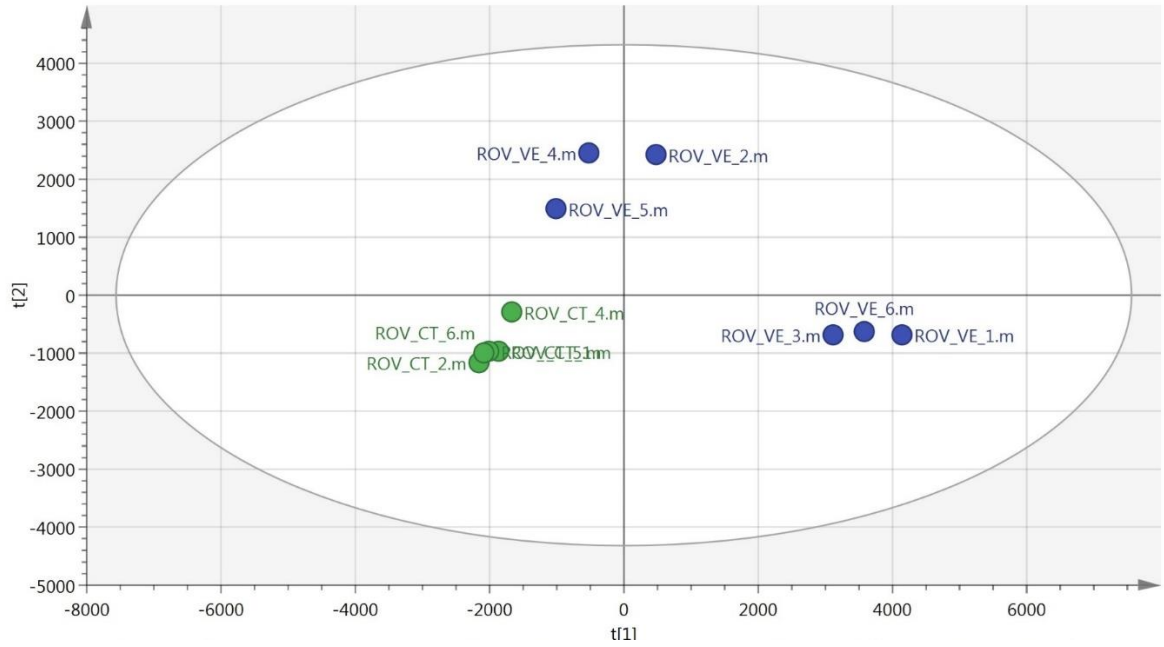

Figure C.2 Multivariate separation (PCA) of replicate samples corresponding to extractions from the NW Rota vent sample (BLUE), the control sample (GREEN). Pool QC's have been removed to better show clustering of ROV samples. Samples were run on the PFP column and ionized in negative mode. Separation is based on the exact mass peak height.

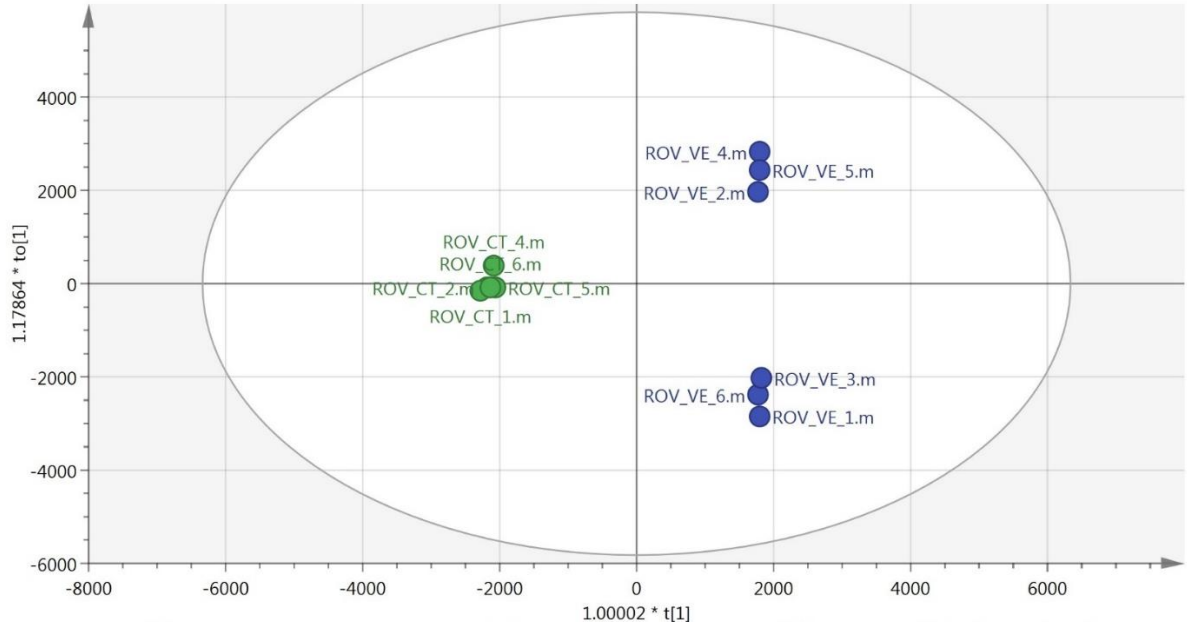

Figure C.3 Classed multivariate separation (OPLS-DA) of replicate samples corresponding to extractions from NW Rota vent samples (BLUE) and ambient ocean control samples (GREEN). Samples were run on the PFP column and ionized in negative mode. Separation is based on the exact mass peak height

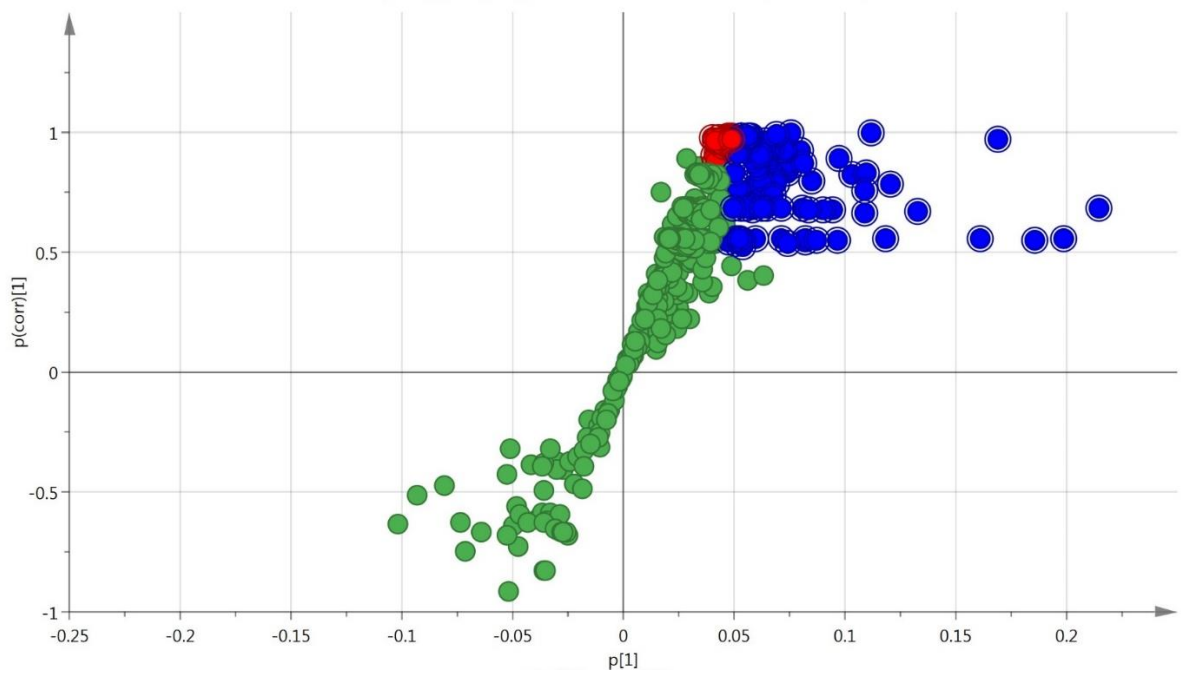

Figure C.4: S-Plot generated from the classed multivariate separation shown in Figure B.3 highlighting features in BLUE being statistically larger (VIP>1) in the vent sample and features in RED being exclusively present in the vent sample but with VIP<1.

Table C.4 Preliminary exact mass matching of features highlighted in BLUE from the Vent samples of the NW Rota ROV dive in Figure 7.20. PFP-negative mode run. All adducts were considered when using the METLIN on-line database and a mass accuracy +/-5 ppm was used

Feature ID	M/Z	VIP-value	Online Database Identification (Metlin) (Exact Mass only, 5ppm)
4224	158.9778(m/z)	5.06633	Benzal chloride or 2,4-Dichlorotoluene [H-] or Arsenobetaine [H2O-H -]:
4295	288.9367(m/z)	4.82226	Cartilagineal $[M+K-2H]^-$
4286	272.9591(m/z)	4.75673	Ribose-1-arsenate **$[M-H]^-$**
3472	158.9779(m/z)	4.11388	Benzal chloride or 2,4-Dichlorotoluene [H-] or Arsenobetaine[H2O-H -]:
3652	304.9143(m/z)	3.30132	No Database Match
4368	402.9172(m/z)	3.03774	No Database Match
4212	130.9827(m/z)	3.02146	1,2-Dichloropropane **$[M+F]^-$**
3516	292.8953(m/z)	2.54656	cis-Chlorobenzene dihydrodiol **$[M+FA-H]^-$** Is a known Bacterial metabolite TcbB
4287	273.9601(m/z)	2.50963	N/A
4288	274.9567(m/z)	2.47251	Plocamene **$[M+K-2H]^-$** or Thiram **[M+Cl]-**
4418	516.8975(m/z)	2.23248	No Database Match
3474	162.8384(m/z)	2.18536	No Database Match
3229	894.8427(m/z)	2.17514	No Database Match
4208	114.9878(m/z)	2.15014	No Database Match

2554	722.2637(m/z)	2.13455	Dihydrostreptomycin 6-phosphate **[M+CH3COO]**$^-$
4357	386.9398(m/z)	2.10294	No Database Match
2872	962.8301(m/z)	2.09252	No Database Match
4375	418.8948(m/z)	2.08741	No Database Match
4228	160.9753(m/z)	2.05172	2-carboxy-Pyrimidine **[M+K-2H]**$^-$
3303	160.8413(m/z)	1.94168	No Database Match
4408	500.9202(m/z)	1.91322	No Database Match
4429	532.8752(m/z)	1.88685	No Database Match
4298	290.9343(m/z)	1.82172	No Database Match
4225	159.9786(m/z)	1.81569	No Database Match
3216	826.8552(m/z)	1.7202	No Database Match
3566	526.7772(m/z)	1.65414	No Database Match
4370	404.9148(m/z)	1.619	No Database Match
3392	902.8292(m/z)	1.58742	No Database Match
2681	793.8648(m/z)	1.53852	No Database Match
4296	289.9378(m/z)	1.52905	No Database Match
2769	861.8522(m/z)	1.49358	No Database Match
2699	808.8354(m/z)	1.4935	No Database Match
3352	443.7743(m/z)	1.48282	No Database Match
3480	170.8831(m/z)	1.48098	No Database Match
4369	403.9177(m/z)	1.46135	No Database Match
3492	196.9229(m/z)	1.44899	No Database Match
2068	442.8946(m/z)	1.44357	No Database Match
2850	929.8398(m/z)	1.40114	No Database Match
3397	997.3255(m/z)	1.39888	No Database Match
4410	502.9176(m/z)	1.39103	No Database Match
4536	847.3117(m/z)	1.38707	No Database Match
3387	861.3506(m/z)	1.38531	Vincristine (K+ -2H-)
4420	517.8984(m/z)	1.38454	No Database Match
2787	876.8229(m/z)	1.36552	No Database Match
2864	944.8103(m/z)	1.3614	No Database Match
3199	758.8675(m/z)	1.35479	No Database Match
3615	827.357(m/z)	1.35356	28-Glucosyl-19(29)-dehydroursolic acid 3-arabinoside (Br-)
2266	578.8696(m/z)	1.35139	No Database Match
4359	388.9374(m/z)	1.33761	No Database Match
3553	444.7822(m/z)	1.33459	No Database Match
4409	501.921(m/z)	1.31513	Gemcitabine diphosphate (Br-)
3923	164.8354(m/z)	1.29867	No Database Match
3237	970.8168(m/z)	1.27837	No Database Match
3600	690.8799(m/z)	1.27499	No Database Match
3396	963.8326(m/z)	1.27053	A phospholipid

3610	793.3631(m/z)	1.25727	No Database Match
3234	936.8236(m/z)	1.25515	No Database Match
4214	132.9803(m/z)	1.2498	No Database Match
3386	834.841(m/z)	1.23467	No Database Match
3612	800.8483(m/z)	1.2278	No Database Match
3398	997.827(m/z)	1.21547	A Phospholipid
4358	387.9402(m/z)	1.21433	2,8-bis-Trifluoromethyl-4-quinoline carboxylic acid, 3-oxobrimonidine (Br-)
3313	219.8452(m/z)	1.18784	No Database Match
3393	929.3383(m/z)	1.18498	No Database Match
3391	895.8451(m/z)	1.18048	A phospholipid
3394	930.8412(m/z)	1.16249	No Database Match
3158	646.8573(m/z)	1.15348	No Database Match
3395	963.3318(m/z)	1.13185	A Peptide
3639	188.8526(m/z)	1.12241	No Database Match
3775	824.8094(m/z)	1.10735	No Database Match
4437	548.8529(m/z)	1.10601	No Database Match
3622	998.8285(m/z)	1.10503	No Database Match
3689	434.8724(m/z)	1.09645	No Database Match
4086	298.2471(m/z)	1.09598	No Database Match
3341	348.8106(m/z)	1.09577	No Database Match
3390	895.3445(m/z)	1.08469	No Database Match
5091	776.294(m/z)	1.08139	No Database Match
3568	580.6966(m/z)	1.07891	No Database Match
3620	971.3188(m/z)	1.07369	No Database Match
3172	688.8341(m/z)	1.0566	No Database Match
3617	850.8201(m/z)	1.04029	No Database Match
3613	809.8391(m/z)	1.03792	No Database Match
4072	165.0914(m/z)	1.03654	Agmatine, Agmatinium (+Cl-) Oleuropeic acid or similar (-H2O-H-)
3532	324.0193(m/z)	1.03624	No Database Match
3854	253.2538(m/z)	1.03597	No Database Match
3795	978.8041(m/z)	1.03119	No Database Match
3781	877.8262(m/z)	1.00695	No Database Match
3388	862.8535(m/z)	1.00344	No Database Match